

Aus dem  
Lehrstuhl für Virologie, Max-von-Pettenkofer-Institut  
Ludwig-Maximilians-Universität München



**Mechanistic insight into the CD32-driven enhancement of HIV-1  
susceptibility of resting CD4 T cells**

Dissertation  
zum Erwerb des Doctor of Philosophy (Ph.D.)  
an der Medizinischen Fakultät der  
Ludwig-Maximilians-Universität München

vorgelegt von  
Madeleine Christine Gapp

aus  
Gunzenhausen

Jahr  
2024

---

Mit Genehmigung der Medizinischen Fakultät der  
Ludwig-Maximilians-Universität München

Erstes Gutachten: Prof. Dr. Oliver T. Keppler  
Zweites Gutachten: Priv. Doz. Dr. Barbara Adler  
Drittes Gutachten: Priv. Doz. Dr. Ulrich von Both  
Viertes Gutachten: Prof. Dr. Marcus Hentrich

Dekan: Prof. Dr. med. Thomas Gudermann

Tag der mündlichen Prüfung: 13.03.2024

## Table of content

<b>Table of content</b> .....	<b>1</b>
<b>Abstract</b> .....	<b>4</b>
<b>List of figures</b> .....	<b>5</b>
<b>List of tables</b> .....	<b>7</b>
<b>List of abbreviations</b> .....	<b>8</b>
<b>1. Introduction</b> .....	<b>12</b>
1.1 HIV-1 and CD4 T cells .....	12
1.1.1 HIV structure and composition.....	12
1.1.2 HIV-1 fusion mediated by its envelope glycoproteins .....	13
1.1.3 After HIV enters the cell: from reverse transcriptase to viral release .....	14
1.1.4 HIV-1 latency and restriction in CD4 T cells .....	16
1.1.5 Potential biomarkers for HIV-1 latency in CD4 T cells.....	18
1.2 Function of Fcγ Receptors (FcγRs) .....	20
1.2.1 Genes and prevalence of FcγR .....	20
1.2.2 The allelic variants of CD32 (FcγRII) .....	22
1.2.3 Immune functions of FcγR .....	23
1.2.4 Antibody binding sites on FcγR .....	24
1.2.5 HIV and FcγRs .....	25
1.2.6 FcγR-mediated trogocytosis .....	26
1.3 Aim of the study .....	28
<b>2. Material and Methods</b> .....	<b>30</b>
2.1 Chemicals and material .....	30
2.1.1 Reagents, drugs, commercial media, buffer, and kits .....	30
2.1.2 Chemokines and enzymes.....	32
2.1.3 Antibodies and cell dyes .....	33
2.1.4 Primers, plasmids, siRNA and gRNA .....	35
2.1.5 Prepared buffers, media and solutions .....	37
2.1.6 Cells and tissue material.....	38
2.1.7 Devices and Software .....	39
2.2 Methods .....	40
2.2.1 Cloning of expression vectors.....	40
2.2.2 Eukaryotic cell isolation, cultivation and differentiation.....	42
2.2.3 Antibody staining for flow cytometer analysis .....	43
2.2.4 Knockdown (KD) generation in 293T cells.....	43
2.2.5 Expression plasmid nucleofection in primary CD4 T cells .....	44
2.2.6 Knockout generation in primary CD4 T cells and monocytic cells.....	44
2.2.7 <i>In vitro</i> trogocytosis and functional assays .....	44
2.2.8 Flow cytometric sorting of cell trace positive cells after co-culture .....	47

2.2.9	Immunoblot Analysis of Vps4 expression .....	47
2.2.10	Viral assays .....	48
<b>3.</b>	<b>Results .....</b>	<b>51</b>
3.1	CD32 exposure on CD4 T cells is cell-contact dependent .....	51
3.2	Investigating CD32 as mediator of trogocytosis .....	55
3.2.1	Testing CD32 genes .....	55
3.2.2	Autoantibodies can mediate trogocytosis enhancement .....	56
3.2.3	Trogocytosis enhancement with the bNAb PGT151 .....	58
3.2.4	Knockdown of ESCRT protein Vps4 in CD32B-expressing cells .....	61
3.3	Fcy-mediated trogocytosis in primary cell co-cultures .....	62
3.3.1	Comprehensive screening of receptor transfer.....	63
3.3.2	CD32 transfer to CD4 T cells is enhanced by autoreactive antibody binding and close cell-cell contact .....	65
3.4	HIV-1 exploits CD32-driven trogocytosis to infect resting CD4 T cells .....	67
3.4.1	Increased HIV-1 fusion to and infection of CD4 T cells after co-culture .....	67
3.4.2	HIV-1 attachment to CD4 T cells is increased following M2 co-culture .....	69
3.5	Deciphering factors involved in enhanced HIV-1 binding to CD32-positive CD4 T cells .....	70
3.5.1	Ablated co-transfer of DC-SIGN does not reduce HIV-1 fusion in co-cultured CD4 T cells .....	71
3.5.2	Macrophage mannose receptor is dispensable for HIV-1 attachment to co-cultured CD32-positive CD4 T cells .....	73
3.5.3	Heparinase and chondroitinase digestion does not reduce HIV-1 binding to CD32-positive CD4 T cells .....	75
3.5.4	Increased HIV-1 binding to transferred membrane patches can be blocked by anti-CD4 antibodies and is mainly Env-dependent.....	76
3.5.5	CD4 expressed <i>de novo</i> by T cells, but not by M2 macrophages, affects HIV-1 viral binding to CD32-positive membrane patches on T cells. ....	79
<b>4.</b>	<b>Discussion .....</b>	<b>84</b>
4.1	CD32 is transferred to CD4 T cells from CD32-expressing cells in a cell contact-dependent manner.....	84
4.2	CD32B is a strong driver of trogocytosis, which can be enhanced by autoantibodies .....	85
4.3	Receptors transferred to CD4 T cells are functional.....	88
4.4	HIV-1 binding, fusion and infection is increased after FcyR-mediated trogocytosis on CD4 T cells .....	90
4.5	HIV-1 binding myeloid C-type lectins receptors and $\beta$ 2-integrin are transferred to CD4 T cells but do not induce FcyR-mediated enhanced HIV-1 binding .....	91
4.6	Heparan sulfate and chondroitin sulfate from CD4 T cells are not responsible for the increased HIV-1 binding.....	93
4.7	M2-derived membrane patches transferred on CD4 T cells recruit endogenous CD4 and create an HIV-1 binding hot spot .....	94
4.8	Outlook.....	96
<b>5.</b>	<b>References.....</b>	<b>98</b>
<b>6.</b>	<b>Supplemental data .....</b>	<b>123</b>
	<b>Acknowledgement.....</b>	<b>134</b>

---

<b>Affidavit .....</b>	<b>135</b>
<b>Confirmation of congruency .....</b>	<b>136</b>
<b>Curriculum vitae .....</b>	<b>Fehler! Textmarke nicht definiert.</b>
<b>List of publications .....</b>	<b>137</b>

## Abstract

The current treatment of HIV-1-infected patients relies on life-long antiretroviral therapy (ART) that can suppress virus replication, but not eradicate the pathogen. The persistence of latent and ART-resistant viral reservoirs, particularly in resting CD4 T cells, remains the major barrier to HIV cure. The current limitation of strategies aiming at reversal of HIV latency or killing of infected cells in a clinical setting, in part results from a lack of biomarkers that are selectively exposed on latently HIV-1-infected, resting CD4 T cells. This knowledge could facilitate the selective elimination of the viral reservoir in infected individuals. Several candidate biomarkers were recently proposed, including the Fcγ receptor (FcγR)-IIa (CD32a), but its role has remained controversial. Here we show, that the FcγR CD32 (FcγRII) is not expressed *de novo* by HIV-1-infected CD4 T cells, but acquired from CD32-positive cells such as macrophages under conditions of close cell-to-cell contact. This cell communication process is referred to as FcγR-mediated trogocytosis. To study it, we established a cell line-based FcγR-mediated trogocytosis model. Here, we tested the functionality and auto-transfer of three isoforms of CD32, i.e. CD32A, B and C, as well as a panel of CD32A and B mutants. This revealed that CD32 drives the transient, cell contact-dependent transfer of itself, but also the co-transfer of other cell surface receptors (CD32B>CD32C≥CD32A) including chemokine coreceptors for HIV-1. Additionally, we explored the role of antibodies in modulating CD32-mediated trogocytosis. We found that the HIV-1 broadly neutralizing antibody (bNAb) PGT151 is autoreactive to CD4 T cells and thereby enhances trogocytosis. Intriguingly, also a subset of patients with chronic HIV-1 infection harbors T cell-reactive IgG autoantibodies with this capacity in their blood. Moreover, in co-cultures of primary macrophages with primary CD4 T cells we detected the transfer of CD32 as well as the co-transfer of a number of other receptors from the plasma membrane of macrophages to that of T cells. Transferred receptors were able to confer cell migration and adhesion properties to recipient cells. By confocal microscopy we were able to visualize transferred receptors on T cells within distinct membrane patches, which originated from the donor cells. Importantly, these macrophage-derived membrane patches served as hotspots for binding and fusion of HIV-1 particles and rendered resting CD4 T cells susceptible to infection.

In order to further elucidate mechanisms that may be directly involved in preferential HIV-1 binding to membrane patches transferred by trogocytosis we investigated a set of receptors, previously implicated in HIV-1 binding to macrophages. While being able to detect the co-transfer of such HIV-1 binding receptors, including DC-SIGN, CD206 and CD11a/b/c, we excluded their functional contribution in this process using highly efficient knockout approaches in donor macrophages. Unexpectedly, we observed that CD4 endogenously expressed by T cells aggregated within transferred CD32<sup>+</sup> ganglioside GM1<sup>+</sup> membrane patches. Based on gene perturbation and antibody inhibition studies, we show that the recruited CD4 is an important factor for preferential virion binding and fusion at these hotspots, resulting in increased infection of these viral reservoir cells.

Taken together, the antibody-enhanced, CD32-driven trogocytotic transfer of membrane patches containing a number of surface receptors can change the proteomic and functional plasticity of primary CD4 T cells. On a more general level, FcγR-mediated trogocytosis should be taken into account when investigating primary immune cells in co-culture and analyzing the expression and functionality of cell surface markers untypical for the respective cell lineage. Even though we can exclude CD32 as a bona fide biomarker for latently HIV-1-infected cells, the discovery of FcγR-driven trogocytosis which enhances the HIV-1 infection rate of resting CD4 T cells is important as this process may contribute to seeding and expansion of the latent reservoir in patients.

## List of figures

Figure 1   Schematic overview of a mature HIV-1 particle. ....	13
Figure 2   Scheme of the complete double stranded HIV-1 DNA encoding the viral proteins, flanked by the LTRs.....	15
Figure 3   Properties of the receptor family FcγR. ....	21
Figure 4   Schematic figure of CD32A, CD32B and CD32C with indicated important amino acids and motifs.....	22
Figure 5   Schematic overview of potential trogocytosis inducing immune cell contacts. ...	28
Figure 6   CD32 exposure on CD4 T cells is independent of infection or activation status, but influenced by the presence of co-cultured cells .....	51
Figure 7   Co-culture with myeloid cells in direct cell contact leads to exposure of CD32 and HLA-DR on CD4 T cells .....	53
Figure 8   HLA-DR and CD32B double-positive CD4 T cells after co-culture with M2 macrophages.....	54
Figure 9   <i>In vitro</i> model to investigate FcγR-mediated trogocytosis.....	55
Figure 10   FcγRs mediate the transfer of CCR5 and CD4. ....	56
Figure 11   CD32 transfer is enhanced by T-cell-autoreactive antibodies frequently seen in chronic infected HIV-1 patients.....	57
Figure 12   Co-transfer of different receptors is promoted by bNAb PGT151 binding to the glycosylated Fc-binding part of CD32. ....	59
Figure 13   CD32 mediates transfer of plasma membrane-associated receptors. ....	60
Figure 14   PGT151 is trapped by hCMV gp34 and gp68, diminishing the bNAb trogocytosis-enhancing effect.....	61
Figure 15   Knockdown of Vps4 in donor cells does not impact CD32B transfer to recipient cell. ....	62
Figure 16   Primary cell <i>in vitro</i> trogocytosis model with CD4 T cells and M2 macrophages. ....	63
Figure 17   A number of receptors is transferred from M2 macrophages to CD4 T cells. ...	64
Figure 18   Transferred receptors remain functional on CD4 T cells. ....	65
Figure 19   CD4 T cell binding antibody Alemtuzumab can enhance receptor transfer from M2 cells to CD4 T cells.....	66
Figure 20   Increased rate of CD32-positive CD4 T cells originating from lymphatic tissue culture.....	67
Figure 21   CD32-mediated trogocytosis enhances HIV-1 fusion to CD4 T cells and can be further enhanced by addition of a T cell-binding antibody (Alemtuzumab).....	68
Figure 22   Productive HIV-1 infection is enhanced in CD4 T cells following M2 co-culture. ....	69
Figure 23   Increased binding of HIV-1 to CD32-positive membrane patches on CD4 T cells after M2 co-culture. ....	70
Figure 24   Functional investigation of potentially trogocytosed HIV-1-binding receptors by gene KO in M2 macrophages.....	71
Figure 25   Knockout of DC-SIGN in macrophages does not impact HIV-1 fusion to co-cultured CD32-positive CD4 T cells. ....	72
Figure 26   Knockout of CD206 in macrophages does not impact HIV-1 attachment to co-cultured CD32-positive CD4 T cells. ....	73
Figure 27   Knockout of CD11a/b/c in macrophages does not impact HIV-1 attachment to co-cultured CD32-positive CD4 T cells. ....	74
Figure 28   HS and Ch digestion can reduce HIV-1 binding to HeLa cells, but not to CD32-positive CD4 T cells.....	75
Figure 29   Blocking a selection of highly transferred surface receptors marginally decreases HIV-1 binding to CD32-positive CD4 T cells.....	76
Figure 30   Addition of anti-CD4 antibodies reduces HIV-1 binding to CD32-positive cells to levels found for CD32-negative cells.....	78

Figure 31   Inoculation with HIV-1 $\Delta$ Env particles reduces HIV-1 binding to CD32-positive T cells to levels found for CD32-negative T cells. ....	79
Figure 32   Absence of CD4 on M2 macrophages does not reduce the binding of HIV-1 to CD32-positive T cells.....	80
Figure 33   Abolishing CD4 expression in T cells reduces HIV-1 binding to the CD32-positive T cell population. ....	81
Figure 34   Aggregation of CD4 at CD32-positive transferred membrane patches promotes HIV-1 binding. ....	82
Figure 35   Trogocytosed membrane patches with increased HIV-1 binding are positive for CD32 and the typical constituent of lipid rafts, GM1. ....	83
Figure 36   CD32-mediated trogocytosis is supplying CD4 T cells with macrophage-like migration behavior. ....	90
Figure 37   Scheme of mechanistic model for Fc $\gamma$ R-mediated enhanced HIV-1 infection. ..	96
Supplemental figure 1   CCR5 transfer is enhanced by T-cell-autoreactive antibodies frequently seen in chronic infected HIV-1 patients. ....	123
Supplemental figure 2   Gating strategy for identification of CD32+ CD4 T cells in PBMCs. ....	124
Supplemental figure 3   Transfer of CD32 isoforms and mutants promoted by bNAbs PGT151 .....	125
Supplemental figure 4   CD32 mediates transfer of plasma membrane-associated receptors.....	125
Supplemental figure 5   Knockdown of Vps4 in 293T monitored overtime. ....	126
Supplemental figure 6   Knockdown of Vps4 in donor cells does not impact CD32B transfer to recipient cell (full immunoblot). ....	126
Supplemental figure 7   Knockout confirmation of CXCR4 in CD4 T cells and transfer of CXCR4 and CCR5 to CD4 T cells. ....	132
Supplemental figure 8   Expression levels of CD32 on CD4 T cells 24 h post nucleofection with expression vector. ....	133
Supplemental figure 9   Flow cytometric staining for heparan sulfate on HeLa cells and CD4 T cells. ....	133

## List of tables

Table 1   Reaction mix for restriction digest of pCMV-CD32B WT-mtagBFP with <i>EcoI</i> and <i>AgeI</i> -HF. ....	40
Table 2   List of corresponding insert sequence, size and the original plasmid. ....	41
Table 3   Ligation reaction of insert and backbone. ....	41
Table 4   SG-PERT reaction steps.....	49
Supplemental table 1   Surface receptor screening on M2 macrophages and autologous CD4 T cells, either co-cultured with M2 cells or kept alone for 48 h (antibodies screening panel of the BD Lyoplate™).....	127

## List of abbreviations

ADCC	antibody dependent cell-mediated cytotoxicity
AHI	acute HIV-1 infection
AIDS	acquired immunodeficiency syndrome
APC	antigen presenting cells
ART	antiretroviral therapy
BCA	bicinchoninic acid
BCR	B cell receptor
BlaM	beta-lactamase
bNAbs	broadly neutralizing antibodies
BSA	bovine serum Albumin
BTK	Bruton's tyrosine kinase
CA	capsid protein
CG	cryoglobulinemia
Ch	chondroitin sulfate
CHI	chronic HIV infection
CHR	C-terminal heptad repeat
CPSF4	cleavage and polyadenylation specificity factor 6
CR3	complement receptor 3
CRP	C-reactive protein
CT	cytoplasmic tail
CT-B	Cholera toxin subunit-B
CTLA-4	cytotoxic T-lymphocyte-associated protein 4
DCs	dendritic cells
DC-SIGN	Dendritic Cell-Specific Intercellular adhesion molecule-3-Grabbing Non-integrin
DENV	dengue virus
dsDNA	double stranded DNA
EBV	Epstein-Barr virus
EC	<i>Echinococcus multilocularis</i>
EDTA	Ethylenediaminetetraacetic acid disodiumsalt-dihydrate
EGFR	epidermal-growth-factor-receptor
env	envelope glycoprotein
ER	endoplasmic reticulum
ESCRT	endosomal sorting complexes required for transport
FBS	Fetal bovine serum
FCS	Fetal calf serum
FcyR	Fcy Receptor
FMO	fluorescence minus one
FP	fusion peptide
FPPR	fusion peptide proximal region
gag	group-specific antigen
GFP	green fluorescent protein
GM1	monosialotetrahexosylganglioside 1
gp	glycoprotein
GPI	glycosylphosphatidylinositol
H2B	histone protein 2B
HAART	highly active ART
hCMV	human cytomegalovirus

---

HCV	hepatitis C virus
HD	healthy donor
HDAC2	Histone Deacetylase 2
HIV	human immunodeficiency virus
HLAC	human lymphoid aggregate culture
HMG1	high mobility group-1
HPV	human papilloma virus
HSPG	heparan sulfate proteoglycan
HSV-1	herpes simplex virus-1
HSV-1	heparan sulfate
HTLV	T-lymphotropic leukemia virus
ICOSL	inducible T cell costimulatory ligand
IFITM1	interferon-induced transmembrane protein 1
IFN- $\gamma$	Interferon- $\gamma$
IL	Interleukin
imIgG	immobilized IgGs
IN	integrase
ITAM	immunoreceptor tyrosine-based activation motif
ITIM	immunoreceptor tyrosine-based inhibition motif
ITP	Idiopathic Thrombocytopenic Purpura
KD	knockdown
KO	knockout
LAG-3	lymphocyte activation gene 3
LB	lysogenic broth
LC-MS/MS	liquid chromatography with tandem mass spectrometry
LEDGF	Lens epithelium–derived growth factor
LPA	latency promoting agents
LPAC	lamina propria lymphocyte culture
LPS	Lipopolysaccharides
LRA	latency reversal agents
LTR	long terminal repeats
MA	matrix protein
mAb	monoclonal antibody
M-CSF	macrophage colony-stimulating factor
MDC	monocyte-derived cytokine
MDM	monocyte-derived macrophage
MFI	mean fluorescence intensity
MMR	macrophage mannose receptor
moDC	monocyte-derived dendritic cells
MOI	multiplicity of infection
MPER	membrane-proximal external region
MS	multiple sclerosis
nef	negative factor
NET	neutrophil extracellular traps
NFAT	nuclear factor of activated T-cells
NF $\kappa$ B	Nuclear Factor kappa B
NHR	N-terminal heptad repeat
NK	Natural Killer cell
NTC	non-targeting control

---

PBMC	peripheral blood mononuclear cells
pbs	primer binding site
PBS	phosphate buffered saline
PD-1	programmed cell death-1
PEI	polyethylenimine
PHA	Phytohemagglutinin from <i>Phaseolus vulgaris</i>
PI3K	Phosphatidylinositol-3 Kinase
PKC	Protein Kinase C
PLCy	phospholipase Cy
pol	polymerase
PR	protease
PTEFb	positive transcription elongation factor b
RA	rheumatoid arthritis
RANTES	regulated upon activation, normal T Cell expressed and presumably secreted
rev	regulator of virus protein expression
RNP	ribonucleoprotein
RT	reverse transcriptase
RT	room temperature
SAMHD1	Sterile Alpha Motif and Histidine-aspartic acid Domain containing protein 1
SAP	serum amyloid P component
SCH	<i>Schistosoma spp</i>
SDF-1 $\alpha$	Stromal cell-derived factor 1
SG-PERT	SYBR green I-based PCR-enhanced reverse transcriptase assays assay
SHIP	SH2 domain inositol 5'-phosphatase
SIV	simian immunodeficiency virus
SLE	systemic lupus erythematosus
SNP	single nucleotide polymorphism
ssRNA	single stranded RNA
SU	surface unit
SYK	spleen tyrosine kinase
tat	transcriptional transactivator
TB	terrific broth
TB	<i>Mycobacterium tuberculosis</i>
TBS	Tris buffered saline
TCR	T cell receptor
TD	transmembrane domain
TIGIT	T cell immunoreceptor with Ig and ITIM domains
TIM-3	T cell immunoglobulin and mucin 3
TM	transmembrane domains
Tris	Tris(hydroxymethyl) aminomethane
U3	upstream region sequences of the ssRNA 3'
U5	upstream region sequences of the ssRNA 5'
vFcyR	viral FcyR
vif	virion infectivity factor
vpr	viral protein R
vpu	viral protein U
vpx	viral protein X
VSG-G	vesicular stomatitis virus G glycoprotein
WT	wild type

YFV            yellow fever virus

# 1. Introduction

## 1.1 HIV-1 and CD4 T cells

### 1.1.1 HIV structure and composition

The human immunodeficiency virus (HIV) was identified in the early 1980s [1, 2] and most likely evolved from a zoonotic transmission of simian immunodeficiency virus (SIV) from chimpanzees to humans at the beginning of the 1920s [3, 4]. Untreated infection leads to acquired immunodeficiency syndrome (AIDS). So far, two types of HIV have been identified, the more abundant type 1 (HIV-1) and the globally less prevalent type 2 (HIV-2) [5]. HIV is a lentivirus and belongs to the family of *retroviridae* with two single stranded RNA copies (ssRNA). Its genome encodes for the group-specific antigen (*gag*), the polymerase (*pol*) and the envelope glycoprotein (*env*). The viral genome also encodes for viral regulatory and accessory proteins such as transcriptional transactivator (*tat*), regulator of virus protein expression (*rev*), viral protein R, U and X (*vpr*, *vpu*, *vpx*), negative factor (*nef*), and virion infectivity factor (*vif*) [6]. Whereas the regulatory proteins Tat and Rev have been reported to be essential for efficient viral replication [7, 8], Vpu and Vif have been reported to enhance infection and Vpx is only found in HIV-2 and among some SIV strains [6, 9]. The retroviral *gag* gene is transcribed as a polyprotein (55 kDa) and later on processed by the viral protease to the viral matrix protein MA (p17), capsid protein CA (p24), the nucleocapsid NC (p7) as well as smaller proteins p1, p2 and p6 [9] with the capsid protein p24 as well as the nucleocapsid p7 are representing half of the mass of the viral particle [10]. The *pol* gene codes for highly conserved enzymatically active proteins: the reverse transcriptase (RT), the integrase (IN), and the protease (PR). The viral *env* gene encodes the glycosylated precursor protein gp160, which is enzymatically cleaved into two parts: the surface (SU, gp120) and the transmembrane domains (TM, gp41) which are later non-covalently bound as heterodimer, with three heterodimers forming the Env protein on the surface of the viral membrane [11, 12].

In the mature virion, the viral genome is protected by the viral core, which itself is surrounded by a lipid bilayer originating from the virus-releasing cell. The lipid membrane is spiked with 8-10 trimeric Env complexes, depending on the virus strain [13-15] (see Figure 1).

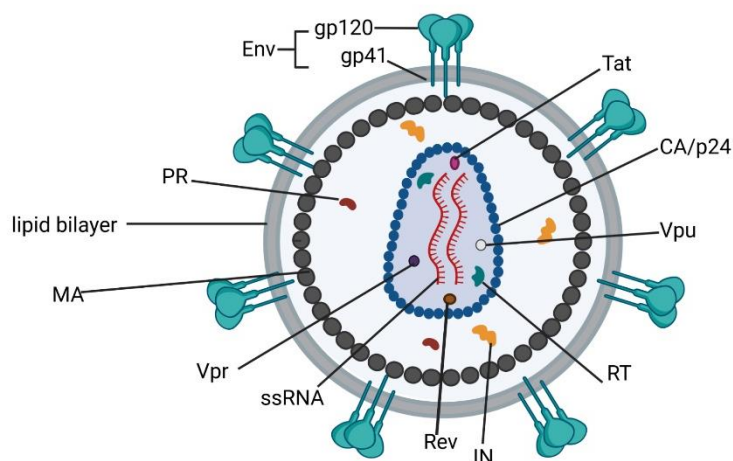


**Figure 1 | Schematic overview of a mature HIV-1 particle.**

A mature HIV particle consists of different viral proteins as well as parts originating from the host cell. The particle is surrounded by a lipid bilayer spiked with envelope protein (env; gp120/gp41), followed by viral matrix proteins (MA). Inside the particle, the viral reverse transcriptase (RT), viral integrase (IN), viral protease (PR) as well as viral regulatory and accessory proteins can be found such as the transcriptional transactivator (Tat), the regulator of virus protein expression (Rev), viral protein R (Vpr) and viral protein U (Vpu). The viral genome consists of two identical ssRNAs which are protected by the viral core formed by capsid/p24 proteins (CA/p24). Schematic created with BioRender.com and adapted from Chen *et al.* [16].

### 1.1.2 HIV-1 fusion mediated by its envelope glycoproteins

HIV fusion occurs between the viral membrane and the cytosolic membrane of the target cell. The two membranes have to come in close proximity and overcome kinetic barriers, such as hydration forces [17, 18]. The viral envelope glycoproteins gp120 and gp41 are the key proteins of the virus for a successful binding and fusion. The surface protein gp120 contains several important binding domains, such as the binding site for the entry receptor CD4 (CD4bs), the co-receptor binding site (revealed upon binding to CD4bs), as well as the site for non-covalent binding to the transmembrane part gp41. The protein sequence of gp120 can be divided into five variable regions (V1-V5), and five conserved regions (C1-C5) [19-21]. The co-receptor binding domain is found on the variable loop V3 and has been reported to play an important role for the viral tropism switch [22, 23] and prediction of the tropism in diagnostics [24, 25]. The tropism is defined by the usage of either the chemokine receptor CCR5 (R5-tropic virus, R5 virus) or CXCR4 (X4-tropic virus, X4 virus) as co-receptor [20, 26]. In the early stage of viral transmission mostly R5 viruses are observed, whereas in later disease stages a switch to X4 or dual-tropic R5/X4 viruses can be found in some patients [27, 28].

The transmembrane protein gp41 is the anchor that places trimers of gp120/gp41 within the viral membrane and induces the membrane fusion later on [29]. Without the specific binding of Env to CD4, no productive infection will occur. Nevertheless, the following cell surface proteins and charged molecules can bind Env and attach the virus to the cell surface, which can play an additional role for cell-to-cell transmission and/or transcytosis through epithelia barriers:

Macrophage Mannose receptors (MMR) [30, 31], Dendritic Cell-Specific Intercellular adhesion molecule-3-Grabbing Non-integrin (DC-SIGN, CD209) [32, 33], glycolipids [34], heparan sulfate [35, 36],  $\alpha 4\beta 7$ -integrin [37, 38], complement receptor 3 (CR3, CD11b/CD18) [39, 40].

gp41 can be divided into three domains: the ectodomain, the transmembrane domain (TD) and the cytoplasmic tail (CT). Upon CD4 and co-receptor binding, gp41 undergoes complex conformational changes to induce viral fusion. The ectodomain part of gp41 mediates the fusion and is composed of five parts: the fusion peptide (FP) with fusion peptide proximal region (FPPR), the N-terminal heptad repeat (NHR), the loop regional the C-terminal heptad repeat (CHR) and the membrane-proximal external region (MPER) [21, 41].

It is proposed that upon the conformational change FP functions as injecting domain by inserting into the host cell membrane [21]. This then also induces the formation of the six-helix bundle (6HB), built by the NHR and CHR of the gp41 trimer, and the so-called viral fusion pore [42, 43]. Even though this was already observed in the late 1990's, there are still some steps of viral entry not fully understood. It had been proposed that cellular components are also needed for the formation of the fusion pore, e.g. triggering of actin dynamics and/or signals triggering through co-receptor dependent signalling [44, 45]. The specific site of fusion on the host cell membrane may also impact fusion and productive infection. Yang *et al.* [46, 47] have shown preferred binding of HIV at lipid membrane domains in the transition from ordered to disordered sites. They suggested a potential lowering tension between the viral and the cellular membrane at these sites [46, 47].

Beside the region of fusion also the location where final fusion occurs is under discussion. Here, Miyauchi *et al.* [48] proposed the fusion pore opening and release of the virus to be endosomal which was supported also by previous and subsequent observations [49-51]. However, controversial findings are still challenging these observations [52] keeping the debate up whether fusion occurs preferentially at the plasma membrane or in endosomes, depending on cell type with different outcomes on productive infection [53-56].

### 1.1.3 After HIV enters the cell: from reverse transcriptase to viral release

After entry, HIV wants to integrate its genomic information into the host cells chromatin. Yet, in order to achieve this, the ssRNA has to be transcribed into complementary DNA and this DNA has to find its way to the host chromatin. Since HIV-1 can infect non-dividing cells, the preintegration complex has to enter the intact nucleus to get in close proximity to chromatin. With the fusion into the host cell, the virus releases its viral core into the cell, but here the following steps have been controversially discussed in the HIV research field. Different options of how and when the viral capsid is uncoated have been proposed by different groups:

**Option A:** Uncoating of the viral core occurs early after virus entry in the cytoplasm and before reverse transcription of the viral genome [57-59].

**Option B:** Uncoating happens during the transport from the cytosol to or directly in the nucleus with the reverse transcription reaction simultaneously already ongoing [60-62].

**Option C:** The intact capsid core is transported through the nuclear pore into the nucleus, where reverse transcription is completed and integration of the proviral DNA occurs.

For a long time, this last option was questioned since the nuclear pore size was expected to be small and therefore excluding the transit of the viral core. Nevertheless, improved electron microscopy-based and ultra-resolution microscopy studies were able to visualize the transport of intact capsid cores [63-65].

The current knowledge is therefore that after fusion the capsid traffics along microtubules towards the nucleus. Here, it enters through the nuclear pore, which is mediated by nuclear pore proteins and the cleavage and polyadenylation specificity factor (CPSF6) protein. The capsid is then

coated by CPSF6 molecules and directed to the site of integration where reverse transcription occurs with subsequent uncoating of the capsid, the release of the cDNA and integration into the host genome [66]. Completion of uncoating and reverse transcription apparently happens simultaneously within the nucleus, which has been also verified by other research groups [67, 68].

In order to perform reverse transcription of its ssRNA, the HIV-1 particle carries its own RNA-dependent DNA polymerase with RNAase H activity, also termed reverse transcriptase (RT). The RT uses the viral ssRNA as template but needs primers for initiation. Here, HIV has incorporated tRNA LysA from its former host cell, which binds at the primer binding site (pbs) of the viral RNA. The pbs is located around 180 nucleotides from the 5'-ssRNA end. On both ends of the viral RNA are direct repeats (3'-R and 5'-R). Since the polymerase reaction starts to create a plus strand DNA by amplifying in the direction of the 5'-end of the ssRNA, only a short part of the viral ssRNA 5'-end including the 5'-R is transcribed at first. The two RNA R sequences then function as bridges between each other, and the DNA amplification then continues at the 3'-end of the RNA to fulfil the transcription of the complete RNA sequences until it reaches again the pbs site (its initial starting point). After amplification of the 3'-5'-complementary DNA (here starting the amplification from the U3 site of the complementary strand) complementary double stranded DNA (dsDNA or cDNA) is complete (see Figure 2).

As a consequence of the bridging of the 5'- and 3'-end during amplification the proviral DNA has on each end parts complementary to the ssRNA ends and is therefore longer than the ssRNA. The 5'-R and the 3'-R are connected to a long terminal repeats (LTR) sequence each flanked by upstream region sequences of the ssRNA 3'-end (U3) and the upstream 5'-ssRNA end (U5). All viral genes are encoded on the viral DNA in-between the two LTR regions [66].

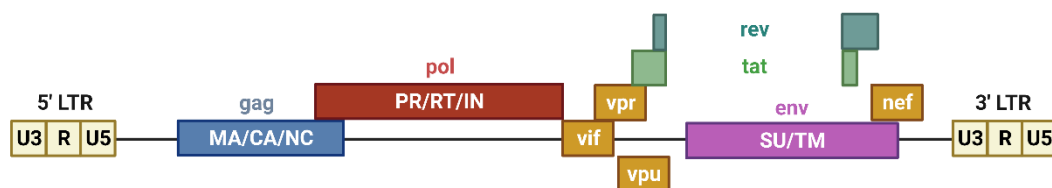


**Figure 2 | Scheme of the complete double stranded HIV-1 DNA encoding the viral proteins, flanked by the LTRs.**

Schematic overview of the proviral DNA with the indicated open reading frames of the viral proteins. The following genomic elements are indicated: *gag* encodes CA, MA, NC. *pol* encodes RT, IN and PR; *env* encodes SU and TM. Different open reading frames encode the viral accessory proteins: *tat*, *rev*, *vpr*, *vpu*, *nef*, and *vif*. All genes are flanked by two long terminal repeats (LTR) on both ends of the DNA [66]. Schematic created by BioRender.com

Integration of the complete proviral DNA into the host genome is mediated by another viral enzyme, the integrase (IN). At the site of integration, IN removes two nucleotides at the 3'-ends of both proviral DNA strands as well as at the host DNA. The corresponding free hydroxyl groups can therefore attack the phosphodiester bonds at the host DNA followed by ligation of the viral DNA into the host DNA. The cellular host repair system then fills in the missing nucleotides at both ends [69]. The proviral DNA preferred integration target site is most likely not highly sequence-specific, however, it has been suggested that HIV preferentially integrates at transcriptional active sites (known as speckles-associated domains) and disfavours sites close to the nuclear lamina [69]. To coordinate the guiding of the pre-integration complex to the integration sites, the virus hijacks different host proteins, such as highly-conserved nucleoproteins comprising the high mobility group-1 (HMG1) [70, 71] or Lens epithelium-derived growth factor (LEDGF/p75) [72-74]. After integration, HIV replication can either remain in a latent state or induce productive replication, resulting in the release of new viral particles [75]. For the production of viral particles,

the integrated proviral DNA is transcribed into viral unspliced RNA or up to 40 different splice variants of viral mRNA due to the different potential frameshift in the sequence. Early phase proteins translated are Tat, Rev and Nef, with Tat and Rev controlling the gene expression of the late phase proteins such as structural proteins (Gag, Pol and Env) and accessory proteins e.g. Vpr [76]. The viral Gag and GagPol polyproteins are transported to the plasma membrane and genomic viral RNAs are recruited by Gag and incorporated during assembly of the virions. The viral envelope proteins, synthesized at the rough endoplasmic reticulum (ER), are transported to the plasma membrane via the secretory pathway. At the plasma membrane, the Env complexes are incorporated into the lipid membrane of the budding virions. To facilitate the release of the viral particle, the host cell endosomal sorting complexes required for transport (ESCRT) machinery is recruited to the assembly site. After release from the plasma membrane, maturation of the viral particle into a conical shaped viral core is catalysed by the viral protease [77].

#### **1.1.4 HIV-1 latency and restriction in CD4 T cells**

HIV latency is until now the main limiting factor to cure from HIV infection. Even life-long anti-retroviral therapy (ART) does not eradicate latently infected cells, which means that the virus can rebound within weeks upon ART disruption [78, 79]. The mechanisms leading to latent infection still remain elusive. First of all, studies investigating the HIV integration site in latently infected resting CD4 T cells of HIV patients under highly active ART (HAART) have demonstrated that the integration target sites are within actively transcribing genes [80] with favourably integration in gene regions with histone modification of active chromatin and a nuclear topography close to nuclear speckles [81, 82]. Later on, the in-line expression of proviral DNA to the host gene expression direction was observed to potentially influence, whether the virus undergoes latency [80, 83, 84]. Additional insight into latency control has been provided by a screening study of integration sites in HIV elite controllers. In these patients, integration is increased within densely packed chromatin, suggesting a state of deep latency that suppresses reactivation of the virus [85]. Besides the modification of histones [86, 87] methylation of CpG islands flanking the transcription start of the integrated proviral genes may induce latency. Methylation of CpG island leads to the binding of Histone Deacetylase 2 (HDAC2) resulting in blocking the binding of transcription factor Nuclear Factor kappa B (NFκB) [88, 89].

##### **Resting CD4 T cells as HIV reservoir**

Already in early studies focusing on the HIV reservoir, the resting CD4 T cell population has been in the focus and defined as the main cellular reservoir [90-92]. In contrast to activated CD4 T cells, HIV-1 encounters many restrictions and replication barriers in resting CD4 T cells. The lower expression levels of the co-receptor CCR5 [93], but also a barrier induced by the cortical actin meshwork have been discussed to limit viral entry and viral trafficking in resting CD4 T cells [94, 95]. In addition, reverse transcription is limited due to the activity of Sterile Alpha Motif and Histidine-Aspartic acid domain containing protein 1 (SAMHD1) [96, 97]. This restriction has also been described to be highly effective in restricting HIV-1 infection in dendritic cells and myeloid cells [98, 99]. HIV-2 and some SIV strains can overcome this restriction by means of the viral protein Vpx, which induces proteasomal degradation of SAMHD1 [100]. Even if integration is completed, up to 90% of the integrated proviral sequences in resting CD4 T cells of cART-treated chronic HIV patients (CHI) are observed to be defective [101]. Even though all these restrictions are present in resting CD4 T cells, these cells represent the major HIV reservoir and explanation for this is still ongoing. However, different reasons may account for this phenomenon. First, previously activated memory CD4 T cells would return to a resting state to survive the infection. Previous

studies support this hypothesis by showing that activated T cells could be reprogrammed to a resting state, inducing thereby latency [102]. Immune regulatory mechanisms, such as cytokines or checkpoint proteins, could further support the cells to return to a resting state [103, 104].

However, even though HIV-1 encounters many barriers and restrictions in resting CD4 T cells, some reports provide evidence that productive infection can occur in resting CD4 T cells, but to a slower extent [105, 106]. In these studies, however, spinoculation was performed to enhance HIV-1 infection, which potentially impacted actin dynamics resulting in a non-physiological state [94].

Second, resting CD4 T cells may formally not be “completely” resting when infected. Even though the cells show no signs of proliferation, they may acquire different states during cell cycle arrest. The cells within the G0/G1a phase have been categorized as “truly quiescent cells” and have also shown no increased levels of proviral DNA, in contrast to the subgroup of resting CD4 T cells in the G1b phase with higher levels of proviral DNA and viral RNA [107]. Furthermore, modulation of the actin cytoskeleton may enhance HIV infectivity when cytokines like Chemokine (C-C motif) ligand 19 (CCL19) and CCL20 are present [108]. In addition higher concentrations of Interleukin-7 (IL-7) can modulate SAMHD1 activity, which could reduce the HIV-restricting environment in resting CD4 T cells [109][110].

### **Reactivation of latency**

Upon stimulation, HIV can be reactivated from latently infected cells, to yield productive replication. Here, the 5'-LTR of the proviral DNA serves as a promotor [111]. Host transcription factors, such as NFκB or nuclear factor of activated T-cells (NFAT), are recruited from the cytosol, initializing viral gene expression by RNA Polymerase II. Upon expression of the regulatory Tat protein, it shuttles back into the nucleus and recruits the cellular transcription factor positive transcription elongation factor b (PTEFb) to boost viral transcription [112, 113].

### **“Shock and Kill” strategy**

Since latently infected cells hinder eradication of HIV in patients, novel concepts to clear the virus are currently being explored, such as one termed “shock and kill” [114]. Here, HIV-1 gene transcription is induced by strong CD4 T cell activation inducers (such as IL-2, TCR agonist and anti-CD3 antibody) to subsequently kill the virus [115]. However, the latency reversal reagents (LRA) globally activate T cells, inducing the expression of pro-inflammatory cytokines, resulting in cytotoxic effects *in vivo* [116]. Therefore, finding LRAs, that productively activate HIV-1 transcription but at the same time keep the activation of the CD4 T cell low, is key for success. Prominent first generation LRAs have targeted the chromatic organization in order to induce HIV proviral transcription, e.g. histone deacetylase (HDAC) inhibitors [117-119], HDACs in combination with a DNA methylation inhibitor [120], or bromodomain and extra terminal domain (BET) inhibitors [121-123]. Yet, *in vivo* studies have either still lacking [124], or have not shown a great impact on HIV reservoir site, yet [125, 126] with severe cytotoxic side effects [127, 128]. LRAs have further been tested to induce transcription factors by activating Protein Kinase C (PKC) [129, 130], but applied concentrations were low and no reduction of the latent reservoir was observed [131, 132].

### **“Block and Lock” strategy**

Beside the approach to eradicate HIV in infected individuals by “shock and kill”, a different approach is to block viral replication and at the same time to ensure maintenance of latency, referred to as “block and lock” [133]. The compounds used for this strategy are latency promoting agents (LPA), overall inducing opposite effects as LRAs, e.g. inhibition of viral transcription elongation [134, 135] or transcription factor recruitment [136], epigenetic remodelling of the chromatin to

generate an HIV promotor repressing environment [137] or recruiting HDACs and Histone methyl transferases [138]. Even though this method is not aimed at curing the patient from HIV, in contrast to the “shock and kill” strategy the success of “block and lock” is more independent from a patient’s functional immune system and therefore seen as advantage for treatment in patients with advanced stages of HIV infection [139]. In addition, “block and lock” may avoid some possible side effects of the “shock” in the central nervous system caused by the viral rebound [140]. A potential disadvantage is the open question whether the clearance of infected cells still appears in patients in the long run, once inflammation is suppressed by LPAs [141].

### 1.1.5 Potential biomarkers for HIV-1 latency in CD4 T cells

Surface markers on latently infected cells have been of high interest, since this could enable specific targeting and more directed killing of the reservoir cells during therapy. Different biomarkers for HIV-1 latency in CD4 T cells have been proposed with some of them highlighted below:

#### CD32a

In 2017, Descours, and Petitjean *et al.* [142] reported the identification of CD32a as a marker of the HIV reservoir in resting CD4 T cells. In this study, they infected PBMC cultures with HIV-1 GFP reporter viruses, 12 h after treatment with virus like particles carrying Vpx to overcome the SAMHD1 restriction. 4 days after infection, they sorted the infected CD4 T cells (CD4<sup>+</sup>/GFP<sup>+</sup>) and uninfected (CD4<sup>+</sup>/GFP<sup>-</sup>) population as well as non-infected controls with subsequent mRNA sequencing. They identified 103 genes being transcriptionally upregulated only in infected CD4 T cells, with CD32a showing the highest increase. They further validated CD32A expression by flow cytometry of HLA-DR/CD4<sup>+</sup> T cells (to ensure resting state of the cells) and observed a CD32A-positive CD4 T cell population in the blood of patients under ART. They further observed a correlation of CD32A expression with HIV proviral load in the cells. Overall, around 50% of the CD4 T cell HIV reservoir was reported to be CD32A-positive [142]. These observations sparked studies in many laboratories to investigate CD32A as a potential marker of latently HIV infection. Other reports have confirmed these findings [143] or have at least suggested a positive correlation of CD32 expression and HIV-1 DNA load in T cells [144-146]. Conversely, other studies did not find HIV-1 DNA enrichment in CD32<sup>+</sup>/CD4<sup>+</sup> T cells [147-150]. Whereas some studies have found CD32 expressed on HIV-infected, yet experienced activated CD4 T cells [144, 151, 152], others have shown CD32 to be most likely a marker for activation, independent of HIV infection [153]. In addition, one report found a similar frequency of CD32<sup>+</sup>/CD4<sup>+</sup> T cells in HIV-infected patients compared to healthy donors [148]. Notably, also the possibility of false positive results due to cell doublets (e.g. CD4 T cells/CD32<sup>+</sup> B cells) or even due to transfer of cell membrane fragments from CD32-expressing positive cells has been proposed [146, 150, 154]. It was also stated that experimental artefacts could have led to misleading observations e.g. detection of intact provirus should rather be performed by quantitative viral outgrowth assay (as described by Laird *et al.* [155]) then by performing p24 ELISA [148] and the antibody used in the study by Descours, and Petitjean *et al.* [142] was actually not specific for CD32A, but also recognize CD32B and CD32C [151].

#### CD30

Hogan *et al.* [156] have proposed CD30 as a marker of residual transcriptionally active HIV-1 in ART-treated individuals. With *in situ* RNA hybridization studies of gut-associated lymphoid tissue

(GALT) they observed a co-localization of CD30 and HIV transcriptional activity. Expression analysis of CD30 on CD4 T cells has also been detected in HIV-1 ART treated individuals compared to healthy donors. Furthermore, CD30-targeting brentuximab vedotin can apparently reduce the total HIV-1 proviral DNA load. In fact, HIV has not been detected in plasma and in purified CD4 T cells of one HIV patient with refractory lymphoma, who had previously been treated with brentuximab vedotin [156]. Co-expression of activation markers, such as HLA-DR or CD69, in a fraction of CD30-positive cells has been reported in addition to increased CD30 expression levels prior to viral rebound in two HIV-1 patients [157]. Yet, further investigations are necessary to define whether CD30 can be used as a marker of persistent HIV-1 infection, as a marker of reactivation, or simply as a marker of CD4 T cell activation, independent of HIV-1 infection.

### **CD98**

Zhang *et al.* [158] have suggested CD98 as a marker for both highly HIV-1-permissive as well as latently infected CD4 T cell populations. Using a liquid chromatography with tandem mass spectrometry (LC-MS/MS) screening of differentially expressed proteins in the latency infection model cell line J-Lat, they have identified more than 1200 differently expressed proteins, of which 126 proteins are plasma membrane proteins. In addition, upregulation for T cell immunoreceptor with Ig and ITIM domains (TIGIT) has been observed, which has previously been reported as a potential latency biomarker [159]. Yet, only for CD98 significant upregulation has been confirmed by RT-qPCR and further verified with other latency T cell lines such as J-d2E GFP and J-mc. Primary CD4 T cells derived from PBMC have further shown differential expression of CD98 in CD4 T cell populations. CD98<sup>high</sup> CD4 T cells have higher CCR5 and CXCR4 expression levels, potentially enhancing the likelihood of HIV entry. Next, CD98<sup>high</sup> CD4 T cells have also been found in PBMC from ART-treated HIV patients, demonstrating higher levels of latently integrated HIV proviruses [158]. Taken together, the results indicate a potential role of CD98 for HIV susceptibility and latency in cell lines but also primary CD4 T cells. However, CD98 is abundantly expressed on CD4 T cells in both healthy and HIV-1 patients, excluding a specific targeting.

### **Immune checkpoint molecules (PD-1, TIGIT, LAG-3)**

Factors suppressing CD4 T cell proliferation and activation may cause a favourable environment for HIV latency and may therefore serve as potential latency biomarkers [90, 160, 161]. In a flow cytometry-based screening approach using CD4 T cells from HIV-1 patients under ART, seven immune checkpoint molecules were analysed: PD-1 (programmed cell death-1), CTLA-4 (cytotoxic T-lymphocyte-associated protein 4), LAG-3 (lymphocyte activation gene 3), TIGIT (T-cell immunoglobulin and ITIM domain), TIM-3 (T cell immunoglobulin and mucin 3), CD160 and 2B4 (CD244). Enrichment in latently HIV-1-infected cells correlated with expression levels for three of the seven markers: TIGIT, PD-1 and LAG-3. An HIV reactivation experiment also verified high expression of at least one of the three markers [160]. Another HIV latency study in humanized mice has also shown a correlation of PD-1 and/or TIGIT expression with enrichment of latent HIV [159]. However, those markers are also found on other cells, such as CD8 T cells. Thus, targeting them may have unwanted impact on the immune system. In addition, it has been reported that a small subset of latently infected CD4 T cells are not positive for the marker [160], so a complete eradication of HIV may not be possible using these markers.

Besides the markers highlighted above a number of other markers have been proposed in the past, such as CD2 [162], interferon-induced transmembrane protein 1 (IFITM1) [163], and CD161 [164]. Still, exclusive expression on latently infected cells and/or reproducibility of such observations are lacking. Therefore, finding a specific “latency” marker is still of high interest for any targeted HIV cure strategy.

## 1.2 Function of Fcγ Receptors (FcγRs)

### 1.2.1 Genes and prevalence of FcγR

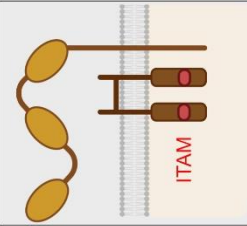
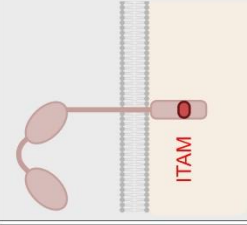
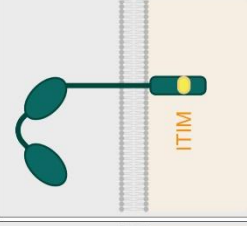
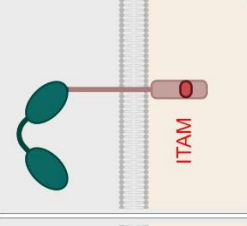
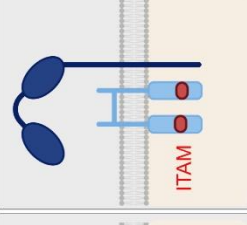
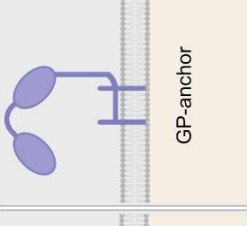
Different subclasses of Fcγ receptors (FcγRs) exist: CD64 (FcγRI), CD32A (FcγRIIA), CD32B (FcγRIIB), CD32C (FcγRIIC), CD16A (FcγRIIIA), and CD16B (FcγRIIIB). All receptors contain an IgG binding domain on their extracellular part, whereas the signal motif is on the intracellular part. FcγRs can be categorized into activating or inhibiting receptors, depending on whether the signal motif carries an immunoreceptor tyrosine-based activation motif (ITAM) or, in the case of CD32B, an immunoreceptor tyrosine-based inhibition motif (ITIM) motif, respectively. CD32 receptors have their signal motif on the same peptide chain as the IgG binding domain, whereas for CD64 and CD16A require an interaction with a separate intracellular transmembrane protein containing the signal motif [165, 166] (Figure 3). In contrast, CD16B does not contain a cytoplasmatic tail but is linked by a glycosylphosphatidylinositol (GPI) anchor into the membrane [166, 167]. The receptor subclasses and their different gene variants can also be classified according to their affinity to bind monomeric IgG with CD64 being classified as high affinity receptor and CD32A/B/C and CD16A/B as low or medium affinity receptors [166, 168]. The affinity is also dependent on the IgG subclasses with CD64 having the highest affinity for IgG1 and IgG3, whereas the other FcγRs not only show an up to 1000-fold lower affinity, but also a broader binding spectrum of IgG subclasses [166, 169, 170]. Upon binding of antibody-opsonized cells or immune complexes to FcγR, phosphorylation of the ITAM or ITIM motif is initiated.

#### ITAM-induced signalling pathway

Phosphorylation of the two tyrosine residues in the ITAM is catalysed by enzymes of the Src kinase family (e.g. Lyn) following recruitment of kinases belonging to the Spleen Tyrosine Kinase (SYK) family. The recruited SYK kinase activates Phosphatidylinositol-3 Kinase (PI3K), resulting in the recruitment of Brutons tyrosine kinase and phospholipase Cγ (PLCγ). This induces downstream signalling for Ca<sup>2+</sup> uptake, but also pathways for cell activation (e.g. ERK and JNK pathway). SYK also activates the Ras signalling pathways, which consequently also triggering cell activation pathways [168]. Selection of the Src kinases depends on the specific FcγR and cell type [171]. Induced signalling cascades lead to phagocytosis, cytokine production and/or antigen processing, depending on the cell type [166].

#### ITIM-induced signalling pathway

In contrast, initialization of the inhibitory ITIM motif has been described to interfere with the ITAM motif-induced pathway. This regulatory pathway is induced by simultaneous crosslinking of an ITAM and the ITIM carrying receptor with an immune complex. For ITIM signal induction, one tyrosine in the motif is phosphorylated by a member of the SRC kinase family [172]. This leads to the recruitment of SH2 domain inositol 5'-phosphatase (SHIP). SHIP activation then counteracts the BTK and PLC signalling pathways as well as inhibits Ras activation, overall muting the ITAM activating signal [173].

					
<b>CD64</b> (FcγRI)	<b>CD32A</b> (FcγRIIA)	<b>CD32B</b> (FcγRIIB)	<b>CD32C</b> (FcγRIIC)	<b>CD16A</b> (FcγRIIA)	<b>CD16B</b> (FcγRIIB)
activating	activating	inhibitory	activating	activating	activating?
high	low	low	low	low	low
7	2	3	3	5	6
	131H/R R: reduced affinity to IgG1/2/3	232T/I I: decreased inhibitory function	57 Q/X X: stop codon (non-functional)	158 F/V V: increased affinity to IgG1/3/4	
	IgG1>IgG3>IgG2=IgG4	IgG1=IgG3=IgG4>IgG2	IgG1=IgG3=IgG4>IgG2	IgG3>IgG1>>IgG4>IgG2	IgG3>IgG1
Dendritic cells Monocytes Macrophages Neutrophils Mast cells	Monocytes Macrophages Langerhans cells Neutrophils Eosinophils Basophils	B cells Monocytes Macrophage Neutrophils Eosinophils Basophils Mast cells	If functionally expressed found on NK cells and Macrophages	Monocytes Macrophage NK cells Mast cells	Neutrophils Basophils
Main function:					
Affinity IgG-binding:					
N-linked glycosylation sites:					
SNP with clinical relevance:					
Affinity to different IgG subclasses:					
Expressed by:					

**Figure 3 | Properties of the receptor family FcγR.**

Overview of features of the different FcγRs. Signal motifs are indicated in the schemes. Table adapted from [169][174][170, 175]. Schematic created with BioRender.com

## 1.2.2 The allelic variants of CD32 (FcγRII)

CD32A, an activating FcγR, is mainly found on cells of the innate immune system such as monocytes, dendritic cells (DC) or macrophages [166]. CD32B, in contrast, is categorized as an inhibitory FcγR with important immune regulatory functions in cells of the innate immune system and is also highly expressed on B cells. CD32C is sort of a chimera between CD32A and B. The four exons of FCGR2C, which encodes the transmembrane and the cytoplasmic tail, are highly homologous to FCGR2A, whereas the exons coding for the extracellular Fc binding part are highly homologous to FCGR2B [176]. The FCGR2C gene is most likely a result from a recombination event between the FCGR2A and FCGR2B genes [177]. Around 10-20% of the Caucasian European people express CD32C on their phagocytes, NK cells and B cells [178, 179], whereas e.g. the black South African population do not express CD32C [180]. Expression of functional CD32C has been proposed to lead to an imbalance between the activating and inhibitory signals in NK cells [178] or B cell receptor (BCR) signalling in B cells [181] and has been linked to autoimmune diseases, such as Systemic Lupus Erythematosus or the blood disorder Idiopathic Thrombocytopenic Purpura (ITP) [179, 181].

Expression of CD32A and CD32B on T cells still remains elusive. While some studies have shown CD32 expression on activated CD4 T cells [153, 182] other studies have implicated rather false positive events due to cell doublets or trogocytic transfer of CD32 [146, 150, 154].

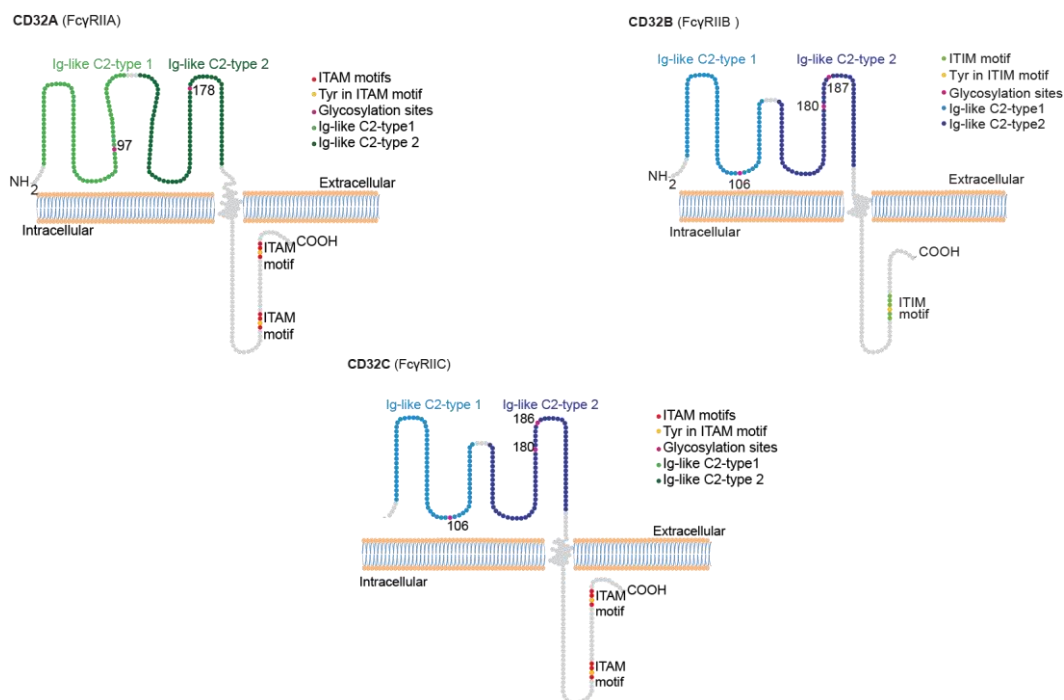


**Figure 4 | Schematic figure of CD32A, CD32B and CD32C with indicated important amino acids and motifs.**

The signal motifs (ITAM or ITIM) are indicated at the intracellular part together with the important tyrosine (Tyr) residues. On the extracellular part, the IgG binding site as well as N-glycosylation sites of the receptors are indicated.

### 1.2.3 Immune functions of FcγR

#### FcγR-mediated phagocytosis

Phagocytosis is described as the uptake of foreign material, senescent cells, apoptotic bodies or cell fragments by phagocytes, such as macrophages or dendritic cells, followed by digestion and degradation in lysosomes [183]. The uptake enables also cross-presentation of foreign antigens to T cells, which induce important immune responses [184]. The binding of opsonized material to FcγR induces phagocytosis by FcγR-expressing cells, which has been mainly observed for activating FcγRs, such as CD64 and CD32A [172, 185]. Mutations in the ITAM motif as well as the point mutation H131R allelic variant of the IgG-binding site of CD32A lead to reduced phagocytic activity of expressing cells [186, 187]. Furthermore, phagocytosis mediated by CD32B on macrophages has also been observed [188]. However, the observations indicate a different antigen processing pathway when phagocytosis is induced by CD32B. Phagocytosis mediated by ITAM carrying receptors, such as CD32A, lead to degradation of the antigen and presentation of antigen peptides to T cells with subsequent T cell activation. In contrast, the CD32B phagocytosis has been observed to keep the antigen intact followed by transfer to B cells [189, 190].

#### FcγR-mediated ADCC and NET formation

Being part of the innate immune defence, Natural Killer (NK) cells attack opsonized pathogens, malignant or infected cells by antibody dependent cell-mediated cytotoxicity (ADCC). The FcγRs on NK cells bind the Fc part of an antibody attached to the target cell [191, 192]. The target cell-IgG-FcγR bridging triggers different pathways with the aim to kill the target cell by e.g. release of cytotoxic granules, release of pro-inflammatory cytokine, or apoptosis induction via tumor necrosis factor family death receptor signalling [192, 193]. The FcγR CD16A is ubiquitously expressed on NK cells and has been described to induce ADCC. It has been described that around 40% of healthy donors have CD16<sup>+</sup>/CD32<sup>+</sup> NK cells [178, 194, 195]. RT-PCR analysis further confirmed either CD32C or CD32B expressing on NK cells, which might have potential clinical relevance, since e.g. NK cells with the inhibitory CD32B have shown reduced ADCC activity [178]. This may also have negative consequences for monoclonal antibody tumor therapy efficacy, since ADCC induction is one of the favoured goals for the success of the treatment [196, 197].

Next to NK cells, neutrophils largely contribute to pathogen elimination. A prominent way to attack opsonized pathogens by neutrophils is the formation of neutrophil extracellular traps (NET) via the release of reactive oxygen species [198-200]. The FcγRs CD32A and CD16B mediate NET formation in neutrophils [201]. The FcγR CD16B lacking cytoplasmic tail is a more “outstanding” FcγR. Even without ITAMs or ITIMs, CD16B also induces signalling events, which lead to actin polymerization or NF-κB activation. Next to opsonized pathogens immune complexes have also been shown to induce NET formation, mediated by an interplay between CD16B and CD32A [202, 203].

#### FcγR-regulated cell activation and maturation

CD32B is expressed on immune cells, such as dendritic or myeloid cells, often together with activating FcγRs, thereby balancing their activation signal within the cells. When cytokines, such as Interleukin-4 (IL-4) or IL-10, are present, CD32B is upregulated and activation of the cell is limited. In contrast, inflammatory cytokines, such as Interferon-γ (IFN-γ) downregulate CD32B, lowering the threshold to activate cells [204, 205]. In B cells, the inhibitory signal is induced upon co-ligation of CD32B with the Fc part of an antibody and simultaneous ligand binding to the activating receptors e.g. B cell Receptor (BCR). This induces the phosphorylation of the ITIM motif by the Lyn kinase followed by phosphorylation and recruiting of SHIP-1 or SHIP-2, regulating the

proliferation and activation of the cell [206, 207]. Co-ligation with the BCR downregulates the cell activation and proliferation induction pathways and therefore balances the peripheral tolerance [172, 206]. If only CD32B is triggered by ligand binding without crosslinking the ligand to an ITAM-carrying BCR, it can induce apoptosis by involving SHIP-independent pathways, where the ITIM motif is directly phosphorylated by the Bruton's tyrosine kinase (BTK) [208]. This additional pathway may be important during B cell development in the spleen, when the cells are interacting with immune complexes presented by follicular DCs. During the later phase of B-cell development, in B cells with a high affinity BCR, the immune complexes will induce signals by the BCR and CD32B within the B cells. Data suggest also a role of CD32B in the exclusion of autoreactive plasma cells with low IgG affinity. Also here, CD32B will induce a signal leading to apoptosis of these immunogenically "unfavourable" cells [168, 173]. The absence of CD32B has been shown to lead to autoreactive diseases [209] and has been linked to lupus-like diseases [210].

The ITAM activating signal induced by immune complex binding is also a potent activation pathway for DCs [211]. Likewise, CD32B plays an important role in controlling the degree of activation. Since immune complexes are always present in the blood stream, undesired activation has to be prevented [168]. This has been demonstrated by recent studies using CD32B-deficient murine DCs, which have caused spontaneous maturation of the DCs even under non-inflammatory conditions [212, 213].

Taken together, the FcγRs are important tools of the immune system. Depending on the cell type, the receptors induce ADCC, phagocytosis of opsonized cells or pathogen, induce cytokine production and have regulatory functions on T cell and B cell activation [166]. Consequently, pathogens have evolved proteins with FcγR-sequestering properties to surmount this immune recognition. Prominent Fc binding proteins from bacteria are e.g. staphylococcal protein A and streptococcal protein G, resulting in decreased binding of antibodies to FcγRs. But also viral proteins have been found to function as viral FcγRs (vFcγR) to trap opsonizing antibodies, such as the glycoproteins gE/gI from herpes simplex virus-1 (HSV-1) [214, 215], gp34, gp68, from Human Cytomegalovirus (hCMV) [216-219]. The vFcγRs expressed on the surface of infected cells capture opsonizing antibodies to impair the Fc recognition by the immune system and induce antibody clearance by internalization into the host cell [217, 220, 221]. The vFcγRs of HSV-1 are also found on the surface of free viral particles, preventing antibody-induced virus neutralization [222].

#### 1.2.4 Antibody binding sites on FcγR

The binding sites of IgGs on FcγRs have been reported to occur at the lower hinge region as well as at residues in the CH2 region. Shield *et al.* [223] have identified point mutations within the CH2 site that vary the binding to the FcγRs, e.g. D270A reduces the binding to CD32, whereas D280A and D280N enhance the binding to CD32 [223]. The CD32 receptors have been classified as low affinity receptors, due to the short dissociation time with monomeric IgGs [224, 225]. However, since the concentration of IgGs in serum is high, it is assumed that the receptors constantly bind antibodies with low affinity. The higher affinity to immune complexes is originating from the higher affinity of immune complexes to the cell surface compared to a monomeric IgGs [170]. The CD32a gene encodes two different allotypes, which having an Arginine or an Histidine at position 131, with H131 being observed to have higher IgG affinity than R131 [226]. The glycosylation pattern of the IgGs has been reported to influence binding to the FcγRs [227, 228], but also the glycosylation pattern of the receptor itself influences the affinity [169, 229, 230]. Two N-glycosylation sites on CD32A and three on CD32B have been reported on the extracellular part [169] (Figure 4).

Besides the binding of IgGs, FcγR bind also proteins of the pentraxin family, such as the C-reactive protein (CRP) and the serum amyloid P component (SAP) [231, 232]. These proteins are pattern recognition proteins and play an important role in sensing damaged cells and microbial antigens. CRP and SAP are acute phase proteins and induced upon infection [233, 234]. It has been reported that CD32 receptors bind to CRP with high affinity [231, 235, 236]. *In vivo* studies with mice as well as clinical data comparing patients with CD32A H131 or R131 alleles have shown that the interaction of FcγR and CRP or SAP regulates inflammation responses [237, 238].

### 1.2.5 HIV and FcγRs

Besides CD32a being proposed as biomarker for latently infected CD4 T cells, FcγRs have also been linked to HIV-1 infection in other ways:

Perez-Bercoff *et al.* [239] have tested the change in susceptibility to HIV-1 infection of monocytes and monocyte-derived macrophages (MDMs), if their FcγRs have been previously primed with immobilized IgGs (imIgGs). Since monocytes and macrophages express CD64 and CD32B, they may induce cellular pathways that could positively or negatively influence infection. They stimulated cells at different time points with immobilized IgGs prior to infection and observed decreased p24 expression. With the stimulation also higher levels of cytokines have been detected, e.g. monocyte-derived cytokines (MDC) [239]. MDCs have previously been reported to suppress HIV-1 infection at a post reverse transcriptional state in macrophages [240]. However, the neutralization of the MDC did not abrogate the infection suppression and, additionally, the suppressed infection with HIV-1 pseudo typed with vesicular stomatitis virus G glycoprotein (VSG-G) virions was also detected, indicating the IgG-induced suppression of infection had to occur after viral entry and was not due to the higher cytokine levels. Later on, these authors detected an accumulation of 2-LTR circles and proposed a potential restriction during integration [239]. In a later study, Bergamaschi *et al.* [241] showed higher levels of the cyclin-dependent kinase inhibitor p21 upon activation of FcγR by immune complexes. Previously, p21 has been observed to bind to the reverse transcription/preintegration complex [242]. However, Bergamaschi *et al.* [241] have not been able to verify this finding. Yet, silencing of p21 has surmounted the FcγR-mediated restriction [241]. Even though the results are preliminary, the studies have shown a potential role of FcγR activation on HIV-1 replication.

Single Nucleotide Polymorphism (SNP) of FcγRs have also been reported to influence HIV-1 infection, disease progression or HIV vaccine responses. The CD32A polymorphism H131R with reduced binding to IgG1, 2 and 3 influences the infection progression of HIV patients [226]. Genotyping of HIV patients have implicated a correlation of the homozygous polymorphism of CD32A R131 (RR131) with accelerated CD4 T cell loss when compared to patients with heterozygous or homozygous HH131 CD32A polymorphism [243]. Yet, even though the patients with homozygous expression for HH131 seem to benefit with a less progressive infection they have also shown to have increased risks for AIDS-related opportunistic diseases, such as *pneumocystis jirovecii pneumonia* [244], and placental malaria [245] and perinatal infections [246] in HIV-infected mothers. Forthal *et al.* [244] have also observed higher antibody-dependent, cell-mediated virus inhibition after treatment with recombinant HIV envelope protein gp120 in patients with HH131 [244].

Similarly, the CD16A SNP F158V has been reported to influence vaccine responses. Forthal *et al.* [247] have demonstrated enhanced HIV-1 infection rates for patients with CD16A homozygote polymorphism for VV158 [247]. Since the polymorphism for CD32A and CD16A have shown to influence the binding and clearance of IgGs and immune complexes [171, 248], this may lower

the clearance of immune complexes in HIV-infected patients, resulting then in higher T cell activation and possibly disease progression [243]. But also targeting of antibody-opsonized, infected cells by FcγR expressing effector cells could be affected and therefore could also influence the outcome of vaccine responses [244].

### 1.2.6 FcγR-mediated trogocytosis

The term trogocytosis has first been defined by Brown *et al.* in 1979 [249], when describing an alternative way of destruction of mammalian cells by the amoeba *Naegleria fowleri*. Here, the partial uptake of cytoplasmic membrane has been described as “nibbling” instead of full internalization as for phagocytosis. Due to this “nibbling” they called this phenotype “trogocytosis” (from the Greek “trogo” for “nibble”) [249]. Up to today this term is generally used when membrane parts or intact surface proteins are transferred from one cell to another cell after close cell-contact. However, the circumstances and the consequences on the involved cells vary widely, raising the question if this topology can be used as a shared term or if there are different underlying molecular mechanisms. Trogocytosis has not only been described for amoebae killing of mammalian cells [249-251], it has also been reported to occur within the immune system [252-256], the central nervous system [257, 258] and also during embryonic development [259].

When the MHC complex loaded with an antigen expressed by an antigen presenting cells (APC) interacts with the T cell receptor (TCR) of T cells, the two cells form an immunological synapse. During this contact, these cells get in close proximity to each other and it has been reported that one of the cells can take over the whole MHC-antigen TCR complex [252-255, 260] (Figure 5 upper panel). This has an impact on immune functions, such as cell survival [252, 261, 262], promoting differentiation [262] and regulatory function [263-265] of the acceptor cells.

Notably, the formation of an immunological synapse is not the only situation this phenomenon occurs with immune cells. Early studies with macrophage-mediated phagocytosis by Griffin *et al.* in 1976 [266] have shown the removal of antibody-antigen complexes on T cells without uptake or even damage of the T cells. They have suggested a different phagocytosis mechanism behind this phenotype with potential dependence on the distribution of the antibody on the lymphocytes [266]. Two years later, Lee *et al.* [267] reported the transfer of soluble FcγRs from macrophages to T and B cells [267].

Soon after, cancer treatment with the first monoclonal antibody (mAb) therapy was initiated, in which specific antigens targeting cancer cells were being applied [268-272]. The strategy for this treatment is either the induction of cell death or stop of cell growth upon binding of the mAb to specific epitopes on the target cells [271-274] as well as induced killing of the cancer cells due to the activation of the complement system [275-281]. But also antibody-induced cell killing by FcγR-expressing cells (e.g. monocytes, neutrophils and macrophages) may lead to the desired effect [196, 276, 282-284]. Disturbingly, early within the studies it became clear that there was a mechanism that also helped the cancer cells to evade this immune cell response. The loss of the antigens from the surface of the target cancer cells has been observed and called “antigenic modulation” [268, 270, 285, 286]. With this, the cancer cell evades the killing by the immune system and it has been discussed whether the loss is due to internalization or due to the uptake of the antigen-mAb complex by other cells. By using *in vitro* co-cultures of FcγR-expressing monocyte cell line THP-1 together with CD20<sup>+</sup> B cell line Raji or ARH 77 cells, Beum *et al.* [287] have observed the actual transfer of the mAb-antigen complexes (trogocytosis of CD20) from the B cell line to the monocytic cells in the presence of rituximab (anti-CD20 Ab) [287]. Similar findings have also been observed with the addition of mAbs targeting other antigens/other cancer cells such as

trastuzumab (antibody against the extracellular domain of the HER-2 tyrosine kinase receptor) or cetuximab (anti-epidermal-growth-factor-receptor (anti-EGFR)), showing an antigen-independent phenotype [288]. The findings have been further verified by other *in vitro* and *in vivo* studies [289-292]. But also, non-therapeutic antibodies this far could induce trogocytosis, implicating a more specific role of antibodies bound to cells to induce trogocytosis [293-295]. The primary focus is the uptake of the antigen-mAb complex by the FcγR expressing cells, however also redirected or bidirected trogocytosis has been reported [263, 295-297]. Also the transfer of membrane fragments from FcγR<sup>+</sup> mastocytoma cell line P815 to CD4 or CD8 T cells (opsonised with anti-CD3 antibody) was observed and was blocked with the addition of anti-CD16/anti-CD32 antibodies. Here a correlation of the binding extent of the antigen-specific antibody to the recipient cell correlated with the levels of membrane fragment transfer [298]. The potential blockage of transfer by anti-CD16/anti-CD32 antibody as well as the correlation of antibody/antigen binding to the levels of membrane transfer indicated that the antibody function as a bridge between the cells. The Fc part of the antibody could bind to the FcγR and, at the same time, the antibody bound the antigen on the surface of the other cell, forming a bridge between the cells and thereby inducing trogocytosis due to the close cell contact formation (Figure 5 lower panel) [297, 298]. In follow-up studies with HEK293T cells transiently expressing the murine CD32B and murine CD16A, the actual capture of both receptors by mAb-opsonized murine CD4 or CD8 T cells in co-culture was shown [297]. Here, the correct orientation of the FcγRs on the T cell membrane after its transfer as well as the remaining capability to bind immune complexes could be demonstrated. However, no potential induction of downstream signals induced by the transferred FcγR was observed, questioning the remaining receptor functionality after transfer [297].

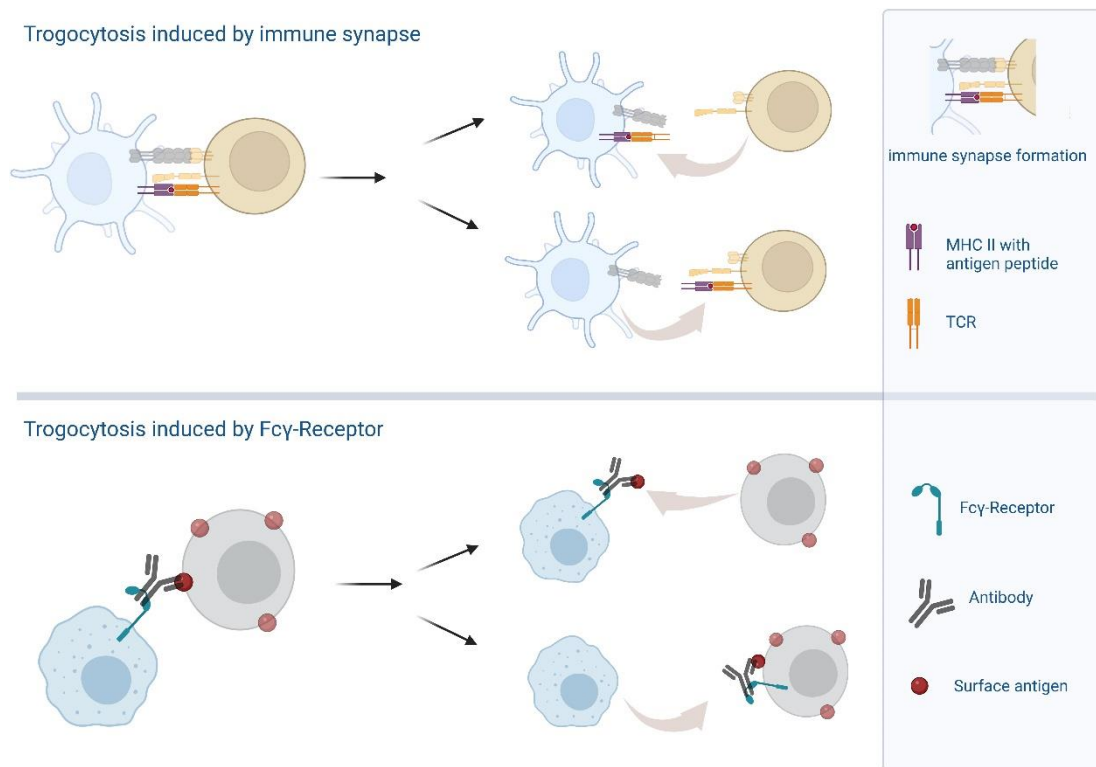


**Figure 5 | Schematic overview of potential trogocytosis inducing immune cell contacts.**

Trogocytosis can be induced after the formation of an immune synapse (upper panel) or upon interaction of an antibody opsonized target cell and the binding of another cell to the Fc part, mediated by Fc $\gamma$ R. Both ways can lead to the uptake of receptors or antigen by one of the involved cells. Schematic was created with BioRender.com

The physiological role and function of Fc $\gamma$ R-mediated trogocytosis is still not fully understood. Fc $\gamma$ R-expressing cells, such as macrophages or neutrophils, attack antibody-opsonized cancer cells via trogocytosis, inducing cell death by active perforation of the cancer cell plasma membrane [299, 300]. Fc $\gamma$ R-mediated trogocytosis regulates inflammation and autoreactivity by removing antibodies bound to self-antigens and thus plays a role in autoimmune diseases inducing autoantibody production, such as systemic lupus [294, 301].

### 1.3 Aim of the study

In 2021, the World Health Organization has counted around 38.8 million HIV-infected people and currently available pharmacotherapies can only suppress viral load and ameliorate disease outcome and viral load but do not cure patients [302]. Due to the viral reservoir, the virus persists and viral rebound can occur, if treatment is interrupted. As a result, the latently infected cells (mainly CD4 T cells) are promising targets to find a cure of HIV infection. It is therefore of high interest, to distinguish latently infected cells from healthy cells by surface latency biomarker. Recently, Descours and Petitjean *et al.* [142] have proposed the Fc $\gamma$ R CD32A as a maker for latently infected CD4 T cells. These findings have sparked enormous interest, with some research groups observing similar findings but also research groups challenging these results. Some research groups have postulated potential false-positive results of CD32-positive CD4 T cells due to cell doublets of CD4 T cells and CD32-expressing cells such as B cells, but also stated to observe CD4 T cells with CD32-positive “cell fragments” on the surface of the T cells, which could have been potentially transferred from another cell.

---

In this study, I aimed to recapitulate the findings of Descours and Petitjean *et al.* [142] and elucidate the potential transfer of CD32 during FcγR-mediated trogocytosis. Here, the three different CD32 receptors and their potential role in FcγR-mediated trogocytosis together with factors, which influence the transfer, will be investigated. Besides mechanistical studies, I aimed to show the potential influence of FcγR-mediated trogocytosis on the susceptibility of primary CD4 T cells to HIV-1, as well as the role of other receptors on the infection outcome.

## 2. Material and Methods

### 2.1 Chemicals and material

#### 2.1.1 Reagents, drugs, commercial media, buffer, and kits

Name	Cat. Nr.	Manufacturer
Agarose	3810.3	Carl Roth
Albumin fraction V (BSA)	8076.3	Carl Roth
AllPrep DNA/RNA Mini Kit (50)	80204	Qiagen
AMD3100	A5602	Sigma Aldrich
Anonymized human serum samples	n.a.	obtained from Diagnostic Department of Max von Pettenkofer Institute with approval of Ethics Committee
BD Trucount™, Absolute Counting Tubes	340334	BD Bioscience
Bolt™ bis tris gel 4-12%, 10 well	NW04120BOX	Thermo Fisher Scientific
CD14 MicroBeads	130-050-201	Miltenyi Biotech
CD4 <sup>+</sup> T Cell Isolation Kit	130-096-533	Miltenyi Biotech
CellTiter-Glo® 2.0 Assay	G9243	Promega
Cholera Toxin B subunit, biotin conjugate	C9972	Merck
CO <sub>2</sub> -independent medium	18045088	Thermo Fisher Scientific
CutSmart Buffer	B7204S	New England Biolabs
dATP	1051440001	Sigma Aldrich
dCTP	11051458001	Sigma Aldrich
dGTP	11051458001	Sigma Aldrich
DharmaFECT 1 Reagent	T-2001-03	Dharmacon
DMEM, high glucose, GlutaMAX	31966047	Thermo Fisher Scientific
dTTP	11051482001	Sigma Aldrich
Dulbecco's phosphate buffered saline (PBS)	P04-36050P	Pan-Biotech
EDTA-free protease inhibitor cocktail complete	11836170001	Roche
Ethylenediaminetetraacetic acid disodiumsalt-dihydrate (EDTA)	22.161.000	Chemsolute, Th. Geyer
Fetal Bovine Serum (FBS/FCS)	F7524	Sigma Aldrich
Fetal Bovine Serum, ultra-low IgG	16250078	Thermo Fisher Scientific
Gel loading dye purple, 6x	B7024S	New England Biolabs
Glycerin	3783.1	Carl Roth

Human AB serum	H4522	Sigma Aldrich
Human Monocyte Isolation Kit II, human	130-091-153	Miltenyi Biotech
Hydrochloride acid (HCl, 32%)	P074.3	Carl Roth
Kanamycin Sulfate	T832.2	Carl Roth
LB-Agar	X969.2	ChemSolute, Th. Geyer
Linear polyethylenimine (PEI)	23966	Polysciences
Lipofectamine™ 2000 transfection	11668019	Thermo Fisher Scientific
Lipopolysaccharides from <i>Escherichia coli</i> O55:B5 (LPS)	L6529	Sigma Aldrich
LiveBLAzer™ FRET-B/G Loading Kit with CCF2-AM	K1032	Thermo Fisher Scientific
Lysogenic broth (LB) acc. Miller powder	88.850.500	ChemSolute, Th. Geyer
Magnesium chloride (MgCl <sub>2</sub> )	M1028-10X1ML	Sigma Aldrich
Methanol, 100%	14.372.511	ChemSolute, Th. Geyer
MS2 RNA	10165948001	SIGMA-Aldrich
Nonidet P40 (NP-40)	A1694	PanReac Applichem
NucleoBond Xtra Midi	740.410.100	Macherey-Nagel
NucleoSpin® Gel and PCR Clean-up	740.609.250	Macherey-Nagel
NuPAGE LDS Sample Buffer (4X)	NP0007	Invitrogen
NuPAGE MOPS SDS running buffer	NP0001	Thermo Fisher Scientific
NuPAGE Transfer Buffer (20x)	NP0006	Thermo Fisher Scientific
Opti-MEM™ I Reduced Serum Medium	31985070	Thermo Fisher Scientific
P3 Primary Cell 96-well Kit (96 RCT)	V4SP-3096	Lonza
Pancoll human, Density 1,077g/ml	P04-60500	P04-60500
Penicillin-Streptomycin	P0781-100ML	Sigma Aldrich
Phytohemagglutinin from <i>Phaseolus vulgaris</i> (PHA)	L1668	Sigma Aldrich
Pierce bicinchoninic acid (BCA) protein assay kit	23227	Thermo Fisher Scientific
Potassium chloride (KCl)	6781.3	Carl Roth
Prolong Diamond Antifade Mountant	P36970	Thermo Fisher Scientific
Quick-Load® 1 kb Extend DNA Ladder	N3239S	New England Biolabs
RosetteSep Human CD4+ T Cells	15062	STEMCELL Technologies
RPMI 1640 GlutaMAX	12027599	Fisher Scientific
siRNA buffer (5x)	B-002000-UB-100	Dharmacon
Sodium Chloride (NaCl)	9265.2	Carl Roth

Streptavidin, Alexa Fluor™ 594 Conjugate	S11227	Thermo Fisher Scientific
SYBR Green I	S4438	Sigma Aldrich
SYBR Safe-D NA Gel Stain	S33102	Thermo Fisher Scientific
Terrific broth (TB) medium	80.490.500	ChemSolute, Th. Geyer
Tris(hydroxymethyl) aminomethane (Tris)	T1503-1KG	Sigma-Aldrich
Triton-X 100	3051.3	Carl Roth
WesternSure Pre-Stained Chemiluminescent Protein Ladder	926-98000	LI-COR Biosciences

## 2.1.2 Chemokines and enzymes

### Chemokines

Name	Cat. Nr.	Manufacturer
Recombinant Human SDF-1 $\alpha$ (CXCL12)	300-28A	Peprtech
Recombinant Human RANTES (CCL5)	300-06	Peprtech
Recombinant Human M-CSF	300-25	Peprtech
Recombinant Human GM-CSF	300-03	Peprtech
Recombinant Human IL-4	200-04	Peprtech
Recombinant Human IL-15	200-15	Peprtech
Recombinant Human IL-2	200-02	Peprtech
Recombinant Human IL-7	200-07	Peprtech
Recombinant Human TNF- $\alpha$	300-01A	Peprtech
Recombinant Human IL-1 $\beta$	200-01b	Peprtech
Recombinant Human IL-6	200-06	Peprtech
Recombinant Human SDF-1 $\alpha$ (CXCL12)	300-28A	Peprtech

### Enzymes

Name	Cat. Nr.	Manufacturer
Liberase TL	05401020001	Sigma Aldrich
DNAase I	04716728001	Sigma Aldrich
NLS-Cas9	1081059	IDT
Accutase	A6964-100ML	Sigma Aldrich
Heparinase I	P0735S	New England Biolabs (NEB)

Heparinase II	P0736S	New England Biolabs (NEB)
Heparinase III	P0737S	New England Biolabs (NEB)
Chondroitinase ABC from <i>Proteus vulgaris</i>	C3667-5UN	Merck
Quick CIP	M0525S	New England Biolabs (NEB)
<i>EcoRI</i>	R0101S	New England Biolabs (NEB)
<i>Agel</i>	R3552S	New England Biolabs (NEB)
Ribolock Rnase	E00381	Thermo Fisher Scientific
GoTag Hot Start Polymerase	M5003	Promega

### 2.1.3 Antibodies and cell dyes

#### Antibodies

##### Used as culture supplement

Name	Cat. Nr.	Manufacturer
Alemtuzumab	n.a.	kindly provided by Central Cytostatics Preparation Facility, LMU hospital Munich
Anti-CD32	303202	Biologend
PGT151	n.a.	kindly provided by Prof. Dr. Ralf Wagner, University of Regensburg
Ultra-LEAF™ Purified Human IgG1	403502	Biologend

##### Used as blocking antibody (used in HIV-1 binding assay)

Name	Cat. Nr.	Manufacturer
Recombinant Human SDF-1 $\alpha$ (CXCL12)	300-28A	Peprtech
Recombinant Human RANTES (CCL5)	300-06	Peprtech
Recombinant Human M-CSF	300-25	Peprtech
Recombinant Human GM-CSF	300-03	Peprtech
Recombinant Human IL-4	200-04	Peprtech
Recombinant Human IL-15	200-15	Peprtech
Recombinant Human IL-2	200-02	Peprtech
Recombinant Human IL-7	200-07	Peprtech
Recombinant Human TNF- $\alpha$	300-01A	Peprtech
Recombinant Human IL-1 $\beta$	200-01b	Peprtech
Recombinant Human IL-6	200-06	Peprtech

Recombinant Human SDF-1 $\alpha$ (CXCL12)	300-28A	Peprotech
---	---------	-----------

#### Used in flow cytometry

Name	Cat. Nr.	Manufacturer
Human BD Fc Block™	564220	BD Bioscience
Anti-hCCR5 APC	556903	BD Bioscience
Anti-hCD11a APC	301212	Biolegend
Anti-hCD11b BV421	301324	Biolegend
Anti-hCD11c FITC	337213	Biolegend
Anti-hCD14 FITC	325603	Biolegend
Anti-hCD19 FITC	302206	Biolegend
Anti-hCD206 APC	550889	BD Bioscience
Anti-hCD209 (DC-SIGN) BV421	330118	Biolegend
Anti-hCD3 APC-Cy7	557832	BD Bioscience
Anti-hCD32 AF647	303212	Biolegend
Anti-hCD32 BV421	564838	BD Bioscience
Anti-hCD32 PE-Cy7	303214	Biolegend
Anti-hCD4 AF594	300544	Biolegend
Anti-hCD4 APC	555349	BD Bioscience
Anti-hCD4 PE-Cy7	300512	Biolegend
Anti-hCXCR7 APC	391405	Biolegend
Anti- Heparan Sulfate	GTX20073	Nordic Biosite
Anti-hHLA-DR FITC	347363	BD Bioscience
Rat anti-mouse IgM BV421	406532	Biolegend
Goat anti-human IgG APC	109-136-170	Jackson Immuno Research

#### Used in immunoblotting

Name	Cat. Nr.	Manufacturer
Anti-hVPS4	sc-133122	Santa Cruz
Anti-Mouse-HRP IgG (H and L)	115-035-062	Jackson Immuno Research
Anti-Rabbit IgG (H and L)	111-035-144	Jackson Immuno Research
Anti-Vinculin	ab129002	abcam

**Drugs**

<b>Name</b>	<b>Cat. Nr.</b>	<b>Manufacturer</b>
CellTrace™ Violet Cell Proliferation Kit	C34571	Thermo Fisher Scientific
CellTrace™ Far Red Cell Proliferation Kit	C34572	Thermo Fisher Scientific
Fixable Yellow Dead Cell Stain Kit	L34967	Thermo Fisher Scientific

**2.1.4 Primers, plasmids, siRNA and gRNA****Primers**

<b>Name</b>	<b>Sequence</b>
SG-PERT forward primer	5'-TAGTTGTTGGGCTTCGCTTT-3'
SG-PERT reverse primer	5'-TTGTCGGCTTTACCTGCTTT-3'

**Plasmids**

<b>Name</b>	<b>Description</b>
HIVivo R5	Used in combination with pCMV-Vpr-BlaM to produce virus stock for HIV-1 fusion assay. Kindly provided by Prof. Michel C. Nussenzweig (Howard Hughes Medical Institute, The Rockefeller University).
HIVivo X4	Generated in the lab by introducing env from NLENG-IRES by using restriction sites <i>EcoRI</i> and <i>HpaI</i> and ligation into the backbone of HIVivo R5. Used in combination with pCMV-Vpr-BlaM to produce virus stock for HIV-1 fusion assay.
NLENG1-I-70	Referred in the thesis as R5 HIV-1 EGFP
NLENG1-IRES	Referred in the thesis as X4 HIV-1 EGFP
pBK-CMV-FynN18-EGFP	Membrane-targeting domains (first 18 amino acid of the N terminal part (SH4 membrane domain) of Fyn fused to EGFP N terminal. Kindly provided by Prof. Dr. Oliver Fackler (Center for Integrative Infectious Disease Research, University of Heidelberg)
pBK-CMV-LckN18-EGFP	Membrane-targeting domains (first 18 amino acid of the N terminal part (SH4 membrane domain) of Lck fused to EGFP N terminal. Kindly provided by Prof. Dr. Oliver Fackler (Center for Integrative Infectious Disease Research, University of Heidelberg)
pCDH-mtagBFP	Expression of mtagBFP. Kindly provided by Prof. Dr. Wolfgang Hammerschmidt, Helmholtz Center Munich
pcDNA3.1_hCXCR7	Expression of human CXCR7. Kindly provided by Prof. Dr. Jürgen Bernhagen (Ludwig-Maximilians-Universität München (LMU Munich))
pcDNA3.1-hCXCR4-Flag	Expression of human CXCR4 with Flag Tag

pHIV-1 YFP X4	Used in combination with pCMV-Vpr-EGFP to generate HIV-1 GFP positive particle for HIV-1 binding assay. Referred in the thesis as HIV-1 Vpr-GFP. Kindly provided by Prof. Dr. Barbara Müller (Center for Integrative Infectious Disease Research, University of Heidelberg) [303]
pHIV-1 ΔEnv	Used in combination with pCMV-Vpr-EGFP to generate HIV-1 GFP positive particle for HIV-1 binding assay. Referred in the thesis as HIV-1ΔEnv Vpr-GFP. Kindly provided by Prof. Dr. Barbara Müller (Center for Integrative Infectious Disease Research, University of Heidelberg)
pCMV-BlaM-Vpr	To incorporate BlaM-Vpr into HIV-1 viral particle
pCMV-CD32A WT-mtagBFP	Expression of human CD32A wild type fused to mtagBFP N terminal
pCMV-CD32A Δglyco-mtagBFP	Expression of human CD32A with point mutation N97G, N178G fused to mtagBFP N terminal
pCMV-CD32B WT-mtagBFP	Expression of human CD32B wildtype fused to mtagBFP N terminal
pCMV-CD32B WT-mtagBFP	Expression of human CD32B wild type fused to mtagBFP N terminal
pCMV-CD32B Δglyco-mtagBFP	Expression of human CD32B with point mutation N106G, N180G, N187T (deletion of glycosylation site) fused to mtagBFP N terminal
pCMV-CD32B ΔITIM-mtagBFP	Expression of human CD32B with point mutation Y292F (deletion of ITIM motif) fused to mtagBFP N terminal
pCMV-CD32C WT-mtagBFP	Expression of human CD32C wild type fused to mtagBFP N terminal
pCMV-Vpr-EGFP	To incorporate Vpr-EGFP into HIV-1 viral particle
pEGFP- CD32A (Δglyco)	Used for cloning of mtagBFP fusion variant
pEGFP- CD32A WT	Used for cloning of mtagBFP fusion variant
pEGFP- CD32B (Δglyco)	Used for cloning of mtagBFP fusion variant
pEGFP- CD32B (ΔITIM)	Used for cloning of mtagBFP fusion variant
pEGFP- CD32C WT	Used for cloning of mtagBFP fusion variant
pEGFP-CD32B	Generated in the lab. CD32B from pCMV6-XL5-CD32B (Cat. No. SC128159) origen amplified by PCR and inserted in pEGFP-N1 (Clontech) using <i>AgeI</i> and <i>EcoRI</i>
pEGFP-CD63	Expression of human CD63 fused to EGFP N terminal
pEGFP-H2B	Expression of human histon protein H2B fused to EGFP N terminal
pEGFP-hCCR5	Expression of human CCR5 fused to EGFP N terminal
pEGFP-hCD4	Expression of human CD4 fused to EGFP N terminal
pEGFP-hCXCR4	Expression of human CXCR4 fused to EGFP N terminal
pHR-CD4	Expression of human CD4
pHR-hCCR5	Expression of human CCR5
pSAMHD1-EGFP (N-term)	Expression of human SAMHD1 fused to EGFP N terminal

**Peptides**

<b>Name</b>	<b>Cat. Nr./ Description</b>	<b>Manufacturer</b>
Soluble hCMV-gp34	kindly provided by Prof. Dr. med. Hartmut Hengel (University of Freiburg)	n.a.
Soluble hCMV-gp34 $\Delta$ IgG binding site	kindly provided by Prof. Dr. med. Hartmut Hengel (University of Freiburg)	n.a.
Soluble hCMV-g68	kindly provided by Prof. Dr. med. Hartmut Hengel (University of Freiburg)	n.a.
Soluble ICOSL	kindly provided by Prof. Dr. med. Hartmut Hengel (University of Freiburg)	n.a.
Recombinant ICAM-1	150-05	Peptotech

**siRNA**

<b>Name</b>	<b>Cat. Nr.</b>	<b>Manufacturer</b>
ON-TARGETplus Non-targeting Pool	D-001810-10-05	Dharmacon
ON-TARGETplus Human VPS4A (27183) siRNA	L-013092-00-0005	Dharmacon

**2.1.5 Prepared buffers, media and solutions**

<b>Name</b>	<b>Description</b>
Adhesion solution	1x PBS, 0.5 % BSA, 1 mM CaCl <sub>2</sub> , 2 nM MgCl <sub>2</sub>
Agar plates	6.25 g LB-Agar in 500 ml LB medium, 50 mg/ml kanamycinsulfat
Antibody solution	1x TBS, 1 % BSA, 0.09 % sodium azide
Blocking buffer for flow cytometry	1x PBS, 2 mM EDTA, 5 % human AB serum
Cyopreservation media	RPMI (w/o supplements), 10 % DMSO, 10 % FBS
Differentiation of monocytes	Seeding of monocytes in RPMI c++; M-CSF (100 ng/ml)
Differentiation of monocytes to monocyte derived macrophage sublineages	MDM: keeping monocytes in RPMI c++; M-CSF (100 ng/ml) for 7 days
	M1 macrophages: addition of LPS (50 ng/ml) and INF- $\gamma$ (20 ng/ml) on day 6/7
	M2 macrophages: addition of IL-4 (20 ng/ml) on day 7
Differentiation of monocytes to mature monocyte-derived dendritic cells (moDC)	Seeding of monocytes in RPMI c++; IL-4 (250 IU/ml; Peptotech) and GM-CSF (800 IU/ml; Peptotech) and keeping in culture for 7 days. Addition of IL-6 (2,000 IU/ml), IL-1 $\beta$ (400 IU/ml), TNF- $\alpha$ (2000 IU/ml)
DMEM c++	DMEM, high glucose, GlutaMAX supplemented with 10% (v/v) FCS, Penicillin-Streptomycin (100 IU/ml)
FACS buffer	1x PBS, 2 mM EDTA, 1% FCS

Hunt lysis buffer	20 mM Tris-HCl pH 8.0, 100 mM NaCl, 1 mM EDTA, 0.5 % NP-40
LB medium	25 g LB powder in 1000 ml H <sub>2</sub> O, 50 mg/ml kanamycin-sulfat
Media for resting primary CD4 T cell media	RPMI c++; IL-7 (1 ng/ml); IL-15 (1 ng/ml).
RPMI c++	RPMI 1640 GlutaMAX supplemented with 10 % (v/v) FCS, Penicillin-Streptomycin (100 IU/ml)
SG-PERT dilution buffer (10x)	50 mM (NH <sub>4</sub> ) <sub>2</sub> SO <sub>4</sub> , 200 mM KCl, 200 mM Tris HCl (pH 8.3) in H <sub>2</sub> O
SG-PERT Lysis buffer (2x)	50 mM KCl, 100 mM Tris HCl (pH 7.4), 40 % Glycerol, 1% Triton-X 100, 0.4 U/μl RNase inhibitor RiboLock, in H <sub>2</sub> O
SG-PERT reaction buffer (2x)	SG-PERT dilution buffer (1x), 10 mM MgCl <sub>2</sub> , 0.2 mg/ml BSA, SYBR Green I (1:10 000), 0.4 mM of each dNTP, 1 μM SG-PERT forward primer, 1 μM SG-PERT reverse primer, 8 ng/μl MS2 RNA, 0.05 U/μl GoTag Hot Start DNA Polymerase
Supplement to activate primary CD4 T cells	Addition of PHA; (5 μg/ml); IL-2 (50 IU/ml) to culture media
TB medium	47.6 g TB powder in 1000 ml H <sub>2</sub> O, 4 ml Glycerol, 50 mg/ml kanamycinsulfat
Tris buffered saline (TBS) buffer, 10x, (pH 7.5)	121 g Tris, 175.2 g NaCl in 2l H <sub>2</sub> O

## 2.1.6 Cells and tissue material

### Bacterial cells

Name	Description
<i>Escherichia coli</i> Stbl2	Chemical competent <i>E.coli</i> ; F-mcr A Δ(mcrBC-hsdRMS-mrr)

### Mammalian cell line

Name	Description	Culture medium
293T	Human embryonic kidney cell line (immortalized via SV 40T antigen and E1A adenovirus protein). Commercially obtained from DSMZ (ACC 635)	DMEM c++
SupT1	T cell lymphoma cell line, originating from an 8-year old male patient with T-lymphoblastic lymphoma in relapse. Commercially obtained from DSMZ (ACC 140).	RPMI c++
HeLa	Epitheloid cervix carcinoma cell line, originating of a female patient. Commercially obtained from ATCC (CCL-2).	DMEM c++

Primary human cells from blood	Isolated from heparinized blood retained in leukocyte reduction system chambers from healthy blood donors with approval by the Ethics Committee of the Medical Faculty of LMU München (Project No. 17-202 UE).	RPMI c++
Primary human PBMCs from HIV-1 patients	Isolated from EDTA whole blood. Approval by the local Ethics Committees of the Medical Faculty of LMU München (Project No. 21-0866) and TUM (Project No. 548/21).	Not cultivated
Human lamina propria lymphocyte culture (LPAC)	Isolated from macroscopically normal human jejunum or ileum tissue samples were obtained from patients undergoing elective abdominal surgery. Approval by the Ethics Committee of the Medical Faculty of the University Duisburg-Essen (Project No. 15-6310-BO).	Not cultivated
Human lymphoid aggregate culture (HLAC)	Isolated from tonsil tissue, from HIV-, hepatitis B virus-, and hepatitis C virus-negative anonymous patients with informed consent and removed during therapeutic tonsillectomy (surgical waste). Approval by the Ethics Committee of the Medical Faculty of LMU München (Project No. 18-209 UE).	Not cultivated

### 2.1.7 Devices and Software

#### Devices

4D-Nucleofector System (Lonza)

FACSAria Fusion cell sorter (BD).

FACSLytic (BD).

CLARIOstar Plus plate reader (BMG Labtech)

CFX96 Touch Real-Time PCR Detection System (BioRad)

Fusion FX (Vilber)

Sorvall WX+ Ultracentrifuge and Rotor SW28 (Beckman Coulter)

---

 Eclipse Ti2 microscope with DS-Qi2 camera (Nikon)
 

---

## Software

---

 Imaris Viewer (Oxford Instruments)
 

---



---

 Image J (National Institute of Health)
 

---



---

 FlowJo™ Software
 

---



---

 GraphPad Software
 

---



---

 CFX Manager™ Software BioRad
 

---



---

 Adobe Illustrator 2023
 

---



---

 Biorender.com
 

---



---

 SnapGene software
 

---

## 2.2 Methods

### 2.2.1 Cloning of expression vectors

Following plasmids expressing mtagBFP fusion variants of FcγRs and their mutants, were specially cloned for the experiments in the thesis: pCMV-CD32A WT-mtagBFP, pCMV-CD32C WT-mtagBFP, pCMV-CD32B N106G N180G N187T (Δglyco)- mtagBFP, pCMV-CD32B Y292F (ΔITIM)- mtagBFP, pCMV-CD32A N97G N178G (Δglyco)- mtagBFP. The cloning strategy is described below:

#### 2.2.1.1 Generation of Backbone and Insert

The desired backbone was generated by digest of pCMV-CD32B WT-mtagBFP with *EcoRI* and *Agel*-HF for 2 h at 37 °C (for digest reaction mix see Table 1).

Table 1 | Reaction mix for restriction digest of pCMV-CD32B WT-mtagBFP with *EcoI* and *Agel*-HF.

Component	Volume
Cutsmart Buffer	9.0 μl
<i>EcoRI</i>	2.0 μl
<i>Agel</i> -HF	2.0 μl
pCMV-CD32B WT-mtagBFP	70.0 μl
H <sub>2</sub> O	7.0 μl

After incubation, 1 μl of Quick CIP enzyme is added to dephosphorylate the 5' ends of the digested DNA. Dephosphorylation was performed for 10 min at 37 °C followed by stopping the reaction by heat-inactivation at 80 °C for 2 min. The digested backbone contained DNA fragments with a size of 947 bp and 4674 bp, which were separated within an 1 % agarose gel (with SYBR Safe DNA

Gel stain 1:10 000 diluted) and 1x TAE buffer through electrophoresis for 1 h at 80 V. The desired DNA fragment of 4674 bp was excised from the gel and cleaned up using the NucleoSpin Gel & PCR clean up Kit.

The desired inserts were generated by restriction digest with *EcoRI* and *AgeI*-HF of pEGFP expressing vectors with the corresponding FcyR sequence (see Table 2) as described for the backbone generation above (without dephosphorylation).

**Table 2 | List of corresponding insert sequence, size and the original plasmid.**

Insert	Digested plasmid	Insert fragment size
CD32A WT	pEGFP- CD32A WT	968 bp
CD32C WT	pEGFP- CD32C WT	986 bp
CD32B ( $\Delta$ glyco)	pEGFP- CD32B ( $\Delta$ glyco)	947 bp
CD32B ( $\Delta$ ITIM)	pEGFP- CD32B ( $\Delta$ ITIM)	947 bp
CD32A ( $\Delta$ glyco)	pEGFP- CD32A ( $\Delta$ glyco)	968 bp

### 2.2.1.2 Ligation and Transformation

For ligation of backbone and the corresponding insert DNA fragments, the cleaned-up DNA fragments were incubated with T4-Ligase overnight (approximately 16-20 h) at 16 °C, with a ratio of about 1:3 backbone to insert (see Table 3).

**Table 3 | Ligation reaction of insert and backbone.**

Component	Amount
Backbone	50 ng
Insert	30 ng
T4-Ligase buffer	1 $\mu$ l
T4-Ligase	1 $\mu$ l
Add to 10 $\mu$ l with H <sub>2</sub> O	

For transformation, an aliquot of 50  $\mu$ l of chemical competent *E. coli* Stabl II was thawed on ice and 10  $\mu$ l of the corresponding ligation mix was added and incubated for 5 min on ice. After incubation the cells were heat shocked at 42 °C for 2 min with subsequent cooling down on ice for 5 min. The cells were then mixed with 1 ml LB Media (without antibiotics) and shaken for 90 min at 37 °C before plating on LB-Agar plates with kanamycin. After incubation of the plates for 20 h at 37 °C, 10 clones were picked from the plate and cultivated overnight in TB medium with kanamycin at 37 °C (shaking). The next day, DNA was isolated from 2/3 of TB culture using the AIIPrep DNA/RNA Mini Kit. The remaining 1/3 of the TB culture was kept at 4 °C until inoculation of TB culture with higher volume. Transformation of the desired ligation product was then validated by sanger sequencing at Eurofins Genomics using the standard CMV forward primer of the company.

### 2.2.1.3 DNA purification

The bacterial clone showing the correct sequence was then selected from the remaining 1/3 TB culture (described above) and used to inoculate 400 ml TB medium with kanamycin. The cultures were shaken overnight (approx. 20 h) at 37 °C. The next day the DNA was isolated using the NucleoBond Xtra Midi Kit. DNA concentration was adjusted to 1 µg/µl DNA with H<sub>2</sub>O and stored at -20 °C until usage.

## 2.2.2 Eukaryotic cell isolation, cultivation and differentiation

If not described differently, cells were cultured at 37 °C (5% CO<sub>2</sub>) and centrifugation steps were performed at 500 g 5 min at room temperature (RT). For corresponding standard culture media of the different cell types see also chapter 2.1.6.

### 2.2.2.1 Isolation of primary human cells from whole blood

Heparinized human blood was retained in leukocyte reduction system chambers from healthy donors (approval by Committee of Medical Faculty of LMU München (Project No. 17-202 UE). The harvested blood was diluted with PBS and CD4 T cells were isolated with EasySep Rosette Human CD4 T cell enrichment kit according to manufacturer protocol. In brief, the approximately 10 ml blood was diluted with 20 ml PBS and 1 ml of the EasySep Rosette Human CD4 T cell enrichment cocktail was added. After inverting the tube 8-10x times, the cell suspension was incubated for 20 min at RT. Then the volume was added to 105 ml with PBS, and 35ml of the cell suspension was carefully mounted on top of 15 ml Pancoll (with a density of 1.077 g/ml). The two layers of cell suspension and Pancoll was then centrifuged for 35 min at 700 g 20°C (without acceleration/break). After centrifugation the plasma layer was removed as much as possible without disturbing the other layers and the layer with CD4 T cells was harvested and cells were counted. The cell was either used directly for functional assays or kept in a resting state [304] (see chapter 2.1.5). For isolation of PBMCs, the harvested blood was directly diluted with PBS to 105 ml total volume and the cell suspension was mounted on Pancoll layer and centrifuged as described above. PBMC were either kept in culture with 2-4 x10<sup>6</sup> cells/ml (see chapter 2.1.6), or cryopreserved in cryopreservation media at a cell density of 1x 10<sup>8</sup> cells/ml.

CD14-positive monocytes were isolated from PBMCs with the human monocyte isolation kit II (negative isolation) or with the CD14 MicroBeads (positive isolation) according to the manufacturer's protocol. During negative isolation all leucocytes except CD14-positive monocytes were targeted by the antibody cocktail mix of the kit, followed by secondary antibody binding with microbeads. With this, the "undesired" cells retain in the column under the magnetic field and CD14-positive monocytes were harvested in the elution. In contrast, during positive isolation CD14-positive monocytes were targeted with an anti-CD14 antibody with microbead tag and here these cells retained in the column during magnetic isolation, whereas the "undesired" cell fraction is eluted from the column. The retained cells are then flushed out of the column, by removing the magnetic field and flushing the column with FACS buffer. After counting of the cells, the monocytes were differentiated by cultivation with different cytokine addition to the culture medium (see chapter 2.1.5).

Alternatively, to the isolation by EasySep Rosette human CD4 T cell enrichment kit, primary CD4 T cells could be isolated from the PBMC culture by magnetic fractioning with microbeads of the CD4 T cell isolation Kit (negative isolation) similarly as described above for monocytes.

### 2.2.2.2 Isolation of tonsillar cells

Tonsil tissue was obtained during therapeutic tonsillectomy from patients (negative tested for HIV, hepatitis B and hepatitis C virus). The anonymous surgical waste was then kindly provided by the LMU hospital Munich Großhadern with the approval of the Ethics Committee of the Medical Faculty of LMU Munich (Project No. 18-209 UE). Single cells were isolated from the tissue by mechanical cutting of the tissue into 2-3 mm tissue piece, which were then passed through 70  $\mu\text{m}$  and 40  $\mu\text{m}$  cell strainers. Remaining tissue was additionally incubated with 1 U/ $\mu\text{l}$  DNase I and 0.4 mg/ml liberase TL for 30 min at 37 °C. After passing through 70  $\mu\text{m}$  strainer these cells were added to the cell suspension. The cells were counted and then cryopreserved with cryopreservation media at -80 °C with a density of  $1 \times 10^8$  cells/ml.

### 2.2.2.3 Isolation of lamina propria mononuclear cells

Cryopreserved lamina propria mononuclear (LPAC) cells were kindly provided by Prof. Dr. Ulf Dittmer, University of Duisburg-Essen. The cells were isolated from macroscopically normal human jejunum or ileum tissue samples (as previously described [305, 306]), with the approval of Ethics Committee of the Medical Faculty of the University Duisburg-Essen. The tissue samples were obtained from patients undergoing elective abdominal surgery.

### 2.2.3 Antibody staining for flow cytometer analysis

Cell were collected from the culture and washed once with PBS. In case of adherent macrophages, the cells were washed once with PBS and then incubated with Accutase for 1-1.5 h at 37 °C to detach the cells before collecting. The cells were then seeded into a 96 Well V-Shape plate (100 000-200 000 cells/well). After spinning down, the cells were resuspended in 25  $\mu\text{l}$  blocking buffer and incubated for 10 min at 4 °C before adding 25  $\mu\text{l}$  antibody staining solution (FACS buffer + corresponding staining antibody, see chapter 2.1.3 and 2.1.5) and incubation of the cells for additional 20 min at 4 °C. After the incubation, 100  $\mu\text{l}$  FACS buffer was added to each well and the cells were spun down and washed twice with FACS buffer before resuspending the cells in 50  $\mu\text{l}$  of 4 % PFA/PBS and incubation for 10 min at 4 °C. Afterwards the cells were diluted with 100  $\mu\text{l}$  FACS buffer per well, spun down at 1100 g for 8 min and resuspended in 100  $\mu\text{l}$  FACS buffer. Flow cytometric analysis was then performed with FACSLyric (BD).

### 2.2.4 Knockdown (KD) generation in 293T cells

293T cells were seeded in a 12 Well plate with 350 000 cells/well. After adhesion of the cells (after 4-5h), the siRNA transfection mix was prepared. For this, siRNA was adjusted to 5  $\mu\text{M}$  with 1x siRNA buffer. Subsequently, 5  $\mu\text{l}$  of 5  $\mu\text{M}$  siRNA is mixed with 95  $\mu\text{l}$  DMEM w/o supplements. In an extra tube 4  $\mu\text{l}$  of DharmaFECT is mixed with 96  $\mu\text{l}$  DMEM w/o supplements. Both tubes are incubated for 5 min at RT before mixing both solutions together. The medium is carefully removed from the 293T cells and 800 $\mu\text{l}$  DMEM with 10% FCS without Penicillin-Streptomycin is added into each well followed by addition of 200  $\mu\text{l}$  siRNA/DharmaFECT transfection mix per well. The next day medium was changed and cells were used for follow up experiments, such as *in vitro* trogocytosis analysis (see chapter 2.2.7.1) and extra wells were harvested (24h, 48h or 72h post KD) for KD efficiency analysis by immunoblotting.

### 2.2.5 Expression plasmid nucleofection in primary CD4 T cells

CD4 T cells were freshly isolated from whole blood as described above (see chapter 2.2.2.1). After washing twice with PBS  $1 \times 10^6$  cells were resuspended in 20  $\mu$ l P3 buffer from P3 Primary Cell 96-well Kit and 0.1-0.5  $\mu$ g plasmid DNA of the corresponding expression vector was added. The cell suspension was then carefully transferred into a 16-well reaction cuvette of the 4D-Nucleofector System (Lonza) and subsequently nucleofected with the program EO-115. Directly after nucleofection, 100  $\mu$ l prewarmed RPMI medium (w/o supplements) was added to the cells and they were incubated for 10 min at 37 °C. The cells were then seeded into culture media with IL-7/IL-15 to keep them in a resting state (see chapter 2.1.5) at a concentration of  $2 \times 10^6$  cells/ml. The day after nucleofection the cells were then used to determine the expression of the gene of interest (by flow cytometry see chapter 2.2.3) as well as tested in HIV-1 Vpr-BlaM fusion assay (see chapter 2.2.10.3).

### 2.2.6 Knockout generation in primary CD4 T cells and monocytic cells

For generation of knockout (KO) CD4 T cells, the cells were used directly after isolation from whole blood as described in chapter 2.2.2. For generation of KO monocytic cells, CD14-positive monocytes were isolated by negative isolation as described in chapter 2.2.2. The KO procedure for CD4 T cells has been previously described [304] and the protocol was adjusted for the generation of KO in primary monocytic cells. Briefly, in order to form CRISPR-Cas9-gRNA ribonucleoprotein (RNP), synthetic 100 pmol sgRNA was incubated with recombinant 40 pmol NLS-Cas9 protein for 10 min at RT. After incubation the RNP complex was diluted with sterile filtered H<sub>2</sub>O (0.22  $\mu$ m pore size) to a final concentration of 20  $\mu$ M. After washing the cells twice with PBS,  $2 \times 10^6$  cells were resuspended in P3 buffer from P3 Primary Cell 96-well Kit and 2  $\mu$ l of the corresponding 20  $\mu$ M RNP suspension was added. Here, to ensure an efficient KO of the gene of interest, two to four RNPs with different sgRNAs specific for the gene of interest were added to suspension. The cell/RNP mixture was then carefully pipetted into a 16-well reaction cuvette of the 4D-Nucleofector System, avoiding the formation of air bubbles in the cuvette. Following the nucleofection with the program EH-100, 100  $\mu$ l pre-warmed RPMI medium (w/o supplements) was added into each cuvette, and the cells were kept at 37 °C for 15 min to recover. In the case of KO in primary CD4 T cells, the cells were seeded into 96 Well flat bottom plates at a concentration of  $2 \times 10^6$  cells/ml, with medium to keep the cells resting (see chapter 2.1.5). For KO generation in monocytic cells, the cells were seeded into 96 well flat bottom plates with 100 000 cells/well and differentiated into M2 macrophages (see chapter 2.1.5).

### 2.2.7 *In vitro* trogocytosis and functional assays

#### 2.2.7.1 Co-culture of 293T/HeLa cells with SupT1/primary CD4 T cells

To create donor cells which transiently express Fc $\gamma$ R and/or other receptors of interest the cells were transfected with the corresponding expressing vector on day 1. For the usage of 293T cells as donor cells, 200 000 293T cells were seeded in 24 well plate and transfected using 520 ng of plasmid DNA with 1  $\mu$ l linear polyethylenimine (PEI) and 100  $\mu$ l DMEM medium (w/o supplements). The DNA/PEI mixture was incubated at RT for 20 min before adding the mixture to the 293T cells. In the case of using HeLa cells as donor cells, the cells were transfected with corresponding plasmid DNA and Lipofectamine 3000, according to manufacturer's protocol. Briefly, 50  $\mu$ l Opti-MEM™ I Reduced Serum Medium was mixed with 1  $\mu$ g plasmid DNA. In an extra tube 2.5

$\mu$ l of Lipofectamine 3000 was mixed with 50  $\mu$ l Opti-MEM™ I Reduced Serum Medium. The tubes were incubated for 5 min at RT before mixing both solutions and incubation for additional 25 min at RT. Subsequently, 100  $\mu$ l transfection mix was added to the culture.

The next day the donor cells were reseeded into 96 well flat bottom plate with  $1 \times 10^5$  cells/well. The day after, recipient cells (SupT1 or primary CD4 T cells) were labeled with cell trace dye. For this, the cells were washed once with PBS and spun down and resuspended in cell trace dye solution (PBS with cell trace dye diluted 1:20 000) with  $1-10 \times 10^6$  cells/ml. The cell suspension was then incubated for 20 min in a water bath at 37°C before stopping the reaction by adding the double amount of RPMI c++. The cells were then washed twice with PBS, before resuspending them in RPMI c++ with a concentration of  $2.5 \times 10^6$  cells/ml.

To start the co-culture, medium was carefully removed from the donor cells without detaching the cells and 100  $\mu$ l of RPMI c++ was added into each well. Subsequently, 100 $\mu$ l with  $2.5 \times 10^6$  cells/ml of recipient cell suspension was carefully added into each well.

If trogocytosis enhancement or inhibition was tested by the addition of antibody or human sera, the antibody/sera were added to the donor cells 30 min before the addition of the recipient cells to the culture (2.5  $\mu$ g/ml final concentration of antibody if not indicated differently, human sera were added to the culture medium with 10% final concentration in the co-culture). Human sera were inactivated at 56 °C for 1 h previously to the addition (HIV-1 viral load of patients was less than 50 copies/ml).

If the experiment was carried out under IgG low conditions, all cells were cultured before the experiment for at least one week in RPMI c++ with low IgG FCS. During the co-culture all steps were performed using also RPMI c++ with low IgG FCS as culture medium.

After 24 h of co-culture the cells were harvested and further analyzed for receptor transfer by flow cytometer (see chapter 2.2.3).

### **2.2.7.2 Co-culture of M2 macrophages and CD4 T cells**

PBMC were freshly isolated from whole blood and monocytes were isolated by magnetic fractioning with anti-CD14 microbeads (positive selection) as described above (see chapter 2.2.2.1) and differentiated to M2 macrophages by the addition of M-CSF and IL-4 to the culture medium (see chapter 2.1.6). The flow through of the magnetic fractioning as well as remaining PBMCs were cryopreserved with cryopreservation media at -80 °C with a density of  $10 \times 10^7$  cells/ml. On the day of co-culture start, the cryopreserved cells were thawed and CD4 T cells were isolated by magnetic fractioning using microbeads of the CD4 T cell isolation Kit (negative isolation, see chapter 2.2.2.1). After isolation, the cells were counted and labeled with a cell trace dye similarly as described above for SupT1 (see chapter 2.2.7.1). The medium of the adherent and differentiated M2 macrophages was then carefully removed and 100 $\mu$ l of RPMI c++ was added on top of the cells. Subsequently, 100  $\mu$ l with  $2 \times 10^6$  cells/well of cell trace labeled CD4 T cells was added to the macrophages.

If trogocytosis was enhanced by the addition of an antibody, the antibody was added to the M2 macrophages 30 min before the addition of primary CD4 T cells to the culture (Alemtuzumab or isotype control with a final concentration of 0.1  $\mu$ g/ml). The cells were then co-cultured for 2 days and subsequently CD4 T cells were harvested from the culture and either directly analyzed for trogocytotic transfer of receptors or further purified by sorting the cell trace positive CD4 T cells by flow cytometry (see chapter 2.2.8), before performing further functional experiments such as testing in HIV-1 infection or fusion assays.

### **2.2.7.3 Screening of transferred receptors by surface marker in BD Lyoplate™**

M2 macrophages and CD4 T cells were co-culture as described in chapter 2.2.7.2. After co-culture, CD4 T cells co-cultured or not co-cultured (control), were harvested and sorted by their cell trace positivity (see chapter 2.2.8). The sorted CD4 T cells (co-cultured or not co-cultured) as well as not co-cultured M2 macrophages were then stained with the BD Lyoplate antibody panel (242 monoclonal primary antibodies and the corresponding secondary antibody conjugated with Alexa Flour 647) as described in chapter 2.2.3.

### **2.2.7.4 Testing the binding of human IgG to primary CD4 T cells**

Freshly isolated CD4 T cells from whole blood (see chapter 2.2.2.1) were incubated with human BD Fc Block in PBS for 20 min at RT in 96 well V-shape plate. After incubation, the cells were spun down and resuspended in 50µl of the selected human serum and incubated for 20 min at 4°C. The cells were washed with FACS buffer to remove excessive primary antibodies and then incubated with APC AffiniPure F(ab')<sub>2</sub> Fragment Goat Anti-Rat IgG (H+L) at 4°C for 20min. After washing the cells with FACS buffer twice, the APC signal was determined by flow cytometry.

### **2.2.7.5 Determination of chemokine migration on CD4 T cells after co-culture**

Primary CD4 T cells were co-cultured with HeLa cells transiently expressing CD32B-EGFP or H2B-EGFP together with CCR5 or CXCR4-HA as described above (see chapter 2.2.7.1). After co-culture, 250 000 CD4 T cells were seeded in the upper part of a transwell system (3.0 µm pore). 500 µl of RPMI medium with 0.2 % FCS and the corresponding chemokine was added in the lower part of the transwell system (SDF-1α 1000 ng/ml; RANTES 800 ng/ml). The upper transwell part with the cells was then carefully laid on top of the medium in the lower part and incubated for 3h at 37°C. After incubation the upper part was carefully removed and the total number of cells that have migrated to the lower part was quantified by flow cytometry using BD Trucount™ Absolute Counting tubes.

### **2.2.7.6 Testing the binding of co-cultured CD4 T cells to ICAM-1**

The method was adapted from a protocol previously described [307]. Briefly, to coat the surface of a 384 well plate with recombinant ICAM-1 (in 1 mM CaCl<sub>2</sub>/ 2 nM MgCl<sub>2</sub> in PBS), each well was filled with ICAM-1 solution and the plate was incubated for 1 h at 37 °C. Until the usage the plate was sealed and kept at 4 °C. Into each well, 20 000 co-cultured and sorted CD4 T cells (see chapter 2.2.7.2 and 2.2.8) were seeded in adhesion solution and incubated for 30 min at 37 °C. Subsequently the cells were washed in the plate with 30 µl adhesion solution three times and loaded with 30 µl adhesion solution and 10µl CellTiter-Glo 2.0 solution. Binding was determined by the number of cells remaining in each well, quantified with CLARIOstar Plus plate reader.

### **2.2.7.7 Trapping of PGT151 with human CMV glycoproteins**

Purified soluble HCMV glycoproteins (gp) and ICOSL were prepared (as described previously [221]) and kindly provided by the lab of Prof. Dr. med. Hartmut Hengel - University of Freiburg. The bNAbs PGT151 was incubated at a concentration of 0.6 µM with different titrated amounts of the soluble gps (or ICOSL) for 30 min at 37°C in RPMI media (w/o supplements). The PGT151/peptide mixture was then added to donor cells (293T cells CD32B-mtagBFP or mtagBFP

positive) in trogocytosis assay (see chapter 2.2.7.1 ) 30 min before adding the recipient cells (SupT1) to the co-culture. The next day, the percentage of mtagBFP positive SupT1 cells was analyzed by flow cytometry.

### **2.2.7.8 Transfer analysis of GM1**

M2 macrophages were differentiated from CD14-positive monocytes in 96 Well flat bottom plates with 100 000 cells/well as described in chapter 2.1.5. In order to label Monosialotetrahexosyl-ganglioside (GM1) the binding of Cholera Toxin B subunit, biotin conjugated, was used. On the day of starting the co-culture with CD4 T cells, the culture medium of the adherent M2 macrophages was carefully removed and the cells were rinsed with cold RPMI c++ before adding 200µl/well of Cholera toxin subunit (CT-B) staining solution (1 µg/ml Cholera Toxin B subunit, biotin conjugated, in RPMI c++) and incubation for 10 min at 4°C. Subsequently the solution was carefully removed and the adherent cells were washed with cold PBS three time. After the washing the M2 macrophages were co-cultured with primary CD4 T cells (as described in chapter 2.2.7.2) and trogocytosis was enhanced by the addition of Alemtuzumab. After co-culture the CD4 T cells were harvested and analyzed and incubated with HIV-1 Vpr-GFP (see chapter 2.2.10.5) and subsequently stained with anti-CD32 AF647 antibody and conjugated streptavidin AF594 followed by confocal microscopy analysis.

### **2.2.8 Flow cytometric sorting of cell trace positive cells after co-culture**

To sort recipient cells from donor cells for further experimental procedure, the recipient cells were sorted for their cell trace positivity by flow cytometry using BD FACS Aria Fusion device. The day before, 15 ml collection tubes were filled with 3 ml FCS for pre-coating and kept rolling over night at 4 °C. The next day, cells were harvested from the co-culture, spun down and resuspended in 500 µl FACS buffer (see chapter 2.1.5) and kept on ice until sorting. FCS from the precoated collection tubes was removed and each tube was filled with 2 ml RPMI medium with 20 % FCS as collection medium. The cells were meshed through a 70 µm cell strainer previous to loading, to ensure a single cell in the suspension and sorted using 70 µm nozzle. After gating for viable single cells, the highly cell trace positive cell population was gated for sorting into the tube. In the case of cell trace far red positive cells the APC channel was used for gating, whereas in the case of cell trace violet stained cells, the BV421 channel was used for gating. After sorting, the cells were spun down and resuspended in RPMI c++ for counting. To ensure the same treatment of the cells, not co-cultured recipient cells were sorted as control in the same way as the co-cultured cells.

### **2.2.9 Immunoblot Analysis of Vps4 expression**

#### **2.2.9.1 Total Protein extraction and BCA-assay**

Cells were harvested and washed with PBS before freezing down the cell pellet at -80°C until total protein extraction was performed. Here, the cell pellet was thawed and resuspended in hunt lysis buffer (see chapter 2.1.5) supplemented with protease inhibitor cocktail (ratio 1:7, protease inhibitor cocktail to hunt lysis buffer). The cell suspension was then repeatedly freeze/thawed by short incubation steps of the tubes in liquid nitrogen to freeze and thawing at RT to ensure physical disruption of the cells. The samples were then centrifuged for 30 min at 4 °C at 20 000 g. The

supernatant was harvested and stored at -20 °C until performing bicinchoninic acid (BCA)-assay for protein quantification.

For BCA-assay the supernatant was thawed and 10 µl of the supernatant (or 1:10 diluted with H<sub>2</sub>O) were added to 96 well flat bottom plate. In separate wells of the 96 well plate a dilution row of bovine serum (concentration reaching from 0.0 to 2.0 mg/ml) was pipetted to generate protein standard samples. 100 µl of solution A of the Pierce (BCA) protein assay kit (previously supplementing solution A with solution B in a 50:1 dilution) was added into each well. The plate was then incubated for 20 min at 37 °C and total protein quantification was colorimetrically measured using CLARIOstar Plus plate reader.

### 2.2.9.2 Immunoblot analysis

From each sample 25 µg protein was mixed with 4x NuPAGE LDS (1:4 dilution) and incubated for 10 min at 70 °C. The samples as well as 5 µl of PageRuler were then loaded on 4-12 % SDS gel (precast gels with neutral pH and Bis-Tris buffering) in 1x NuPAGE MOPS SDS running buffer for 1.5 h at 150 V. Subsequently the proteins were blotted from the gel to 0.45 µm nitrocellulose membrane at 30 V for 1 h in 1x NuPAGE transfer buffer with 10 % methanol. Blocking of the membrane after blotting was performed in 5 % milk in 1x TBS for 30 min at RT (shaking). After washing the membrane 3 x 10 min in 1x TBS, the membrane was incubated with primary antibody solution (anti-Vps4 1:500 diluted in antibody solution) overnight at RT shaking. The next day the membrane was washed 3x 10 min in 1x TBS buffer before incubation with the secondary antibody (anti-mouse-HRP IgG (H and L) diluted 1:10 000 in 5 % milk) for 1 h at RT shaking. After washing the membrane 3x 10min with 1x TBS buffer, the membrane was incubated with developing solution (Clarity wester ECL substrate kit). To detect the chemiluminescence and developing digital images, the membrane was analyzed using Vilber Fusion FX. Subsequently, the membrane was washed 3x 10min with 1x TBS before incubating with the next primary antibody (anti-Vinculin 1:2000 diluted in antibody solution) overnight as described above. The next day the membrane was washed and incubated as described above with the secondary antibody (anti-rabbit IgG (H and L) diluted 1: 10 000 in 5% milk) as well as developed and analyzed as described above.

### 2.2.10 Viral assays

#### 2.2.10.1 Production of sucrose cushion-purified HIV-1 stocks

The day before transfection, 8x 10<sup>6</sup> 293T cells were seeded into 15 cm cell culture dishes. After 24 h, the cells were transfected with plasmid DNA encoding the viral DNA (see chapter 2.1.4) and 112.5 µl of linear PEI in 2.5 ml DMEM (w/o supplement). Here, for the production of viral vectors to perform HIV-1 infection assay, 18.75 µg viral DNA was used in the transfection mix. In order to produce viral stocks for HIV-1-fusion assay, 15 µg of viral DNA was used together with 12.5 µg of pCMV BlaM-Vpr vector in the transfection mix. In the case of production of viral stocks for the HIV-1-binding assay, 17 µg of viral vector plasmid was combined with 17 µg of pCMV GFP-Vpr vector. The transfection mix was then incubated for 20 min at RT and subsequently added on top of the cells. After 72h, the supernatant of the cells was harvest, filtered (0.45 µm) and then 32 ml supernatant was overlaid on ml sucrose (25 %). The samples were then ultra-centrifuged at 28 000 rpm for 1.5 h at 4° C. The concentrated virus was then harvested after removing the supernatant and resuspended in 100 µl PBS. Until usage the viral stocks were stored at -80°C.

### 2.2.10.2 SG-PERT

To determine the amount of virus particles after sucrose cushion-purification, the reverse transcriptase activity was quantified by qPCR using the SYBR Green I-based PCR-enhanced reverse transcriptase assays assay (SG-PERT) described previously [308]. Briefly, the virus stocks and SG-PERT standard (pHIV #528 virus) were lysed with SG-PERT lysis buffer (ratio 1:2) to release the RT from the particles and further diluted with SG-PERT dilution buffer (1x diluted with H<sub>2</sub>O), with increasing 1:10 dilution steps. Each sample was then added to SG-PERT reaction buffer (1:2) in 96 Well PCR plate and reaction is started in the qPCR cycler (see Table 4). During the first reaction step, the RT transcribed the supplied RNA (from MS2 bacteriophage) in the reaction buffer to cDNA. The generated cDNA was then used as a template by the GoTag Hotstar Polymerase using the supplied primers in the reaction buffer. The generated DNA copies were then subsequently quantified by the signal of the fluorescence of the SYBR green dye intercalating into the amplified DNA. For final quantification the *cq* values of the SG-PERT standard was used to define the amount of RT units in the viral stock samples. Analysis performed with CFX-Manager V3 BioRad. Composition of the SG-PERT buffers are listed in chapter 2.1.5.

**Table 4 | SG-PERT reaction steps.**

reaction step	temperature	duration	cycle repeats
RT activity	42°C	20 min	1
RT inactivation	95 °C	2 min	1
Initial denaturation	95 °C	5 sec	1
Denaturation	60 °C	5 sec	40x
Annealing	72 °C	15 sec	
Extension	80 °C	7 sec	
Meltingcurve	60 °C	30 sec	1
Meltingcurve	60 °C (+0.5 °C/cycle)	5 sec	70x

### 2.2.10.3 HIV-1 BlaM-Vpr fusion assay

The protocol was adjusted from the protocol previously described [309]. Here, 200 000 co-cultured and sorted CD4 T cells per 96 V-shaped well were incubated with either X4 HIVivo [304] or R5 HIVivo [310] containing BlaM-Vpr (as described above) for 4 h at 37 °C. After the incubation the cells were spun down and washed twice in CO<sub>2</sub>-independent medium, and then resuspended in 100µl CCF2/AM staining suspension (2 µl CCF2, 8 µl of solution B of the kit together with 10 µl 250 nM probencid and 1 ml CO<sub>2</sub>-independent medium with 10% FCS). The cells were then incubated in the staining suspension for 16 h at RT in the dark and subsequently washed twice with PBS. After resuspending in 4% PFA the cells were incubated at RT for 90 min, for inactivation of the virus and fixation of the cells. Subsequently, the cells were spun down at 1100 g 8 min and resuspended in 100 µl FACS buffer for flow cytometric analysis.

#### 2.2.10.4 HIV-1 infection assay

To study full infection of CD4 T cells, the cells were inoculated with GFP-reporter viruses (for X4 tropic virus infection study NLENG1-IRES [311] and for R5 tropic virus infection study NLENG1-I-70 [311] was used). Therefore, the cells were seeded in a 96 V-shape well plate with 200 000 cells/well in RPMI c++ and virus was added with an MOI of 0.5-1 (if not indicated differently). Subsequently spinoculation for 2.5 h at 650 g and 37 °C was performed (if not indicated differently), before resuspending the cells and cultivating for 3 days at 37°C. On the day of analysis, the cells were spun down, washed once with PBS and resuspended in 4% PFA and incubated at RT for 90 min in order to inactivate the virus and fixing the cells. After the incubation, the cells were spun down at 1100 g for 8 min and resuspended in FACS buffer for flow cytometric analysis. Previously to infection study, the viral stocks were titrated with freshly isolated CD4 T cells (200 000 cells/well) from whole, by inoculation with different viral stock volumes (as described above) and MOI was determined according to the GFP-positive cell population frequency and total cell number per well.

#### 2.2.10.5 HIV-1 Vpr-GFP binding assay

After sorting co-cultured CD4 T cells (see chapter 2.2.8), 200 000 CD4 T cells per well were seeded in to 96 V-shape well plate in CO<sub>2</sub>-independent medium (with 10 % FCS). In case of treatment with antiviral drug/and blocking antibody, AMD3100 (16 µg/ml) and blocking antibody (25 µg/ml) (see chapter 2.1.3) were, added to the cells. After incubation for 15 min at 16 °C, HIV-1 Vpr-GFP virus was added to the cells and cells were incubated for 1 h at 16°C. After the incubation, the cells were spun down and washed with FACS buffer, following antibody staining for flow cytometric analysis (see chapter 2.2.3) or confocal microscopy (see chapter 2.2.10.6).

In the condition of enzymatic digest with heparinase/chondroitinase of the sorted co-cultured CD4 T cells (or HeLa cells), the cells were incubated with 1 U/ml of heparinase I/II/III and chondroitinase ABC from *Proteus vulgaris* for 15 min at 37 °C in PBS stopping the reaction by addition of medium supplemented with 10 % FBS. The cells were then spun down and washed twice with PBS before inoculation with the virus as described above.

#### 2.2.10.6 Confocal microscopy analysis of HIV-1 Vpr-GFP binding and co-localization

After co-culture of CD4 T cells and M2 macrophages as described above (see 2.2.7.2), CD4 T cells were sorted by flow cytometry and incubated with HIV-1 Vpr-GFP followed by staining for cell surface receptors of interest, as described before (see chapter 2.2.3 and 2.2.10.5). After the staining the cells were washed twice and fixed with 4 % PFA for 10 min at RT and washed again. Cells were then fixed on culture plates with ProLong Diamond Antifade Mountant. To analyze the images the software Imaris Viewer was used and Intensity profiles were evaluated with Image J software.

### 3. Results

#### 3.1 CD32 exposure on CD4 T cells is cell-contact dependent

In a pilot experiment conducted with the intention to recapitulate experiments by Descours and Petitjean *et al.* [142], a culture of peripheral blood mononuclear cells (PBMC) was infected with X4 HIV-1 Green fluorescent protein (GFP) reporter virus. Subsequently, the infection rate as well as CD32 surface levels were analyzed three days post infection on the fraction of CD4 T cells. This determined 9.3% of the cells to be GFP positive, of which 28% (2.6% of all CD4 T cells) were also CD32 positive. However, CD32 positivity (4.59% among all cells) was observed also in the GFP-negative population (Figure 6A, left panel). In parallel, CD4 T cells were isolated from the PBMC culture prior to viral inoculation. The sample with the isolated CD4 T cells showed also a high infection rate with 5.26% GFP-positive cells. However, the frequency of CD32-positive cells was very low (Figure 6A, right panel), indicating a potential influence by other immune cells on CD32 positivity of CD4 T cells.

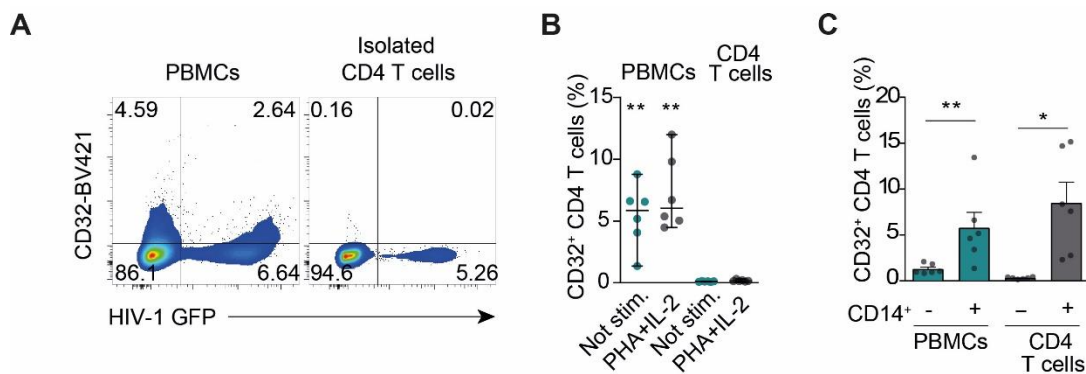


**Figure 6 | CD32 exposure on CD4 T cells is independent of infection or activation status, but influenced by the presence of co-cultured cells**

**A**, Infection of freshly isolated PBMCs or CD4 T cells highly purified by negative selection with HIV-1 GFP reporter virus. After 3 days CD32 and GFP expression was assessed by flow cytometry. One representative donor is shown ( $n=3$ ). **B**, Activation with PHA/IL-2 or left untreated PBMCs and negative-selected CD4 T cells were analyzed for CD32 expression after 3 days of culture. Median with 95% CI are shown ( $n=6$ ). Asterisks indicate statistical significance by one-way ANOVA relative to unstimulated (Not stim.) CD4 T cells.  $P$  values were corrected for multiple comparison (Tukey). **C**, Depletion of CD14<sup>+</sup> cells from PBMC. Cultivation for 3 days of PBMC +/- CD14<sup>+</sup> cells or isolated CD4 T cells cultured +/- CD14<sup>+</sup> cells, following CD32 expression analysis. Mean  $\pm$  s.e.m. are shown ( $n=6$ ). Asterisks indicate statistical significance by one-way ANOVA.  $P$  values were corrected for multiple comparison (Tukey). \* $P \leq 0.05$ ; \*\* $P \leq 0.01$ . Experiments performed by Maximilian Münchhoff and Manuel Albanese.

To assess whether CD32 expression on CD4 T cells is dependent on HIV-1 infection or on activation, we stimulated cells with Phytohemagglutinin (PHA) + Interleukin-2 (IL-2). The CD32 exposure was only detected on CD4 T cells when kept in PBMC co-culture. Isolated cells remained negative, also following stimulation (Figure 6B), indicating an HIV-1 infection-independent and activation-independent CD32 expression on CD4 T cells.

Aiming at investigating the dependency of the CD32 exposure to cell culture composition, we isolated CD14-positive monocytes from the PBMC culture. As a consequence, the CD4 T cells showed a decrease of CD32 positivity in the CD14-negative PBMC culture, whereas in the presence of CD14-positive cells, the levels of CD32-positive CD4 T cells remained high. Consistent with these findings, addition of CD14-positive cell fraction to the isolated autologous CD4 T cells

showed CD32 levels on CD4 T cells comparable to the whole PBMC culture condition (Figure 6C).

So far, we demonstrated that the presence of CD14-positive monocytes and monocyte-derived cells strongly influenced the CD32 exposure on CD4 T cells and that this event is independent of HIV-1 infection. We next aimed to examine whether the CD32 exposure on the surface was cell-contact-dependent, and which type of monocyte-derived cells influenced its surface exposure. For this purpose, monocytes were differentiated into monocyte-derived macrophages (MDM), M1 macrophages or M2 macrophages and subsequently co-cultured with autologous CD4 T cells. The cells were either kept in cell-contact co-cultures or separated by a transwell membrane system (Figure 7A). Analyses of the CD4 T cells for their CD32 positivity after co-culture revealed a strong cell-contact interaction dependency, since the separation of the cells by transwell resulted in CD4 T cells being largely negative for CD32. As expected, also the CD4 T cells that had migrated through the transwell membrane and harvested from the bottom of the transwell, which therefore had cell-contact to the monocytic cell layer, showed high CD32 percentages similar in magnitude to the CD4 T cells kept in direct contact co-culture from the beginning of the experiment (Figure 7B).

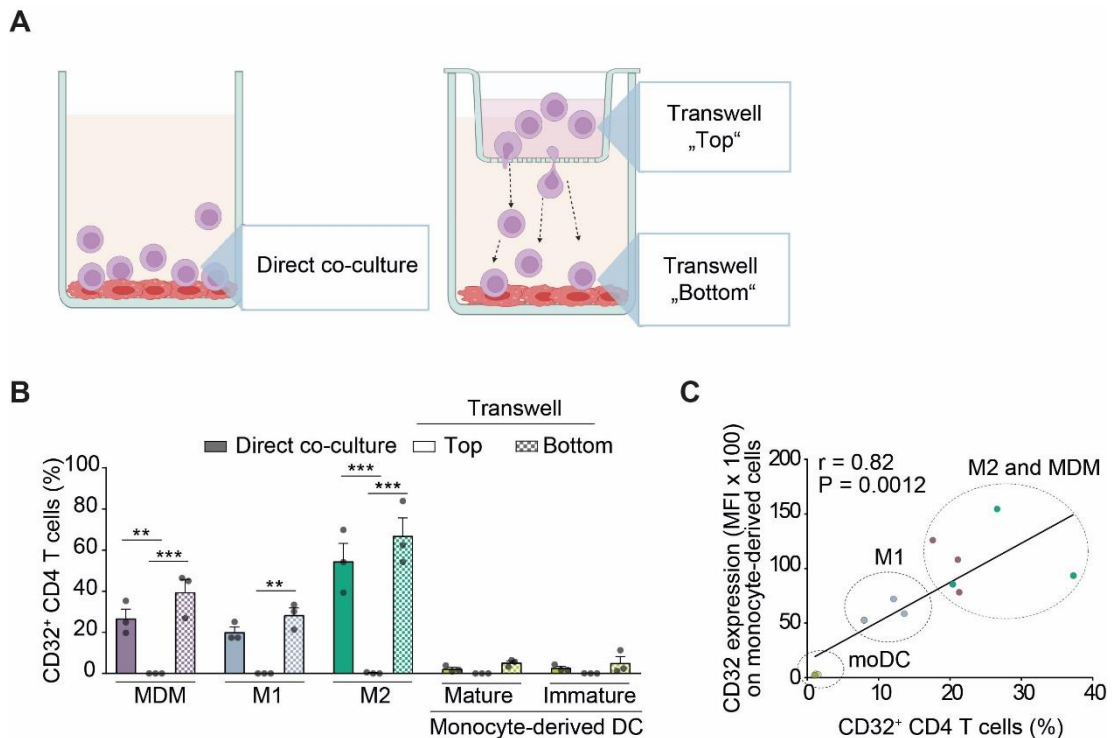


**Figure 7 | Co-culture with myeloid cells in direct cell contact leads to exposure of CD32 and HLA-DR on CD4 T cells**

**A, B**, Schematic of the experimental set up: After isolation of CD14<sup>+</sup> monocytes, cells were differentiated into different myeloid lineages for 7 days followed by co-culture with autologous CD4 T cells. The co-culture was either in direct cell-cell contact or T cells separated from the other cells in the upper part of a transwell setup (schematic overview (**A**)). (**B**) Analysis for CD32 exposure on CD4 T cells kept isolated in transwell (top), CD4 T cells kept in close contact with the differentiated myeloid cells (direct co-culture), as well as CD4 T cells that had migrated to the bottom of the transwell and which therefore had cell-cell contact with differentiated myeloid cells (bottom). Mean  $\pm$  s.e.m. are shown ( $n=3$ ). Asterisks indicate statistical significance by two-way ANOVA.  $P$  values were corrected for multiple comparison (Tukey). The illustration was created with BioRender.com. **C**, Pearson correlation plot for frequency of CD32- positive CD4 T cells, which had been in a 2 day co-culture with indicated differentiated myeloid cells and the expression levels of CD32 given as mean fluorescence intensity (MFI) on the corresponding myeloid cells. \*\* $P \leq 0.01$ ; \*\*\* $P \leq 0.001$ . Experiments performed by Manuel Albanese.

The M2 macrophage lineage showed the strongest effect with 66.8% of the CD4 T cell being CD32 positive after direct co-culture (Figure 7B), followed by co-culture with MDM or M1 macrophages. In contrast, only low percentages of CD32-positive CD4 T cells were found in the co-culture with monocyte-derived DC.

The CD32 expression on myeloid cells was different for each sublineage (Figure 7, y-axis). Therefore, we aimed to analyze the CD32 percentage of CD4 T cells together with the CD32 expression levels on the monocyte-derived cells and observed a strong correlation ( $r=0.82$ ;  $P=0.0012$ ; Figure 7C). Notably, besides CD32 also the percentage of HLA-DR demonstrated an increase among direct co-cultured T cells, and also here the culture with M2 macrophages, showed the highest percentages (data not shown).

Interestingly, CD32 expression correlated with HLA-DR expression on CD4 T cells, after M2 co-culture, with more than 15% of the cells being double-positive (Figure 8).

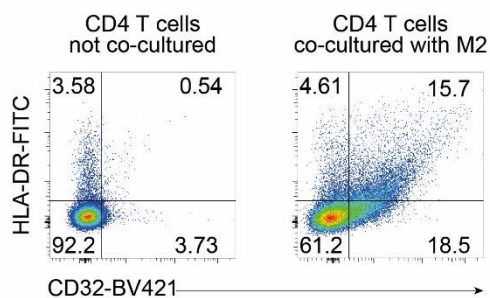


**Figure 8 | HLA-DR and CD32B double-positive CD4 T cells after co-culture with M2 macrophages.**

CD4 T cells directly co-cultured with M2 macrophages (as described in Figure 7) were co-stained for CD32 and HLA-DR. One representative donor out of three is shown.

In a follow-up experiment, we could exclude the possibility that the CD32 levels on T cells was induced by T cell's activation, since even long-term culture after activation did not show CD32-positive T cells (data not shown).

The capture of FcγRs by non-expressing cells has previously been reported [297], which could explain the dependency of cell-cell contact and correlation of CD32 exposure on T cells to the expression on the co-cultured cells (Figure 7 B and C). Together with the transfer of FcγRs some reports showed also a “co-transfer” of other cell surface receptors or even membrane parts in an FcγR-dependent manner in a process called “trogoncytosis” [267, 287, 293, 295, 296]. We therefore hypothesized that CD32 on CD4 T cells was actually not expressed *de novo*, but previously transferred from a CD32-expressing cell such as an M2 macrophage and this also could induce transfer of other receptors such as HLA-DR.

To assess whether the increased HLA-DR levels on CD4 T cells after co-culture was also due to transfer from M2 macrophages to CD4 T cells we designed a CRISPR/Cas9 knockout (KO) experiment. In this approach, HLA-DR expression was abrogated by nucleofection of specific Cas9–gRNA ribonucleoprotein complex (RNP) [304], targeting the first exon of *HLA-DR*. In a first experimental setup, HLA-DR was knocked out in M2 macrophages (KO M2) to prevent the potential transfer of HLA-DR from macrophages to T cells. We then analyzed the HLA-DR positivity of CD4 T cells co-cultured with HLA-DR KO M2, wildtype M2 (WT) or not co-cultured CD4 T cells. In the co-culture of WT M2 and CD4 T cells, an increase of HLA-DR-positive CD4 T cells was detected as observed previously. However, the percentage of HLA-DR on CD4 T cells co-cultured with HLA-DR KO M2 cells was comparable to levels on the not co-cultured T cells (data not shown).

In a second part of the experiment, we addressed the question from a different angle by performing the HLA-DR KO in CD4 T cells. Again, we analyzed the HLA-DR expression on CD4 T cells after co-culture with WT M2 cells, HLA-DR KO M2 cells or not co-cultured cells. CD4 T cells not co-cultured and co-cultured with HLA-DR KO M2 cells showed no expression of HLA-DR on their surface. Nevertheless, co-culture of HLA-DR KO CD4 T cells with WT M2 cells resulted in HLA-DR percentages similar to the percentages seen in WT CD4 T cells/WT M2 cells co-culture (data not shown).

These experiments demonstrated that the HLA-DR observed on CD4 T cells after co-culture was the result primarily of the transfer of HLA-DR from M2 macrophages. Given the similar expression of CD32 on the co-cultured CD4 T cells we speculated that also CD32, similar to HLA-DR, was transferred from macrophages.

The CD32-mediated transfer of cell surface receptors and antigens has been reported and investigated, yet is not fully understood [293, 294, 297]. Therefore, it was of interest for us to investigate further this phenomenon and its possible impact on the surface proteome of CD4 T cells.

## 3.2 Investigating CD32 as mediator of trogocytosis

### 3.2.1 Testing CD32 genes

Human CD32 is encoded by three different genes named FCGR2A, FCGR2B, and FCGR2C. To investigate, which subclass can be transferred from one cell to another and, in addition, also whether CD32 mediates the transfer of other receptors or membrane patches, we established a trogocytosis *in vitro* model. Here, 293T cells are used as donor cells, transiently expressing the FcγR fused to a fluorescent protein. The receptor of interest is also co-expressed transiently by the donor cells and can be detected by staining with a specific antibody. The T cell line SupT1 is used as recipient cell in the model. To distinguish the two cell populations in subsequent flow cytometer analysis, the recipient cells, prior to co-culture, are stained with a cell trace dye. By gating for the cell trace-positive cell population, the transfer of the protein of interest can be investigated (Figure 9).

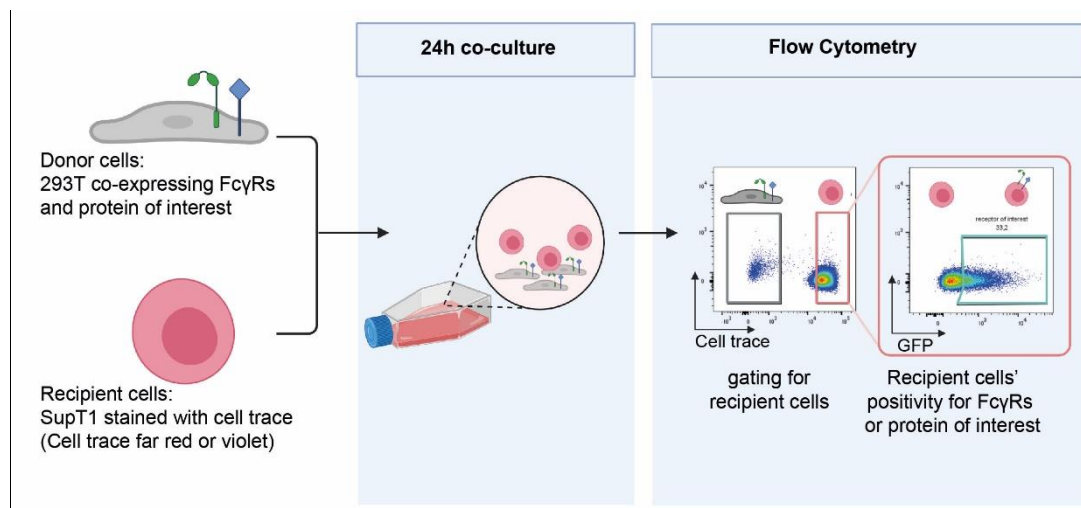


**Figure 9** | *In vitro* model to investigate FcγR-mediated trogocytosis.

Experimental workflow: 293T cells (donor cells) transiently expressing the FcγRs together with the protein of interest, are cultured together with SupT1 cells (recipient cells, previously stained with a cell trace dye) for 24 h. After co-culture, the cells are harvested and analyzed by flow cytometry, gating the recipient cell population according to the cell trace-positivity and analyzing the transfer of receptors from the 293T cells. The illustration was created with BioRender.com.

To ensure we can distinguish FcγR-mediated trogocytosis from other potential membrane transfer mechanisms such as exosome uptake, 293T expressing the intracellular protein Sterile Alpha Motif and Histidine-Aspartic acid domain containing protein 1-GFP (SAMHD1-GFP) instead of FcγRs, was used as control and the transfer detected in this co-culture condition was set as baseline. With this approach we could observe the transfer of CD32A-, -B- and -C-GFP as well as the FcγRI (CD64-GFP). We also co-expressed on 293T cells CCR5 or CD4 to investigate the potential co-transfer of these receptors, in the context of expression of one of the FcγRs. By using this setup, we could show that CD32A, B and C can be transferred and also mediate co-transfer of the receptors of interests tested. Nevertheless, transfer of CD4 was only detected above the baseline in the presence of CD32A, B or C and CCR5 only in the presence of CD32B and C. In

all cases CD32B-GFP showed the highest transfer efficiency (21-39% GFP positive cells) and also mediated the highest transfer of the receptors of interest (CCR5 31.25% and CD4 16.2% positive cells). The deletion of the cytoplasmic tail of CD32B (CD32B  $\Delta$ CT-GFP) diminished the transfer of the receptor itself but also of CD32-dependent transfer of other receptors (CCR5 11.2% and CD4 4.2% (Figure 10).

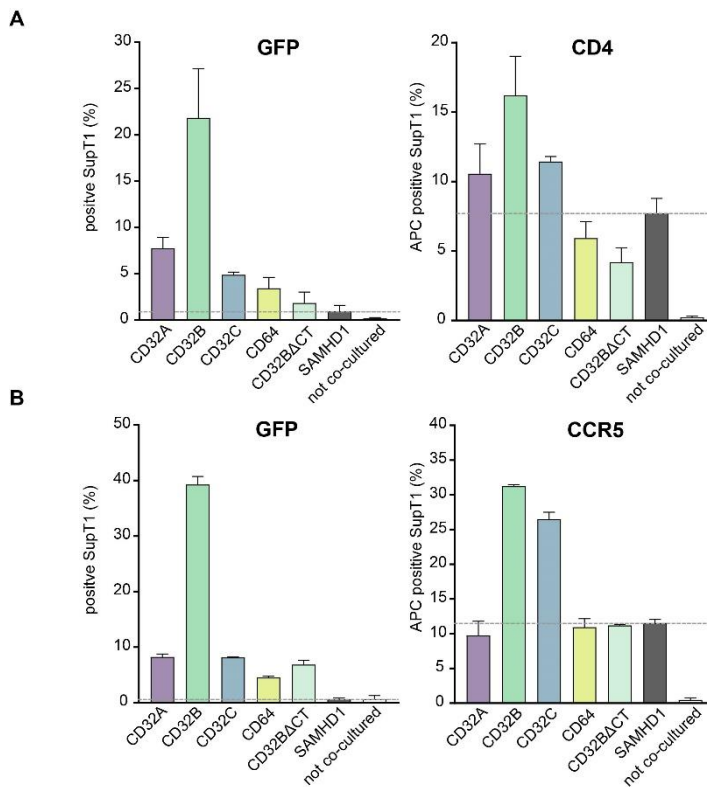


**Figure 10 | Fc $\gamma$ R<sub>s</sub> mediate the transfer of CCR5 and CD4.**

After co-culture (as described in Figure 9) with 293T cells expressing GFP fusion proteins of Fc $\gamma$ R<sub>s</sub> variants or SAMHD1 together with CD4 (A) or CCR5 (B) the transfer of the receptors to SupT1 cells was investigated and compared with detection on not co-cultured SupT1 cells. The transfer levels in the control condition with SAMHD1 were set as baseline (dashed line). Mean  $\pm$  SD of technical replicates.

### 3.2.2 Autoantibodies can mediate trogocytosis enhancement

In the following experiments, we used fetal calf serum (FCS) with depleted IgG (“IgG low” FCS) as supplement in the culture medium for cultivating the donor cells, recipient cells and during co-culture. In previous experiments, we could observe with this culture condition a decrease of Fc $\gamma$ R-mediated trogocytosis (“IgG low” vs “regular” FCS, data not shown). After this initial observation, a possible role of antibody-induced trogocytosis was raised since this was also reported in the context of Fc $\gamma$ R-mediated trogocytosis [289, 295, 300]. This was then examined by testing the trogocytosis effect of sera from patients with either infectious diseases or autoimmune diseases known to induce autoantibody production in patients (Figure 11A).

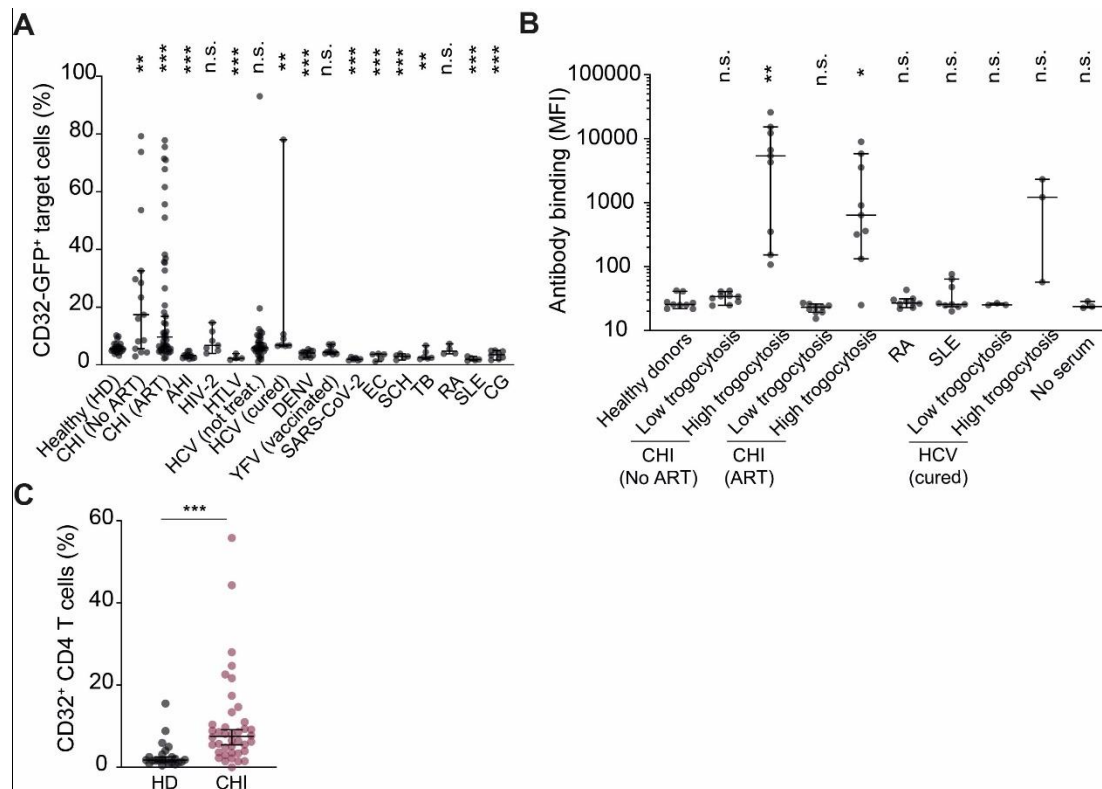


**Figure 11 | CD32 transfer is enhanced by T-cell-autoreactive antibodies frequently seen in chronic infected HIV-1 patients.**

**A**, SupT1 cells were co-cultured with 293T cells expressing CD32B-GFP and CCR5. Prior to co-culture the 293T cells were pre-treated with sera from patients with different diseases. Chronic HIV-1 infection (CHI); ART: Anti-retroviral therapy; Acute HIV-1 infection (AHI); Fiebig stages II-III of acute HIV-1 infection, HIV-2: HIV type 2; HTLV-1: Human T-cell lymphotropic virus type 1; HCV: Hepatitis C virus; DENV: Dengue virus; YFV: Yellow-fever virus-vaccinated; SARS-CoV-2: Severe acute respiratory syndrome coronavirus type 2; EC: *Echinococcus multilocularis*; SCH: *Schistosoma spp.*; TB: *Mycobacterium tuberculosis*; RA: Rheumatoid arthritis; SLE: Systemic lupus erythematosus; CG: Cryoglobulinemia or healthy donors (HD). After 20h co-culture the SupT1 population was analyzed and the percentage of CD32B-GFP and CCR5 positive target cells) was determined by flow cytometry (see CCR5 transfer Supplemental figure 1). Median with 95% CI are shown, each dot represents a different patient. Asterisks indicate statistical significance by Mann-Whitney test. **B**, IgG binding of selected serum to primary CD4 T cells. CD4 T cells were incubated with selected sera samples, followed by staining with fluorochrome-coupled anti-human IgG Ab. selected sera: Six HIV-1 serum samples with high trogocytosis levels from (A) were selected. Median with 95% CI are shown. Kruskal-Wallis test is corrected with Dunn's multiple-testing. Experiments performed by Hong-Ru Chen. **C**, Flow cytometry analysis of CD3/CD4-positive T cell population was analyzed for CD32 expression derived from peripheral blood of healthy donors (n=23) and chronic HIV-1-infected patients (CHI) (n=39) (for gating strategy see Supplemental figure 2). Median with 95% CI are shown. Asterisks indicate statistical significance by Mann-Whitney test. n.s.: not significant; \*P ≤0.05; \*\*P ≤0.01; \*\*\*P ≤0.001.

Intriguingly, a number of sera from patients with chronic HIV-1 infection (CHI) could enhance trogocytosis of CD32B-GFP (Figure 11A) as well as CCR5 co-transfer (Supplemental figure 1). In contrast, sera from acute HIV-1 infection as well as samples from patients with chronic HIV-2 infection showed no significance compared to the sera of healthy donors. Moreover, besides two hepatitis C virus (HCV) patient sera, none of the other tested sera from viral infectious diseases like T-lymphotropic leukemia virus (HTLV, n=4), SARS-CoV-2 (n=6), dengue virus (DENV, n=11), attenuated yellow fever virus (YFV) vaccine (n=10) or autoimmune diseases (rheumatoid arthritis (RA; n=4), systemic lupus erythematosus (SLE; n=5) or cryoglobulinemia (CG; n=8)), nor from parasitic or bacterial infections (*Echinococcus multilocularis*, (EC; n=5), *Schistosoma spp.* (SCH; n=5) or *Mycobacterium tuberculosis* (TB; n=6)) could affect trogocytosis (Figure 11A).

Since “cell-bridging” antibodies have been reported to induce FcγR dependent trogocytosis [291, 293, 295, 312], we wondered whether the trogocytotic effect observed with some sera could be explained by auto-antibody binding to the surface of CD4 T cells (Figure 11B). Next, primary CD4 T cells were incubated with the corresponding patient sera followed by staining for human IgG. In the analysis, the CHI as well as the HCV patient sera were divided into two groups: one group of sera previously shown to enhance trogocytosis (“High trogocytosis”) and the ones with low or no effect (“low trogocytosis”). This revealed medium/high binding of antibodies to CD4 T cells for those sera with a high trogocytosis boosting effect, but no binding was observed in the group of “low trogocytosis” sera as well as for the other tested sera (Figure 11B). A correlation of antibody binding and trogocytosis boosting was further demonstrated by removal with IgG from the sera of two selected CHI “highly boosting sera”. Here, the trogocytosis-enhancing effect was lost but could be partially reversed by reconstituting the co-cultures with the column-eluted IgGs (data not shown). Notably, also screening PBMC cultures from healthy donors or HIV-1-positive patients, displayed an increased rate for CD3/CD4/CD32-positive T cells in PBMC from HIV-1 patients (Figure 11C). These findings showed the possibility of increased CD32-dependent trogocytosis rate *in vivo* for CHI patients, and gave insight into a potential role of increased trogocytosis-inducing antibodies in the blood of chronic HIV-1-infected individuals.

In a subset of HIV-1 infected-individuals, HIV-1 broadly neutralizing antibodies (bNAbs) are found [313-315] and are of high interest for the research and development of HIV-1 drugs and vaccines. However, bNAbs showed various unfavorable properties for the use in patients, such as autoreactivity to human lipids and proteins [316, 317]. This type of autoreactivity could explain the binding of IgGs to CD4 T cells as in the serum of some of the tested HIV-1 sera samples.

We therefore screened 10 known HIV-1 bNAbs in 293T/SupT1 cell co-cultures. Here, we found the bNAb PGT151 as trogocytosis enhancer of CD32B-GFP and also the co-transfer of CCR5 to SupT1 cells (data not shown). Besides the trogocytosis “boosting” effect, we observed a strong CD4 T cell-reactive binding of PGT151 (known to bind the HIV-1 envelope [318]), compared to the other bNAbs tested. In follow-up experiments, in which the Fab and Fc part of PGT151 were separated by the treatment with papain, neither the F(ab')<sub>2</sub> fragments nor the Fc part alone were able to enhance trogocytosis (data not shown).

These findings demonstrate a critical role of T cell autoreactive antibodies in the CD32-dependent trogocytosis and suggested the usage of such antibodies to modulate trogocytosis.

### 3.2.3 Trogocytosis enhancement with the bNAb PGT151

In previous experiments, we could show that the transfer of CCR5 could be enhanced with the bNAb PGT151. Following this we wanted to investigate whether PGT151 enhances also co-transfer of other receptors such as the tetraspanin receptor CXCR7 as well as single transmembrane receptor CD4. Similar to the transfer of CCR5 (with ~47-fold increase) also the CD32B-GFP mediated transfer of CXCR7 (~32-fold) and of CD4 (~55-fold) could be highly increased by the addition of PGT151 to the co-culture (Figure 12A). The CD32B dependency was underscored by low or no differences of receptor transfer in the control condition, here with, co-expressed GFP-tagged histone protein 2B (H2B-GFP).

This property of PGT151 enabled us to more easily differentiate between CD32-dependent and independent receptor transfer. For a better understanding on the influence of antibodies on the CD32-mediated transfer, we cloned CD32A and B constructs with different mutations, substituting either the N-glycosylation sites (observed to play a role in IgG binding [319]) or mutating the ITIM

motif of CD32B (see Figure 12C and Supplemental figure 3). The FcγR genes have different N-glycosylation sites but share a common structure, also displayed by CD32C representing a chimera of CD32A and CD32B. Here, the intracellular sequence of CD32C has a high homology with the intracellular part of CD32A with the ITAM motif, but has more sequence homology with CD32B in the extracellular part [177, 320]. The chimeric properties of the wild type CD32C construct therefore were of interest.

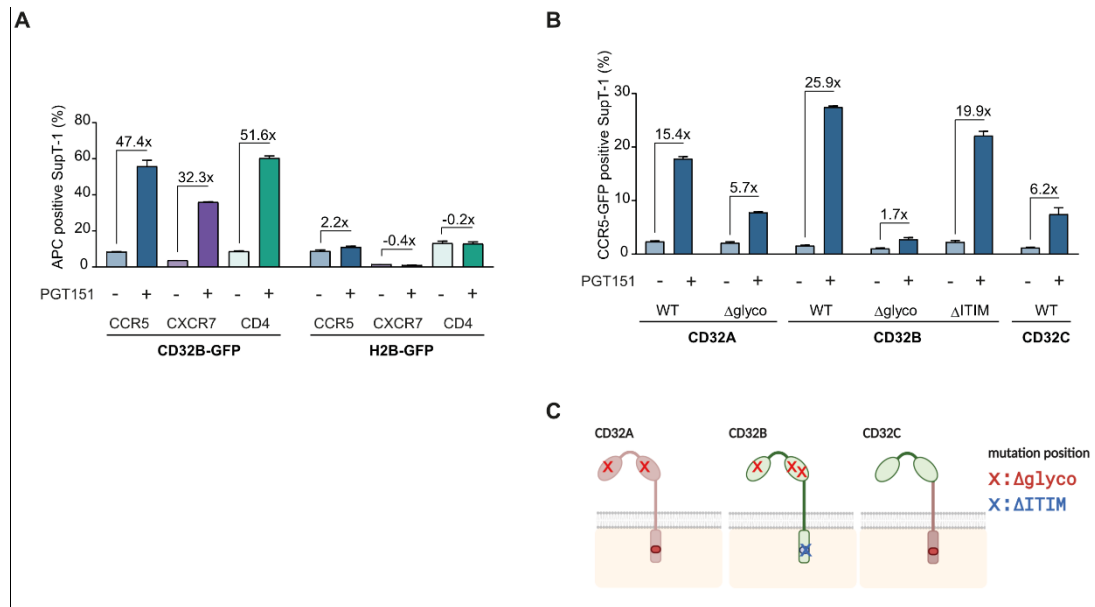


**Figure 12 | Co-transfer of different receptors is promoted by bNAb PGT151 binding to the glycosylated Fc-binding part of CD32.**

**A** 293T cells were transfected to transiently express CD32B-GFP together with CCR5, CXCR7 or CD4. After co-culture in the presence or absence of PGT151, the transfer of CCR5, CXCR7 and CD4 to the SupT1 cells was determined as described in Figure 9. Mean of technical replicates  $\pm$  SD. are shown. **B**, in a similar co-culture approach as in **(A)** the transfer of CCR5 mediated by either CD32A, B, C or indicated mutant was assessed in comparison to their indicated mutants (presented in scheme **(C)**) as well as CD32C WT. Means of technical replicates  $\pm$  SD. are shown. Schematic created by BioRender.com.

To further exclude any background staining caused by the staining antibodies in the flow cytometry analysis, we designed plasmids to express all FcγRs as well as their mutated versions (see scheme Figure 12B) fused to mtagBFP, and a N-terminal GFP fusion construct of CCR5 as receptor of interest (Figure 12B). This enabled a simplified detection of the transfer of the receptors by flow cytometry without the need of antibody-based staining. The mutation of the N-glycosylation sites on the extracellular part ( $\Delta$ glyco) reduced the PGT151-enhanced trogocytosis to a high extent, which was even more dramatic for CD32B (from ~26-fold with CD32BWT, to ~2-fold with CD32B $\Delta$ glyco). In contrast, the depletion of the signaling motif ITIM of CD32B (CD32B $\Delta$ ITIM ~20-fold increase) only slightly affected the antibody-mediated trogocytosis. PGT151 could also improve the transfer of CCR5 mediated by CD32CWT, but to a lower extent, than with CD32AWT and CD32BWT (Figure 12B, transfer of FcγRs-mtagBFP variants see also Supplemental figure 3).

Since bNAb PGT151 enabled us to investigate antibody-mediated, CD32-dependent transfer, we also investigated the co-transfer of receptors located in different cellular compartments. As representative of transmembrane receptors we analyzed the transfer of CCR5, CXCR4, CD63 and CD4, intracellular, but membrane-associated proteins were represented by the membrane-targeting domains of Lck and Fyn. SAMHD1 was selected as a non-membrane-associated intracellular protein with both cytoplasmic and nuclear localization (Figure 13).

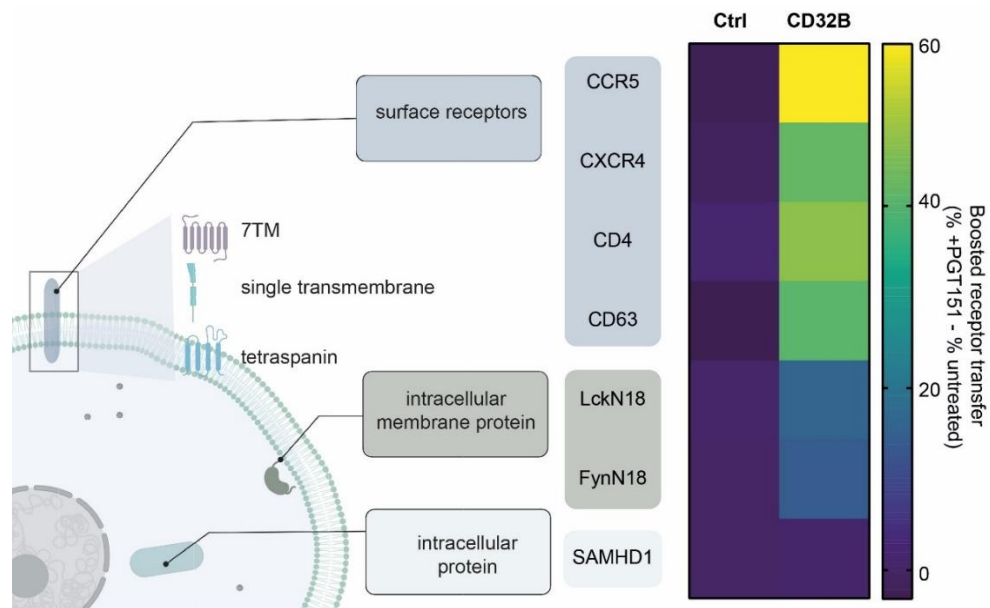


**Figure 13 | CD32 mediates transfer of plasma membrane-associated receptors.**

293T cells were co-transfected with plasmids encoding either CD32B-mtagBFP or mtagBFP alone (Ctrl), together with a plasmid encoding one of the indicated surface receptors (CCR5, CXCR4, CD4 or CD63), the first 18 amino acid of the N-terminal part of the intracellular membrane-anchored proteins of the Src kinase receptors Lck or Fyn or the intracellular protein SAMHD1. Cells were co-cultured for 24 h as described in Figure 9, with or without addition of PGT151. Transfer of the receptors to SupT1 T cells was assessed and percentage difference between +PGT151 condition and untreated cells was determined (see also Supplemental figure 4). Means of two experiments are shown as a heatmap. The illustration was created with BioRender.com.

When the transfer of a specific receptor is CD32-dependent, this is reflected by increased transfer in the presence of PGT151 during the co-culture. The CD32B-dependent transfer was highly increased for the transmembrane receptors (CCR5 ~58%; CXCR4 ~42%; CD4 ~47% and CD63 ~41%) or medium increased with intracellular membrane located proteins FyN and Lck (LckN18 ~16%, FckN18 ~14% difference). No CD32-dependent transfer was seen for the intracellular protein SAMHD1 (0.8% increase) (Figure 13 and Supplemental figure 4).

The immune evasion strategy of the Human Cytomegalosus Virus (hCMV) includes the manipulation of the Fc $\gamma$ R activation by the viral glycoproteins virus-encoded gp34 and gp68. These glycoproteins were reported to bind the Fc part of antibodies in immune complexes, impairing the binding to the Fc $\gamma$ R and therefore surmounting immune reactions such as antibody-dependent cellular cytotoxicity [217, 221]. To explore whether the Fc trapping properties of gp34 and gp68 could potentially also influence PGT151-enhanced trogocytosis, we added soluble purified hCMV glycoproteins in increasing amounts to the 293T/SupT1 co-culture. As a presentative readout, the transfer of CD32B-mtagBFP to SupT1 cells was assessed. The transfer observed without addition of PGT151 was defined as baseline. The T cell inducible co-stimulator ligand (ICOSL) glycoprotein and the non-Fc-binding point mutant of gp34 (gp34  $\Delta$ IgG binding site) [221] served as controls, since both proteins should not bind antibodies (Figure 14).

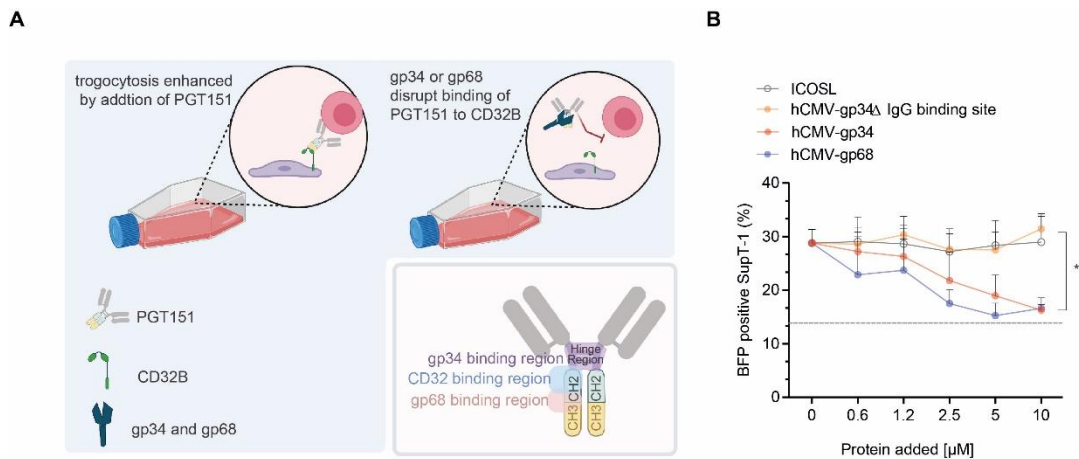


**Figure 14 | PGT151 is trapped by hCMV gp34 and gp68, diminishing the bNAbs trogocytosis-enhancing effect.**

**A**, Schematic overview: proposed bridging effect of PGT151 in the co-culture system (as described in Figure 9) and the disruption of the binding by the addition of hCMV glycoproteins 34 and 68 (gp34 and gp68) (upper part). Schematic of an antibody and the different binding sites of gp34 or gp68 and CD32 (lower part) [221, 223]. The illustration was created with BioRender.com. **B**, Purified hCMV glycoproteins gp34, gp8, ICOSL as well as the non-Fcγ-binding point mutant (W65F) gp34 (gp34 ΔIgG binding site) were added at indicated molarity to 293T cells expressing CD32B-mtagBFP. SupT1 T cells were added to start the co-culture (as described in Figure 9) for 24 h in the presence of PGT151 followed by CD32B-mtagBFP transfer analysis (dashed line indicating the transfer of CD32B in the co-culture condition without PGT151). The Asterisk indicates statistical significance by two-way ANOVA.

As expected, we observed decreasing transfer of CD32B with increasing amounts of purified gp34 as well as gp68 (~30% positive cells without glycoproteins to ~16% positive cells with 10 μM gp34 or gp68) close to the baseline (with ~14% positive cells), even though equal concentration of PGT151 had been present. This revealed a potential interference of hCMV glycoproteins with PGT151. The control glycoproteins ICOSL as well as gp34ΔIgG binding control glycoproteins, did not impair PGT151-enhancing trogocytosis effect, with stable transfer levels (~30%) observed independently of the amount of the proteins (Figure 14B).

Overall, these results confirmed PGT151 as a powerful tool to investigate CD32-dependent transfer and the factors influencing its outcome. The Fc binding domain of CD32 receptors as well as the plasma membrane association of proteins were observed to play an important role for their FcγR-dependent transfer. Interference with antibody binding by trapping the Fc part also could suppress the transfer to some extent, in together verifying the previously observed crucial role of antibody bridging of donor and target cells.

### 3.2.4 Knockdown of ESCRT protein Vps4 in CD32B-expressing cells

In order to release a vesicle during microvesicle fission cells have to ensure to release vesicles with an intact membrane, but at the same time exclude potential damage to the cell membrane itself. In order to ensure this, eukaryotic cells recruit endosomal sorting complexes required for transport (ESCRT) [321-324]. The complex itself consists of various proteins and also recruits enzymes and transport machinery [325, 326]. Additionally, ESCRT, is also hijacked by viruses such as HIV-1 for viral release [327, 328]. The core units' compounds of the complex are ALIX, ESCRT-I, ESCRT-II, ESCRT-III, and the AAA ATPase Vps4. Since the membranes of the two cells get into close proximity during CD32-dependent trogocytosis, membrane scissoring could take place and therefore ESCRT could play a mechanistic role in this process.

We addressed this question in a pilot experiment by knockdown (KD) of Vps4 as an important modulator of the ESCRT complex in the donor 293T cell and subsequently investigating its impact on CD32B-mediated transfer. This was achieved by transfection of siRNA for Vps4 or a non-targeting control siRNA (NTC) in 293T cells stably expressing CD32B-T2A-mtagBFP. One day after transfection, the analysis of Vps4 expression showed an efficient knockdown of the protein (Figure 15A). On the same day the co-culture with SupT1 T cells was started. The time point to start the co-culture after siRNA transfection was chosen, due to a previous monitoring of Vps4 expression 24 h, 48 h and 72 h post siRNA transfection and showed an efficient knockdown after 24 h with a continuous loss observed after 72 h (Supplemental figure 5). NTC or the Vps4 KD 293T cells were co-cultured with SupT1 T cells for an additional 24 h.

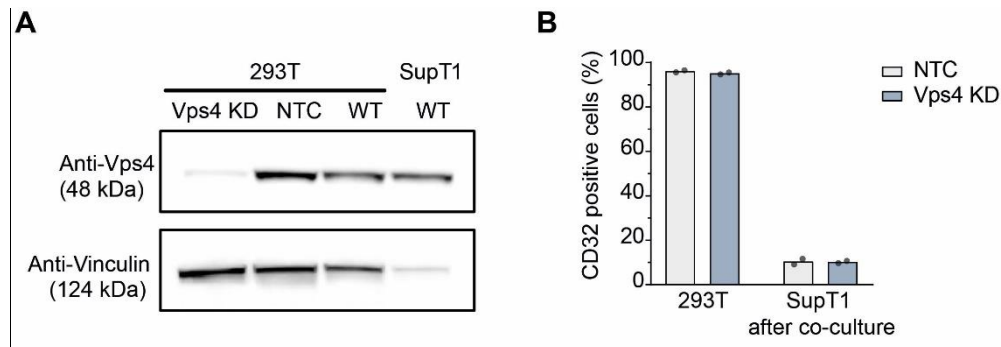


**Figure 15 | Knockdown of Vps4 in donor cells does not impact CD32B transfer to recipient cell.**

**A, B,** Stably CD32B-T2A-mtagBFP expressing 293T cells were transfected with siRNA specific for human Vps4 or a non-targeting control siRNA (NTC). The next day, SupT1 cells were added and cells were co-cultured as described (Figure 9). **(A)** Vps4 expression in the 293T KD, NTC and wild type (WT) as well as in SupT1 T cells was analyzed by western blotting, 24 h post transfection. Shown are immunoblots for either Vps4 or vinculin (loading control) (full image of immunoblots see Supplemental figure 6). **(B)** CD32B expression on 293T cells as well as transfer to SupT1 cells was determined, the following day by flow cytometry. Mean of technical replicate shown.

Analyzing both donor and recipient cells for CD32B expression after co-culture showed, no negative impact of the Vps4 KD on the CD32B expression in the 293T cells. However, also the transfer of CD32B to SupT1 T cells was unaltered, independently of the Vps4 status in 293T cells. Since the knockdown highly reduced the expression of Vps4 in the 293T cell, but had no effect on the transfer of CD32, we concluded that the ESCRT complex was not recruited by the donor cell to transfer CD32B to T cells.

In the previous experiments the mechanisms of CD32-dependent trogocytosis were investigated using controlled *in vitro* cell culture conditions with cell lines. This helped to understand the induction of CD32-dependent trogocytosis by close cell-cell contact, the role of autoreactive antibodies and preferential co-transfer of plasma membrane-associated receptors. Next, it was of further interest to investigate the CD32-dependent transfer in a primary cell context.

### 3.3 Fcy-mediated trogocytosis in primary cell co-cultures

The monocyte-derived M2 macrophages showed the highest CD32 expression and highest transfer of CD32 to CD4 T cells (Figure 7). We therefore established a primary cell co-culture model with M2 macrophages as donor cells and autologous CD4 T cells as recipient cells. In this experimental setup, the CD4 T cells are isolated from cryo-conserved PBMC by negative isolation and stained with a cell trace dye (similar to the 293T/SupT1 cell co-culture) before starting a 48 h co-culture with autologous M2 cells. The M2 macrophages are previously differentiated from CD14-positive monocytes for 7 days by addition of macrophage colony-stimulating factor (M-CSF) for 6

days and subsequent 24 h addition of M-CSF and IL-4, to the culture medium. The aim was to create a model that is closer to *in vivo* conditions using primary human cells. This model enables further investigation of CD32 transfer from the M2 to the CD4 T cells and also enables a closer investigation of the co-transfer of other receptors and factors influencing trogocytosis in primary HIV target cells (Figure 16).

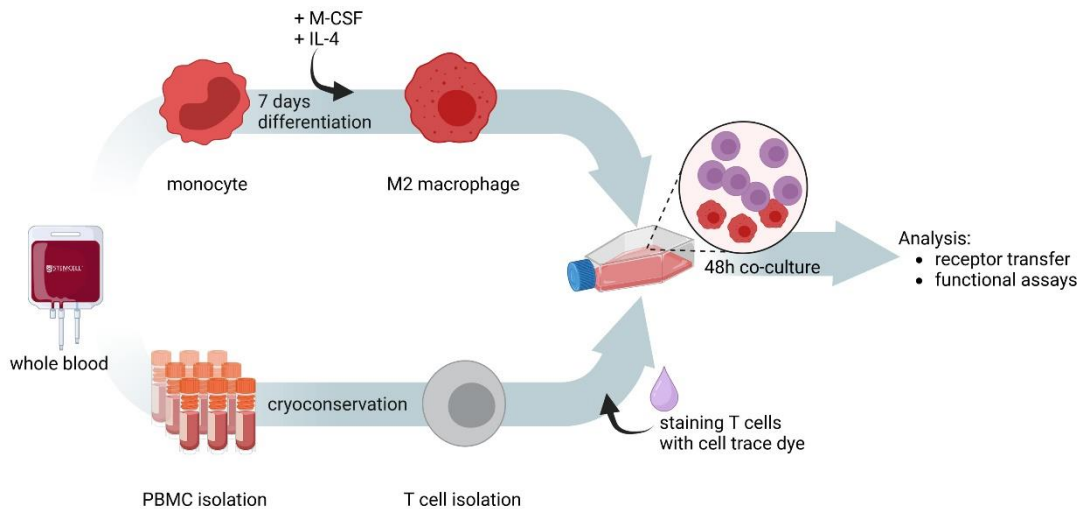


**Figure 16 | Primary cell *in vitro* trogocytosis model with CD4 T cells and M2 macrophages.**

Schematic overview of the experimental setup of CD4 T cell-M2 macrophage trogocytosis model. Monocytes isolated from whole blood are differentiated to M2 macrophages followed by 48 h co-culture with autologous CD4 T cells (previously stained with cell trace dye). After co-culture, CD4 T cells are analyzed for receptor transfer and/or used in functional assays.

### 3.3.1 Comprehensive screening of receptor transfer

In previous experiments, we saw the co-transfer of HLA-DR and CD32 to CD4 T cells from M2 macrophages (Figure 7C). Following this observation, we aimed to broadly screen for the transfer of other M2 receptors. This was performed by staining for 273 different receptors using the BD Lyoplate™ (BD) Kit. Of the total receptors included in the kit, we found 116 receptors that were moderately or highly expressed on M2 cells from 3 pooled donors (moderate: MFI  $\leq 6000$ , but higher than the MFI of the isotype control; highly expressed: MFI  $> 6000$ ). After CD4 T cells/M2 macrophage co-culture (as described before; Figure 16), we sorted the CD4 T cells, pooled the 3 donors and then determined the “ratio of receptor exposure” by dividing the MFI for each receptor on co-cultured cells by the MFI on not co-cultured CD4 T cells. A ratio  $> 1$  indicates an increase of the receptor after co-culture and therefore implying a transfer from M2 cells to T cells. By ranking the receptors for their “ratio of receptor exposure”, the macrophage receptor DC-SIGN (CD209) showed the highest ratio of  $\sim 6.2$  followed by HLA-DR with a ratio of  $\sim 5.8$ , confirming our previous observations (Figure 17A and Supplemental table 1). A ratio above 2 was considered as “highly transferred” receptor, which was also confirmed for 10 out of the 116 receptors (Figure 17B). Interestingly, not all receptors of the “top 10” were highly expressed on M2 cells. Vice versa, also receptors highly expressed on M2 cells not always exhibited a high ratio of transfer (such as CD44 or CD43). This was also depicted by ranking seven receptors that were highly expressed by M2 macrophages but not detected on CD4 T cells independently of co-cultured or not (Figure 17C).

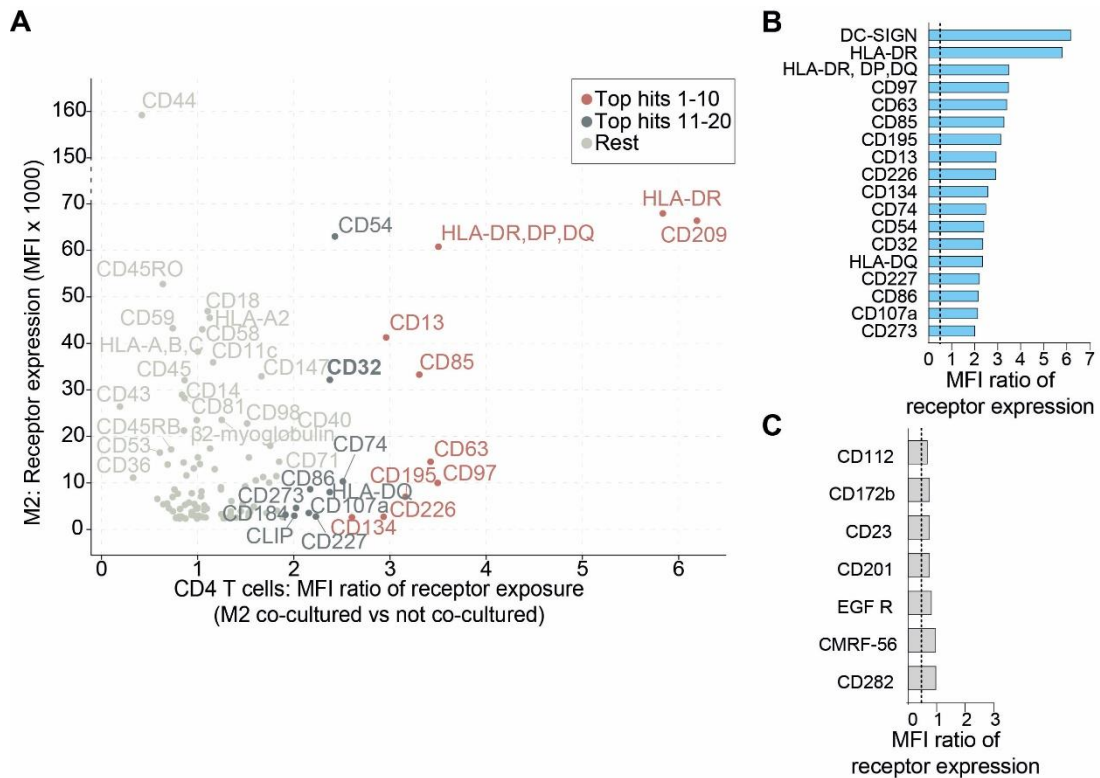


**Figure 17 | A number of receptors is transferred from M2 macrophages to CD4 T cells.**

**A**, Surface receptor screening on M2 macrophages and autologous CD4 T cells, either co-cultured with M2 cells or kept alone for 48 h (antibody screening panel of the BD Lyoplate™). CD4 T cells were sorted and then the pool of 3 donors was stained for the receptors detected as moderate or highly expressed by the M2 macrophages. Here, ratio of mean fluorescence intensity (MFI) detected on the not co-cultured to the MFI of co-cultured CD4 T cells was determined. Expression on M2 macrophages (Y-axis) towards MFI ratio on CD4 T cells (X-axis) was analyzed. Receptors with a high ratio were categorized into “top hits 1-10” and “top hits 11-20” transferred receptors, respectively. Data analysis performed together with Simon Besson-Girard generated using ggplot2. **B**, Ranking of receptors with a ratio of expression above 2, categorized as highly transferred surface receptors. **C**, Ranking of the receptors not detectable on CD4 T cells regardless of previous culture condition and with a ratio lower than 1 (indicating no transfer).

Follow-up experiments sought to test the functionality of the transferred receptors after co-culture. Chemokine receptors CXCR4 or CCR5 could be transferred to CD4 T cells in a CD32B-dependent manner from transiently expressing donor cells (HeLa cells). CD4 T cells with a low (CCR5) or genetically ablated (KO CXCR4, see also Supplemental figure 7) expression of the corresponding chemokine receptor, were enabled to migrate towards the natural chemokine ligand for CCR5 (Regulated upon Activation, Normal T Cell Expressed and Presumably Secreted (RANTES)) or for CXCR4 (stromal-derived factor-1 $\alpha$  (SDF-1 $\alpha$ ), if the chemokine receptors were transferred (Figure 18A and B). The induced migration of the CD4 T cells was not observed if the cells had been previously co-cultured with H2B-GFP/chemokine receptor co-expressing HeLa cells or if transfer was blocked by the addition of anti-CD32 antibody to the co-culture involving CD32B-GFP/chemokine receptor-positive HeLa cells and the T cells.

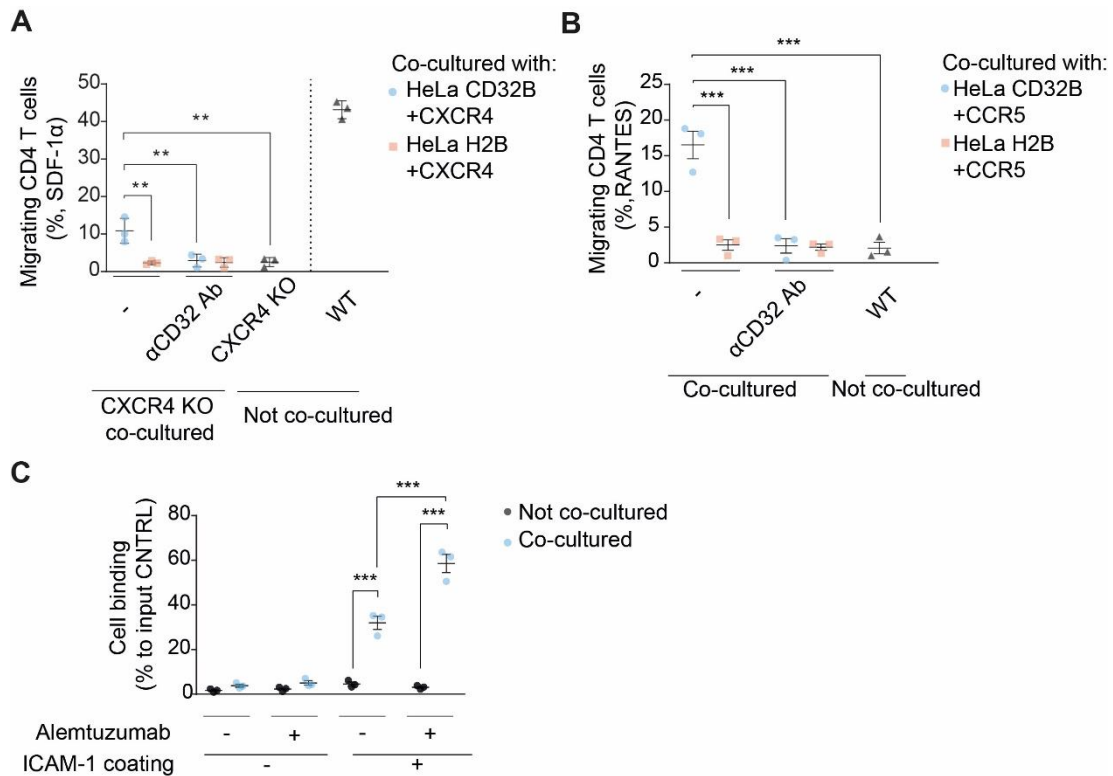


**Figure 18 | Transferred receptors remain functional on CD4 T cells.**

**A, B** Testing chemotaxis of CD4 T cells after co-culture with HeLa cell transiently co-expressing CD32B-GFP or H2B-GFP (control) together with chemokine receptor (A) CXCR4 or (B) CCR5. HeLa cells were treated with or without anti-CD32 mAbs before co-culture with (A) CXCR4 KO or WT CD4 T cells or (B) WT CD4 T cells. One day after co-culture CD4 T cells were harvested and placed in top chamber of transwell and chemokine (A) SDF-1α or (B) RANTES (CCL-5) was added to the lower chamber of the transwell. Migrating cells were collected and counted by flow cytometry. Mean  $\pm$  s.e.m. are shown (n=3). Asterisks indicate statistical significance by one-way ANOVA. P values were corrected for multiple comparison (Tukey). **C**, ICAM-1/CD11b binding of CD4 T cells after co-culture with M2 macrophages. CD4 T cells and M2 macrophages were co-cultured for 48 h as described before (see Figure 16) with or without trogocytosis enhancing antibody Alemtuzumab (see next chapter 3.3.2). CD4 T cells were then harvested and sorted and then cultured in plates with or without coated with ICAM-1. Cells attached to plate were quantified by luminometry. Cell binding values were normalized to wells with input cells without washing. Mean  $\pm$  s.e.m. are shown (n=3). Asterisks indicate statistical significance by two-way ANOVA. P values were corrected for multiple comparison (Tukey). Experiments performed by Hong-Ru Chen.

Similar to this experiment also CD11b transferred in the primary co-culture of M2 macrophages to CD4 T cells increased the binding of the co-cultured CD4 T cells to the surface coated with CD11b ligand ICAM-1 (Figure 18C). The transfer of CD11b and, as consequence, the binding to ICAM-1 could be enhanced by T cell-specific binding antibody (Alemtuzumab, described and tested in the following chapter 3.2.2).

The findings from the receptor screening indicated a strong impact on the surface proteome of CD4 T cells, following close cell-cell contact with M2 macrophages. The newly acquired ability to migrate after receptor transfer indicated a potential impact on the migration behavior of primary CD4 T cells.

### 3.3.2 CD32 transfer to CD4 T cells is enhanced by autoreactive antibody binding and close cell-cell contact

In the *in vitro* trogocytosis model with 293T and SupT1 cells, we could boost the CD32-dependent transfer by adding bNAbs PGT151. The binding of PGT151 to the surface of SupT1 cells was

observed, confirming the cell-antibody-cell bridging effect as transfer booster (chapter 3.2.2 & 3.2.3).

Following this observation, we decided to test a second antibody that binds specifically to the surface of CD4 T cells and hereby potentially inducing the bridging between the M2 and CD4 T cells in co-culture. The monoclonal humanized anti-CD52 antibody matches these criteria. CD52 is expressed by T cells, B cells and monocytes [329, 330]. This antigen is a target of relapsing multiple sclerosis (MS) therapy using the IgG1 kappa monoclonal humanized anti-CD52 antibody: Alemtuzumab (Lemtrada®) [331, 332]. Alemtuzumab is used to decrease the number of T cells and B cells, thereby reducing the main inflammatory inducing factors in MS [333, 334]. Its properties of (i) targeting an antigen mainly expressed on T cells and (ii) its humanized IgG, made it to a promising candidate to test it for boosting FcγR-dependent trogocytosis. We therefore first cultured CD4 T cells in the presence of Alemtuzumab and could define a concentration of the antibody with no severe cytotoxic effect (data not shown). This antibody concentration was then used to pre-incubate M2 macrophages following the addition of CD4 T cells to start the co-culture. To show the specific trogocytosis effect of Alemtuzumab, human IgG1 (isotype control) was tested in comparison. After co-culture, CD4 T cells were analyzed for the transfer of CD32 as well as the co-transfer of HLA-DR. In both co-culture conditions, we could see the transfer of the two receptors, but in the presence of Alemtuzumab this was significantly increased (%CD32 ~26-fold, %HLA-DR ~8-fold, Figure 19).

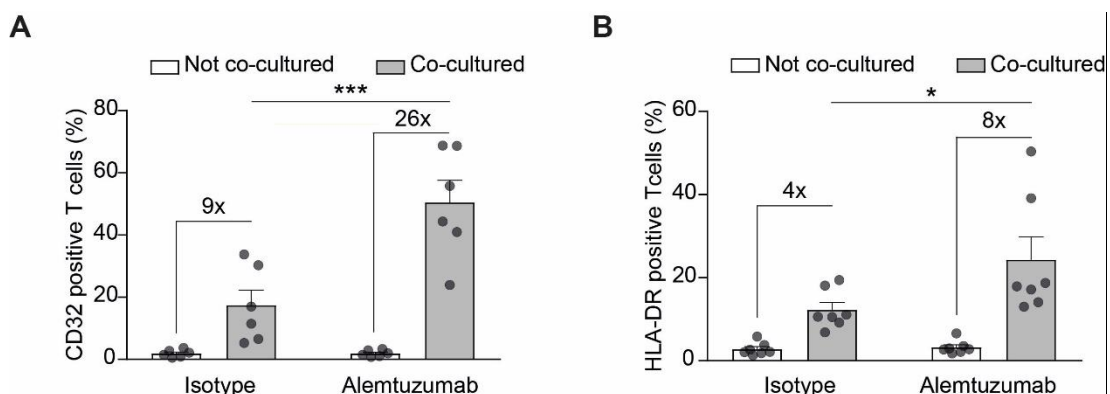


**Figure 19 | CD4 T cell binding antibody Alemtuzumab can enhance receptor transfer from M2 cells to CD4 T cells.**

Addition of mAb Alemtuzumab or isotype control antibody to the M2 cell culture prior to co-culture with autologous CD4 T cells. Subsequently, the cells were kept in co-culture for 48 h together with the indicated antibody. After co-culture CD4 T cells were sorted and the transfer of CD32 (A) and HLA-DR (B) was determined by flow cytometry. Mean  $\pm$  s.e.m. is shown (n=6-7). Asterisks indicate statistical significance by two-way ANOVA. *P* values were corrected for multiple comparison (Šidák). \**P*  $\leq$  0.05; \*\*\**P*  $\leq$  0.001.

So far, we demonstrated that also in a primary cell context, CD32 is transferred from donor to recipient cells together with a variety of other receptors and this process can be enhanced with CD4 T cell-binding antibodies. The aim of the next experiment was to further explore the relevance of CD32-dependent trogocytosis for CD4 T cells *in vivo*. Since CD4 T cells are found in different compartments of the body, this can influence the number of trogocytic events, especially if there is a close cell-cell contact with CD32-expressing cells. Therefore, the CD3/CD4-positive T cells, originating from different tissues, were analyzed for their CD32 positivity as following: i) PBMC cultures from whole blood, ii) Human lymphoid aggregate culture (HLAC) from tonsil tissue and iii) Lamina propria lymphocyte culture (LPAC) from L. propria of the intestinal tract (Figure 20). For the analysis, the CD14<sup>-</sup>/CD19<sup>-</sup>/CD3<sup>+</sup> population was gated from the living cells to exclude monocytes and B cells with further gating for CD4-positive cells and assessment of the frequency

of CD32-positive cells (gating strategy as for experiment in Figure 11, see Supplemental figure 2).

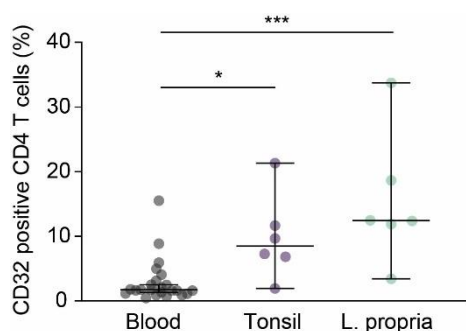


**Figure 20 | Increased rate of CD32-positive CD4 T cells originating from lymphatic tissue culture.**

Flow cytometry analysis shows frequency of CD32-positive CD3<sup>+</sup>/CD4<sup>+</sup> T cells, originating from peripheral blood lymphocyte culture (n=23), tonsil tissue culture (n=6) or lamina propria of jejunum or ileum tissue culture (n=6) samples (for gating strategy see also Supplemental figure 2). Median with 95% CI are shown. Asterisks indicate statistical significance by one-way ANOVA. *P* values were corrected for multiple comparison (Dunnnett)\**P* ≤0.05; \*\*\**P* ≤0.001.

The rate of CD32-positive CD4 T cells was higher in tissue with higher cell density and therefore induces more frequent T cell-macrophages contacts [335], such as the lamina propria and tonsil tissue, with the highest rate seen for the L. propria tissue samples.

The close macrophage cell contact of CD4 T cells has been shown to have a strong impact on their surface proteome and can equip CD4 T cells with macrophage-like properties. CD4 T cell binding auto-antibodies also strongly enhance this phenotype. Taking these observations into account we next addressed the question whether CD32-dependent trogocytosis has an impact on the susceptibility of primary CD4 T cells to HIV-1.

## 3.4 HIV-1 exploits CD32-driven trogocytosis to infect resting CD4 T cells

### 3.4.1 Increased HIV-1 fusion to and infection of CD4 T cells after co-culture

Since the examination of PBMC cultures showed an increased rate of CD32-positive CD4 T cells in HIV-1 patients (Figure 11), we further characterized whether CD32-mediated trogocytosis affects HIV-1 fusion to and infection of CD4 T cells. For this, the primary cell co-culture model which was described in Figure 16 was used. Here, CD4 T cells were sorted 48 h after co-culture and used for HIV-1 fusion or infection.

The HIV-1 fusion assay was performed as described by Cavrois *et al.* [336] with macrophage-co-cultured and not co-cultured CD4 T cells. Briefly, HIV-1 fusion can be detected by the change of fluorescent wavelength resulting from the enzymatic cleavage of CCF2 dye by beta-lactamase (BlaM) activity. The enzyme is incorporated into the virion during virus production mediated by the fusion to the viral protein Vpr. Later on, the fusion protein Vpr-BlaM is released into CCF2-stained CD4 T cells upon viral entry, allowing thereby the cleavage of the dye.

As demonstrated in the experiments above, the addition of Alemtuzumab could increase CD32-dependent trogocytosis (Figure 19) and we therefore added the CD52-targeting antibody also to the co-culture to increase the rate of trogocytosis to investigate if this affects capacity of cells for

HIV-1 fusion. The fusion of X4- and R5-tropic HIV-1 showed, in both cases, enhanced virus entry following M2 co-culture in comparison to the not co-cultured CD4 T cells (X4 ~5-fold increase; R5 ~20-fold increase, Figure 21A).

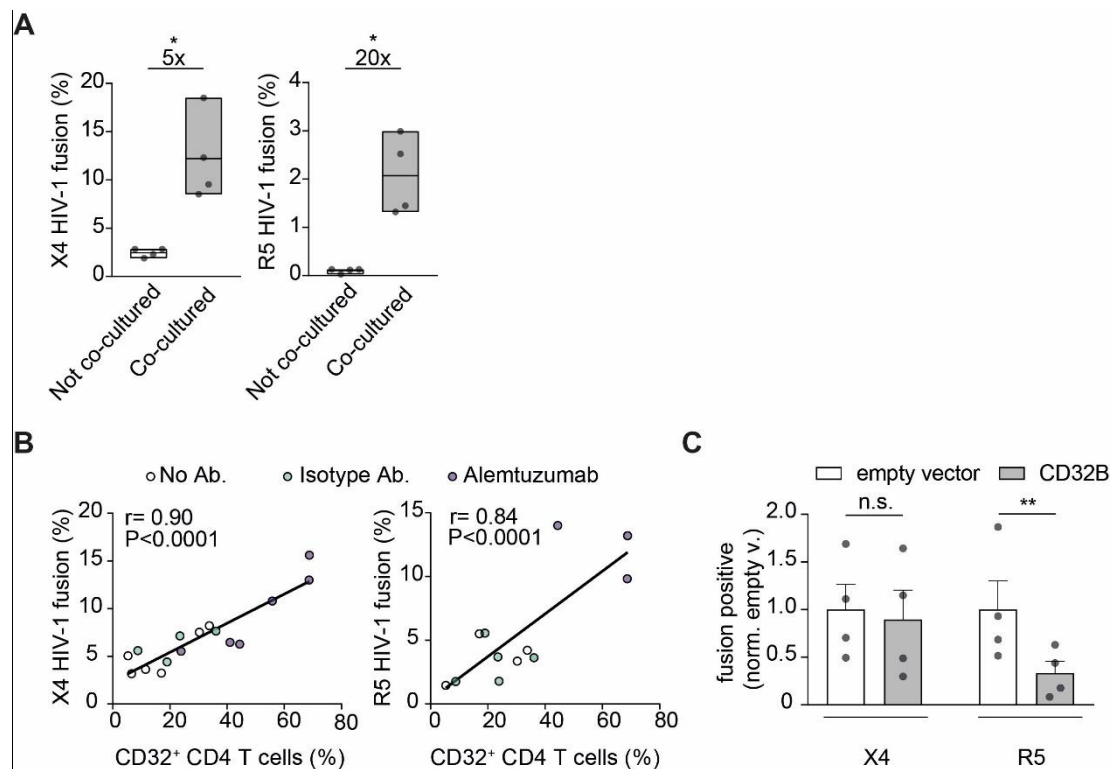


**Figure 21 | CD32-mediated trogocytosis enhances HIV-1 fusion to CD4 T cells and can be further enhanced by addition of a T cell-binding antibody (Alemtuzumab).**

**A**, M2 macrophages were pre-treated with Alemtuzumab followed by 48 h co-culture with autologous CD4 T cells. CD4 T cells were then sorted and the HIV-1 fusion assay performed with either X4- or R5-tropic HIV-1 virion carrying Vpr-BlaM. The rate of HIV-1 fusion was determined by flow cytometry. Mean  $\pm$  s.e.m. are shown (n=4). Asterisks indicate significance by two-tailed paired t-test. **B**, M2 macrophages were pre-treated with Alemtuzumab or an isotype control antibody and then co-cultured with autologous CD4 T cells. CD4 T cells were sorted after 48 h co-culture and viral fusion was performed (as in A), as well as stained for CD32 and analyzed by flow cytometry. Pearson correlations between CD32 positivity and HIV-1 fusion are shown. **C**, Overexpression of CD32B in primary CD4 T cells by nucleofection with a CD32B-encoding plasmid. Cells were then incubated either HIV-1 Vpr-BlaM virion X4- or R5-tropic and viral fusion was determined by flow cytometry. The fusion percentages were normalized with fusion percentages in empty vector-expressing cells. Mean  $\pm$  s.e.m. is shown (n=4). Asterisks indicate significance by two-tailed paired t-test. \*P  $\leq$  0.05; \*\*P  $\leq$  0.01; n.s.: not significant.

The amount of trogocytic events in the co-culture was represented by the percentage of CD32-positive T cells afterwards and was detected for all co-culture conditions (untreated, +isotype Ab. or + Alemtuzumab). The assessment of CD32 transfer and HIV-1 fusion in the same cells demonstrated a direct positive correlation (X4 tropic  $r=0.90$  (right panel), R5 tropic  $r=0.84$  left panel; Figure 21B).

To exclude a direct involvement of CD32 in the enhanced HIV-1 susceptibility, we transiently expressed CD32B in primary CD4 T cells. This was performed by nucleofection of a CD32B-expression plasmid in CD4 T cells, followed by an HIV-1 fusion assay. Here, even though the CD4 T cells had high expression levels of CD32B (see Supplemental figure 8) nucleofected cells did not show a higher HIV-1 fusion percentage than the control cells (for R5-tropic the rate was even lower than the control cells; Figure 21C).

Since HIV-1 encounters several restrictions after fusion in resting CD4 T cells [337], we addressed in the next experiment whether the increased fusion translates into increased productive infection after M2 co-culture.

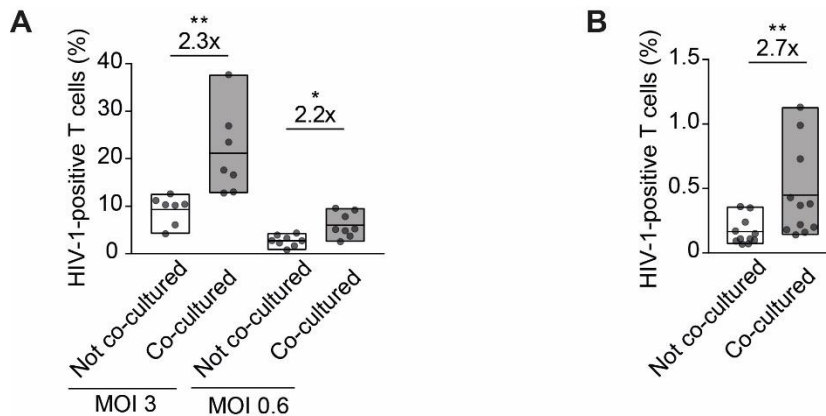


**Figure 22 | Productive HIV-1 infection is enhanced in CD4 T cells following M2 co-culture.**

**A, B.** Following co-culture with M2 macrophages, CD4 T cells were sorted and spinoculated (2.5 h, 650 g, 35 °C) with either X4- (**A**, with different MOI) or R5-tropic (**B**) HIV-1 GFP reporter viruses. After 2 days in culture, the cells were analyzed by flow cytometry for their GFP expression compared to the frequency of infected not co-cultured CD4 T cells. Mean  $\pm$  s.e.m. is shown (n=7-11). Asterisks indicate significance by two-tailed paired t-test. \*P  $\leq$  0.05; \*\*P  $\leq$  0.01; \*\*\*P  $\leq$  0.001. Experiments performed together with Manuel Albanese.

Spinoculation of HIV-1 GFP reporter viruses onto sorted CD4 T cells after co-culture was performed to study productive infection. Infection-positive cells were detected by GFP expression 2 days post infection. The X4 HIV-1 GFP infection rate was  $\sim$ 2.3 fold increased when CD4 T cells had previously been in culture with M2 cells, regardless of the multiplicity of infection (MOI) (Figure 22A). Analogue to these findings also spinoculation with R5 HIV-1 GFP resulted in an  $\sim$ 3-fold increase upon co-culture (Figure 22B).

Thus, CD32-positive CD4 T cells showed enhanced HIV-1 susceptibility, but here CD32 was a marker of previous trogocytosis and was not the contributing factor of increased HIV-1 fusion and infection in co-cultured CD4 T cells. The next step was to combine this observation and investigate which factors may be involved in increased HIV-1 fusion and whether this enhancement is already during the binding of the virus to the target cells.

### 3.4.2 HIV-1 attachment to CD4 T cells is increased following M2 co-culture

To address this question, CD4 T cells were prepared and co-cultured with M2 macrophages as described in Figure 16. After co-culture, CD4 T cells were sorted and incubated with X4 HIV-1 Vpr-GFP particles for 1 h at 16 °C with subsequent staining for CD32. In the analysis, the HIV-1 binding to CD32-positive cells was compared with the CD32-negative cells. The CD32-positive cells reflect those cells that had been in close proximity with M2 macrophages, resulting in trogocytosis of CD32 and co-transferred receptors. Whereas within the CD32-negative cell population most likely trogocytosis had not occurred during co-culture.

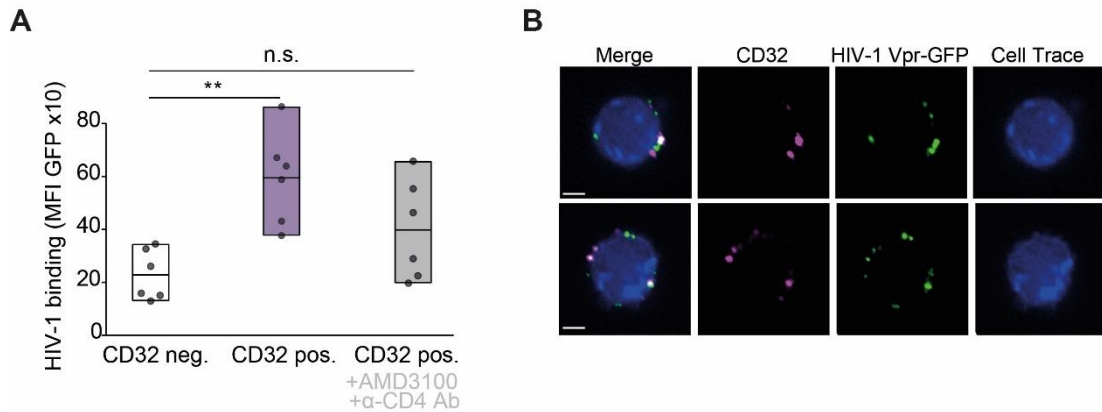


**Figure 23 | Increased binding of HIV-1 to CD32-positive membrane patches on CD4 T cells after M2 co-culture.**

**A, B**, HIV-1 binding assay. M2-co-cultured CD4 T cells were sorted and incubated with HIV-1 Vpr-GFP particles with subsequent staining for CD32. GFP and CD32 positivity of target CD4 T cells were determined by either flow cytometry (**A**) or by spinning disc confocal microscopy (**B**). Scale bar = 2  $\mu$ m. Mean  $\pm$  s.e.m. are shown (n=6). Asterisks indicate statistical significance by one-way ANOVA. P values were corrected for multiple comparison (Dunnett's). \*\*P  $\leq$  0.01; n.s. = not significant. Microscopy analysis performed by Manuel Albanese and Hong-Ru Chen.

Increased HIV-1 binding was detected on CD32-positive CD4 T cells compared to CD32-negative cells (~2-fold). The increased trogocytosis-dependent binding was reduced, following the addition of anti-CD4 antibody and the CXCR4 antagonist AMD3100 (Figure 23A). Confocal microscopy studies of co-cultured CD4 T cells also showed a co-localization of CD32 and HIV-1 Vpr-GFP particles. Of note, CD32 was not homogenously distributed on the surface of T cell but rather observed as distinct spots (Figure 23B).

Taking together, the results showed a relationship of the transferred CD32 positive membrane patches and the preferential binding of HIV-1.

### 3.5 Deciphering factors involved in enhanced HIV-1 binding to CD32-positive CD4 T cells

Next, we sought to identify key factors located within the trogocytosed membrane patches that mediate this virological phenotype. In "receptor transfer screening experiment" (Figure 17), we already identified a variety of receptors being transferred from M2 macrophages to T cells. It was therefore of particular interest whether specific transferred receptors or proteins may underlie the higher binding of HIV-1 to the trogocytosed membrane patches.

To approach this question, we focused on receptors reported to be expressed on myeloid cells and previously implicated in increased viral attachment or entry [30-33]. These receptors of interest were then knocked out in monocytes, followed by differentiation to M2 macrophages. As a control we nucleofected the M2 with non-targeting control gRNA (NTC). If the knockout efficiency was sufficient ( $\geq$  80% negative cells for the target protein) the next step was to co-culture these KO M2 with autologous CD4 T cells. The CD4 T cells were then sorted and viral assay (fusion or binding assay) was performed. This experimental setup included three different flow cytometry readouts: i) the knockout efficiency on the M2 macrophages before co-culture, to ensure no or very low expression of the targeted receptor ii) the transfer of CD32 on CD4 T cells after co-culture, to ensure a high trogocytosis rate, but lack of transfer of the receptor of interest from the KO M2 macrophages iii) the HIV-1 binding or fusion analysis comparing CD4 T cells that had been co-cultured with either NTC M2 macrophage or KO M2 macrophages (Figure 24).

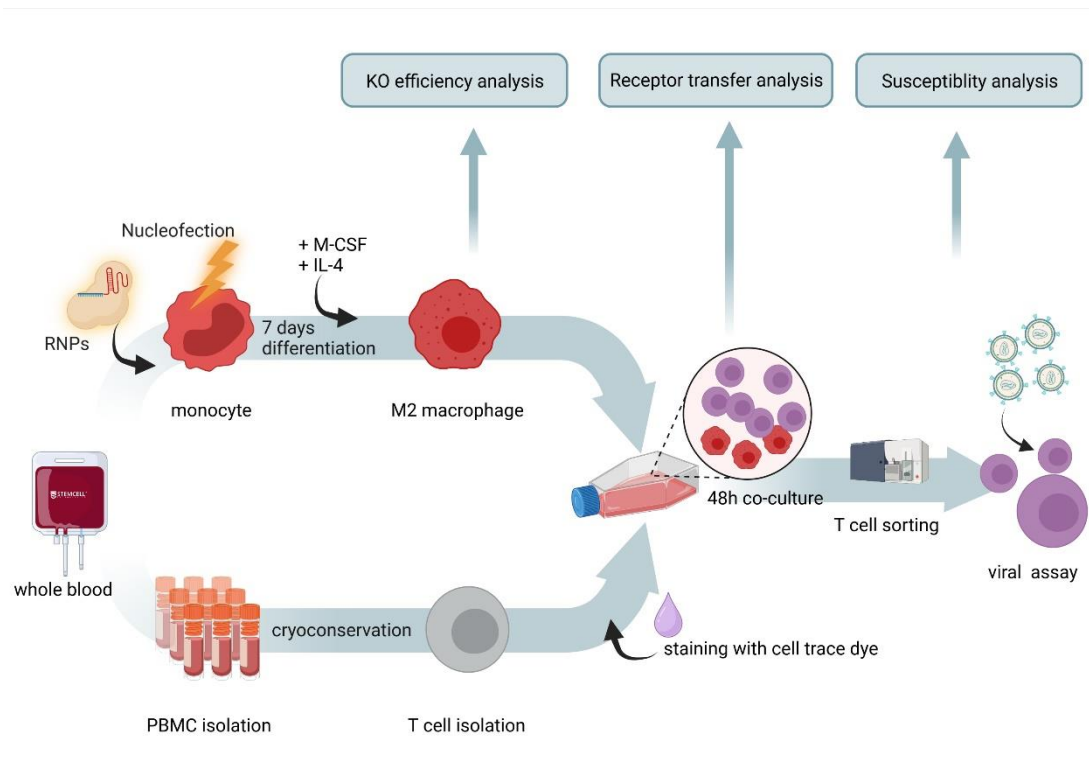


**Figure 24 | Functional investigation of potentially trogocytosed HIV-1-binding receptors by gene KO in M2 macrophages.**

Schematic overview: Monocytes were isolated from PBMCs and the receptor of interest was knocked out by nucleofection with specific Cas9–gRNA ribonucleoproteins (RNP). After differentiation, the KO efficiency was analyzed followed by co-culture as described in Figure 16. Subsequently to co-culture, the transfer of CD32B and the receptor of interest is determined. The co-cultured CD4 T cells are then sorted and examined in viral assays for HIV-1 binding or fusion.

### 3.5.1 Ablated co-transfer of DC-SIGN does not reduce HIV-1 fusion in co-cultured CD4 T cells

One of the first candidates we focused on was DC-SIGN. This receptor has been reported to increase HIV-1 binding to the surface of dendritic cells (DC) or macrophages and being involved in the trans-infection of CD4 T cells [338-340]. It was also reported that co-expression of DC-SIGN together with the HIV-1 entry receptors lead to an increased infection rate in a CD4 T cell line [33, 341]. DC-SIGN was also found in our studies to be one of the receptors with the highest relative transfer ratio from M2 macrophages to CD4 T cells (Figure 17). The following experiments therefore focused on DC-SIGN as receptor of interest with the experimental setup as described above (Figure 24).

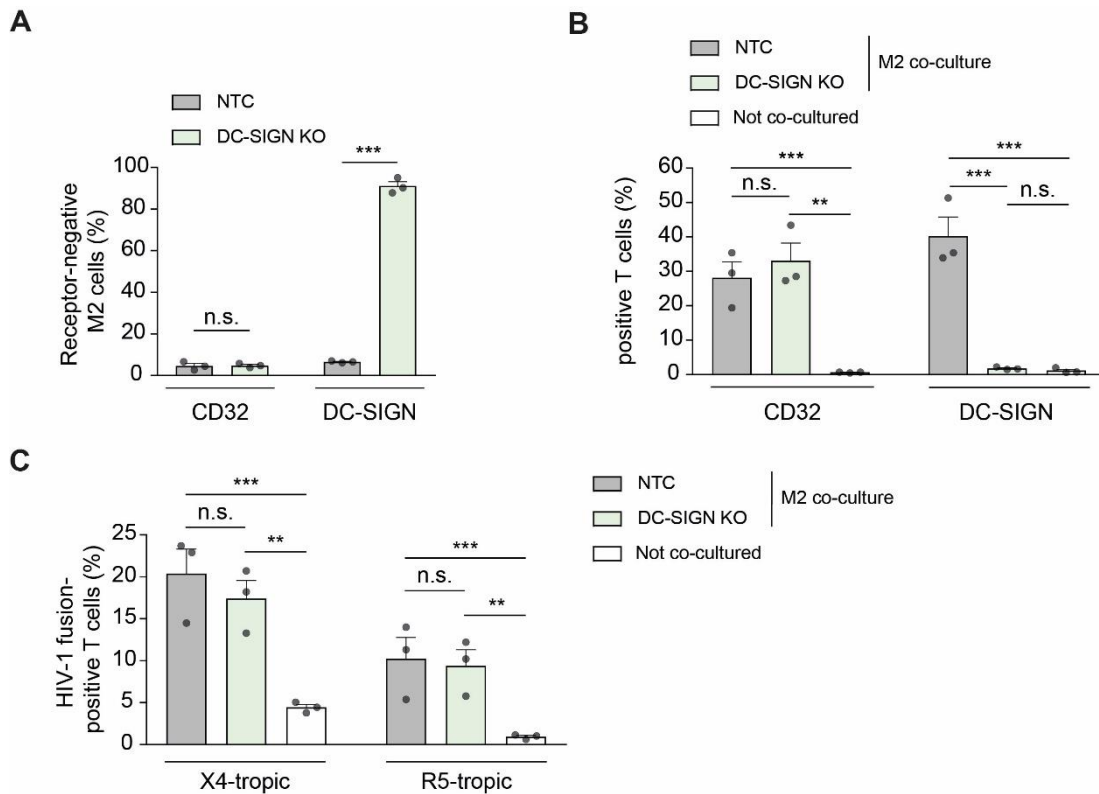


**Figure 25 | Knockout of DC-SIGN in macrophages does not impact HIV-1 fusion to co-cultured CD32-positive CD4 T cells.**

**A**, Monocytes were isolated from PBMCs as previously described (Figure 16) followed by knockout of DC-SIGN using specific RNPs or NTC RNPs as control (Figure 24). After differentiation of the NTC and KO monocytes to M2 macrophages, the expression of CD32 and DC-SIGN was assessed by flow cytometry. Mean  $\pm$  s.e.m. is shown ( $n = 3$ ). **B**, Autologous CD4 T cells were co-cultured with DC-SIGN KO or NTC M2 cells for 2 days followed by staining for CD32 and DC-SIGN on co-cultured and not-cultured T cells. Mean  $\pm$  s.e.m. is shown ( $n = 3$ ). **C**, CD4 T cells were sorted and X4 as well as R5 HIV-1 fusion assays were performed comparing CD4 T cells co-cultured with NTC or DC-SIGN KO M2 cells as well as not co-cultured cells. Mean  $\pm$  s.e.m. is shown ( $n=3$ ). Asterisks indicate statistical significance by two-way ANOVA. P values were corrected for multiple comparison (Šídák) n.s.: not significant \* $P \leq 0.05$ ; \*\* $P \leq 0.01$ ; \*\*\* $P \leq 0.001$ . Experiments performed together with Manuel Albanese.

The KO of DC-SIGN in M2 macrophages was validated by flow cytometry (91% DC-SIGN-negative cells). As expected, the M2 DC-SIGN KO did not show differences in their CD32 expression compared to the NTC (Figure 25A). This was also reflected by the comparable transfer of CD32 to CD4 T cells in both co-culture scenarios (~30% CD32-positive CD4 T cells) (Figure 25B). The virtual absence of DC-SIGN-positive CD4 T cells, when co-cultured with DC-SIGN KO M2 cells, further validated the actual transfer of DC-SIGN onto CD4 T cells from donor M2 macrophages. However, the abrogated transfer of DC-SIGN from the M2 KO co-cultured CD4 T cells, did not negatively influence HIV-1 fusion to co-cultured CD4 T cells. The co-cultured CD4 T cells still showed increased fusion compared to the not-cultured CD4 T cells, irrespective of the DC-SIGN status (Figure 25C).

These findings excluded DC-SIGN as a potential factor within the transferred membrane patches that is directly involved in the increased HIV-1 binding and fusion to co-cultured CD4 T cells.

### 3.5.2 Macrophage mannose receptor is dispensable for HIV-1 attachment to co-cultured CD32-positive CD4 T cells

An analogous experiment was performed with a different receptor candidate: the macrophage mannose receptor CD206. CD206 recognizes different polysaccharide structures such as mannose, fucose and GlcNAc and is involved in the recognition of pathogen's glycan structures as innate immune sensor in macrophages [342]. It was shown to bind the HIV envelope glycoprotein gp120 and potentially playing a role in transmission of bound HIV particles from macrophages to CD4 T cells [30, 31].

Similar to the DC-SIGN KO experiment (Figure 25), we achieved a high KO efficiency for CD206 (99% CD206-negative M2 KO cells) in M2 macrophages (Figure 26A). The CD206 KO had no effect on CD32 expression (Figure 26A) with efficient transfer of CD32, ranging between 35 and 40% in both co-culture conditions. We examined also the co-transfer of CD206 (14.5% positive CD4 T cells) after co-culture with the NTC M2 cells, which was completely suppressed in the M2 CD206 KO co-culture condition (0.5% CD206 positive CD4 T cells) (Figure 26B).

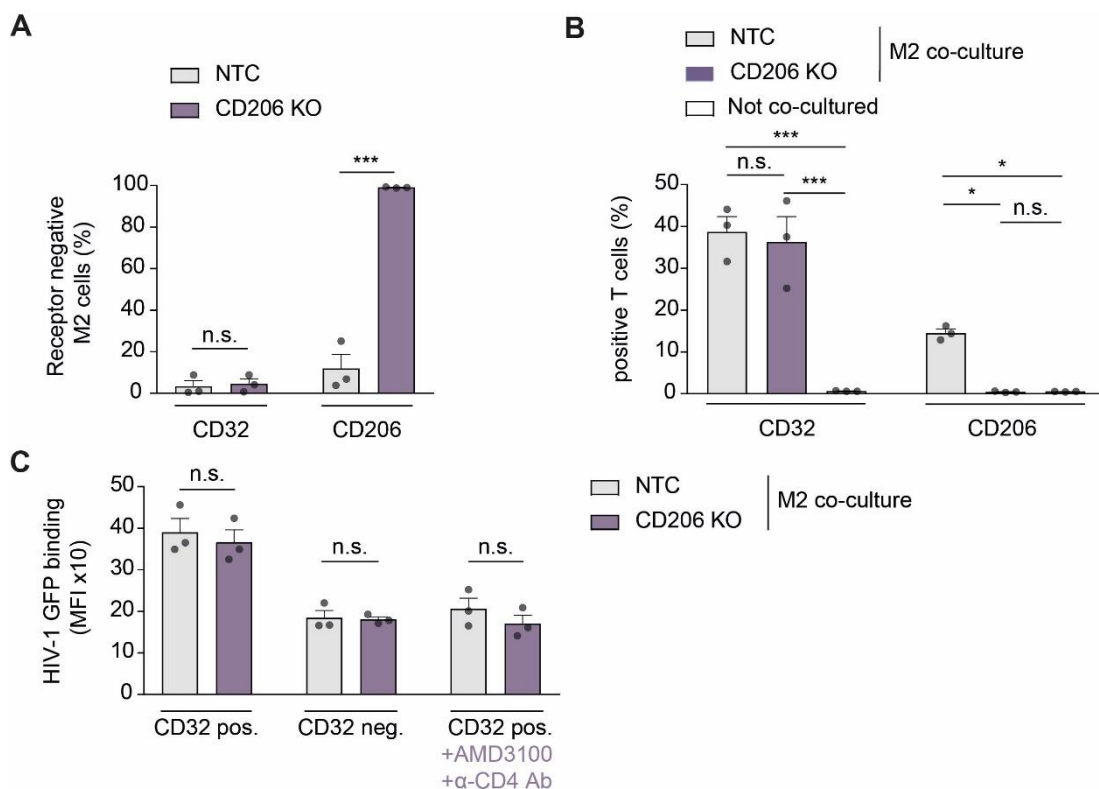


**Figure 26 | Knockout of CD206 in macrophages does not impact HIV-1 attachment to co-cultured CD32-positive CD4 T cells.**

**A**, Monocytes were isolated from PBMCs as previously described (Figure 11), followed by knockout of CD206 using specific RNPs, or NTC RNPs as control (Figure 18). After differentiation of the NTC and KO monocytes to M2 macrophages the expression of CD32 and CD206 was assessed by flow cytometry. Mean  $\pm$  s.e.m. are shown ( $n=3$ ). **B**, Autologous CD4 T cells were co-cultured with CD206 KO or NTC M2 cells for 2 days followed by staining for CD32 and CD206 on co-cultured and not-cultured T cells. Mean  $\pm$  s.e.m. is shown ( $n=3$ ). **C**, T cells from (**B**) were sorted after co-culture and then challenged with X4 HIV-1 particles carrying Vpr-GFP, followed by staining for CD32. CD32 frequency and GFP MFI were assessed by flow cytometry. Mean  $\pm$  s.e.m. is shown ( $n=3$ ). Asterisks indicate statistical significance by two-way ANOVA. P values were corrected for multiple comparison (Šídák). n.s.: not significant; \* $P \leq 0.05$ ; \*\*\* $P \leq 0.001$ .

However, also comparable to the DC-SIGN KO experiment, the absence of CD206 transfer did not affect the binding of HIV-1 virions to the CD32-positive T cells. In both co-culture conditions, HIV-1 binding to CD32-positive cells was increased compared to CD32-negative cells, which excluded also CD206 as relevant factor influencing HIV-1 binding to the transferred membrane patches (Figure 26C). With a similar approach we also excluded the receptor family CD11a/b and c. The  $\beta$ -integrin CD11c has been reported recently to bind HIV-1 when expressed on cervical epithelial cells. However, CD11c is also expressed on monocytes and macrophages, which induced our focus on also investigating this receptor. In order to exclude the influence of other receptors of the CD11 receptor family, we aimed to perform a “triple” KO in the macrophages, targeting CD11a, b and c simultaneously in the cells (Figure 27A).

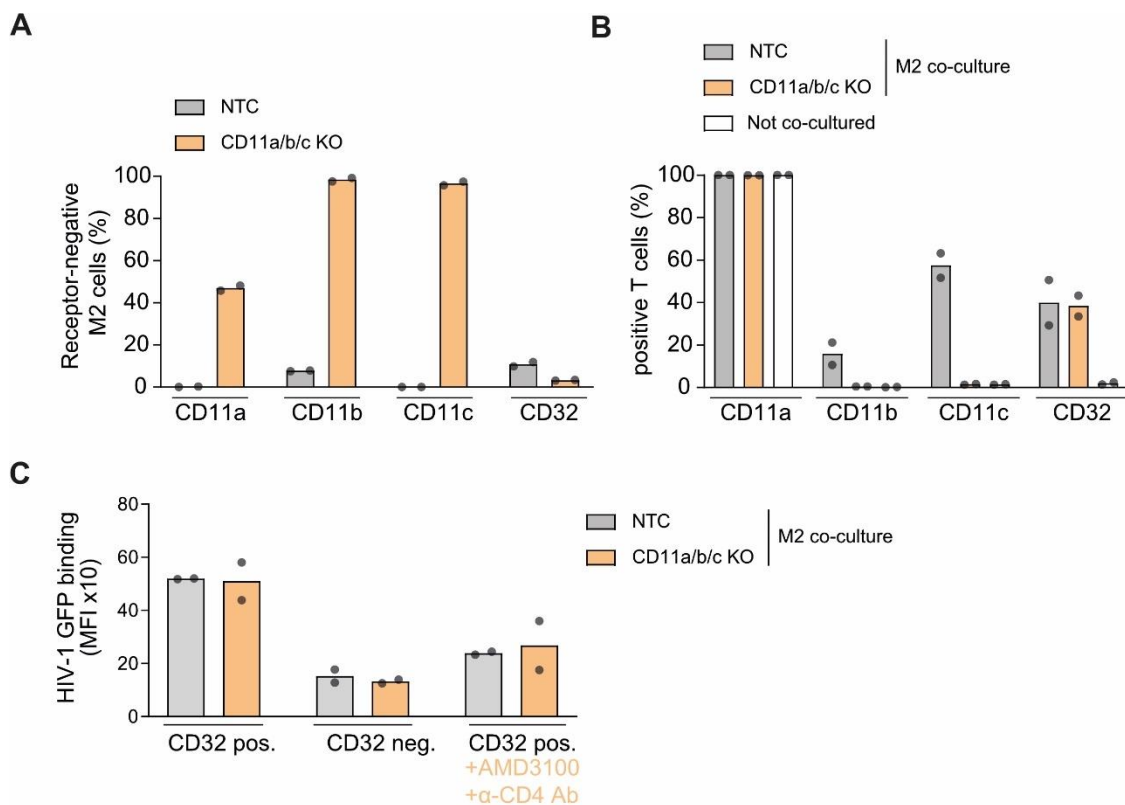


**Figure 27 | Knockout of CD11a/b/c in macrophages does not impact HIV-1 attachment to co-cultured CD32-positive CD4 T cells.**

**A**, Monocytes were isolated from PBMCs as previously described (Figure 11) followed by knockout of CD11a, b and c using specific RNPs, or NTC RNPs as control (Figure 18). After differentiation of the NTC and KO monocytes to M2 macrophages, the expression of CD32 and CD11a, b and c was assessed by flow cytometry. Mean  $\pm$  s.e.m. are shown ( $n=3$ ). **B**, Autologous CD4 T cells were co-cultured with CD11a/b/c KO or NTC M2 cells for 2 days followed by staining for CD32 and CD11a, b and c on co-cultured and not-cultured T cells. Mean  $\pm$  s.e.m. is shown ( $n=3$ ). **C**, T cells from **(B)** were sorted after co-culture and then challenged with X4 HIV-1 particles carrying Vpr-GFP, followed by staining for CD32. CD32 frequency and GFP MFI were assessed by flow cytometry. Mean of two independent donors are shown. Experiment performed by Hong-Ru Chen.

The KO of CD11b and c ablated the expression of these receptors nearly completely, with over 90% of the macrophages being negative after KO. In the case of CD11a, the KO efficiency was reduced, over 50% of the macrophages were still positive for CD11a. Analyzing the T cells after co-culture with the KO or NTC macrophages, allowed us to verify the transfer of CD11b and CD11c to the cells after co-culture, which was ablated if co-cultured with CD11a/b/c KO macrophages (Figure 27B). The expression levels of CD11a on the T cells were high, regardless of the culture condition, so transfer of CD11a could not be verified. Yet, even though the transfer of

CD11b and c was prevented in the co-culture of CD4 T cells and CD11a/b/c KO M2 cells, the binding of HIV-1 to CD32-positive T cells remained similarly high as in the condition of NTC co-cultured T cells (Figure 27C). This also excluded CD11a/b and c as potential receptors to induce HIV-1 binding to the transferred CD32-positive membrane patches on CD4 T cells after co-culture with M2 cells.

### 3.5.3 Heparinase and chondroitinase digestion does not reduce HIV-1 binding to CD32-positive CD4 T cells

The anionic polysaccharide Heparan sulfate (HS) is found on cell surfaces as well as extracellular matrix. Here it is covalently bound to proteoglycans (Heparan sulfate proteoglycan, HSPG) e.g. syndecans [343]. HSPGs have been reported to interact and help viruses such as hepatitis viruses [344-346], human papilloma virus (HPV) [347], herpes virus [348, 349] as well as HIV-1 [350] to attach on cell surfaces. In the case of HIV-1 binding it was found that HS on syndecans can bind the viral particle on spermatozoa supporting the transmission of the virus to the target cells such as macrophages and CD4 T cells [351]. HS was found to interact with the virus envelope glycoprotein gp120 [352] and was observed to bind HIV-1 on the cell surface independently of the presence of CD4 on the cells [35]. Syndecan expressed by macrophages could help the virus to surmount the restriction of low CD4 and positively influence the entry of the virus [353]. Heparan sulfate was therefore considered to play a potential role in increased HIV-1 binding to the trogocytically transferred membrane patches on CD4 T cells following M2 co-culture.

The antibody staining for HS on CD4 T cells (not co-cultured compared to co-cultured cells) did not show HS regardless of culture condition (Supplemental figure 9). Hereby we could not exclude a possible limit of detection of HS expressed on CD4 T cells and therefore continued with the strategy to enzymatically digest and remove potentially transferred HS, and additionally, also chondroitin sulfate (Ch) on co-cultured CD4 T cells. After digestion, we investigated HIV-1 binding to CD32-positive and negative cells. HeLa cells had shown high expression of HS (Supplemental figure 9) and served as digestion and HIV-1 binding control cells. Here the binding was strongly reduced upon HS/Ch digestion (Figure 28A).

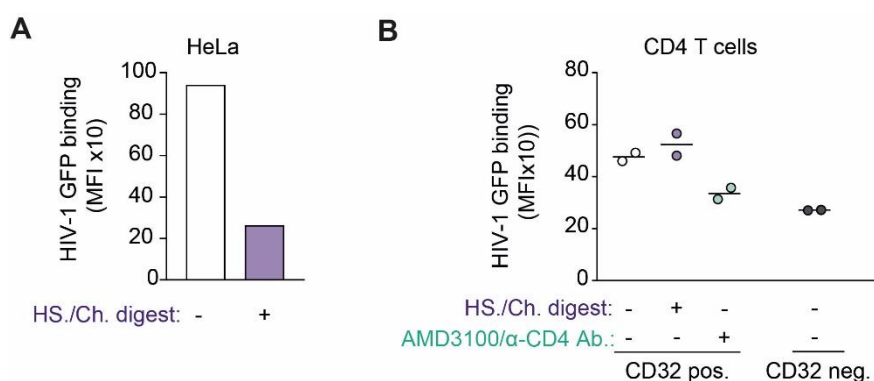


**Figure 28 | HS and Ch digestion can reduce HIV-1 binding to HeLa cells, but not to CD32-positive CD4 T cells.**

**A, B,** Heparinase I/II/III (HS) and chondroitinase ABC (Ch) digestion of HeLa cells (**A**), or on M2-co-cultured sorted CD4 T cells (**B**). HIV-1 Vpr-GFP binding was performed after digestion with subsequent staining for CD32 on the co-cultured T cells. MFI of GFP on CD32-positive and negative population was assessed by flow cytometry. Mean of two independent donors is shown.

In contrast, the enzymatic digestion of the co-cultured CD4 T cells did not reduce HIV-1 binding and did not reduce the differences of HIV-1 binding to CD32-positive (Figure 28B). CD32-positive

cells (MFI ~500) showed nearly twice as high binding of HIV-1 compared to CD32-negative cells (MFI ~270) irrespective of prior HS/Ch treatment.

The enzymatic treatment of the HeLa cells was in line with previous reports of high HIV-1 binding to these cells due to HS [35]. This could also validate the effectiveness of the performed HS/Ch digestion in our experimental setup. Since the digestion did not affect the HIV-1 binding to the CD32-positive CD4 cells, we largely excluded heparan sulfate- and chondroitin sulfate-carrying structures as potential factor of HIV-1 binding to CD32-positive membrane patches.

### 3.5.4 Increased HIV-1 binding to transferred membrane patches can be blocked by anti-CD4 antibodies and is mainly Env-dependent

The receptor KO approach as well as the enzymatic reduction of factors of interest allowed a structured investigation of potential factors one by one. We next extended this approach implementing a “receptor screening” procedure. Hereby we used antibodies specific for receptors that we found to be highly transferred after trogocytosis (Figure 17). The antibodies were added to the CD4 T cells after co-culture, followed by performing a HIV-1 Vpr-GFP binding assay. The hypothesis was that if one of these receptors is responsible of the higher HIV-1 binding capacity observed, it could be potentially blocked by a specific antibody.

To raise the number of screened receptors in one round of experiments, we simultaneously used a mixture of different antibodies for each sample. If one of the antibody mixtures showed an effect on HIV-1 binding, we further tested the individual antibodies in the mix.

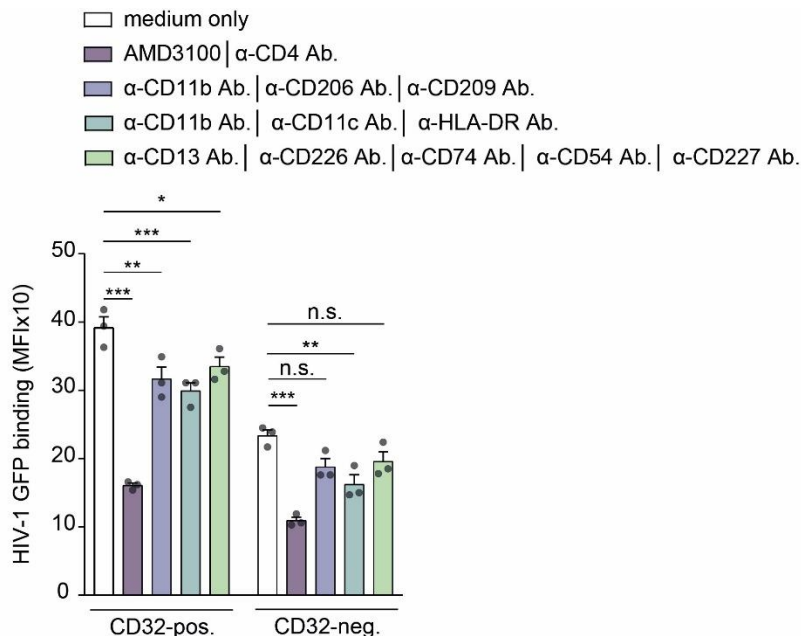


**Figure 29 | Blocking a selection of highly transferred surface receptors marginally decreases HIV-1 binding to CD32-positive CD4 T cells.**

CD4 T cells were sorted after co-cultured with M2 and challenged with X4 HIV-1 Vpr-GFP in the presence of different antibody combinations and/or antiviral drugs. Mean  $\pm$  s.e.m. are shown (n=3). Asterisks indicate statistical significance by two-way ANOVA. P values were corrected for multiple comparison (Šídák). n.s.: not significant; \*P  $\leq$  0.05; \*\*P  $\leq$  0.01; \*\*\*P  $\leq$  0.001.

All three antibody mixtures showed a significant reduction of HIV-1 binding to CD32-positive cells, albeit only to a minor extent (Figure 28). Since the three antibody mixes did not share the same targets, we concluded that the binding reduction was most likely caused by steric hindrance than

of bound antibodies by specific blocking of one receptor. In the control condition, where X4 HIV-1 entry receptors were blocked by the addition of AMD3100/anti-CD4 antibody, the MFI was markedly decreased. Here, the reduction was seen within the CD32-positive as well as the CD32-negative CD4 T cell population. However, binding decreased within the CD32-positive cells upon drug treatment, stronger than the level of binding seen within the untreated CD32-negative population (CD32-pos. +AMD3100/ $\alpha$ -CD4: MFI ~160; CD32-neg. medium only: MFI ~234). This indicated a strong loss of increased HIV-1 binding phenotype in the CD32-positive CD4 T cell population and raised the question of whether the increased HIV-1 binding within the transferred membrane patches strongly depends on the viral entry receptors.

We therefore targeted in an analogous experiment, the blockages of CXCR4 by AMD3100 or of CD4 by anti-CD4 antibody separately to investigate the impact of each compound (Figure 30A). This approach revealed that only in the presence of anti-CD4 antibody the binding was strongly reduced (no treatment MFI ~664; AMD3100/ $\alpha$ -CD4 Ab. MFI ~248; AMD3100/Isotype ~649). Already with the addition of anti-CD4 antibody only, the difference of HIV-1 binding to CD32-positive cells was restored to levels seen in CD32-negative cells. The addition of AMD3100 and isotype control had no significant effect ( $\alpha$ -CD4 Ab. MFI ~225).

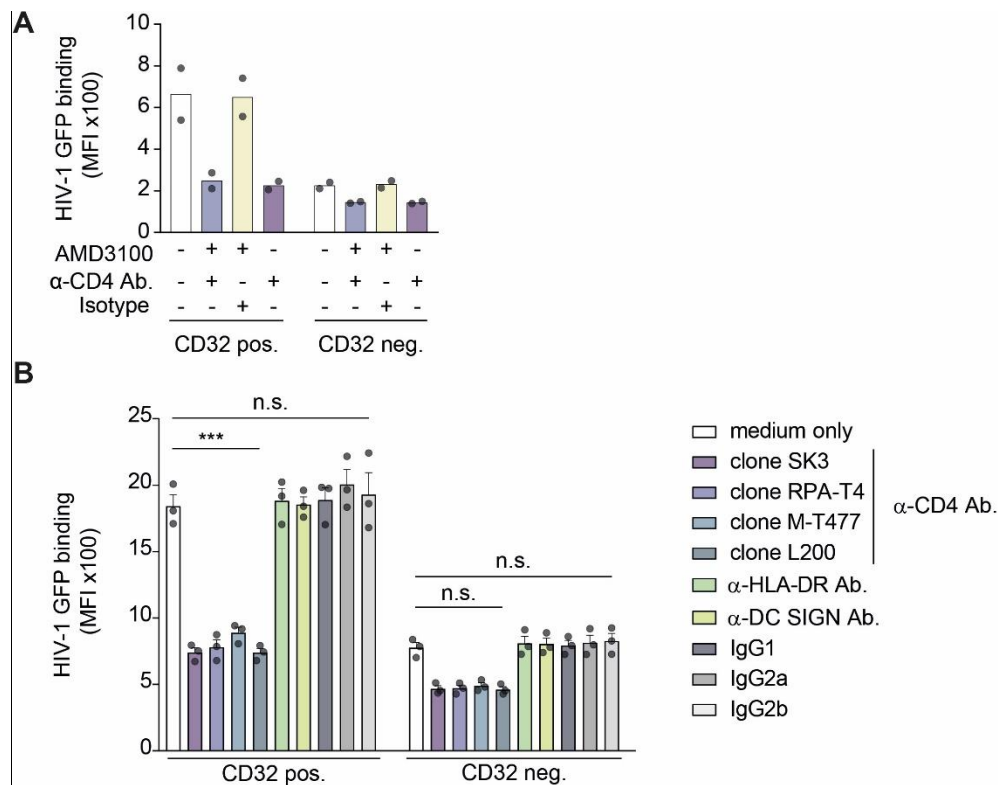


**Figure 30 | Addition of anti-CD4 antibodies reduces HIV-1 binding to CD32-positive cells to levels found for CD32-negative cells.**

**A, B,** HIV-1 binding to M2 co-cultured and sorted CD4 T cells following addition of **(A)** anti-CD4 antibody, isotype control and or CXCR4 antagonist AMD3100 in different combinations. Mean of two independent donors shown. Using a similar approach, the binding of HIV-1 Vpr-GFP to CD4 T cells was investigated in the presence of **(B)** either different anti-CD4 antibody clones, isotype control antibodies or antibodies against receptors known to be highly transferred to the T cells during M2 co-culture. Mean  $\pm$  s.e.m. are shown (n=3). Asterisks indicate statistical significance by two-way ANOVA. P values were corrected for multiple comparison (Šídák). n.s.: not significant; \*\*\*P  $\leq$  0.001.

The specificity of blocking CD4 in the binding assay by the antibody clone SK3 used in the previous experiments was confirmed in the following experiment (Figure 30B) in which we tested different anti-CD4 antibodies. As controls, we used antibodies against prominently transferred receptors such as HLA-DR and DC-SIGN or isotype controls, which should not interfere with binding. All four anti-CD4 antibody clones prevented the increased HIV-1 binding to CD32-positive cells, whereas the addition of neither anti-HLA-DR, anti-DC-SIGN nor isotype control antibody had an effect on HIV-1 binding. Addition of anti-CD4 antibodies showed a slight reduction in HIV-1 viral binding also within the CD32-negative population, which did not react statistically significant.

Following these findings, we addressed the HIV-1 envelope dependency of increased binding of HIV-1 to CD32-positive cells. For this aim, we inoculated CD4 T cells after co-culture with increasing MOIs of either X4 HIV-1 Vpr-GFP or HIV-1 $\Delta$ Env Vpr-GFP particles (Figure 24). The amount of viral particles had been previously quantified by SYBR Green I-based real-time PERT assay (SG- PERT) for both virus stocks, to ensure the inoculation with the same number of viral particles in both conditions.

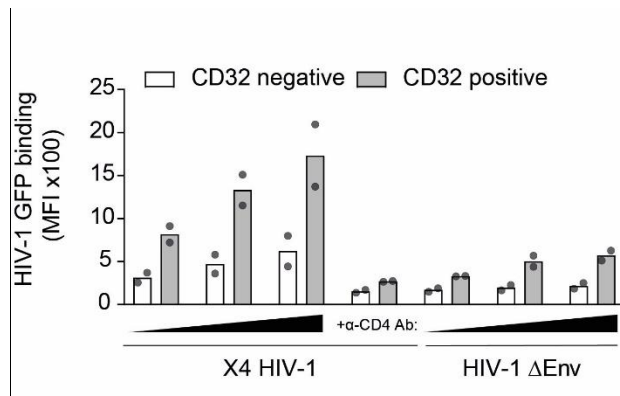


**Figure 31 | Inoculation with HIV-1 ΔEnv particles reduces HIV-1 binding to CD32-positive T cells to levels found for CD32-negative T cells.**

In an experiment analogous to the setup of Figure 30 and Figure 29, sorted CD4 T cells were inoculated after co-culture with increasing amounts of X4 HIV-1 or HIV-1ΔEnv particles carrying Vpr-GFP, followed by staining for CD32. CD32 expression and GFP MFI were assessed by flow cytometry. Mean of two independent donors are shown.

With increasing amounts of X4 HIV-1 particles also the GFP MFI differences between the CD32-positive and CD32-negative T cells increased. In contrast, this phenotype was only observed to a minor extent for the binding of HIV-1ΔEnv GFP. Consistent with previous experiments, the binding of X4 HIV-1 Vpr-GFP could be strongly decreased by addition of anti-CD4 antibody, to similar levels as the lowest MOI with HIV-1ΔEnv Vpr-GFP.

Overall, these findings provided insight into increased binding to CD32-positive T cells being partially HIV-1 Env-dependent and strongly influenced by the binding to CD4.

### 3.5.5 CD4 expressed *de novo* by T cells, but not by M2 macrophages, affects HIV-1 viral binding to CD32-positive membrane patches on T cells.

In previous experiments, we excluded pre-selected receptors/host factors of co-cultured M2 macrophages to play a role in preferential binding of HIV-1 to CD32-positive CD4 T cells. Among all receptors tested, blocking with anti-CD4 antibodies had the strongest effect on the increase in HIV-1 binding.

Following up on this observation, we considered CD4 could be co-transferred from the M2 macrophages during co-culture, resulting in a concentrated localization within the transferred CD32-positive membrane patches and inducing a preferential virus binding environment compared to the CD4 highly endogenously expressed on T cells. We assessed this hypothesis with a similar experimental setup as implemented for the previous investigation of CD206 (Figure 24 & Figure 26). We knocked out CD4 in monocytes, differentiated them to M2 macrophages, resulting in a highly effective loss of CD4 expression of 99% (Figure 31A). In parallel, also the CD32 expression was monitored and was not found to be affected by the CD4 KO. In the following co-culture with autologous CD4 T cells, both co-culture conditions showed lower transfer of CD32 compared to previous experiments (7-9% CD32 positive cells). However, we concluded that the KO of CD4 did not generally influence the transfer since the NTC M2 co-cultured showed similarly low levels (Figure 32B). Since CD4 is highly expressed on T cells, we could not detect differences of CD4 levels after co-culture (data not shown) leaving the question unsolved whether CD4 is transferred from M2 macrophages during co-culture.

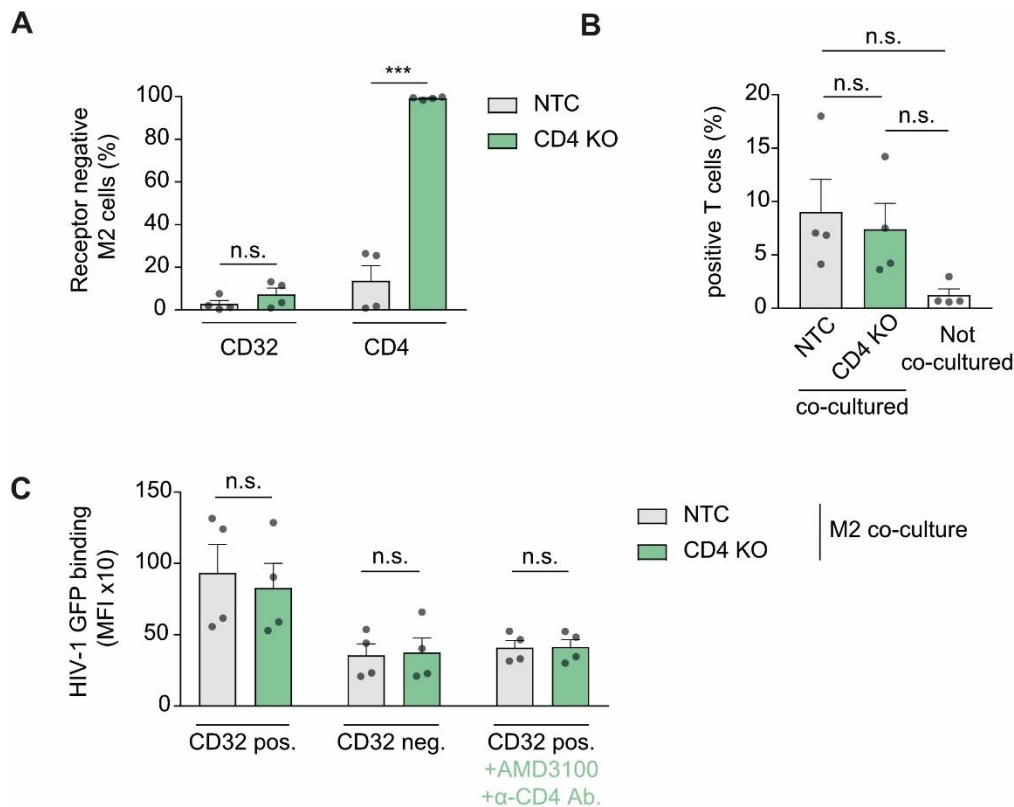


**Figure 32 | Absence of CD4 on M2 macrophages does not reduce the binding of HIV-1 to CD32-positive T cells.**

**A**, Monocytes were isolated from PBMC as previously described (Figure 11) followed by knockout of CD4 using specific RNPs, or NTC RNPs as control (Figure 18). After differentiation of the NTC and KO monocytes to M2 macrophages the expression of CD32 and CD4 was assessed by flow cytometry. Mean  $\pm$  s.e.m. are shown ( $n=4$ ). Asterisks indicate statistical significance by two-way ANOVA. P values were corrected for multiple comparison (Šídák). **B**, Autologous CD4 T cells were co-cultured with CD4 KO or NTC M2 cells for 2 days followed by staining for CD32 and CD4 on co-cultured and not-cultured T cells. Mean  $\pm$  s.e.m. is shown ( $n=4$ ). Asterisks indicate statistical significance by one-way ANOVA. P values were corrected for multiple comparison (Tukey). **C**, CD4 T cells in (**B**) were sorted and inoculated after co-culture with X4 HIV-1 particles carrying Vpr-GFP, followed by staining for CD32. The percentage of CD32-positive cells and GFP MFI was assessed by flow cytometry. Mean  $\pm$  s.e.m. are shown ( $n=4$ ). Asterisks indicate statistical significance by two-way ANOVA. P values were corrected for multiple comparison (Šídák). n.s.: not significant. \*\*\* $P \leq 0.001$

In the final step of the CD4 KO co-culture experiment, we analyzed the binding of HIV-1 Vpr-GFP particles to the CD32-positive or negative CD4 T cells after M2 co-culture and sorting. The CD4 KO in M2 macrophages did not affect the binding of HIV-1 to CD32-positive CD4 T cells. Furthermore, the blocking of binding by addition of AMD3100/anti-CD4 showed to be efficient for NTC and CD4 KO M2-co-cultured T cells. The drug/antibody treatment reduced the levels of bound HIV-1 particles on CD32-positive cells to levels similar seen for those untreated or CD32-negative cells for the NTC and the CD4 KO M2 co-cultured T cells (Figure 31).

Until now the focus was on identifying cellular factors transferred from M2 macrophages to explain the increase in HIV-1 binding on CD32-positive membrane patches on CD4 T cells. However, since the blocking with anti-CD4 antibody was observed in all conditions tested, irrespective of the CD4 expression on co-cultured M2 cells, the question arose whether CD4 endogenously expressed by the T cells may be involved in this virological phenotype.

Accordingly, we re-designed the experimental setup, genetically modifying this time the recipient cells before co-culture instead of the myeloid donor cells. We therefore aimed to knock out CD4 in resting CD4 T cells applying protocol recently established in the Keppler laboratory [304]. To ensure a complete loss of CD4 after KO in resting CD4 T cells, the cells had to be kept in culture

for more than 10 days (based on pilot experiment, data not shown). The CD4 T cells were directly isolated from whole blood and on the same day nucleofected with specific RNPs to knock out CD4, NTC RNPs served as control. The autologous WT monocytes were kept in culture and the differentiation period was extended until the start of the co-culture (~14 days instead of ~7 days). Following confirming the effective loss of CD4 (data not shown) on the T cells, these cells were seeded for the co-culture with the autologous wildtype M2 macrophages. CD4 (Figure 33A) and CD32 (Figure 33B) levels were analyzed on the CD4 T cells after co-culture compared to not co-cultured cells. First, the complete depletion of CD4 within the KO T cells confirmed the absence of CD4 transfer from M2 cells, in line with the previous experimental outcome with CD4 KO M2 cells (Figure 32). Second, the efficient transfer of CD32 was seen independently of the editing condition of the T cells (Figure 33B).

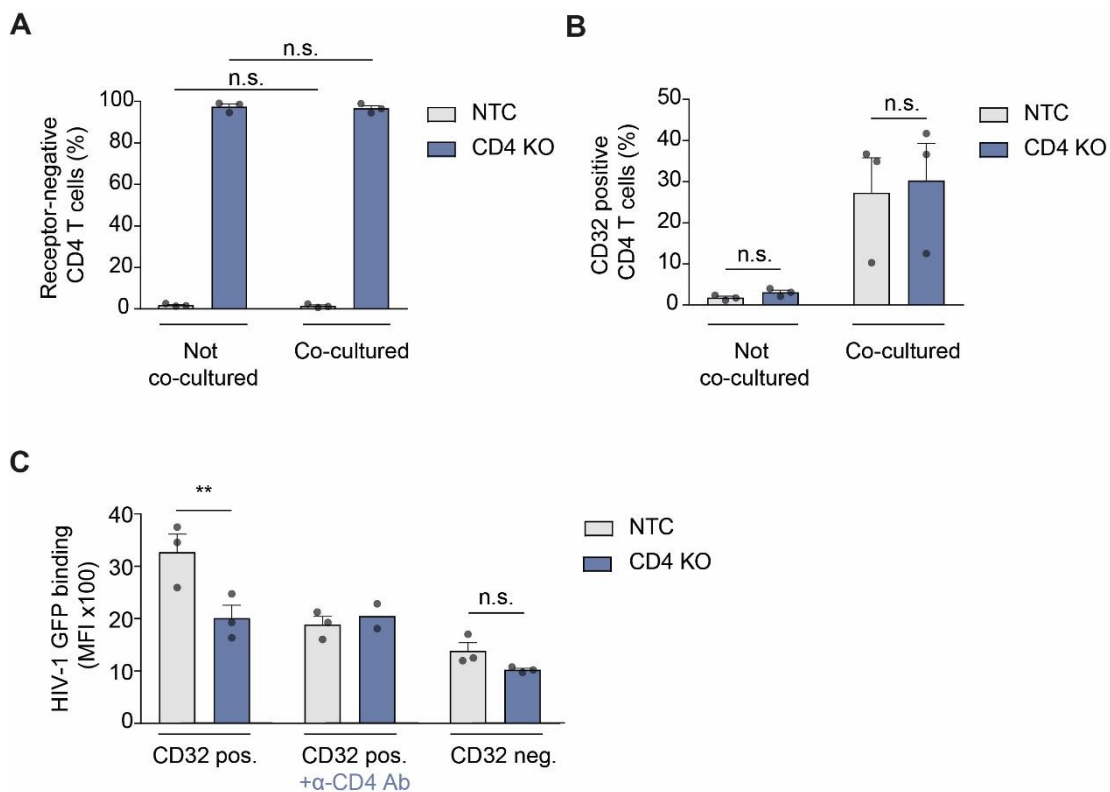


**Figure 33 | Abolishing CD4 expression in T cells reduces HIV-1 binding to the CD32-positive T cell population.**

**A, B**, Freshly isolated CD4 T cells were nucleofected with either specific RNPs to knock out CD4 or, as control nucleofected with NTC RNPs. The cells were kept in a resting state by addition of IL-7/IL-15 [304] for 16 days before starting a 48 h co-culture with autologous wild type M2 macrophages. After co-culture, the cells were analyzed for CD4 (**A**) or CD32 surface levels (**B**). Mean  $\pm$  s.e.m. are shown ( $n=3$ ). Asterisks indicate statistical significance by two-way ANOVA. P values were corrected for multiple comparison (Šídák). **C**, the sorted T cells from (**A**) and (**B**) were then seeded for the X4 HIV-1 Vpr-GFP binding assay as described previously. Mean  $\pm$  s.e.m. are shown ( $n=2-3$ ). Asterisks indicate statistical significance by two-way ANOVA. P values were corrected for multiple comparison (Šídák). n.s.: not significant; \*\* $P \leq 0.01$ .

Subsequent analysis of HIV-1 Vpr-GFP binding to the co-cultured T cells showed a decline of HIV-1 binding to CD32-positive cells, when CD4 was not present on T cells. This nearly completely abrogated the enhanced binding to CD32-positive compared to CD32-negative cells (Figure 33C). Consistently, with the addition of anti-CD4 antibodies to the NTC T cells the binding declined to similar levels as within the untreated CD4 KO T cells. In these cells, HIV-1 binding levels to the CD32-positive CD4 KO T cells was not affected by the addition of anti-CD4 antibod-

ies, further confirming that CD4 had to be expressed *de novo* by T cells to recapitulate this phenotype (Figure 33C). Overall these results implicated the crucial role of endogenously expressed CD4 in the enhanced HIV-1 binding to T cells observed after co-culture.

Next, a fluorescent microscopic analysis of co-cultured CD4 T cells was performed. Here, the endogenously expressed CD4 receptor was observed to be homogeneously distributed on the surface of wild type CD4 T cells. However, at the site of CD32-positive membrane patches, where also high levels of HIV-1 Vpr-GFP particles were found to be bound, the CD4 staining indicated an aggregation of CD4 receptors. Intensity profile analysis of the membrane verified the co-localization of CD32, HIV-1 GFP particles and CD4 (Figure 34).

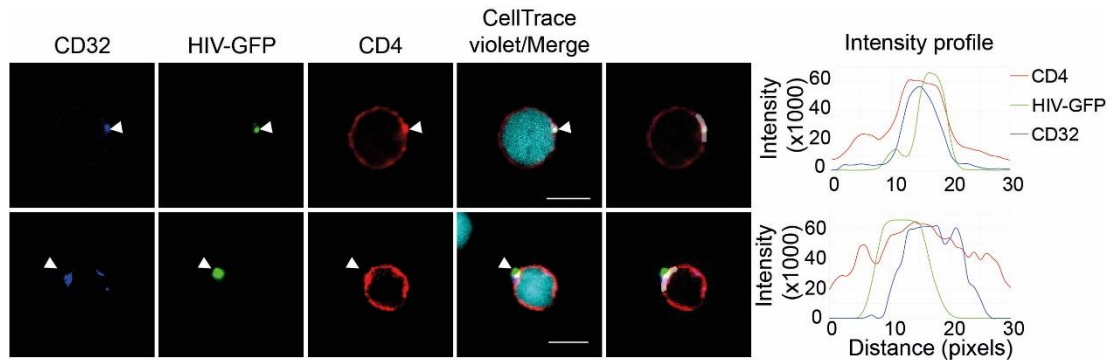


**Figure 34 | Aggregation of CD4 at CD32-positive transferred membrane patches promotes HIV-1 binding.**

CD4 T cells co-cultured with M2 macrophages for two days (as in Figure 16), were sorted and subsequently incubated with HIV-1 Vpr-GFP followed by staining for CD32 and CD4 as in (Figure 30). After fixation, the images were taken with a spinning disc confocal microscope. White arrow heads indicate the co-localization of CD32, HIV-1 Vpr-GFP and clustered CD4. The intensity profiles were analyzed along selected regions on the cell surface with ImageJ. Scale bar: 5  $\mu$ m. Microscopic picture and intensity profile performed by Hong-Ru Chen.

The CD4 KO T cell experiments (Figure 33) with analysis of HIV-1 binding as well as the following microscopic analysis (Figure 34) indicated that the increased susceptibility of T cells seen after myeloid cell co-culture, is induced by the aggregation of endogenously expressed CD4 receptors within the M2-derived trogocytotically transferred membrane spots. We speculated that these higher levels of CD4 created a more favorable environment for the interaction with the virus, resulting increased binding, fusion and infection of these otherwise infection-refractory CD4 T cells.

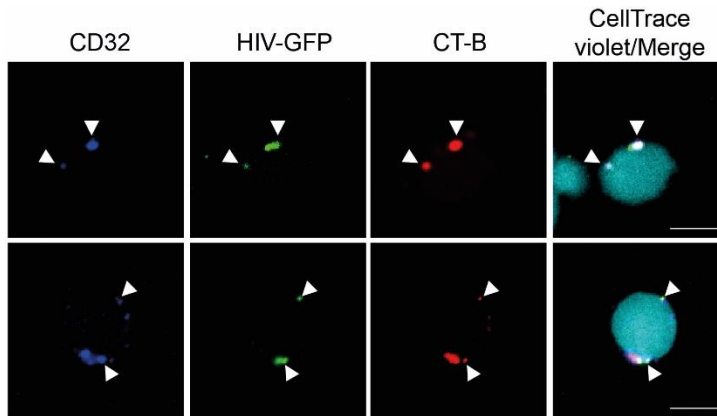


**Figure 35 | Trogocytosed membrane patches with increased HIV-1 binding are positive for CD32 and the typical constituent of lipid rafts, GM1.**

CD4 T cells were co-cultured with M2 macrophages as described before (Figure 16). M2 macrophages were pre-labeled with biotin-xx-conjugated CT-B- prior to co-culture to detect ganglioside monosialotetrahexosylganglioside (GM1). After co-culture, CD4 T cells were sorted by flow cytometry and incubated with HIV-1 Vpr-GFP. Subsequently CD4 T cells were stained for CD32 and fluorochrome-conjugated streptavidin followed by fixation of the cells. The cells were then analyzed by spinning disc confocal microscope. The white arrow heads indicate the co-localization of CD32, HIV-1 Vpr-GFP and CT-B. Scale bar: 5  $\mu\text{m}$ . Microscopic pictures and intensity profile performed by Hong-Ru Chen.

Moreover, pre-labeling M2 macrophages with cholera toxin subunit-B (CT-B) prior to co-culture with CD4 T cells enabled the detection of the ganglioside monosialotetrahexosylganglioside (GM1) and its transfer within the CD32-positive membrane patches with high HIV-1 binding capacity on T cells (Figure 35). In the field of membrane lipid research GM1 has been used as a marker for lipid rafts [354-356], which was mainly detected within the transferred membrane patches but not in other parts of on the surface of the CD4 T cells. This further verified the transfer of complete membrane patches with remaining M2 membrane composition to the T cells.

## 4. Discussion

### 4.1 CD32 is transferred to CD4 T cells from CD32-expressing cells in a cell contact-dependent manner

The persistence of HIV in latently infected cells is still one of the major limitations to the cure of HIV-infected patients. A selectively expressed biomarker in this HIV reservoir (mostly resting CD4 T cells), would facilitate the specific targeting and elimination of latently infected cells. In the past several surface markers have been proposed to have this potential property, such as CD30 [156], CD98 [158] and CD32a [142]. Descours and Petitjean *et al.* [142] proposed CD32a to be a highly exclusive biomarker for latently infected cells, since they could not detect CD32-positive CD4 T cells within the uninfected controls, while over 50% of the latently infected cells were CD32a-positive. This electrified the HIV field with some groups partially confirming the findings, reporting CD32 expression on HIV transcriptionally active CD4 T cells [144, 151, 152]. However, also contradictory findings have been found, observing e.g. no enrichment of HIV-1 proviral DNA in CD32-positive cells [147-150] and comparable CD32-positive CD4 T cell frequencies in healthy donors [148, 150], or even proposing for the original discovery of Descours and Petitjean *et al.* [142] experimental artifacts [148, 151] that had caused false positive results. In our hands, the culturing conditions turned out to have a strong impact on the exposure of CD32 positivity on CD4 T cells. Keeping the cells in a PBMCs co-culture (similar to the settings Descours and Petitjean *et al.* [142] had used), we could detect CD32-positive CD4 T cells in the infected and uninfected cell population. However, isolation of the CD4 T cells from PBMC prior to infection, diminished this phenotype drastically with low to no detectable CD32-positive CD4 T cells (Figure 6A, p.51). This indicated a potential dependency on the presence of other immune cells for the CD32 exposure on CD4 T cells. CD32 was also proposed to be induced in CD4 T cells upon activation [144, 151, 153]. We therefore investigated a scenario with induced activation of the CD4 T cells within the PBMC culture, which could explain the previous experimental outcome. Yet, strong T cells activation with PHA+IL-2 treatment did not induce CD32 expression, if the CD4 T cells were cultured alone. This therefore further supported the dependency of CD32 positivity on the presence of other immune cell types (Figure 6B, p.51). This was further verified by the depletion of CD14-positive cells from the PBMC culture, that strongly reduced the CD32 frequency in the CD4 T cell population (from ~6% CD32-positive CD4 T cells with PBMC culture to ~1% within the CD14-depleted PBMC culture) and furthermore, the co-culturing of the isolated CD14-positive cells with CD4 T cells induced similar or even higher CD32 positivity (~8% CD32-positive CD4 T cells) (Figure 6C, p.51). Together these findings suggested that CD32 expression on CD4 T cells depends on the presence of monocytic cells in the culture and is independent of HIV-1 infection.

The co-culture in a transwell system, which physically separates CD4 T cells from myeloid cells demonstrated the cell contact-dependency and shaped the hypothesis of CD32 being transferred from CD32-expressing myeloid cells and not being *de novo* expressed by CD4 T cells. No CD32 exposure was detected on CD4 T cells, if cells were kept separated from myeloid cells (Figure 7B, p. 53). In addition, the frequency of CD32-positive CD4 T cells strongly correlated with the levels of CD32 expressed on the surface of myeloid cells (Figure 7C, p.53). The higher the expression of the primary donor cells (myeloid cells) the higher the level of CD32 exposure on CD4 T cells could be detected. The highest exposure of CD32 on CD4 T cells after co-culture was seen with M2 macrophages, followed by MDM and M1 macrophages. Macrophages have been

reported to express CD32A and B and also the FcγRI (CD64), whereas DC cells have been reported to express CD64, but are not thought to express CD32 [169, 175] (Figure 3, p.21). Likewise, we could not detect CD32 on the monocyte-derived DC cells and, correspondingly, no CD32 was found on co-cultured CD4 T cells (Figure 7, p.53). As also described by Abdel-Mohsen *et al.* [151] the commercially available anti-CD32 antibodies for the detection by flow cytometry cannot distinguish between CD32A, CD32B or CD32C, because of their high degree of amino acid sequence similarity in the extracellular part [151]. We therefore could not define which gene product is actually expressed by the macrophages and was transferred to co-cultured CD4 T cells. Also, qPCR analysis could not satisfyingly distinguish between the different mRNAs (data not shown). Interestingly the co-culture with M2 macrophages also showed double-positive CD4 T cells for CD32 and HLA-DR (Figure 8, p.54). The actual transfer of HLA-DR could be proven by the depletion of HLA-DR expression on CD4 T cells by gene perturbation, which still showed comparable HLA-DR exposure after co-culture with wild type (WT) M2 macrophages. In contrast, the co-culture with HLA-DR KO macrophages and WT T cells showed no increase of HLA-DR exposure on CD4 T cells (data not shown, description in chapter 3.1 p.54). Descours and Petitjean *et al.* [142] had excluded HLA-DR-positive CD4 T cells from their analysis to exclude activated CD4 T cells. However, taking into account that HLA-DR can also be transferred from macrophages together with CD32 this might have excluded a high number of CD32-positive CD4 T cells from their investigation. It also has to be considered that HLA-DR transfer to T cells could also result in their false categorization as “activated T cells”. Other groups have stated that CD32 could be a marker of activation, since they saw co-expression of HLA-DR and CD32 on T cells [143, 151]. However, when analyzing CD32-positive T cells after co-culture over 16 days, we could not observe its induction by activation while other activation marker such as CD69, CD25, CD38 and Ki67 responded as expected (data not shown). Other groups have also noted that CD32 could be transferred within membrane fragments from CD32-expressing cells to CD4 T cells and these cell fragments could also include other cell surface markers such as CD19 and HLA-DR [150].

## 4.2 CD32B is a strong driver of trogocytosis, which can be enhanced by autoantibodies

In an attempt to gain further insight into the dynamics of the transfer of CD32 and potential co-transfer of other receptors we turned to design an *in vitro* FcγR-mediated trogocytosis cell line model. Similarly, also Hudrisier *et al.* had designed an *in vitro* trogocytosis protocol to investigate the transfer of receptors from one cell to another, in which the target cells are stained with a lipophilic probe, DiO, before co-culturing with the donor cells for 1 h at 37 °C [297, 298]. With this model they were able to observe the transfer of murine CD32B and CD16A from transiently expressing 293T cells (donor cells) to primary CD4 or CD8 T cells (recipient cells). Yet, the T cells had previously been opsonized with mAb, binding to antigens on the T cell surface e.g. anti-CD2 antibody [297]. In comparison we used in our *in vitro* model a cell trace dye that in contrast to DiO does not stain the lipid membrane but reacts with intracellular compounds. In our hands this minimized the transfer of the dye to the co-cultured cell population and ensured a clear distinction of the cell populations later on (Figure 4, p.22). We also extended the co-culture duration to 24 h at 37 °C. With this setup we could monitor the transfer of human FcγRs CD32A, B and C as well as CD64 to human T cell line SupT1 (Figure 10A and B (left panel), p.56). Here, the inhibitory FcγR CD32B showed the highest transfer efficiency and, interestingly, we could detect the co-transfer of other receptors (CD4 and CCR5) in the presence of CD32A (for CD4) and CD32B and CD32C (for CD4 and CCR5) (Figure 10A and B (right panel), p.56). However, in contrast to the findings

of Hudrisier *et al.* [297] we had not previously opsonized the T cell line with antibodies to induce trogocytosis. Follow up experiments showed a role of the bovine IgGs in the fetal calf serum supplemented to the culture media in the co-culture to enhance trogocytosis (data not shown). This indicated that not only specific antibodies could enhance trogocytosis, but potentially unspecifically bound IgGs from another species could also enhance trogocytosis.

Since CD32 is an IgG binding receptor, we sought to investigate whether the trogocytosis rate was enhanced by the presence of antibodies. To this end we tested human serum as addition to the regular co-culture. Additionally, we not only tested sera from healthy donors, but also sera from patients with different virologic, bacterial or parasitic infections as well as autoimmune diseases (Figure 11A, p.57), which are known diseases that are characterized by the presence of auto-antibodies. Interestingly, neither the healthy donor sera nor most of sera of other diseases enhanced trogocytosis. In contrast, two HCV patient samples and a subset of chronic HIV-1-infected patient sera (non-treated and ART-treated) enhanced the trogocytosis rate to different degrees. When incubating a selection of these HIV-1 and HCV patient sera with primary CD4 T cells, the same sera that had shown trogocytosis-enhancing properties also showed high levels of IgG bound to the surface to primary CD4 T cells (Figure 11B, p.57). This further supported the notion that antibodies bound to the surface of the target cells, may form a cell-to-cell bridge with the CD32-expressing donor cells to enhance trogocytosis, as proposed by Daubeuf *et al.* [295]. This raised the question why this was almost exclusively seen for sera of chronic HIV-1 patients? In HIV infection auto-antibody levels are known to increase already in the early acute phase of infection and these levels stay high also in chronic infection [357, 358]. However, auto-antibody production is also reported for some of the other viral infections studied (SARS-CoV-2 [359], DENV [360], HTLV [361] and HCV [362]) and autoimmune diseases (SLE [363] or RA [364]). Yet, for the trogocytosis-enhancing effect it seems like the autoantibody specifically has to bind to the recipient cells (in this case CD4 T cells). Autoantibodies targeting CD4 T cells are observed only in HIV-1-infected patients [357, 358, 365], which could explain the exclusive phenotype for a subset of HIV-1 patient sera. In contrast, the infection or diseases reported to induce more broadly binding autoantibody production such as antibodies against intracellular components [359, 362, 363, 366] or antigens on other cells such as platelets and endothelia cells [360] might not produce autoantibodies with the properties to bind to the CD4 T cells. Trogocytosis-enhancing autoantibodies present in HIV-1 patients can also explain the increased rate of CD32-positive CD4 T cells in chronic disease in comparison to CD4 T cells from healthy donors (Figure 11C, p.57). If CD4 T cells are opsonized with autoantibodies in HIV-1 patients, this will also induce and enhance the interaction with CD32-expressing cells such as macrophages with CD4 T cells, leading to increased rate of CD32 transfer to the CD4 T cells. Interestingly, the limited number of HIV-2 sera tested did not show trogocytosis-enhancing effects, indicating potential differences in autoantibodies between chronic HIV-1- or HIV-2-infected patients, as it is also seen for other clinical manifestations such as lower viral load and more frequent non-progressors in HIV-2 disease [367].

In a subset of bNAbs we screened for potential trogocytosis-enhancing properties, bNAb PGT151 markedly enhanced CD32 transfer and strongly bound to CD4 T cells (data not shown). Since the trogocytosis-enhancing effect in our model is believed to be induced by the antibody binding to FcγRs on the surface of donor cells with their Fc part and targeting an antigen on the recipient cell surface, an enhancement of trogocytosis by the antibody should only be observed if trogocytosis is mediated by an FcγR. Consequently, transfer of receptors enhanced by antibodies can be described as FcγR-dependent trogocytosis and therefore we used PGT151 as a tool to better characterize CD32-dependent co-transfer of other receptors.

The co-transfer of seven-transmembrane receptors CCR5 and CXCR7 as well as the single transmembrane receptor CD4 could be enhanced with the addition of bNAb PGT151, whenever CD32 was co-expressed on the 293T cells (Figure 12A, p.59). If the donor 293T cells expressed instead of CD32B the control protein H2B, low basal levels of transfer of CCR5, CXCR7 or CD4 to SupT1 target cells were observed with no increase of transfer when PGT151 was present. The CD32 dependency on the trogocytosis-enhancing effect of PGT151 was also supported by mutating the N-glycosylation site on CD32B IgG binding sites ( $\Delta$ glyco CD32B: N106G, N18G, N187T): Here, the increased transfer of CCR5 was strongly reduced with the  $\Delta$ glyco CD32B mutant compared to the increased transfer by PGT151 with CD32B WT (from ~26-fold increase with WT to ~2-fold  $\Delta$ glyco). In contrast, deleting the intracellular signaling motif ( $\Delta$ ITIM CD32B) only slightly decreased the enhancing effect i.e. from ~26-fold increase with WT to ~20-fold with  $\Delta$ ITIM. Deglycosylation of Fc $\gamma$ R has been shown to affect the binding of antibodies [319], for CD32B, mutation especially of the N-glycosylation site N187 has been reported to decrease the binding of the therapeutic antibody trastuzumab [368]. However, in that study the mutation of CD32A on the N-glycosylation sites showed no strong effect on the interaction of trastuzumab and the mutated CD32A. In contrast, our finding also showed a decrease of PGT151-enhancing trogocytosis with  $\Delta$ glyco CD32A (N97G, N178G). Since the mutation of the N-glycosylation sites presumably decrease the binding of the Fc part to CD32B this then can potentially decrease the capability of the antibodies to form a bridge between the two cells and enhance trogocytosis. Since CCR5 transfer was still highly detected with a “silenced” ITIM motif in CD32B, the signaling function of the Fc $\gamma$ R seems to be not essential for CD32B to mediate trogocytosis, this implies that the transfer mechanistically relies more on the binding and the close cell-cell contact than on the known signaling function of the receptor.

Using PGT151 as a tool to investigate CD32B-dependent transfer of receptors, we could determine a certain selectivity of transferred receptors/proteins in dependency on their cellular localization (Figure 13, p.60). Here, the cell surface receptors with large extracellular domains CCR5, CXCR4, CD4 as well as CD63 showed to be highly transferred. But also intracellular plasma membrane proteins could be transferred by CD32B e.g. LckN18, however to a lower extent. Transfer of cytoplasmic-nuclear protein SAMHD1 was not observed. This provided the insight that mainly receptors or proteins located in or at the cell membrane were actually transferred together with CD32B. In trogocytosis *in vitro* models performed by others, fluorescent chemical probes were used for discriminating subcellular compartments, reporting similar observations, with mainly cell membrane components being transferred [369, 370].

The crucial role of an accessible Fc part of bNAb PGT151 to enhance CD32B-mediated transfer was observed when neutralizing the antibody with soluble viral Fc $\gamma$ R gp34 or gp68 from hCMV (scheme Figure 14A, p. 61). With increasing amount of soluble gp34 or gp68 in the co-culture of CD32B-mtagBFP-positive 293T cells and SupT1 cells, we detected an increased loss of PGT151-enhanced CD32B-mediated trogocytosis (Figure 14B, p.61). Both soluble viral Fc $\gamma$ Rs bind different parts in the Fc $\gamma$  part of IgGs. The binding site of gp34 is located within the lower hinge region [221] whereas gp68 binds the CH2–CH3 interdomain region of Fc $\gamma$  [216]. This may lead to sterical hindrance of the Fc-CD32B interaction since the binding site of CD32 and CD16 have been shown to involve the CH2 region as well as the lower hinge region of IgG [216, 223, 371].

The selectivity of mainly membrane-associated proteins and receptors being transferred during CD32-dependent trogocytosis raised the question whether there are cell machineries involved to ensure a transfer of membrane parts without damaging of the cells. Here we sought to investigate the potential role of the ESCRT machinery as a prominent membrane scissoring machinery [323].

This hypothesis was investigated by generating a knockdown of Vps4 in CD32B-positive 293T donor cells (Figure 15, p.62). Vps4 is an ATPase and is a component of the ESCRT machinery. Its catalytic activity is important in the late phase of membrane scissoring performed by the ESCRT machinery [323]. The lack of Vps4 ATPase activity has been observed to lead to accumulation of ESCRT machinery compounds at the membrane and defective vesicle release [372, 373]. However, even though the knockdown showed an efficient decrease of Vps4 protein compared to the NTC control CD32-positive or WT 293T (Figure 15A) the transfer of CD32B to SupT1 cells was not affected (Figure 15B). This indicates that the ESCRT machinery does not play part in the membrane transfer during CD32B-dependent trogocytosis in the donor cells. However, the protein analysis of the SupT1 target cells showed high expression of Vps4 (Figure 15A). Therefore, to better clarify the role of Vps4 during trogocytosis, follow-up experiments are needed to investigate a potential role of the ESCRT machinery in the recipient cell that “receives” CD32B. For example, by knocking down Vps4 in both, donor and in the recipient cells. Investigation of trogocytosis mediated by the immunological synapse, Aucher *et al.* observed inhibition of trogocytosis in the presence of actin polarization inhibitors. Yet, this was only observed between T cells and their target cells, but not in co-culture of B cells and their target cells [374]. This may indicate that there are different types of mechanism for the trogocytic transfer of cell surface receptors and might not always include an active process in immune synapse-induced trogocytosis. This could also be the case in FcγR-mediated trogocytosis. We observed that the signaling motif of CD32B is not crucial to trogocytosis mediation by CD32B (Figure 12B), implying that the well-known FcγR-signaling is not important for the process but leaving an uncertainty if there are other signaling or actin polarization induction is needed. Therefore, the question if FcγRs-mediated trogocytosis is an active or potentially a passive process still remains to be solved.

### 4.3 Receptors transferred to CD4 T cells are functional

In earlier experiments co-culturing M2 macrophages with CD4 T cells we assessed the co-transfer of HLA-DR and CD32 to CD4 T cells in a cell contact-dependent manner (Figure 8, p.54). Introducing HLA-DR KOs in donor and recipient cells we demonstrated that M2 macrophages were the source of the increased surface-exposed HLA-DR on co-cultured CD4 T cells (data not shown, described on p. 54). Also in the *in vitro* model with 293T cells and SupT1 cells, the co-transfer of FcγR and other receptors was shown (Figure 10, p.56 and Figure 12A, p.59). With this in mind we aimed to assess the breadth of receptors that can be co-transferred with CD32 from M2 macrophages to co-cultured CD4 T cells. This was assessed by an antibody-based screening by flow cytometry. We analyzed the donor cells (M2 macrophages) to investigate the surface expression profile as well as that of co-cultured the CD4 T cells or T cells left in culture alone to determine changes of surface exposure of each receptor (Figure 17, p.64). Of the 242 receptors examined, 116 receptors were expressed by the M2 macrophages, of which some also showed increased surface exposure on the CD4 T cells after co-culture (indicated by a high ratio of MFI on not co-cultured T cells to the MFI on co-cultured T cells, see also Supplemental table 1). This increased surface exposure indicated the transfer of a number of receptors, of which we ranked receptors that showed an MFI ratio higher than 2 to be potentially “highly transferred”. Importantly, HLA-DR receptor ranked among the top transferred receptors (Figure 17B, p.64). Yet also other members of the MHC class II receptors were found to be increased on co-cultured CD4 T cells (HLA-DP and -DQ). The highly ranked receptors showed a broad diversity ranging from single membrane anchored receptors (CD74 and CD227), over tetraspanin receptors (CD63) to seven transmembrane receptors (CD97, CD195 (CCR5)). This demonstrated that the variety of receptors being

potentially co-transferred was indeed broad. Yet, the screening also indicated some level of selectivity. We ranked receptors that were highly expressed on the M2 macrophages, but not detected on the CD4 T cells regardless of prior co-culture or not (Figure 17C, p.64). Already in a study by Hudrisier *et al.* investigating trogocytosis induced by immunological synapse formation, a selectivity was observed [254]. In their Westernblot analysis of biotinylated proteins after transfer to T or NK cells indicated that not all proteins present on the donor cells were also transferred to the recipient cells [254]. Later studies of CD32B-induced trogocytosis, analyzed the CD32B transfer and different proteins/receptors of interest from transiently expressing 293T cells to T or B cells [375]. Here, they observed higher transfer efficiencies for proteins or receptors anchored in the inner leaflet of the plasma membrane compared to proteins residing in the extracellular leaflet of the plasma membrane and observed highly transfer of tetraspanin receptors. Yet, some level of selectivity for cytoplasm membrane receptors, which were not transferred were not observed with this model. Interestingly, HIV-1 binding receptor DC-SIGN (CD209) was the receptor with the highest ratio in the screening as well as the R5 HIV-1 entry co-receptor CCR5 (CD195). This hinted a potential influence on viral infection of resting CD4 T cells after trogocytosis. Taken together the screening showed, that the cell-contact dependent transfer of receptors from M2 macrophages can have a marked impact on the cell surface proteome of CD4 T cells which in turn could have an impact on the behavior of these cells. Nevertheless, using this method of detection we cannot entirely rule out that the increase of cell surface exposure seen after co-culture on the CD4 T cells is in part due to *de novo* expression triggered by the close cell contact with the myeloid cells. This possible scenario could only be addressed by a receptor KO approach of each receptor, similar to the approach we performed to validate the actual transfer of HLA-DR (data not shown, described on p. 54).

Observing a broad variety of receptors and proteins being transferred to the co-cultured CD4 T cells, we next sought to address the question whether the transferred receptors remain functional and exert biological activity on CD4 T cells. The transfer of both chemokine receptor CXCR4 and CCR5 markedly induced migration towards their corresponding chemokine (Figure 18A and B, p.65). Here the chemokine receptors were transferred from transiently expressing HeLa cells which had a high expression levels for these receptors together with CD32B. Yet, also the transfer of CD11b from M2 macrophages to primary CD4 T cells induced the enhanced binding of the co-cultured T cells to the CD11b ligand ICAM-1 (Figure 18C, p.65). Transfer of functional receptors has also been seen in another study e.g. NK cells could acquire CCR7 from an APC cell line and the acquired CCR7 could induce migration activity of NK cells [376]. Also, TCR exchange between CD8 T cell clones has been detected. The acquired TCR remained functional and the recipient CD8 T cells could induce lysis of tumor target cells [377]. For FcγR-mediated trogocytosis, Hudrisier *et al.* [297] showed that the transferred FcγRs could still efficiently bind immune complexes, however, they could not detect downstream signaling induction [297]. The missing signal transduction might be explained by downstream transmitting signal partners that are either missing or not present, since the transferred FcγRs might not be connected to the signaling machinery in CD4 T cells which usually do not express FcγR receptors themselves. Nevertheless, this shows that the transferred receptors are in a correct topological orientation integrated into the membrane and can be potentially functionally used by the recipient cells. Transferred chemokine receptors from macrophages to CD4 T cells therefore could equip T cells with macrophage-like migration properties, with potential induced migration to inflammatory tissue (Figure 36).

With the primary cell *in vitro* model, we also showed that CD32-dependent trogocytosis can be enhanced by using T cell-reactive antibody (here anti-CD52 mAb, Alemtuzumab) (Figure 19, p.66). Not only CD32 transfer was increased when Alemtuzumab was present, but also the co-

transfer of HLA-DR could be enhanced. The application of primary cells can underline the relevance CD4 T cell reactive antibodies inducing trogocytosis under physiological condition. Furthermore, comparing the frequency of CD32-positive CD4 T cells isolated from peripheral blood to cells isolated from lymphatic tissue such as tonsil and lamina propria (Figure 20, p.67), revealed that increased frequency of cell contact of CD4 T cells with macrophage as observed in tissues with enriched cell density (as it is the case in lymphatic tissue [335]), can potentially elevate CD32-dependent trogocytosis.

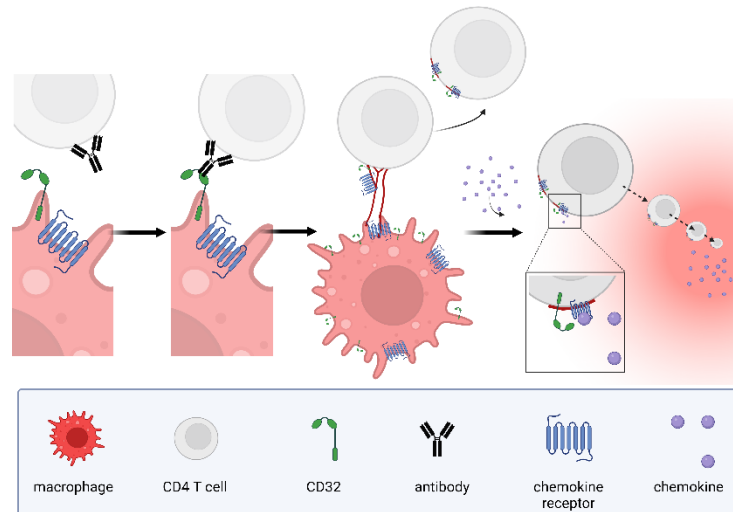


**Figure 36 | CD32-mediated trogocytosis is supplying CD4 T cells with macrophage-like migration behavior.**

CD32-mediated trogocytosis could induce the transfer of functional chemokine receptors from macrophages to CD4 T cells. The functional receptor then can bind its corresponding chemokine ligand and induce the migration of the T cells to inflammatory hot spots.

#### 4.4 HIV-1 binding, fusion and infection is increased after FcγR-mediated trogocytosis on CD4 T cells

After observing that the co-culture with M2 macrophages can have a huge impact on the plasticity of the surface proteome of CD4 T cells, we next addressed whether this could also influence the susceptibility of the CD4 T cells for HIV-1. This was tested by analyzing HIV-1 fusion into CD4 T cells either previously co-cultured with M2 macrophages or not (Figure 21A, p.68). Here, we tested both X4-tropic and R5-tropic HIV-1 virions. In both cases enhanced fusion was observed in CD4 T cells that had previously been co-cultured with M2 macrophages, indicating that the previous cell contacts strongly enhance the susceptibility for HIV-1. Furthermore, since we could enhance CD32-dependent transfer by addition of Alemtuzumab, we analyzed the correlation of enhanced CD32-dependent trogocytosis and enhanced fusion (Figure 21B, p.68). For the X4- and the R5-tropic fusion experiments we could see a positive correlation between trogocytosis and HIV-1 fusion. Here, trogocytosis efficiency was detected by the transfer of CD32. We could further exclude that CD32B itself is enhancing fusion, we used CD4 T cells transiently expressing CD32B endogenously. Here no increased fusion was seen for CD32B-positive CD4 T cells compared to cells nucleofected with an empty vector (Figure 21C, p.68). This verified CD32 as the mediator of trogocytosis but not the factor causing the increased HIV-1 fusion in the cells.

Beside fusion, we also tested a full HIV-1 infection (with both X4- or R5-tropic HIV-1). Co-cultured CD4 T cells showed over ~2-fold increase of infected cells compared to the not-co-cultured cells (Figure 22, p.69). Here, the differences between co-cultured and not co-cultured cells was less

than in the fusion experiments. This could be explained by post-entry restriction of HIV-1 infection present in resting CD4 T cells, such as SAMHD1 [96, 97]. Nevertheless, these experiments clearly showed a change of susceptibility for HIV-1 infection. Testing the binding of X4 HIV-1 Vpr-GFP particle on either CD32-positive or CD32-negative co-cultured CD4 T cells indicated that the CD32-positive CD4 T cells were binding HIV-1 particle to a higher extent than CD4 T cells that were negative for CD32 (Figure 23A, p.70). In confocal microscopy analysis, this was also visualized by CD32-positive membrane patches on the CD4 T cells and preferential binding of a high number of HIV-1 Vpr-GFP particle within these membrane patches (Figure 23B, p.70). These results could explain why some groups observed HIV-1 enrichment or increased transcriptionally active HIV-1 in CD32-positive cells [142-144, 146]. After trogocytosis, the membrane patches are positive for CD32, which could lead to the wrong assumption that this is a marker of HIV-1 reservoir or transcriptionally active cells. Conversely, these cells are more likely to be infected due to the higher binding and fusion of the virus and therefore more likely included in HIV-1 positive cell population analysis. In line with this are also observation of increased CD32 expression together with transcriptional active HIV-1 in lymph nodes and gut tissue [144, 151, 378]. Correspondingly, here trogocytosis can be enhanced due to more frequent cell contact, which then increase HIV-1 infection of the cells. In addition, the testing of sera of HIV-1 patients for increased CD4 T cell binding and enhancing trogocytosis ability (Figure 11, p.57) also indicated that CD32-mediated trogocytosis can be elevated in subset of patients but not others. This would give explanation why some have reported increased CD32-positive T cells frequency in HIV-1 patients [142] whereas others saw no difference to healthy donors [150].

Since CD32 itself is the driver of trogocytosis but not the factor transferred that increase HIV-1 fusion, we aimed to investigate what was transferred from the M2 macrophages, residing within the membrane patches, that then caused increased binding, fusion and infection of the CD4 T cells. Transferred receptors that lead to virus binding has been reported in the case of Epstein-Barr virus (EBV) binding after membrane transfer on NK cells. Here the membrane transfer was induced after the formation of immunological synapse of NK cells and CD21-positive target cells. Within the transfer of membrane fragments also CD21 was transferred to the NK cells, which is one of the entry receptors of EBV and increased EBV binding to the NK cells was detected after contact with the CD21-positive target cells [379]. In the receptor screening experiment, we found HIV-1 binding receptor DC-SIGN and HIV-1 co-receptor CCR5 among the top 10 of the highest transferred receptors (Figure 17). Since the increased binding/fusion and infection after CD32-dependent trogocytosis on CD4 T cell was detected for X4- and R5-tropic, it implied that this infection enhancement is viral tropism independent. We therefore set our focus on investigating which factors increase HIV-1 binding in the case of both viral tropism.

#### **4.5 HIV-1 binding myeloid C-type lectins receptors and $\beta$ 2-integrin are transferred to CD4 T cells but do not induce Fc $\gamma$ R-mediated enhanced HIV-1 binding**

The envelope glycoprotein gp120 of HIV-1 is a heavily N-glycosylated protein with high density of oligomannose [380]. It therefore is recognized by C-type lectin receptors such as DC-SIGN [32] or the macrophage mannose receptor 1 (also known as CD206) [30], which are expressed by antigen presenting cells like dendritic cells and macrophages. The binding to the receptors can then induce immune reaction such as chemokine/cytokine production or phagocytosis of the foreign material [381]. However, both receptors are also reported to be hijacked by HIV-1 to attach

on the surface of DC or macrophages and then being further transported and transmitted to their actual target cells (CD4 T cells) in e.g. lymphoid tissue [31, 382]. Since we hypothesized that within the transferred membrane patches from macrophages, there is a factor residing within the macrophage membrane patches, which then increase binding of HIV-1 within these patches after transfer to the T cells, DC-SIGN as well as CD206 were at first of interest to be investigated. Both receptors were highly expressed by the M2 macrophages (over 80% positive cells (Figure 25A, p. 72 and Figure 26A, p.73) as also previously reported [383, 384]. Additionally, these receptors were also identified to be highly co-transferred with CD32 in our receptor-transfer screening previously. Here, DC-SIGN was the second highest receptor in the “top hits 1-10” of the receptors with an MFI ratio above 2 and CD206 had also a high ratio of 1.7 (Supplemental table 1). Their properties to be (i) expressed on M2 macrophages, (ii) binding of HIV-1 by these receptors as well as their (iii) potential co-transfer with CD32 made both receptors to very promising candidates to investigate. Their expression on M2 macrophages could be then efficiently ablated (less than 1% positive cells upon KO of each receptor in the macrophages (Figure 25A & Figure 26A)). Using M2 KO cells in co-culture with CD4 T cells confirmed that both receptors found on CD4 T cells after co-culture were originating from the macrophages and are not *de novo* expressed by the T cells, since in the co-culture with KO M2 macrophages the surface exposure was on a similar level as in the only T cells culture condition (Figure 25B & Figure 26B). With these results we could confirm three receptors being co-transferred from the M2 macrophages together with CD32 to CD4 T cells: HLA-DR, DC-SIGN and CD206. However, even though transfer of DC-SIGN and CD206 was abolished, within the co-culture of CD4 T cells with KO M2 macrophages, HIV-1 fusion (Figure 25C) or HIV-1 binding to CD32-positive cells (Figure 26C) was unchanged compared to the WT control. This was in contradiction of our initial expectations, since previous studies for DC-SIGN had shown increased HIV infection rate if CD4 T cell line co-expressed DC-SIGN, CD4 and CCR5 [341]. Yet, there was no difference of HIV-1 fusion in co-cultured CD4 T cells that had received high amounts of DC-SIGN from M2 macrophages to T cells with no/low DC-SIGN surface exposure after co-culture (Figure 25C). Similarly, CD4 T cells that had received CD206 in the co-cultured did not show more HIV binding than T cells that had been co-cultured but transfer of CD206 was ablated (Figure 26, p.73). These finding not only excluded DC-SIGN or CD206 as potential key factors for increased HIV-1 binding to the transferred membrane patches, it also was contradicting the expectation that if these receptors are present this should enhance HIV-1 binding and fusion similar to the finding in T cells lines expressing DC-SIGN [341]. However, our experiments were performed with CD4 T cells highly expressing CD4, therefore the entry receptor is not a limiting factor as seen on macrophages. Lee *et al.* [341] showed that the increased viral infection under the presence of DC-SIGN was especially the case if there were low levels of CD4 or CCR5. Additionally, we had used MOI between 0.5 and 1. Potentially the advanced binding due to the presence of DC-SIGN or CD206 is only seen with lower viral loads. This could be of interest in follow-up experiments, in which the transferred DC-SIGN and CD206 could be tested to bind HIV-1 with lower MOI on the CD4 T cells. Nevertheless, since it also did not affect the phenotype of increased fusion or binding to CD32-positive cells, we turned to explore other potential factors that could cause the increase binding to the co-cultured CD4 T cells observed by us.

With a similar approach, we also investigated CD11a/b/c as factors inducing the virological phenotype in the transferred membrane patches. CD11c/CD18 has recently been reported to potentially bind HIV-1 through CD11c on the surface of cervical epithelial cells, mediating then transcytosis of the virus through the epithelium to the target cells [40]. Since CD11c is also expressed to high levels on monocytes and macrophages, we aimed at investigating the potential

role of CD11c, using a M2 macrophage KO/CD4 T cell co-culture. To address in parallel the potential role of other members of the  $\beta$ 2-integrin family, we performed in this experimental setup simultaneous KO of three genes: CD11a, CD11b and CD11c in the macrophages. With this method we could nearly completely ablate the expression of CD11b and c on the macrophages and reduce the CD11a-positive M2 macrophages by ~ 50% (Figure 27A, p.74). CD11a was already highly expressed by the CD4 T cells without co-culture, so its transfer from M2 macrophages could not be readily quantified. Yet, transfer of CD11b and c was documented by their increase of cell surface exposure on T cells after co-culture with the NTC M2 macrophages, but lack of exposure after co-culture with KO M2 macrophages (Figure 27A, p.74). However, the follow-up experiment of HIV-1 binding to the co-cultured CD4 T cells did not show changes of binding when the transfer was ablated in the M2 macrophage KO co-culture condition. Even though the set up excluded CD11a/b and c as key driver involved in the virological phenotype, the experiment nevertheless demonstrated the transfer of both CD11b and CD11c from M2 macrophages to CD4 T cells during co-culture. Furthermore, this confirmed our observed Fc $\gamma$ R-mediated increase in binding of co-cultured CD4 T cells to ICAM-1 (Figure 18, p.65).

#### **4.6 Heparan sulfate and chondroitin sulfate from CD4 T cells are not responsible for the increased HIV-1 binding**

Besides receptors such as DC-SIGN and CD206 or CD11a/b/c, heparan sulfate (HS) is also reported to play a potential role for HIV-1 attachment to macrophages. Heparan sulfate chains are covalently bound to proteoglycans e.g. syndecans, on the cell surface. The chains are large anionic polysaccharides and can be used by pathogens such as HIV-1 to bind to the surface of cells such as mucosal epithelial cells or spermatozoa for transport and transmission to the actual target cells such as CD4 T cells, macrophages and DCs [350, 351, 385, 386]. Expressed on macrophages, HS was observed to enhance the binding of HIV-1 to these cells and to overcome the restriction of low CD4 expression. In a study of Saphire *et al.* [353] treatment of MDMs with heparinase showed a strong decrease of HIV-1 attachment (X4 and R5 HIV-1) whereas the treatment with anti-CD4 antibody did not. In contrast, the treatment of activated CD4 T cells in their hands with heparinase did not affect the binding of HIV-1, whereas incubation with anti-CD4 antibodies strongly decreased binding [353]. Since this indicated that Heparan sulfate proteoglycans (HSPGs) could play an important role for HIV-1 binding to the surface of macrophages, but not on CD4 T cells, we hypothesized that proteoglycans with heparan sulfate chains have no/low physiological expression on CD4 T cells, yet HSPGs can be potentially transferred from macrophages during co-culture, residing in the macrophage-derived membrane patches. The HSPGs may then enhance the binding of HIV-1 locally. In a first attempt to stain for HS on the CD4 T cells (co-cultured with M2 cells or not), we could not detect HS on CD4 T cells regardless of their previous culture condition (Supplemental figure 9). CD4 T cells have only low levels of HSPGs on their surface [353, 387] and we therefore concluded that our staining procedure to detect HS was here at limit of detection, since we could stain for HS on HeLa cells, used here as positive control (Supplemental figure 9), which have been reported to highly express HSPGs [35, 353]. As a consequence of the heparinase/chondroitinase treatment, we observed a strong decrease of HIV-1 binding to HeLa cells. However, this enzymatical digestion of CD4 T cells after co-culture showed no effect on binding of HIV-1 to CD32-positive cells compared to CD32-negative cells. Since we had seen a strong effect of the treatment on the HIV-1 binding capacity of HeLa cells, we concluded that even if small amounts of HS on CD32-positive CD4 T cells had been trans-

ferred from the macrophages, these amounts should have been effectively removed by the enzymatic digestion. Collectively, this largely excluded HS or chondroitin sulfate as important factors in the virological phenotype following trogocytotic membrane transfer from M2 macrophages to CD4 T cells.

#### **4.7 M2-derived membrane patches transferred on CD4 T cells recruit endogenous CD4 and create an HIV-1 binding hot spot**

When testing the blocking of HIV-1 binding by different antibodies, which target transferred receptors (Figure 29, p.76), our interest was sparked by the investigation of the actual drug/antibody control condition with AMD3100 and anti-CD4 (clone SK3). This control reduced the virus binding to CD32-positive CD4 T cells to a lower level than observed on CD32-negative cells, therefore completely abolished the virological phenotype for CD32-positive CD4 T cells. In a follow up experiment, we then found that the anti-CD4 antibody decreased HIV-1 binding, yet not AMD3100 (Figure 30A, p. 78). AMD3100 is a small molecule that downregulates CXCR4 from the surface and thus blocks the binding of HIV to the co-receptor and therefore the fusion of the virus to the cell. When cells are treated with AMD3100, HIV can potentially still bind to the cell surface, since the binding to CXCR4 occurs subsequently to CD4 binding [20]. In our experiment, we analyzed the binding after one hour of inoculation with viral particles at 16 °C. Temperatures below 25 °C should ensure an inhibition of HIV-1 fusion and endocytosis [388, 389] and should thus assess only the attachment of the virus to the cell surface. Looking at this early step of viral entry the actual inhibition of fusion by AMD3100 might not be present and therefore detectable at this time point. The anti-CD4 antibody clone SK3 binds to the extracellular immunoglobulin domain D1[390] of CD4, which is also the binding side of HIV-1 gp120 [391-393]. This antibody can be efficiently used to inhibit viral binding and entry[390]. To ensure in our experiment that the reduction of viral binding to CD32-positive T cells by anti-CD4 mAb clone SK3 was specific, we also tested the anti-CD4 mAb clone RPA-T4, which is also reported to bind at the D1 domain, as well as two other commercially available mAbs (clone M-T477, clone L200). All four antibodies reduced the CD32-mediated enhancement of HIV-1 binding to a similar extent as anti-CD4 mAb clone SK3. The isotype controls as well as anti-HLA-DR and anti-DC-SIGN mAbs did not affect the binding. This confirmed that the blocking of CD4 strongly reduced the increased binding observed in CD32-positive T cells. Furthermore, testing HIV-1  $\Delta$ Env binding to the cells, demonstrated that the increased HIV-1 binding to CD32-positive T cells was partially Env-dependent (Figure 31, p.79).

Building on this observation, we further characterized the potential role of CD4 in the increased HIV-1 binding to CD32-positive T cells. At first, we hypothesized that CD4, even though highly expressed on T cells, is also transferred from the macrophages to T cells by trogocytosis. The transferred CD4 would then reside within the densely packed membrane patches that might cause a preferential binding of HIV-1 to these CD4 molecules instead of the endogenously expressed CD4. A similar idea was hypothesized by Aucher *et al.* [374], which observed the Fc $\gamma$ R-mediated transfer of CD4 to CD8. In their study CD4-GFP fusion protein was transferred from the CD32/CD16-expressing mast cell line P815 to activated CD8 T cells. However, they could not detect an increase of HIV-1 p24 associated with CD8 T cells following transfer of CD4-GFP. Yet they also stated that they had a high background for p24 and the limit of detection may have limited the value of the findings [394]. We tested the potential transfer from M2 macrophages

with a similar M2 macrophage KO approach as for DC-SIGN and CD206 (Figure 32, p.80). Using this KO approach almost 100% CD4-negative M2 macrophages were achieved. However, the absence of CD4 on M2 cells in the co-culture did not reduce subsequent HIV-1 binding to CD32-positive T cells (Figure 32C, p.80). Since the CD4 T cells endogenously highly expressed CD4, the lack of detectable CD4 transfer could also be due to a smaller absolute increase of CD4 by a potential transfer. However, since the virological phenotype was not influenced, it indicated that CD4 expressed by M2 macrophages does not promote the trogocytosis-mediated enhanced HIV-1 binding. In the follow-up experiment, we performed the KO in the CD4 T cells (also with a high CD4 KO efficiency, Figure 33, p.81). This experiment revealed then the crucial role of the endogenously expressed CD4 on T cells for the increased binding of HIV-1 to CD32-positive CD4 T cells. After co-culture with WT M2 macrophages the CD4 KO T cells positive for CD32 showed reduced binding to levels similar to those seen in CD32-negative T cells (Figure 33C). Microscopic analysis of CD4 T cells co-cultured with M2 macrophages revealed a strong clustering of CD4 within the CD32-positive membrane patches and co-localization of HIV-1 particles (Figure 34, p.82). The CD4 receptor has been reported to cluster in membrane islands [395] and is also observed to localize in lipid raft/detergent resident membranes [396, 397]. Similarly, CD32 is localized in lipid raft membrane domains after immune complex binding to the receptor [398-400]. Since antibody binding induces the FcγR-mediated trogocytosis, CD32 may be recruited to lipid raft membrane domains subsequently to the antibody bridging between M2 macrophages and CD4 T cells. The receptor is then transferred to the T cells together with the membrane parts with lipid raft properties. This was also supported by the observation of co-localized GM1 within the transferred membrane patches (Figure 35, p.83). GM1 is a ganglioside belonging to the sphingolipids, and is used as a marker for lipid rafts [354-356]. Popik *et al.* [401] reported a potentially crucial role of lipid raft for the entry of HIV-1, since they observed a strong decrease of HIV-1 infectivity when depleting raft-resistant membrane cholesterol, without altering the number of HIV entry receptors on the cells. Our current working model of the trogocytosis-mediated enhanced HIV-1 binding, fusion and infection is therefore the following: endogenously expressed CD4 on T cells is preferentially recruited and clustered within the transferred membrane patches (potentially with lipid raft properties), creating then a preferential hot spot for HIV-1 binding and entry (Figure 37).

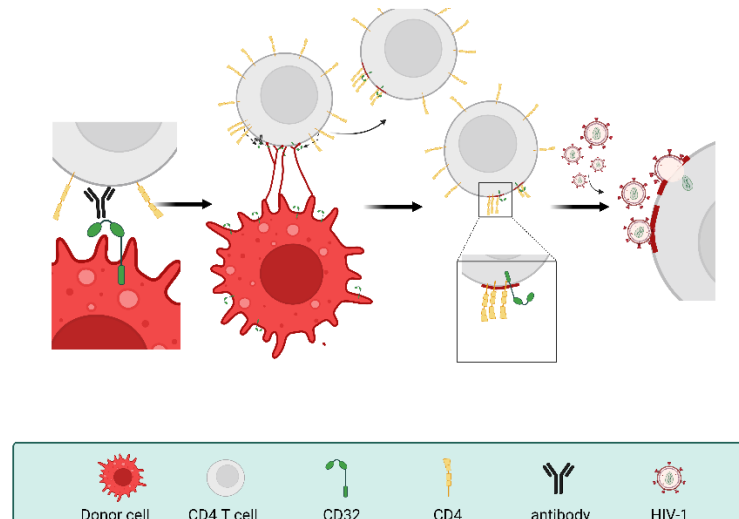


**Figure 37 | Scheme of mechanistic model for Fc $\gamma$ R-mediated enhanced HIV-1 infection.**

Membrane patches are transferred from macrophages to CD4 T cells. Within the membrane patches endogenously expressed CD4 receptors are recruited and clustered. This clustering leads then to enhanced HIV-1 binding and entry resulting in enhancement of HIV-1 infection of CD4 T cells.

## 4.8 Outlook

Even though this study excludes CD32 as a biomarker for HIV-1 latency in CD4 T cells, it highlighted the capacity of CD32 as a key mediator and driver of trogocytosis and the functional impact this can have on the recipient cells. We had initially screened for receptors transferred from M2 macrophages to CD4 T cells, and here the breadth and selectivity of transferred receptors were observed. However, further investigations could be performed to gain a more detailed picture. Daubeuf *et al.* [375] already investigated the transfer of biotinylated surface proteins by Western blotting [375]. In future experiments biotinylating of surface proteins on the donor cells could allow identification by mass spectrometry (MS) analysis of proteins transferred to recipient cells and could create a list of transferred receptors as well of those receptors who remain on the surface of macrophages. We also saw that Fc $\gamma$ R-mediated trogocytosis is also happening under physiological conditions in healthy individuals in blood and lymphoid tissue and that transferred receptors can remain functional. This can expand the intrinsic properties of immune cells, and therefore should be considered in the research of immune cells and their functions. Additionally, this has to be considered as a potential explanation when investigating subpopulations of immune cells with surface receptors, which are usually expressed only by other immune cell subtypes [402-406]. Furthermore, when investigating PBMC cultures there also has to be an awareness that Fc $\gamma$ R-mediated trogocytosis between these cells can occur under common cell culture conditions. This problem has been already addressed by other groups [294], but has not reached a high level of awareness in the scientific community.

Since the results also showed how HIV-1 can exploit Fc $\gamma$ R-mediated trogocytosis to enhance the infection of resting CD4 T cells this could also lead *in vivo* to enhanced seeding of the HIV-1 reservoir in the patients. Future experiments therefore could also focus on the investigation of latency development in CD4 T cells in the context of Fc $\gamma$ R-mediated enhancement of HIV-1 infection. For this, infected GFP-positive CD32-positive or CD32-negative T cell population could be sorted and kept in culture to study the induction frequency from latency in the two populations also in comparison to infected, but not co-cultured CD4 T cells. Additionally, also the frequency

---

of productive virus release after reactivation could be determined. Since the reactivation of HIV-1 production in latently infected resting CD4 T cells has been observed with a high number of defective viral genome [101], it could be of interest to investigate whether the increased infection by FcγR-mediated trogocytosis may lead to more productive reactivation, giving further insights into how these cells can be used by HIV-1 as its major cellular reservoir.

## 5. References

- [1] F. Barré-Sinoussi *et al.*, "Isolation of a T-lymphotropic retrovirus from a patient at risk for acquired immune deficiency syndrome (AIDS)," (in eng), *Science*, vol. 220, no. 4599, pp. 868-71, May 20 1983, doi: 10.1126/science.6189183.
- [2] M. Popovic *et al.*, "Isolation and transmission of human retrovirus (human t-cell leukemia virus)," (in eng), *Science*, vol. 219, no. 4586, pp. 856-9, Feb 18 1983, doi: 10.1126/science.6600519.
- [3] B. H. Hahn, G. M. Shaw, K. M. De Cock, and P. M. Sharp, "AIDS as a zoonosis: scientific and public health implications," (in eng), *Science*, vol. 287, no. 5453, pp. 607-14, Jan 28 2000, doi: 10.1126/science.287.5453.607.
- [4] B. Korber, B. Gaschen, K. Yusim, R. Thakallapally, C. Kesmir, and V. Detours, "Evolutionary and immunological implications of contemporary HIV-1 variation," (in eng), *Br Med Bull*, vol. 58, pp. 19-42, 2001, doi: 10.1093/bmb/58.1.19.
- [5] M. Peeters, M. Jung, and A. Ayoub, "The origin and molecular epidemiology of HIV," (in eng), *Expert Rev Anti Infect Ther*, vol. 11, no. 9, pp. 885-96, Sep 2013, doi: 10.1586/14787210.2013.825443.
- [6] E. O. Freed, "HIV-1 replication," (in eng), *Somat Cell Mol Genet*, vol. 26, no. 1-6, pp. 13-33, Nov 2001, doi: 10.1023/a:1021070512287.
- [7] M. B. Feinberg, R. F. Jarrett, A. Aldovini, R. C. Gallo, and F. Wong-Staal, "HTLV-III expression and production involve complex regulation at the levels of splicing and translation of viral RNA," (in eng), *Cell*, vol. 46, no. 6, pp. 807-17, Sep 12 1986, doi: 10.1016/0092-8674(86)90062-0.
- [8] J. Sodroski *et al.*, "Replicative and cytopathic potential of HTLV-III/LAV with sor gene deletions," (in eng), *Science*, vol. 231, no. 4745, pp. 1549-53, Mar 28 1986, doi: 10.1126/science.3006244.
- [9] M. R. Ferguson, D. R. Rojo, J. J. von Lindern, and W. A. O'Brien, "HIV-1 replication cycle," (in eng), *Clin Lab Med*, vol. 22, no. 3, pp. 611-35, Sep 2002, doi: 10.1016/s0272-2712(02)00015-x.
- [10] L. A. Carlson *et al.*, "Three-dimensional analysis of budding sites and released virus suggests a revised model for HIV-1 morphogenesis," (in eng), *Cell Host Microbe*, vol. 4, no. 6, pp. 592-9, Dec 11 2008, doi: 10.1016/j.chom.2008.10.013.
- [11] B. K. Ganser-Pornillos, M. Yeager, and W. I. Sundquist, "The structural biology of HIV assembly," (in eng), *Curr Opin Struct Biol*, vol. 18, no. 2, pp. 203-17, Apr 2008, doi: 10.1016/j.sbi.2008.02.001.
- [12] S. Hallenberger, V. Bosch, H. Angliker, E. Shaw, H. D. Klenk, and W. Garten, "Inhibition of furin-mediated cleavage activation of HIV-1 glycoprotein gp160," (in eng), *Nature*, vol. 360, no. 6402, pp. 358-61, Nov 26 1992, doi: 10.1038/360358a0.
- [13] P. Zhu *et al.*, "Electron tomography analysis of envelope glycoprotein trimers on HIV and simian immunodeficiency virus virions," (in eng), *Proc Natl Acad Sci U S A*, vol. 100, no. 26, pp. 15812-7, Dec 23 2003, doi: 10.1073/pnas.2634931100.
- [14] P. Zhu *et al.*, "Distribution and three-dimensional structure of AIDS virus envelope spikes," (in eng), *Nature*, vol. 441, no. 7095, pp. 847-52, Jun 15 2006, doi: 10.1038/nature04817.
- [15] E. Yuste, J. D. Reeves, R. W. Doms, and R. C. Desrosiers, "Modulation of Env content in virions of simian immunodeficiency virus: correlation with cell surface expression and virion infectivity," (in eng), *J Virol*, vol. 78, no. 13, pp. 6775-85, Jul 2004, doi: 10.1128/jvi.78.13.6775-6785.2004.
- [16] L. Chen, O. T. Keppler, and C. Schölz, "Post-translational Modification-Based Regulation of HIV Replication," (in eng), *Front Microbiol*, vol. 9, p. 2131, 2018, doi: 10.3389/fmicb.2018.02131.

- [17] V. A. Parsegian, N. Fuller, and R. P. Rand, "Measured work of deformation and repulsion of lecithin bilayers," (in eng), *Proc Natl Acad Sci U S A*, vol. 76, no. 6, pp. 2750-4, Jun 1979, doi: 10.1073/pnas.76.6.2750.
- [18] R. P. Rand and V. A. Parsegian, "Physical force considerations in model and biological membranes," (in eng), *Can J Biochem Cell Biol*, vol. 62, no. 8, pp. 752-9, Aug 1984, doi: 10.1139/o84-097.
- [19] O. Hartley, P. J. Klasse, Q. J. Sattentau, and J. P. Moore, "V3: HIV's switch-hitter," (in eng), *AIDS Res Hum Retroviruses*, vol. 21, no. 2, pp. 171-89, Feb 2005, doi: 10.1089/aid.2005.21.171.
- [20] C. B. Wilen, J. C. Tilton, and R. W. Doms, "HIV: cell binding and entry," (in eng), *Cold Spring Harb Perspect Med*, vol. 2, no. 8, Aug 1 2012, doi: 10.1101/cshperspect.a006866.
- [21] G. Negi, A. Sharma, M. Dey, G. Dhanawat, and N. Parveen, "Membrane attachment and fusion of HIV-1, influenza A, and SARS-CoV-2: resolving the mechanisms with biophysical methods," (in eng), *Biophys Rev*, vol. 14, no. 5, pp. 1109-1140, Oct 2022, doi: 10.1007/s12551-022-00999-7.
- [22] F. Cocchi, A. L. DeVico, A. Garzino-Demo, A. Cara, R. C. Gallo, and P. Lusso, "The V3 domain of the HIV-1 gp120 envelope glycoprotein is critical for chemokine-mediated blockade of infection," (in eng), *Nat Med*, vol. 2, no. 11, pp. 1244-7, Nov 1996, doi: 10.1038/nm1196-1244.
- [23] R. A. Fouchier *et al.*, "Phenotype-associated sequence variation in the third variable domain of the human immunodeficiency virus type 1 gp120 molecule," (in eng), *J Virol*, vol. 66, no. 5, pp. 3183-7, May 1992, doi: 10.1128/jvi.66.5.3183-3187.1992.
- [24] M. A. Jensen *et al.*, "Improved coreceptor usage prediction and genotypic monitoring of R5-to-X4 transition by motif analysis of human immunodeficiency virus type 1 env V3 loop sequences," (in eng), *J Virol*, vol. 77, no. 24, pp. 13376-88, Dec 2003, doi: 10.1128/jvi.77.24.13376-13388.2003.
- [25] K. Bozek *et al.*, "An expanded model of HIV cell entry phenotype based on multi-parameter single-cell data," (in eng), *Retrovirology*, vol. 9, p. 60, Jul 25 2012, doi: 10.1186/1742-4690-9-60.
- [26] E. A. Berger *et al.*, "A new classification for HIV-1," (in eng), *Nature*, vol. 391, no. 6664, p. 240, Jan 15 1998, doi: 10.1038/34571.
- [27] C. Verhofstede, M. Nijhuis, and L. Vandekerckhove, "Correlation of coreceptor usage and disease progression," (in eng), *Curr Opin HIV AIDS*, vol. 7, no. 5, pp. 432-9, Sep 2012, doi: 10.1097/COH.0b013e328356f6f2.
- [28] R. I. Connor, K. E. Sheridan, D. Ceradini, S. Choe, and N. R. Landau, "Change in coreceptor use correlates with disease progression in HIV-1--infected individuals," (in eng), *J Exp Med*, vol. 185, no. 4, pp. 621-8, Feb 17 1997, doi: 10.1084/jem.185.4.621.
- [29] S. C. Harrison, "Mechanism of membrane fusion by viral envelope proteins," (in eng), *Adv Virus Res*, vol. 64, pp. 231-61, 2005, doi: 10.1016/s0065-3527(05)64007-9.
- [30] J. Lai, O. K. Bernhard, S. G. Turville, A. N. Harman, J. Wilkinson, and A. L. Cunningham, "Oligomerization of the macrophage mannose receptor enhances gp120-mediated binding of HIV-1," (in eng), *J Biol Chem*, vol. 284, no. 17, pp. 11027-38, Apr 24 2009, doi: 10.1074/jbc.M809698200.
- [31] D. G. Nguyen and J. E. Hildreth, "Involvement of macrophage mannose receptor in the binding and transmission of HIV by macrophages," (in eng), *Eur J Immunol*, vol. 33, no. 2, pp. 483-93, Feb 2003, doi: 10.1002/immu.200310024.
- [32] T. B. Geijtenbeek *et al.*, "DC-SIGN, a dendritic cell-specific HIV-1-binding protein that enhances trans-infection of T cells," (in eng), *Cell*, vol. 100, no. 5, pp. 587-97, Mar 3 2000, doi: 10.1016/s0092-8674(00)80694-7.
- [33] C. Trumpheller, C. G. Park, J. Finke, R. M. Steinman, and A. Granelli-Piperno, "Cell type-dependent retention and transmission of HIV-1 by DC-SIGN," (in eng), *Int Immunol*, vol. 15, no. 2, pp. 289-98, Feb 2003, doi: 10.1093/intimm/dxg030.

- [34] J. Fantini, D. G. Cook, N. Nathanson, S. L. Spitalnik, and F. Gonzalez-Scarano, "Infection of colonic epithelial cell lines by type 1 human immunodeficiency virus is associated with cell surface expression of galactosylceramide, a potential alternative gp120 receptor," (in eng), *Proc Natl Acad Sci U S A*, vol. 90, no. 7, pp. 2700-4, Apr 1 1993, doi: 10.1073/pnas.90.7.2700.
- [35] I. Mondor, S. Ugolini, and Q. J. Sattentau, "Human immunodeficiency virus type 1 attachment to HeLa CD4 cells is CD4 independent and gp120 dependent and requires cell surface heparans," (in eng), *J Virol*, vol. 72, no. 5, pp. 3623-34, May 1998, doi: 10.1128/jvi.72.5.3623-3634.1998.
- [36] B. J. Connell and H. Lortat-Jacob, "Human immunodeficiency virus and heparan sulfate: from attachment to entry inhibition," (in eng), *Front Immunol*, vol. 4, p. 385, Nov 20 2013, doi: 10.3389/fimmu.2013.00385.
- [37] J. Arthos *et al.*, "HIV-1 envelope protein binds to and signals through integrin alpha4beta7, the gut mucosal homing receptor for peripheral T cells," (in eng), *Nat Immunol*, vol. 9, no. 3, pp. 301-9, Mar 2008, doi: 10.1038/ni1566.
- [38] C. Cicala *et al.*, "The integrin alpha4beta7 forms a complex with cell-surface CD4 and defines a T-cell subset that is highly susceptible to infection by HIV-1," (in eng), *Proc Natl Acad Sci U S A*, vol. 106, no. 49, pp. 20877-82, Dec 8 2009, doi: 10.1073/pnas.0911796106.
- [39] Z. Bajtay, C. Speth, A. Erdei, and M. P. Dierich, "Cutting edge: productive HIV-1 infection of dendritic cells via complement receptor type 3 (CR3, CD11b/CD18)," (in eng), *J Immunol*, vol. 173, no. 8, pp. 4775-8, Oct 15 2004, doi: 10.4049/jimmunol.173.8.4775.
- [40] C. J. Day *et al.*, "Complement Receptor 3 Mediates HIV-1 Transcytosis across an Intact Cervical Epithelial Cell Barrier: New Insight into HIV Transmission in Women," (in eng), *mBio*, vol. 13, no. 1, p. e0217721, Jan 11 2022, doi: 10.1128/mbio.02177-21.
- [41] R. Blumenthal, S. Durell, and M. Viard, "HIV entry and envelope glycoprotein-mediated fusion," (in eng), *J Biol Chem*, vol. 287, no. 49, pp. 40841-9, Nov 30 2012, doi: 10.1074/jbc.R112.406272.
- [42] D. C. Chan, D. Fass, J. M. Berger, and P. S. Kim, "Core structure of gp41 from the HIV envelope glycoprotein," (in eng), *Cell*, vol. 89, no. 2, pp. 263-73, Apr 18 1997, doi: 10.1016/s0092-8674(00)80205-6.
- [43] W. Weissenhorn, A. Dessen, S. C. Harrison, J. J. Skehel, and D. C. Wiley, "Atomic structure of the ectodomain from HIV-1 gp41," (in eng), *Nature*, vol. 387, no. 6631, pp. 426-30, May 22 1997, doi: 10.1038/387426a0.
- [44] M. J. Lehmann, N. M. Sherer, C. B. Marks, M. Pypaert, and W. Mothes, "Actin- and myosin-driven movement of viruses along filopodia precedes their entry into cells," (in eng), *J Cell Biol*, vol. 170, no. 2, pp. 317-25, Jul 18 2005, doi: 10.1083/jcb.200503059.
- [45] S. Iyengar, J. E. Hildreth, and D. H. Schwartz, "Actin-dependent receptor colocalization required for human immunodeficiency virus entry into host cells," (in eng), *J Virol*, vol. 72, no. 6, pp. 5251-5, Jun 1998, doi: 10.1128/jvi.72.6.5251-5255.1998.
- [46] S. T. Yang, V. Kiessling, and L. K. Tamm, "Line tension at lipid phase boundaries as driving force for HIV fusion peptide-mediated fusion," (in eng), *Nat Commun*, vol. 7, p. 11401, Apr 26 2016, doi: 10.1038/ncomms11401.
- [47] S. T. Yang, A. J. B. Kreutzberger, V. Kiessling, B. K. Ganser-Pornillos, J. M. White, and L. K. Tamm, "HIV virions sense plasma membrane heterogeneity for cell entry," (in eng), *Sci Adv*, vol. 3, no. 6, p. e1700338, Jun 2017, doi: 10.1126/sciadv.1700338.
- [48] K. Miyauchi, Y. Kim, O. Latinovic, V. Morozov, and G. B. Melikyan, "HIV enters cells via endocytosis and dynamin-dependent fusion with endosomes," (in eng), *Cell*, vol. 137, no. 3, pp. 433-44, May 1 2009, doi: 10.1016/j.cell.2009.02.046.
- [49] B. L. Fredericksen, B. L. Wei, J. Yao, T. Luo, and J. V. Garcia, "Inhibition of endosomal/lysosomal degradation increases the infectivity of human immunodeficiency virus," (in eng), *J Virol*, vol. 76, no. 22, pp. 11440-6, Nov 2002, doi: 10.1128/jvi.76.22.11440-11446.2002.

- [50] J. Daecke, O. T. Fackler, M. T. Dittmar, and H. G. Kräusslich, "Involvement of clathrin-mediated endocytosis in human immunodeficiency virus type 1 entry," (in eng), *J Virol*, vol. 79, no. 3, pp. 1581-94, Feb 2005, doi: 10.1128/jvi.79.3.1581-1594.2005.
- [51] M. Marin, Y. Kushnareva, C. S. Mason, S. K. Chanda, and G. B. Melikyan, "HIV-1 Fusion with CD4+ T cells Is Promoted by Proteins Involved in Endocytosis and Intracellular Membrane Trafficking," (in eng), *Viruses*, vol. 11, no. 2, Jan 25 2019, doi: 10.3390/v11020100.
- [52] N. Herold, M. Anders-Ößwein, B. Glass, M. Eckhardt, B. Müller, and H. G. Kräusslich, "HIV-1 entry in SupT1-R5, CEM-ss, and primary CD4+ T cells occurs at the plasma membrane and does not require endocytosis," (in eng), *J Virol*, vol. 88, no. 24, pp. 13956-70, Dec 2014, doi: 10.1128/jvi.01543-14.
- [53] L. Chauveau *et al.*, "HIV Fusion in Dendritic Cells Occurs Mainly at the Surface and Is Limited by Low CD4 Levels," (in eng), *J Virol*, vol. 91, no. 21, Nov 1 2017, doi: 10.1128/jvi.01248-17.
- [54] C. M. Finnegan and R. Blumenthal, "Fenretinide inhibits HIV infection by promoting viral endocytosis," (in eng), *Antiviral Res*, vol. 69, no. 2, pp. 116-23, Feb 2006, doi: 10.1016/j.antiviral.2005.11.002.
- [55] G. Filice *et al.*, "Endocytosis constitute the infectious route of HIV-1 entry in human and rabbit monocytes lacking the CD4 receptor," (in eng), *Microbiologica*, vol. 14, no. 2, pp. 77-93, Apr 1991.
- [56] A. Pelchen-Matthews, B. Kramer, and M. Marsh, "Infectious HIV-1 assembles in late endosomes in primary macrophages," (in eng), *J Cell Biol*, vol. 162, no. 3, pp. 443-55, Aug 4 2003, doi: 10.1083/jcb.200304008.
- [57] B. M. Forshey, U. von Schwedler, W. I. Sundquist, and C. Aiken, "Formation of a human immunodeficiency virus type 1 core of optimal stability is crucial for viral replication," (in eng), *J Virol*, vol. 76, no. 11, pp. 5667-77, Jun 2002, doi: 10.1128/jvi.76.11.5667-5677.2002.
- [58] V. B. Shah and C. Aiken, "In vitro uncoating of HIV-1 cores," (in eng), *J Vis Exp*, no. 57, Nov 8 2011, doi: 10.3791/3384.
- [59] R. Welker, H. Hohenberg, U. Tessmer, C. Huckhagel, and H. G. Kräusslich, "Biochemical and structural analysis of isolated mature cores of human immunodeficiency virus type 1," (in eng), *J Virol*, vol. 74, no. 3, pp. 1168-77, Feb 2000, doi: 10.1128/jvi.74.3.1168-1177.2000.
- [60] A. E. Hulme, O. Perez, and T. J. Hope, "Complementary assays reveal a relationship between HIV-1 uncoating and reverse transcription," (in eng), *Proc Natl Acad Sci U S A*, vol. 108, no. 24, pp. 9975-80, Jun 14 2011, doi: 10.1073/pnas.1014522108.
- [61] J. I. Mamede, G. C. Cianci, M. R. Anderson, and T. J. Hope, "Early cytoplasmic uncoating is associated with infectivity of HIV-1," (in eng), *Proc Natl Acad Sci U S A*, vol. 114, no. 34, pp. E7169-e7178, Aug 22 2017, doi: 10.1073/pnas.1706245114.
- [62] S. Rankovic, J. Varadarajan, R. Ramalho, C. Aiken, and I. Rousso, "Reverse Transcription Mechanically Initiates HIV-1 Capsid Disassembly," (in eng), *J Virol*, vol. 91, no. 12, Jun 15 2017, doi: 10.1128/jvi.00289-17.
- [63] T. G. Müller, V. Zila, B. Müller, and H. G. Kräusslich, "Nuclear Capsid Uncoating and Reverse Transcription of HIV-1," (in eng), *Annu Rev Virol*, vol. 9, no. 1, pp. 261-284, Sep 29 2022, doi: 10.1146/annurev-virology-020922-110929.
- [64] S. Schifferdecker *et al.*, "Direct Capsid Labeling of Infectious HIV-1 by Genetic Code Expansion Allows Detection of Largely Complete Nuclear Capsids and Suggests Nuclear Entry of HIV-1 Complexes via Common Routes," (in eng), *mBio*, vol. 13, no. 5, p. e0195922, Oct 26 2022, doi: 10.1128/mbio.01959-22.
- [65] V. Zila *et al.*, "Cone-shaped HIV-1 capsids are transported through intact nuclear pores," (in eng), *Cell*, vol. 184, no. 4, pp. 1032-1046.e18, Feb 18 2021, doi: 10.1016/j.cell.2021.01.025.

- [66] W. S. Hu and S. H. Hughes, "HIV-1 reverse transcription," (in eng), *Cold Spring Harb Perspect Med*, vol. 2, no. 10, Oct 1 2012, doi: 10.1101/cshperspect.a006882.
- [67] A. Selyutina, M. Persaud, K. Lee, V. KewalRamani, and F. Diaz-Griffero, "Nuclear Import of the HIV-1 Core Precedes Reverse Transcription and Uncoating," (in eng), *Cell Rep*, vol. 32, no. 13, p. 108201, Sep 29 2020, doi: 10.1016/j.celrep.2020.108201.
- [68] A. Dharan, N. Bachmann, S. Talley, V. Zwickelmaier, and E. M. Campbell, "Nuclear pore blockade reveals that HIV-1 completes reverse transcription and uncoating in the nucleus," (in eng), *Nat Microbiol*, vol. 5, no. 9, pp. 1088-1095, Sep 2020, doi: 10.1038/s41564-020-0735-8.
- [69] R. Craigie and F. D. Bushman, "HIV DNA integration," (in eng), *Cold Spring Harb Perspect Med*, vol. 2, no. 7, p. a006890, Jul 2012, doi: 10.1101/cshperspect.a006890.
- [70] C. M. Farnet and F. D. Bushman, "HIV-1 cDNA integration: requirement of HMG I(Y) protein for function of preintegration complexes in vitro," (in eng), *Cell*, vol. 88, no. 4, pp. 483-92, Feb 21 1997, doi: 10.1016/s0092-8674(00)81888-7.
- [71] L. Li, K. Yoder, M. S. Hansen, J. Olvera, M. D. Miller, and F. D. Bushman, "Retroviral cDNA integration: stimulation by HMG I family proteins," (in eng), *J Virol*, vol. 74, no. 23, pp. 10965-74, Dec 2000, doi: 10.1128/jvi.74.23.10965-10974.2000.
- [72] M. C. Shun *et al.*, "LEDGF/p75 functions downstream from preintegration complex formation to effect gene-specific HIV-1 integration," (in eng), *Genes Dev*, vol. 21, no. 14, pp. 1767-78, Jul 15 2007, doi: 10.1101/gad.1565107.
- [73] P. Cherepanov *et al.*, "HIV-1 integrase forms stable tetramers and associates with LEDGF/p75 protein in human cells," (in eng), *J Biol Chem*, vol. 278, no. 1, pp. 372-81, Jan 3 2003, doi: 10.1074/jbc.M209278200.
- [74] P. K. Singh, G. J. Bedwell, and A. N. Engelman, "Spatial and Genomic Correlates of HIV-1 Integration Site Targeting," (in eng), *Cells*, vol. 11, no. 4, Feb 14 2022, doi: 10.3390/cells11040655.
- [75] J. Symons, P. U. Cameron, and S. R. Lewin, "HIV integration sites and implications for maintenance of the reservoir," (in eng), *Curr Opin HIV AIDS*, vol. 13, no. 2, pp. 152-159, Mar 2018, doi: 10.1097/coh.0000000000000438.
- [76] J. Karn and C. M. Stoltzfus, "Transcriptional and posttranscriptional regulation of HIV-1 gene expression," (in eng), *Cold Spring Harb Perspect Med*, vol. 2, no. 2, p. a006916, Feb 2012, doi: 10.1101/cshperspect.a006916.
- [77] E. O. Freed, "HIV-1 assembly, release and maturation," (in eng), *Nat Rev Microbiol*, vol. 13, no. 8, pp. 484-96, Aug 2015, doi: 10.1038/nrmicro3490.
- [78] R. T. Davey, Jr. *et al.*, "HIV-1 and T cell dynamics after interruption of highly active antiretroviral therapy (HAART) in patients with a history of sustained viral suppression," (in eng), *Proc Natl Acad Sci U S A*, vol. 96, no. 26, pp. 15109-14, Dec 21 1999, doi: 10.1073/pnas.96.26.15109.
- [79] T. W. Chun, R. T. Davey, Jr., D. Engel, H. C. Lane, and A. S. Fauci, "Re-emergence of HIV after stopping therapy," (in eng), *Nature*, vol. 401, no. 6756, pp. 874-5, Oct 28 1999, doi: 10.1038/44755.
- [80] Y. Han *et al.*, "Orientation-dependent regulation of integrated HIV-1 expression by host gene transcriptional readthrough," (in eng), *Cell Host Microbe*, vol. 4, no. 2, pp. 134-46, Aug 14 2008, doi: 10.1016/j.chom.2008.06.008.
- [81] A. R. Schröder, P. Shinn, H. Chen, C. Berry, J. R. Ecker, and F. Bushman, "HIV-1 integration in the human genome favors active genes and local hotspots," (in eng), *Cell*, vol. 110, no. 4, pp. 521-9, Aug 23 2002, doi: 10.1016/s0092-8674(02)00864-4.
- [82] B. Marini *et al.*, "Nuclear architecture dictates HIV-1 integration site selection," (in eng), *Nature*, vol. 521, no. 7551, pp. 227-31, May 14 2015, doi: 10.1038/nature14226.
- [83] L. Shan *et al.*, "Influence of host gene transcription level and orientation on HIV-1 latency in a primary-cell model," (in eng), *J Virol*, vol. 85, no. 11, pp. 5384-93, Jun 2011, doi: 10.1128/jvi.02536-10.

- [84] T. Lenasi, X. Contreras, and B. M. Peterlin, "Transcriptional interference antagonizes proviral gene expression to promote HIV latency," (in eng), *Cell Host Microbe*, vol. 4, no. 2, pp. 123-33, Aug 14 2008, doi: 10.1016/j.chom.2008.05.016.
- [85] C. Jiang *et al.*, "Distinct viral reservoirs in individuals with spontaneous control of HIV-1," (in eng), *Nature*, vol. 585, no. 7824, pp. 261-267, Sep 2020, doi: 10.1038/s41586-020-2651-8.
- [86] S. C. Hsia and Y. B. Shi, "Chromatin disruption and histone acetylation in regulation of the human immunodeficiency virus type 1 long terminal repeat by thyroid hormone receptor," (in eng), *Mol Cell Biol*, vol. 22, no. 12, pp. 4043-52, Jun 2002, doi: 10.1128/mcb.22.12.4043-4052.2002.
- [87] J. J. Coull *et al.*, "The human factors YY1 and LSF repress the human immunodeficiency virus type 1 long terminal repeat via recruitment of histone deacetylase 1," (in eng), *J Virol*, vol. 74, no. 15, pp. 6790-9, Aug 2000, doi: 10.1128/jvi.74.15.6790-6799.2000.
- [88] J. Blazkova *et al.*, "CpG methylation controls reactivation of HIV from latency," (in eng), *PLoS Pathog*, vol. 5, no. 8, p. e1000554, Aug 2009, doi: 10.1371/journal.ppat.1000554.
- [89] S. E. Kauder, A. Bosque, A. Lindqvist, V. Planelles, and E. Verdin, "Epigenetic regulation of HIV-1 latency by cytosine methylation," (in eng), *PLoS Pathog*, vol. 5, no. 6, p. e1000495, Jun 2009, doi: 10.1371/journal.ppat.1000495.
- [90] N. Chomont *et al.*, "HIV reservoir size and persistence are driven by T cell survival and homeostatic proliferation," (in eng), *Nat Med*, vol. 15, no. 8, pp. 893-900, Aug 2009, doi: 10.1038/nm.1972.
- [91] T. W. Chun *et al.*, "Presence of an inducible HIV-1 latent reservoir during highly active antiretroviral therapy," (in eng), *Proc Natl Acad Sci U S A*, vol. 94, no. 24, pp. 13193-7, Nov 25 1997, doi: 10.1073/pnas.94.24.13193.
- [92] D. Finzi *et al.*, "Identification of a reservoir for HIV-1 in patients on highly active antiretroviral therapy," (in eng), *Science*, vol. 278, no. 5341, pp. 1295-300, Nov 14 1997, doi: 10.1126/science.278.5341.1295.
- [93] T. Pierson, J. McArthur, and R. F. Siliciano, "Reservoirs for HIV-1: mechanisms for viral persistence in the presence of antiviral immune responses and antiretroviral therapy," (in eng), *Annu Rev Immunol*, vol. 18, pp. 665-708, 2000, doi: 10.1146/annurev.immunol.18.1.665.
- [94] J. Guo, W. Wang, D. Yu, and Y. Wu, "Spinoculation triggers dynamic actin and cofilin activity that facilitates HIV-1 infection of transformed and resting CD4 T cells," (in eng), *J Virol*, vol. 85, no. 19, pp. 9824-33, Oct 2011, doi: 10.1128/jvi.05170-11.
- [95] P. Matarrese and W. Malorni, "Human immunodeficiency virus (HIV)-1 proteins and cytoskeleton: partners in viral life and host cell death," (in eng), *Cell Death Differ*, vol. 12 Suppl 1, pp. 932-41, Aug 2005, doi: 10.1038/sj.cdd.4401582.
- [96] B. Descours *et al.*, "SAMHD1 restricts HIV-1 reverse transcription in quiescent CD4(+) T-cells," (in eng), *Retrovirology*, vol. 9, p. 87, Oct 23 2012, doi: 10.1186/1742-4690-9-87.
- [97] H. M. Baldauf *et al.*, "SAMHD1 restricts HIV-1 infection in resting CD4(+) T cells," (in eng), *Nat Med*, vol. 18, no. 11, pp. 1682-7, Nov 2012, doi: 10.1038/nm.2964.
- [98] C. St Gelais *et al.*, "SAMHD1 restricts HIV-1 infection in dendritic cells (DCs) by dNTP depletion, but its expression in DCs and primary CD4+ T-lymphocytes cannot be upregulated by interferons," (in eng), *Retrovirology*, vol. 9, p. 105, Dec 11 2012, doi: 10.1186/1742-4690-9-105.
- [99] N. Laguette *et al.*, "SAMHD1 is the dendritic- and myeloid-cell-specific HIV-1 restriction factor counteracted by Vpx," (in eng), *Nature*, vol. 474, no. 7353, pp. 654-7, May 25 2011, doi: 10.1038/nature10117.
- [100] B. Kim, L. A. Nguyen, W. Daddacha, and J. A. Hollenbaugh, "Tight interplay among SAMHD1 protein level, cellular dNTP levels, and HIV-1 proviral DNA synthesis kinetics in human primary monocyte-derived macrophages," (in eng), *J Biol Chem*, vol. 287, no. 26, pp. 21570-4, Jun 22 2012, doi: 10.1074/jbc.C112.374843.

- [101] K. M. Bruner *et al.*, "Defective proviruses rapidly accumulate during acute HIV-1 infection," (in eng), *Nat Med*, vol. 22, no. 9, pp. 1043-9, Sep 2016, doi: 10.1038/nm.4156.
- [102] D. Finzi *et al.*, "Latent infection of CD4+ T cells provides a mechanism for lifelong persistence of HIV-1, even in patients on effective combination therapy," (in eng), *Nat Med*, vol. 5, no. 5, pp. 512-7, May 1999, doi: 10.1038/8394.
- [103] C. Dobrowolski *et al.*, "Entry of Polarized Effector Cells into Quiescence Forces HIV Latency," (in eng), *mBio*, vol. 10, no. 2, Mar 26 2019, doi: 10.1128/mBio.00337-19.
- [104] V. A. Evans *et al.*, "Programmed cell death-1 contributes to the establishment and maintenance of HIV-1 latency," (in eng), *Aids*, vol. 32, no. 11, pp. 1491-1497, Jul 17 2018, doi: 10.1097/qad.0000000000001849.
- [105] W. J. Swiggard *et al.*, "Human immunodeficiency virus type 1 can establish latent infection in resting CD4+ T cells in the absence of activating stimuli," (in eng), *J Virol*, vol. 79, no. 22, pp. 14179-88, Nov 2005, doi: 10.1128/jvi.79.22.14179-14188.2005.
- [106] L. M. Agosto, J. J. Yu, J. Dai, R. Kaletsky, D. Monie, and U. O'Doherty, "HIV-1 integrates into resting CD4+ T cells even at low inoculums as demonstrated with an improved assay for HIV-1 integration," (in eng), *Virology*, vol. 368, no. 1, pp. 60-72, Nov 10 2007, doi: 10.1016/j.virol.2007.06.001.
- [107] Y. D. Korin and J. A. Zack, "Progression to the G1b phase of the cell cycle is required for completion of human immunodeficiency virus type 1 reverse transcription in T cells," (in eng), *J Virol*, vol. 72, no. 4, pp. 3161-8, Apr 1998, doi: 10.1128/jvi.72.4.3161-3168.1998.
- [108] P. U. Cameron *et al.*, "Establishment of HIV-1 latency in resting CD4+ T cells depends on chemokine-induced changes in the actin cytoskeleton," (in eng), *Proc Natl Acad Sci U S A*, vol. 107, no. 39, pp. 16934-9, Sep 28 2010, doi: 10.1073/pnas.1002894107.
- [109] M. Coiras *et al.*, "IL-7 Induces SAMHD1 Phosphorylation in CD4+ T Lymphocytes, Improving Early Steps of HIV-1 Life Cycle," (in eng), *Cell Rep*, vol. 14, no. 9, pp. 2100-2107, Mar 8 2016, doi: 10.1016/j.celrep.2016.02.022.
- [110] F. Hsiao *et al.*, "Tissue memory CD4+ T cells expressing IL-7 receptor-alpha (CD127) preferentially support latent HIV-1 infection," (in eng), *PLoS Pathog*, vol. 16, no. 4, p. e1008450, Apr 2020, doi: 10.1371/journal.ppat.1008450.
- [111] B. R. Cullen, "Regulation of HIV-1 gene expression," (in eng), *Faseb j*, vol. 5, no. 10, pp. 2361-8, Jul 1991, doi: 10.1096/fasebj.5.10.1712325.
- [112] C. Dingwall *et al.*, "HIV-1 tat protein stimulates transcription by binding to a U-rich bulge in the stem of the TAR RNA structure," (in eng), *Embo j*, vol. 9, no. 12, pp. 4145-53, Dec 1990, doi: 10.1002/j.1460-2075.1990.tb07637.x.
- [113] M. E. Garber, P. Wei, and K. A. Jones, "HIV-1 Tat interacts with cyclin T1 to direct the P-TEFb CTD kinase complex to TAR RNA," (in eng), *Cold Spring Harb Symp Quant Biol*, vol. 63, pp. 371-80, 1998, doi: 10.1101/sqb.1998.63.371.
- [114] S. Sengupta and R. F. Siliciano, "Targeting the Latent Reservoir for HIV-1," (in eng), *Immunity*, vol. 48, no. 5, pp. 872-895, May 15 2018, doi: 10.1016/j.immuni.2018.04.030.
- [115] J. M. Prins *et al.*, "Immuno-activation with anti-CD3 and recombinant human IL-2 in HIV-1-infected patients on potent antiretroviral therapy," (in eng), *Aids*, vol. 13, no. 17, pp. 2405-10, Dec 3 1999, doi: 10.1097/00002030-199912030-00012.
- [116] C. Fraser *et al.*, "Reduction of the HIV-1-infected T-cell reservoir by immune activation treatment is dose-dependent and restricted by the potency of antiretroviral drugs," (in eng), *Aids*, vol. 14, no. 6, pp. 659-69, Apr 14 2000, doi: 10.1097/00002030-200004140-00005.
- [117] G. Lehrman *et al.*, "Depletion of latent HIV-1 infection in vivo: a proof-of-concept study," (in eng), *Lancet*, vol. 366, no. 9485, pp. 549-55, Aug 13-19 2005, doi: 10.1016/s0140-6736(05)67098-5.
- [118] N. M. Archin *et al.*, "Administration of vorinostat disrupts HIV-1 latency in patients on antiretroviral therapy," (in eng), *Nature*, vol. 487, no. 7408, pp. 482-5, Jul 25 2012, doi: 10.1038/nature11286.

- [119] J. H. Elliott *et al.*, "Activation of HIV transcription with short-course vorinostat in HIV-infected patients on suppressive antiretroviral therapy," (in eng), *PLoS Pathog*, vol. 10, no. 10, p. e1004473, Oct 2014, doi: 10.1371/journal.ppat.1004473.
- [120] S. Bouchat *et al.*, "Sequential treatment with 5-aza-2'-deoxycytidine and deacetylase inhibitors reactivates HIV-1," (in eng), *EMBO Mol Med*, vol. 8, no. 2, pp. 117-38, Feb 1 2016, doi: 10.15252/emmm.201505557.
- [121] P. Lu *et al.*, "BET inhibitors RVX-208 and PFI-1 reactivate HIV-1 from latency," (in eng), *Sci Rep*, vol. 7, no. 1, p. 16646, Nov 30 2017, doi: 10.1038/s41598-017-16816-1.
- [122] Z. Li, J. Guo, Y. Wu, and Q. Zhou, "The BET bromodomain inhibitor JQ1 activates HIV latency through antagonizing Brd4 inhibition of Tat-transactivation," (in eng), *Nucleic Acids Res*, vol. 41, no. 1, pp. 277-87, Jan 7 2013, doi: 10.1093/nar/gks976.
- [123] C. Banerjee *et al.*, "BET bromodomain inhibition as a novel strategy for reactivation of HIV-1," (in eng), *J Leukoc Biol*, vol. 92, no. 6, pp. 1147-54, Dec 2012, doi: 10.1189/jlb.0312165.
- [124] T. Salahong, C. Schwartz, and R. Sungthong, "Are BET Inhibitors yet Promising Latency-Reversing Agents for HIV-1 Reactivation in AIDS Therapy?," (in eng), *Viruses*, vol. 13, no. 6, May 29 2021, doi: 10.3390/v13061026.
- [125] J. D. Siliciano *et al.*, "Stability of the latent reservoir for HIV-1 in patients receiving valproic acid," (in eng), *J Infect Dis*, vol. 195, no. 6, pp. 833-6, Mar 15 2007, doi: 10.1086/511823.
- [126] N. M. Archin *et al.*, "Valproic acid without intensified antiviral therapy has limited impact on persistent HIV infection of resting CD4+ T cells," (in eng), *Aids*, vol. 22, no. 10, pp. 1131-5, Jun 19 2008, doi: 10.1097/QAD.0b013e3282fd6df4.
- [127] A. T. Boateng, A. Abaidoo-Myles, E. Y. Bonney, and G. B. Kyei, "Isoform-Selective Versus Nonselective Histone Deacetylase Inhibitors in HIV Latency Reversal," (in eng), *AIDS Res Hum Retroviruses*, vol. 38, no. 8, pp. 615-621, Aug 2022, doi: 10.1089/aid.2021.0195.
- [128] S. Matalon, T. A. Rasmussen, and C. A. Dinarello, "Histone deacetylase inhibitors for purging HIV-1 from the latent reservoir," (in eng), *Mol Med*, vol. 17, no. 5-6, pp. 466-72, May-Jun 2011, doi: 10.2119/molmed.2011.00076.
- [129] A. Biancotto *et al.*, "Dual role of prostratin in inhibition of infection and reactivation of human immunodeficiency virus from latency in primary blood lymphocytes and lymphoid tissue," (in eng), *J Virol*, vol. 78, no. 19, pp. 10507-15, Oct 2004, doi: 10.1128/jvi.78.19.10507-10515.2004.
- [130] G. Jiang and S. Dandekar, "Targeting NF- $\kappa$ B signaling with protein kinase C agonists as an emerging strategy for combating HIV latency," (in eng), *AIDS Res Hum Retroviruses*, vol. 31, no. 1, pp. 4-12, Jan 2015, doi: 10.1089/aid.2014.0199.
- [131] C. Gutiérrez *et al.*, "Bryostatins for latent virus reactivation in HIV-infected patients on antiretroviral therapy," (in eng), *Aids*, vol. 30, no. 9, pp. 1385-92, Jun 1 2016, doi: 10.1097/qad.0000000000001064.
- [132] A. M. Spivak and V. Planelles, "Novel Latency Reversal Agents for HIV-1 Cure," (in eng), *Annu Rev Med*, vol. 69, pp. 421-436, Jan 29 2018, doi: 10.1146/annurev-med-052716-031710.
- [133] G. Vansant, A. Bruggemans, J. Janssens, and Z. Debyser, "Block-And-Lock Strategies to Cure HIV Infection," (in eng), *Viruses*, vol. 12, no. 1, Jan 10 2020, doi: 10.3390/v12010084.
- [134] C. F. Kessing *et al.*, "In Vivo Suppression of HIV Rebound by Didehydro-Cortistatin A, a "Block-and-Lock" Strategy for HIV-1 Treatment," (in eng), *Cell Rep*, vol. 21, no. 3, pp. 600-611, Oct 17 2017, doi: 10.1016/j.celrep.2017.09.080.
- [135] M. J. Jean *et al.*, "Curaxin CBL0100 Blocks HIV-1 Replication and Reactivation through Inhibition of Viral Transcriptional Elongation," (in eng), *Front Microbiol*, vol. 8, p. 2007, 2017, doi: 10.3389/fmicb.2017.02007.
- [136] E. Besnard *et al.*, "The mTOR Complex Controls HIV Latency," (in eng), *Cell Host Microbe*, vol. 20, no. 6, pp. 785-797, Dec 14 2016, doi: 10.1016/j.chom.2016.11.001.

- [137] C. Ahlenstiel *et al.*, "Novel RNA Duplex Locks HIV-1 in a Latent State via Chromatin-mediated Transcriptional Silencing," (in eng), *Mol Ther Nucleic Acids*, vol. 4, no. 10, p. e261, Oct 27 2015, doi: 10.1038/mtna.2015.31.
- [138] C. Méndez, S. Ledger, K. Petoumenos, C. Ahlenstiel, and A. D. Kelleher, "RNA-induced epigenetic silencing inhibits HIV-1 reactivation from latency," (in eng), *Retrovirology*, vol. 15, no. 1, p. 67, Oct 4 2018, doi: 10.1186/s12977-018-0451-0.
- [139] A. Mukim, D. M. Smith, S. Deshmukh, A. A. Qazi, and N. Beliakova-Bethell, "A Camptothetin Analog, Topotecan, Promotes HIV Latency via Interference with HIV Transcription and RNA Splicing," (in eng), *J Virol*, vol. 97, no. 2, p. e0163022, Feb 28 2023, doi: 10.1128/jvi.01630-22.
- [140] L. Gama *et al.*, "Reactivation of simian immunodeficiency virus reservoirs in the brain of virally suppressed macaques," (in eng), *Aids*, vol. 31, no. 1, pp. 5-14, Jan 2 2017, doi: 10.1097/qad.0000000000001267.
- [141] M. M. Nühn *et al.*, "Shock and kill within the CNS: A promising HIV eradication approach?," (in eng), *J Leukoc Biol*, vol. 112, no. 5, pp. 1297-1315, Nov 2022, doi: 10.1002/jlb.5vmr0122-046rrr.
- [142] B. Descours *et al.*, "CD32a is a marker of a CD4 T-cell HIV reservoir harbouring replication-competent proviruses," (in eng), *Nature*, vol. 543, no. 7646, pp. 564-567, Mar 23 2017, doi: 10.1038/nature21710.
- [143] G. Darcis *et al.*, "CD32(+)CD4(+) T Cells Are Highly Enriched for HIV DNA and Can Support Transcriptional Latency," (in eng), *Cell Rep*, vol. 30, no. 7, pp. 2284-2296.e3, Feb 18 2020, doi: 10.1016/j.celrep.2020.01.071.
- [144] J. J. Vásquez *et al.*, "CD32-RNA Co-localizes with HIV-RNA in CD3+ Cells Found within Gut Tissues from Viremic and ART-Suppressed Individuals," (in eng), *Pathog Immun*, vol. 4, no. 1, pp. 147-160, 2019, doi: 10.20411/pai.v4i1.271.
- [145] A. Astorga-Gamaza *et al.*, "Identification of HIV-reservoir cells with reduced susceptibility to antibody-dependent immune response," (in eng), *Elife*, vol. 11, May 26 2022, doi: 10.7554/eLife.78294.
- [146] P. Adams *et al.*, "CD32(+)CD4(+) memory T cells are enriched for total HIV-1 DNA in tissues from humanized mice," (in eng), *iScience*, vol. 24, no. 1, p. 101881, Jan 22 2021, doi: 10.1016/j.isci.2020.101881.
- [147] G. E. Martin *et al.*, "CD32-Expressing CD4 T Cells Are Phenotypically Diverse and Can Contain Proviral HIV DNA," (in eng), *Front Immunol*, vol. 9, p. 928, 2018, doi: 10.3389/fimmu.2018.00928.
- [148] L. N. Bertagnolli *et al.*, "The role of CD32 during HIV-1 infection," (in eng), *Nature*, vol. 561, no. 7723, pp. E17-e19, Sep 2018, doi: 10.1038/s41586-018-0494-3.
- [149] L. Pérez *et al.*, "Conflicting evidence for HIV enrichment in CD32(+) CD4 T cells," (in eng), *Nature*, vol. 561, no. 7723, pp. E9-e16, Sep 2018, doi: 10.1038/s41586-018-0493-4.
- [150] C. E. Osuna *et al.*, "Evidence that CD32a does not mark the HIV-1 latent reservoir," (in eng), *Nature*, vol. 561, no. 7723, pp. E20-e28, Sep 2018, doi: 10.1038/s41586-018-0495-2.
- [151] M. Abdel-Mohsen *et al.*, "CD32 is expressed on cells with transcriptionally active HIV but does not enrich for HIV DNA in resting T cells," (in eng), *Sci Transl Med*, vol. 10, no. 437, Apr 18 2018, doi: 10.1126/scitranslmed.aar6759.
- [152] R. Badia *et al.*, "CD32 expression is associated to T-cell activation and is not a marker of the HIV-1 reservoir," (in eng), *Nat Commun*, vol. 9, no. 1, p. 2739, Jul 16 2018, doi: 10.1038/s41467-018-05157-w.
- [153] M. P. Holgado, I. Sananez, S. Raiden, J. R. Geffner, and L. Arruvito, "CD32 Ligation Promotes the Activation of CD4(+) T Cells," (in eng), *Front Immunol*, vol. 9, p. 2814, 2018, doi: 10.3389/fimmu.2018.02814.

- [154] J. P. Thornhill *et al.*, "CD32 expressing doublets in HIV-infected gut-associated lymphoid tissue are associated with a T follicular helper cell phenotype," (in eng), *Mucosal Immunol*, vol. 12, no. 5, pp. 1212-1219, Sep 2019, doi: 10.1038/s41385-019-0180-2.
- [155] G. M. Laird, D. I. Rosenbloom, J. Lai, R. F. Siliciano, and J. D. Siliciano, "Measuring the Frequency of Latent HIV-1 in Resting CD4<sup>+</sup> T Cells Using a Limiting Dilution Coculture Assay," (in eng), *Methods Mol Biol*, vol. 1354, pp. 239-53, 2016, doi: 10.1007/978-1-4939-3046-3\_16.
- [156] L. E. Hogan *et al.*, "Increased HIV-1 transcriptional activity and infectious burden in peripheral blood and gut-associated CD4<sup>+</sup> T cells expressing CD30," (in eng), *PLoS Pathog*, vol. 14, no. 2, p. e1006856, Feb 2018, doi: 10.1371/journal.ppat.1006856.
- [157] T. J. Henrich *et al.*, "HIV-1 persistence following extremely early initiation of antiretroviral therapy (ART) during acute HIV-1 infection: An observational study," (in eng), *PLoS Med*, vol. 14, no. 11, p. e1002417, Nov 2017, doi: 10.1371/journal.pmed.1002417.
- [158] W. Zhang *et al.*, "Identification of CD98 as a Novel Biomarker for HIV-1 Permissiveness and Latent Infection," (in eng), *mBio*, vol. 13, no. 6, p. e0249622, Oct 10 2022, doi: 10.1128/mbio.02496-22.
- [159] G. N. Llewellyn *et al.*, "Humanized Mouse Model of HIV-1 Latency with Enrichment of Latent Virus in PD-1(+) and TIGIT(+) CD4 T Cells," (in eng), *J Virol*, vol. 93, no. 10, May 15 2019, doi: 10.1128/jvi.02086-18.
- [160] R. Fromentin *et al.*, "CD4<sup>+</sup> T Cells Expressing PD-1, TIGIT and LAG-3 Contribute to HIV Persistence during ART," (in eng), *PLoS Pathog*, vol. 12, no. 7, p. e1005761, Jul 2016, doi: 10.1371/journal.ppat.1005761.
- [161] R. Fromentin *et al.*, "PD-1 blockade potentiates HIV latency reversal ex vivo in CD4(+) T cells from ART-suppressed individuals," (in eng), *Nat Commun*, vol. 10, no. 1, p. 814, Feb 18 2019, doi: 10.1038/s41467-019-08798-7.
- [162] M. Iglesias-Ussel, C. Vandergeeten, L. Marchionni, N. Chomont, and F. Romerio, "High levels of CD2 expression identify HIV-1 latently infected resting memory CD4<sup>+</sup> T cells in virally suppressed subjects," (in eng), *J Virol*, vol. 87, no. 16, pp. 9148-58, Aug 2013, doi: 10.1128/jvi.01297-13.
- [163] R. A. S. Raposo *et al.*, "IFITM1 targets HIV-1 latently infected cells for antibody-dependent cytolysis," (in eng), *JCI Insight*, vol. 2, no. 1, p. e85811, Jan 12 2017, doi: 10.1172/jci.insight.85811.
- [164] X. Li *et al.*, "CD161(+) CD4(+) T Cells Harbor Clonally Expanded Replication-Competent HIV-1 in Antiretroviral Therapy-Suppressed Individuals," (in eng), *mBio*, vol. 10, no. 5, Oct 8 2019, doi: 10.1128/mBio.02121-19.
- [165] T. Takai, M. Li, D. Sylvestre, R. Clynes, and J. V. Ravetch, "FcR gamma chain deletion results in pleiotropic effector cell defects," (in eng), *Cell*, vol. 76, no. 3, pp. 519-29, Feb 11 1994, doi: 10.1016/0092-8674(94)90115-5.
- [166] M. Guillems, P. Bruhns, Y. Saeys, H. Hammad, and B. N. Lambrecht, "The function of Fcγ receptors in dendritic cells and macrophages," (in eng), *Nat Rev Immunol*, vol. 14, no. 2, pp. 94-108, Feb 2014, doi: 10.1038/nri3582.
- [167] C. Rosales and E. Uribe-Querol, "Fc receptors: Cell activators of antibody functions," *Advances in Bioscience and Biotechnology*, vol. Vol.04No.04, p. 13, 2013, Art no. 30589, doi: 10.4236/abb.2013.44A004.
- [168] F. Nimmerjahn and J. V. Ravetch, "Fcγ receptors as regulators of immune responses," (in eng), *Nat Rev Immunol*, vol. 8, no. 1, pp. 34-47, Jan 2008, doi: 10.1038/nri2206.
- [169] J. M. Hayes, M. R. Wormald, P. M. Rudd, and G. P. Davey, "Fc gamma receptors: glycobiology and therapeutic prospects," (in eng), *J Inflamm Res*, vol. 9, pp. 209-219, 2016, doi: 10.2147/jir.S121233.
- [170] A. W. Barb, "Fc γ receptor compositional heterogeneity: Considerations for immunotherapy development," (in eng), *J Biol Chem*, vol. 296, p. 100057, Jan-Jun 2021, doi: 10.1074/jbc.REV120.013168.

- [171] J. V. Ravetch and S. Bolland, "IgG Fc receptors," (in eng), *Annu Rev Immunol*, vol. 19, pp. 275-90, 2001, doi: 10.1146/annurev.immunol.19.1.275.
- [172] J. V. Ravetch and L. L. Lanier, "Immune inhibitory receptors," (in eng), *Science*, vol. 290, no. 5489, pp. 84-9, Oct 6 2000, doi: 10.1126/science.290.5489.84.
- [173] F. Nimmerjahn and J. V. Ravetch, "Fc-receptors as regulators of immunity," (in eng), *Adv Immunol*, vol. 96, pp. 179-204, 2007, doi: 10.1016/s0065-2776(07)96005-8.
- [174] L. T. Vogelpoel, D. L. Baeten, E. C. de Jong, and J. den Dunnen, "Control of cytokine production by human fc gamma receptors: implications for pathogen defense and autoimmunity," (in eng), *Front Immunol*, vol. 6, p. 79, 2015, doi: 10.3389/fimmu.2015.00079.
- [175] J. C. Anania, A. M. Chenoweth, B. D. Wines, and P. M. Hogarth, "The Human FcγRII (CD32) Family of Leukocyte FcR in Health and Disease," (in eng), *Front Immunol*, vol. 10, p. 464, 2019, doi: 10.3389/fimmu.2019.00464.
- [176] J. van der Heijden, W. B. Breunis, J. Geissler, M. de Boer, T. K. van den Berg, and T. W. Kuijpers, "Phenotypic variation in IgG receptors by nonclassical FCGR2C alleles," (in eng), *J Immunol*, vol. 188, no. 3, pp. 1318-24, Feb 1 2012, doi: 10.4049/jimmunol.1003945.
- [177] P. A. Warmerdam, N. M. Nabben, S. A. van de Graaf, J. G. van de Winkel, and P. J. Capel, "The human low affinity immunoglobulin G Fc receptor IIC gene is a result of an unequal crossover event," (in eng), *J Biol Chem*, vol. 268, no. 10, pp. 7346-9, Apr 5 1993.
- [178] L. K. Ernst, D. Metes, R. B. Herberman, and P. A. Morel, "Allelic polymorphisms in the FcγRIIC gene can influence its function on normal human natural killer cells," (in eng), *J Mol Med (Berl)*, vol. 80, no. 4, pp. 248-57, Apr 2002, doi: 10.1007/s00109-001-0294-2.
- [179] W. B. Breunis *et al.*, "Copy number variation of the activating FCGR2C gene predisposes to idiopathic thrombocytopenic purpura," (in eng), *Blood*, vol. 111, no. 3, pp. 1029-38, Feb 1 2008, doi: 10.1182/blood-2007-03-079913.
- [180] R. Lassaunière and C. T. Tiemessen, "Variability at the FCGR locus: characterization in Black South Africans and evidence for ethnic variation in and out of Africa," (in eng), *Genes Immun*, vol. 17, no. 2, pp. 93-104, Mar 2016, doi: 10.1038/gene.2015.60.
- [181] X. Li *et al.*, "Allelic-dependent expression of an activating Fc receptor on B cells enhances humoral immune responses," (in eng), *Sci Transl Med*, vol. 5, no. 216, p. 216ra175, Dec 18 2013, doi: 10.1126/scitranslmed.3007097.
- [182] W. Engelhardt, J. Matzke, and R. E. Schmidt, "Activation-dependent expression of low affinity IgG receptors Fc gamma RII(CD32) and Fc gamma RI(CD16) in subpopulations of human T lymphocytes," (in eng), *Immunobiology*, vol. 192, no. 5, pp. 297-320, Apr 1995, doi: 10.1016/s0171-2985(11)80172-5.
- [183] M. Gray and R. J. Botelho, "Phagocytosis: Hungry, Hungry Cells," (in eng), *Methods Mol Biol*, vol. 1519, pp. 1-16, 2017, doi: 10.1007/978-1-4939-6581-6\_1.
- [184] O. P. Joffre, E. Segura, A. Savina, and S. Amigorena, "Cross-presentation by dendritic cells," (in eng), *Nat Rev Immunol*, vol. 12, no. 8, pp. 557-69, Jul 13 2012, doi: 10.1038/nri3254.
- [185] M. K. Kim *et al.*, "Fc gamma receptors differ in their structural requirements for interaction with the tyrosine kinase Syk in the initial steps of signaling for phagocytosis," (in eng), *Clin Immunol*, vol. 98, no. 1, pp. 125-32, Jan 2001, doi: 10.1006/clim.2000.4955.
- [186] M. A. Mitchell, M. M. Huang, P. Chien, Z. K. Indik, X. Q. Pan, and A. D. Schreiber, "Substitutions and deletions in the cytoplasmic domain of the phagocytic receptor Fc gamma RIIA: effect on receptor tyrosine phosphorylation and phagocytosis," (in eng), *Blood*, vol. 84, no. 6, pp. 1753-9, Sep 15 1994.
- [187] A. L. Hepburn *et al.*, "Both Fcγ and complement receptors mediate transfer of immune complexes from erythrocytes to human macrophages under physiological flow conditions in vitro," (in eng), *Clin Exp Immunol*, vol. 146, no. 1, pp. 133-45, Oct 2006, doi: 10.1111/j.1365-2249.2006.03174.x.

- [188] S. Amigorena and C. Bonnerot, "Fc receptor signaling and trafficking: a connection for antigen processing," (in eng), *Immunol Rev*, vol. 172, pp. 279-84, Dec 1999, doi: 10.1111/j.1600-065x.1999.tb01372.x.
- [189] A. Bergtold, D. D. Desai, A. Gavhane, and R. Clynes, "Cell surface recycling of internalized antigen permits dendritic cell priming of B cells," (in eng), *Immunity*, vol. 23, no. 5, pp. 503-14, Nov 2005, doi: 10.1016/j.immuni.2005.09.013.
- [190] S. Amigorena, J. Salamero, J. Davoust, W. H. Fridman, and C. Bonnerot, "Tyrosine-containing motif that transduces cell activation signals also determines internalization and antigen presentation via type III receptors for IgG," (in eng), *Nature*, vol. 358, no. 6384, pp. 337-41, Jul 23 1992, doi: 10.1038/358337a0.
- [191] H. D. Kay, G. D. Bonnard, W. H. West, and R. B. Herberman, "A functional comparison of human Fc-receptor-bearing lymphocytes active in natural cytotoxicity and antibody-dependent cellular cytotoxicity," (in eng), *J Immunol*, vol. 118, no. 6, pp. 2058-66, Jun 1977.
- [192] E. Vivier, E. Tomasello, M. Baratin, T. Walzer, and S. Ugolini, "Functions of natural killer cells," (in eng), *Nat Immunol*, vol. 9, no. 5, pp. 503-10, May 2008, doi: 10.1038/ni1582.
- [193] C. Lo Nigro, M. Macagno, D. Sangiolo, L. Bertolaccini, M. Aglietta, and M. C. Merlano, "NK-mediated antibody-dependent cell-mediated cytotoxicity in solid tumors: biological evidence and clinical perspectives," (in eng), *Ann Transl Med*, vol. 7, no. 5, p. 105, Mar 2019, doi: 10.21037/atm.2019.01.42.
- [194] P. A. Morel, L. K. Ernst, and D. Metes, "Functional CD32 molecules on human NK cells," (in eng), *Leuk Lymphoma*, vol. 35, no. 1-2, pp. 47-56, Sep 1999, doi: 10.3109/10428199909145704.
- [195] C. A. Dutertre, E. Bonnin-Gélizé, K. Pulford, D. Bourel, W. H. Fridman, and J. L. Teillaud, "A novel subset of NK cells expressing high levels of inhibitory FcγRIIB modulating antibody-dependent function," (in eng), *J Leukoc Biol*, vol. 84, no. 6, pp. 1511-20, Dec 2008, doi: 10.1189/jlb.0608343.
- [196] R. A. Clynes, T. L. Towers, L. G. Presta, and J. V. Ravetch, "Inhibitory Fc receptors modulate in vivo cytotoxicity against tumor targets," (in eng), *Nat Med*, vol. 6, no. 4, pp. 443-6, Apr 2000, doi: 10.1038/74704.
- [197] W. Wang, A. K. Erbe, J. A. Hank, Z. S. Morris, and P. M. Sondel, "NK Cell-Mediated Antibody-Dependent Cellular Cytotoxicity in Cancer Immunotherapy," (in eng), *Front Immunol*, vol. 6, p. 368, 2015, doi: 10.3389/fimmu.2015.00368.
- [198] A. Mócsai, "Diverse novel functions of neutrophils in immunity, inflammation, and beyond," (in eng), *J Exp Med*, vol. 210, no. 7, pp. 1283-99, Jul 1 2013, doi: 10.1084/jem.20122220.
- [199] V. Brinkmann *et al.*, "Neutrophil extracellular traps kill bacteria," (in eng), *Science*, vol. 303, no. 5663, pp. 1532-5, Mar 5 2004, doi: 10.1126/science.1092385.
- [200] B. G. Yipp *et al.*, "Infection-induced NETosis is a dynamic process involving neutrophil multitasking in vivo," (in eng), *Nat Med*, vol. 18, no. 9, pp. 1386-93, Sep 2012, doi: 10.1038/nm.2847.
- [201] K. Futosi, S. Fodor, and A. Mócsai, "Neutrophil cell surface receptors and their intracellular signal transduction pathways," (in eng), *Int Immunopharmacol*, vol. 17, no. 3, pp. 638-50, Nov 2013, doi: 10.1016/j.intimp.2013.06.034.
- [202] M. J. Zhou, D. M. Lublin, D. C. Link, and E. J. Brown, "Distinct tyrosine kinase activation and Triton X-100 insolubility upon Fc γRII or Fc γRIIIB ligation in human polymorphonuclear leukocytes. Implications for immune complex activation of the respiratory burst," (in eng), *J Biol Chem*, vol. 270, no. 22, pp. 13553-60, Jun 2 1995, doi: 10.1074/jbc.270.22.13553.
- [203] Z. Jakus, T. Németh, J. S. Verbeek, and A. Mócsai, "Critical but overlapping role of FcγRIII and FcγRIV in activation of murine neutrophils by immobilized immune complexes," (in eng), *J Immunol*, vol. 180, no. 1, pp. 618-29, Jan 1 2008, doi: 10.4049/jimmunol.180.1.618.

- [204] S. K. Panda *et al.*, "IL-4 controls activated neutrophil FcγR2b expression and migration into inflamed joints," (in eng), *Proc Natl Acad Sci U S A*, vol. 117, no. 6, pp. 3103-3113, Feb 11 2020, doi: 10.1073/pnas.1914186117.
- [205] L. Pricop *et al.*, "Differential modulation of stimulatory and inhibitory Fc gamma receptors on human monocytes by Th1 and Th2 cytokines," (in eng), *J Immunol*, vol. 166, no. 1, pp. 531-7, Jan 1 2001, doi: 10.4049/jimmunol.166.1.531.
- [206] S. Bolland and J. V. Ravetch, "Inhibitory pathways triggered by ITIM-containing receptors," (in eng), *Adv Immunol*, vol. 72, pp. 149-77, 1999, doi: 10.1016/s0065-2776(08)60019-x.
- [207] O. Malbec *et al.*, "Fc epsilon receptor I-associated lyn-dependent phosphorylation of Fc gamma receptor IIB during negative regulation of mast cell activation," (in eng), *J Immunol*, vol. 160, no. 4, pp. 1647-58, Feb 15 1998.
- [208] S. J. Tzeng, S. Bolland, K. Inabe, T. Kurosaki, and S. K. Pierce, "The B cell inhibitory Fc receptor triggers apoptosis by a novel c-Abl family kinase-dependent pathway," (in eng), *J Biol Chem*, vol. 280, no. 42, pp. 35247-54, Oct 21 2005, doi: 10.1074/jbc.M505308200.
- [209] T. Takai, M. Ono, M. Hikida, H. Ohmori, and J. V. Ravetch, "Augmented humoral and anaphylactic responses in Fc gamma RII-deficient mice," (in eng), *Nature*, vol. 379, no. 6563, pp. 346-9, Jan 25 1996, doi: 10.1038/379346a0.
- [210] M. C. Blank *et al.*, "Decreased transcription of the human FCGR2B gene mediated by the -343 G/C promoter polymorphism and association with systemic lupus erythematosus," (in eng), *Hum Genet*, vol. 117, no. 2-3, pp. 220-7, Jul 2005, doi: 10.1007/s00439-005-1302-3.
- [211] A. Regnault *et al.*, "Fcγ receptor-mediated induction of dendritic cell maturation and major histocompatibility complex class I-restricted antigen presentation after immune complex internalization," (in eng), *J Exp Med*, vol. 189, no. 2, pp. 371-80, Jan 18 1999, doi: 10.1084/jem.189.2.371.
- [212] A. M. Boruchov, G. Heller, M. C. Veri, E. Bonvini, J. V. Ravetch, and J. W. Young, "Activating and inhibitory IgG Fc receptors on human DCs mediate opposing functions," (in eng), *J Clin Invest*, vol. 115, no. 10, pp. 2914-23, Oct 2005, doi: 10.1172/jci24772.
- [213] K. M. Dhodapkar *et al.*, "Selective blockade of inhibitory Fcγ receptor enables human dendritic cell maturation with IL-12p70 production and immunity to antibody-coated tumor cells," (in eng), *Proc Natl Acad Sci U S A*, vol. 102, no. 8, pp. 2910-5, Feb 22 2005, doi: 10.1073/pnas.0500014102.
- [214] I. Frank and H. M. Friedman, "A novel function of the herpes simplex virus type 1 Fc receptor: participation in bipolar bridging of antiviral immunoglobulin G," (in eng), *J Virol*, vol. 63, no. 11, pp. 4479-88, Nov 1989, doi: 10.1128/jvi.63.11.4479-4488.1989.
- [215] E. R. Sprague, C. Wang, D. Baker, and P. J. Bjorkman, "Crystal structure of the HSV-1 Fc receptor bound to Fc reveals a mechanism for antibody bipolar bridging," (in eng), *PLoS Biol*, vol. 4, no. 6, p. e148, Jun 2006, doi: 10.1371/journal.pbio.0040148.
- [216] E. R. Sprague *et al.*, "The human cytomegalovirus Fc receptor gp68 binds the Fc CH2-CH3 interface of immunoglobulin G," (in eng), *J Virol*, vol. 82, no. 7, pp. 3490-9, Apr 2008, doi: 10.1128/jvi.01476-07.
- [217] E. Corrales-Aguilar *et al.*, "Human cytomegalovirus Fcγ binding proteins gp34 and gp68 antagonize Fcγ receptors I, II and III," (in eng), *PLoS Pathog*, vol. 10, no. 5, p. e1004131, May 2014, doi: 10.1371/journal.ppat.1004131.
- [218] R. Atalay *et al.*, "Identification and expression of human cytomegalovirus transcription units coding for two distinct Fcγ receptor homologs," (in eng), *J Virol*, vol. 76, no. 17, pp. 8596-608, Sep 2002, doi: 10.1128/jvi.76.17.8596-8608.2002.
- [219] B. N. Lilley, H. L. Ploegh, and R. S. Tirabassi, "Human cytomegalovirus open reading frame TRL11/IRL11 encodes an immunoglobulin G Fc-binding protein," (in eng), *J Virol*, vol. 75, no. 22, pp. 11218-21, Nov 2001, doi: 10.1128/jvi.75.22.11218-11221.2001.

- [220] G. Dubin, E. Socolof, I. Frank, and H. M. Friedman, "Herpes simplex virus type 1 Fc receptor protects infected cells from antibody-dependent cellular cytotoxicity," (in eng), *J Virol*, vol. 65, no. 12, pp. 7046-50, Dec 1991, doi: 10.1128/jvi.65.12.7046-7050.1991.
- [221] P. Kolb *et al.*, "Human cytomegalovirus antagonizes activation of Fcγ receptors by distinct and synergizing modes of IgG manipulation," (in eng), *Elife*, vol. 10, Mar 16 2021, doi: 10.7554/eLife.63877.
- [222] K. W. Dowler and R. W. Veltri, "In vitro neutralization of HSV-2: inhibition by binding of normal IgG and purified Fc to virion Fc receptor (FcR)," (in eng), *J Med Virol*, vol. 13, no. 3, pp. 251-9, 1984, doi: 10.1002/jmv.1890130307.
- [223] R. L. Shields *et al.*, "High resolution mapping of the binding site on human IgG1 for Fc gamma RI, Fc gamma RII, Fc gamma RIII, and FcRn and design of IgG1 variants with improved binding to the Fc gamma R," (in eng), *J Biol Chem*, vol. 276, no. 9, pp. 6591-604, Mar 2 2001, doi: 10.1074/jbc.M009483200.
- [224] F. Nimmerjahn and J. V. Ravetch, "FcγRs in health and disease," (in eng), *Curr Top Microbiol Immunol*, vol. 350, pp. 105-25, 2011, doi: 10.1007/82\_2010\_86.
- [225] A. M. Chenoweth, B. D. Wines, J. C. Anania, and P. Mark Hogarth, "Harnessing the immune system via FcγR function in immune therapy: a pathway to next-gen mAbs," (in eng), *Immunol Cell Biol*, vol. 98, no. 4, pp. 287-304, Apr 2020, doi: 10.1111/imcb.12326.
- [226] P. Bruhns *et al.*, "Specificity and affinity of human Fcγ receptors and their polymorphic variants for human IgG subclasses," (in eng), *Blood*, vol. 113, no. 16, pp. 3716-25, Apr 16 2009, doi: 10.1182/blood-2008-09-179754.
- [227] R. Wada, M. Matsui, and N. Kawasaki, "Influence of N-glycosylation on effector functions and thermal stability of glycoengineered IgG1 monoclonal antibody with homogeneous glycoforms," (in eng), *MABs*, vol. 11, no. 2, pp. 350-372, Feb/Mar 2019, doi: 10.1080/19420862.2018.1551044.
- [228] G. Dekkers *et al.*, "Decoding the Human Immunoglobulin G-Glycan Repertoire Reveals a Spectrum of Fc-Receptor- and Complement-Mediated-Effector Activities," (in eng), *Front Immunol*, vol. 8, p. 877, 2017, doi: 10.3389/fimmu.2017.00877.
- [229] J. M. Hayes *et al.*, "Identification of Fc Gamma Receptor Glycoforms That Produce Differential Binding Kinetics for Rituximab," (in eng), *Mol Cell Proteomics*, vol. 16, no. 10, pp. 1770-1788, Oct 2017, doi: 10.1074/mcp.M117.066944.
- [230] G. P. Subedi, D. J. Falconer, and A. W. Barb, "Carbohydrate-Polypeptide Contacts in the Antibody Receptor CD16A Identified through Solution NMR Spectroscopy," (in eng), *Biochemistry*, vol. 56, no. 25, pp. 3174-3177, Jun 27 2017, doi: 10.1021/acs.biochem.7b00392.
- [231] D. Bharadwaj, M. P. Stein, M. Volzer, C. Mold, and T. W. Du Clos, "The major receptor for C-reactive protein on leukocytes is fcgamma receptor II," (in eng), *J Exp Med*, vol. 190, no. 4, pp. 585-90, Aug 16 1999, doi: 10.1084/jem.190.4.585.
- [232] J. Lu, L. L. Marnell, K. D. Marjon, C. Mold, T. W. Du Clos, and P. D. Sun, "Structural recognition and functional activation of FcγR by innate pentraxins," (in eng), *Nature*, vol. 456, no. 7224, pp. 989-92, Dec 18 2008, doi: 10.1038/nature07468.
- [233] L. Deban, S. Jaillon, C. Garlanda, B. Bottazzi, and A. Mantovani, "Pentraxins in innate immunity: lessons from PTX3," (in eng), *Cell Tissue Res*, vol. 343, no. 1, pp. 237-49, Jan 2011, doi: 10.1007/s00441-010-1018-0.
- [234] J. Lu, C. Mold, T. W. Du Clos, and P. D. Sun, "Pentraxins and Fc Receptor-Mediated Immune Responses," (in eng), *Front Immunol*, vol. 9, p. 2607, 2018, doi: 10.3389/fimmu.2018.02607.
- [235] L. L. Marnell, C. Mold, M. A. Volzer, R. W. Burlingame, and T. W. Du Clos, "C-reactive protein binds to Fc gamma RI in transfected COS cells," (in eng), *J Immunol*, vol. 155, no. 4, pp. 2185-93, Aug 15 1995.
- [236] M. P. Stein *et al.*, "C-reactive protein binding to FcγRIIIa on human monocytes and neutrophils is allele-specific," (in eng), *J Clin Invest*, vol. 105, no. 3, pp. 369-76, Feb 2000, doi: 10.1172/jci7817.

- [237] R. V. Jimenez, T. T. Wright, N. R. Jones, J. Wu, A. W. Gibson, and A. J. Szalai, "C-Reactive Protein Impairs Dendritic Cell Development, Maturation, and Function: Implications for Peripheral Tolerance," (in eng), *Front Immunol*, vol. 9, p. 372, 2018, doi: 10.3389/fimmu.2018.00372.
- [238] N. Cox, D. Pilling, and R. H. Gomer, "Serum amyloid P: a systemic regulator of the innate immune response," (in eng), *J Leukoc Biol*, vol. 96, no. 5, pp. 739-43, Nov 2014, doi: 10.1189/jlb.1MR0114-068R.
- [239] D. Perez-Bercoff, A. David, H. Sudry, F. Barré-Sinoussi, and G. Pancino, "Fcγ receptor-mediated suppression of human immunodeficiency virus type 1 replication in primary human macrophages," (in eng), *J Virol*, vol. 77, no. 7, pp. 4081-94, Apr 2003, doi: 10.1128/jvi.77.7.4081-4094.2003.
- [240] M. Cota *et al.*, "Selective inhibition of HIV replication in primary macrophages but not T lymphocytes by macrophage-derived chemokine," (in eng), *Proc Natl Acad Sci U S A*, vol. 97, no. 16, pp. 9162-7, Aug 1 2000, doi: 10.1073/pnas.160359197.
- [241] A. Bergamaschi, A. David, E. Le Rouzic, S. Nisole, F. Barré-Sinoussi, and G. Pancino, "The CDK inhibitor p21Cip1/WAF1 is induced by FcγR activation and restricts the replication of human immunodeficiency virus type 1 and related primate lentiviruses in human macrophages," (in eng), *J Virol*, vol. 83, no. 23, pp. 12253-65, Dec 2009, doi: 10.1128/jvi.01395-09.
- [242] J. Zhang, D. T. Scadden, and C. S. Crumpacker, "Primitive hematopoietic cells resist HIV-1 infection via p21," (in eng), *J Clin Invest*, vol. 117, no. 2, pp. 473-81, Feb 2007, doi: 10.1172/jci28971.
- [243] D. N. Forthal, G. Landucci, J. Bream, L. P. Jacobson, T. B. Phan, and B. Montoya, "FcγRIIIa genotype predicts progression of HIV infection," (in eng), *J Immunol*, vol. 179, no. 11, pp. 7916-23, Dec 1 2007, doi: 10.4049/jimmunol.179.11.7916.
- [244] D. N. Forthal, P. B. Gilbert, G. Landucci, and T. Phan, "Recombinant gp120 vaccine-induced antibodies inhibit clinical strains of HIV-1 in the presence of Fc receptor-bearing effector cells and correlate inversely with HIV infection rate," (in eng), *J Immunol*, vol. 178, no. 10, pp. 6596-603, May 15 2007, doi: 10.4049/jimmunol.178.10.6596.
- [245] K. C. Brouwer *et al.*, "Polymorphism of Fc receptor IIa for IgG in infants is associated with susceptibility to perinatal HIV-1 infection," (in eng), *Aids*, vol. 18, no. 8, pp. 1187-94, May 21 2004, doi: 10.1097/00002030-200405210-00012.
- [246] K. C. Brouwer *et al.*, "Polymorphism of Fc receptor IIa for immunoglobulin G is associated with placental malaria in HIV-1-positive women in western Kenya," (in eng), *J Infect Dis*, vol. 190, no. 6, pp. 1192-8, Sep 15 2004, doi: 10.1086/422850.
- [247] D. N. Forthal, E. E. Gabriel, A. Wang, G. Landucci, and T. B. Phan, "Association of Fcγ receptor IIIa genotype with the rate of HIV infection after gp120 vaccination," (in eng), *Blood*, vol. 120, no. 14, pp. 2836-42, Oct 4 2012, doi: 10.1182/blood-2012-05-431361.
- [248] B. A. Vance, T. W. Huizinga, K. Wardwell, and P. M. Guyre, "Binding of monomeric human IgG defines an expression polymorphism of Fc γRIII on large granular lymphocyte/natural killer cells," (in eng), *J Immunol*, vol. 151, no. 11, pp. 6429-39, Dec 1 1993.
- [249] T. Brown, "Observations by immunofluorescence microscopy and electron microscopy on the cytopathogenicity of *Naegleria fowleri* in mouse embryo-cell cultures," (in eng), *J Med Microbiol*, vol. 12, no. 3, pp. 363-71, Aug 1979, doi: 10.1099/00222615-12-3-363.
- [250] K. S. Ralston, M. D. Solga, N. M. Mackey-Lawrence, Somlata, A. Bhattacharya, and W. A. Petri, Jr., "Trogoncytosis by *Entamoeba histolytica* contributes to cell killing and tissue invasion," (in eng), *Nature*, vol. 508, no. 7497, pp. 526-30, Apr 24 2014, doi: 10.1038/nature13242.
- [251] D. R. Waddell and G. Vogel, "Phagocytic behavior of the predatory slime mold, *Dictyostelium caveatum*. Cell nibbling," (in eng), *Exp Cell Res*, vol. 159, no. 2, pp. 323-34, Aug 1985, doi: 10.1016/s0014-4827(85)80006-9.

- [252] D. G. Osborne and S. A. Wetzel, "Trogoctosis results in sustained intracellular signaling in CD4(+) T cells," (in eng), *J Immunol*, vol. 189, no. 10, pp. 4728-39, Nov 15 2012, doi: 10.4049/jimmunol.1201507.
- [253] S. A. Wetzel, T. W. McKeithan, and D. C. Parker, "Peptide-specific intercellular transfer of MHC class II to CD4+ T cells directly from the immunological synapse upon cellular dissociation," (in eng), *J Immunol*, vol. 174, no. 1, pp. 80-9, Jan 1 2005, doi: 10.4049/jimmunol.174.1.80.
- [254] D. Hudrisier, J. Riond, H. Mazarguil, J. E. Gairin, and E. Joly, "Cutting edge: CTLs rapidly capture membrane fragments from target cells in a TCR signaling-dependent manner," (in eng), *J Immunol*, vol. 166, no. 6, pp. 3645-9, Mar 15 2001, doi: 10.4049/jimmunol.166.6.3645.
- [255] J. F. Huang *et al.*, "TCR-Mediated internalization of peptide-MHC complexes acquired by T cells," (in eng), *Science*, vol. 286, no. 5441, pp. 952-4, Oct 29 1999, doi: 10.1126/science.286.5441.952.
- [256] F. D. Batista, D. Iber, and M. S. Neuberger, "B cells acquire antigen from target cells after synapse formation," (in eng), *Nature*, vol. 411, no. 6836, pp. 489-94, May 24 2001, doi: 10.1038/35078099.
- [257] D. P. Schafer *et al.*, "Microglia sculpt postnatal neural circuits in an activity and complement-dependent manner," (in eng), *Neuron*, vol. 74, no. 4, pp. 691-705, May 24 2012, doi: 10.1016/j.neuron.2012.03.026.
- [258] L. Weinhard *et al.*, "Microglia remodel synapses by presynaptic trogoctosis and spine head filopodia induction," (in eng), *Nat Commun*, vol. 9, no. 1, p. 1228, Mar 26 2018, doi: 10.1038/s41467-018-03566-5.
- [259] Y. Abdu, C. Maniscalco, J. M. Heddleston, T. L. Chew, and J. Nance, "Developmentally programmed germ cell remodelling by endodermal cell cannibalism," (in eng), *Nat Cell Biol*, vol. 18, no. 12, pp. 1302-1310, Dec 2016, doi: 10.1038/ncb3439.
- [260] M. Nakayama, K. Takeda, M. Kawano, T. Takai, N. Ishii, and K. Ogasawara, "Natural killer (NK)-dendritic cell interactions generate MHC class II-dressed NK cells that regulate CD4+ T cells," (in eng), *Proc Natl Acad Sci U S A*, vol. 108, no. 45, pp. 18360-5, Nov 8 2011, doi: 10.1073/pnas.1110584108.
- [261] J. Zhou, Y. Tagaya, R. Tolouei-Semnani, J. Schlom, and H. Sabzevari, "Physiological relevance of antigen presentosome (APS), an acquired MHC/costimulatory complex, in the sustained activation of CD4+ T cells in the absence of APCs," (in eng), *Blood*, vol. 105, no. 8, pp. 3238-46, Apr 15 2005, doi: 10.1182/blood-2004-08-3236.
- [262] J. Reed and S. A. Wetzel, "Trogoctosis-Mediated Intracellular Signaling in CD4(+) T Cells Drives T(H)2-Associated Effector Cytokine Production and Differentiation," (in eng), *J Immunol*, vol. 202, no. 10, pp. 2873-2887, May 15 2019, doi: 10.4049/jimmunol.1801577.
- [263] P. Gu, J. F. Gao, C. A. D'Souza, A. Kowalczyk, K. Y. Chou, and L. Zhang, "Trogoctosis of CD80 and CD86 by induced regulatory T cells," (in eng), *Cell Mol Immunol*, vol. 9, no. 2, pp. 136-46, Mar 2012, doi: 10.1038/cmi.2011.62.
- [264] J. LeMaout *et al.*, "Immune regulation by pretenders: cell-to-cell transfers of HLA-G make effector T cells act as regulatory cells," (in eng), *Blood*, vol. 109, no. 5, pp. 2040-8, Mar 1 2007, doi: 10.1182/blood-2006-05-024547.
- [265] M. S. Ford McIntyre, K. J. Young, J. Gao, B. Joe, and L. Zhang, "Cutting edge: in vivo trogoctosis as a mechanism of double negative regulatory T cell-mediated antigen-specific suppression," (in eng), *J Immunol*, vol. 181, no. 4, pp. 2271-5, Aug 15 2008, doi: 10.4049/jimmunol.181.4.2271.
- [266] F. M. Griffin, Jr., J. A. Griffin, and S. C. Silverstein, "Studies on the mechanism of phagocytosis. II. The interaction of macrophages with anti-immunoglobulin IgG-coated bone marrow-derived lymphocytes," (in eng), *J Exp Med*, vol. 144, no. 3, pp. 788-809, Sep 1 1976, doi: 10.1084/jem.144.3.788.

- [267] S. T. Lee and F. Paraskevas, "Macrophage--T cell interactions. I. The uptake by T cells of Fc receptors released from macrophages," (in eng), *Cell Immunol*, vol. 40, no. 1, pp. 141-53, Sep 15 1978, doi: 10.1016/0008-8749(78)90322-2.
- [268] J. Ritz *et al.*, "Serotherapy of acute lymphoblastic leukemia with monoclonal antibody," (in eng), *Blood*, vol. 58, no. 1, pp. 141-52, Jul 1981.
- [269] L. M. Nadler *et al.*, "Serotherapy of a patient with a monoclonal antibody directed against a human lymphoma-associated antigen," (in eng), *Cancer Res*, vol. 40, no. 9, pp. 3147-54, Sep 1980.
- [270] J. H. Bertram *et al.*, "Monoclonal antibody T101 in T cell malignancies: a clinical, pharmacokinetic, and immunologic correlation," (in eng), *Blood*, vol. 68, no. 3, pp. 752-61, Sep 1986.
- [271] P. Carter, "Improving the efficacy of antibody-based cancer therapies," (in eng), *Nat Rev Cancer*, vol. 1, no. 2, pp. 118-29, Nov 2001, doi: 10.1038/35101072.
- [272] M. Stern and R. Herrmann, "Overview of monoclonal antibodies in cancer therapy: present and promise," (in eng), *Crit Rev Oncol Hematol*, vol. 54, no. 1, pp. 11-29, Apr 2005, doi: 10.1016/j.critrevonc.2004.10.011.
- [273] R. Gruber, E. Holz, and G. Riethmüller, "Monoclonal antibodies in cancer therapy," (in eng), *Springer Semin Immunopathol*, vol. 18, no. 2, pp. 243-51, 1996, doi: 10.1007/bf00820669.
- [274] M. J. Glennie and P. W. Johnson, "Clinical trials of antibody therapy," (in eng), *Immunol Today*, vol. 21, no. 8, pp. 403-10, Aug 2000, doi: 10.1016/s0167-5699(00)01669-8.
- [275] K. Jurianz *et al.*, "Complement resistance of tumor cells: basal and induced mechanisms," (in eng), *Mol Immunol*, vol. 36, no. 13-14, pp. 929-39, Sep-Oct 1999, doi: 10.1016/s0161-5890(99)00115-7.
- [276] P. Johnson and M. Glennie, "The mechanisms of action of rituximab in the elimination of tumor cells," (in eng), *Semin Oncol*, vol. 30, no. 1 Suppl 2, pp. 3-8, Feb 2003, doi: 10.1053/sonc.2003.50025.
- [277] N. Di Gaetano *et al.*, "Complement activation determines the therapeutic activity of rituximab in vivo," (in eng), *J Immunol*, vol. 171, no. 3, pp. 1581-7, Aug 1 2003, doi: 10.4049/jimmunol.171.3.1581.
- [278] Z. Fishelson, N. Donin, S. Zell, S. Schultz, and M. Kirschfink, "Obstacles to cancer immunotherapy: expression of membrane complement regulatory proteins (mCRPs) in tumors," (in eng), *Mol Immunol*, vol. 40, no. 2-4, pp. 109-23, Sep 2003, doi: 10.1016/s0161-5890(03)00112-3.
- [279] F. Hong *et al.*, "Mechanism by which orally administered beta-1,3-glucans enhance the tumoricidal activity of antitumor monoclonal antibodies in murine tumor models," (in eng), *J Immunol*, vol. 173, no. 2, pp. 797-806, Jul 15 2004, doi: 10.4049/jimmunol.173.2.797.
- [280] J. L. Teeling *et al.*, "Characterization of new human CD20 monoclonal antibodies with potent cytolytic activity against non-Hodgkin lymphomas," (in eng), *Blood*, vol. 104, no. 6, pp. 1793-800, Sep 15 2004, doi: 10.1182/blood-2004-01-0039.
- [281] R. P. Taylor, "Use of biological response modifiers to enhance the action of Rituximab," (in eng), *Leuk Res*, vol. 29, no. 6, pp. 599-600, Jun 2005, doi: 10.1016/j.leukres.2004.12.014.
- [282] F. J. Hernandez-Ilizaliturri *et al.*, "Neutrophils contribute to the biological antitumor activity of rituximab in a non-Hodgkin's lymphoma severe combined immunodeficiency mouse model," (in eng), *Clin Cancer Res*, vol. 9, no. 16 Pt 1, pp. 5866-73, Dec 1 2003.
- [283] J. Uchida *et al.*, "The innate mononuclear phagocyte network depletes B lymphocytes through Fc receptor-dependent mechanisms during anti-CD20 antibody immunotherapy," (in eng), *J Exp Med*, vol. 199, no. 12, pp. 1659-69, Jun 21 2004, doi: 10.1084/jem.20040119.
- [284] Y. Hamaguchi *et al.*, "The peritoneal cavity provides a protective niche for B1 and conventional B lymphocytes during anti-CD20 immunotherapy in mice," (in eng), *J Immunol*, vol. 174, no. 7, pp. 4389-99, Apr 1 2005, doi: 10.4049/jimmunol.174.7.4389.

- [285] N. L. Letvin *et al.*, "In vivo administration of lymphocyte-specific monoclonal antibodies in nonhuman primates: I. Effects of anti-T11 antibodies on the circulating T cell pool," (in eng), *Blood*, vol. 66, no. 4, pp. 961-6, Oct 1985.
- [286] R. A. Miller, D. G. Maloney, J. McKillop, and R. Levy, "In vivo effects of murine hybridoma monoclonal antibody in a patient with T-cell leukemia," (in eng), *Blood*, vol. 58, no. 1, pp. 78-86, Jul 1981.
- [287] P. V. Beum, A. D. Kennedy, M. E. Williams, M. A. Lindorfer, and R. P. Taylor, "The shaving reaction: rituximab/CD20 complexes are removed from mantle cell lymphoma and chronic lymphocytic leukemia cells by THP-1 monocytes," (in eng), *J Immunol*, vol. 176, no. 4, pp. 2600-9, Feb 15 2006, doi: 10.4049/jimmunol.176.4.2600.
- [288] P. V. Beum, D. A. Mack, A. W. Pawluczko, M. A. Lindorfer, and R. P. Taylor, "Binding of rituximab, trastuzumab, cetuximab, or mAb T101 to cancer cells promotes trogocytosis mediated by THP-1 cells and monocytes," (in eng), *J Immunol*, vol. 181, no. 11, pp. 8120-32, Dec 1 2008, doi: 10.4049/jimmunol.181.11.8120.
- [289] E. A. Rossi, D. M. Goldenberg, R. Michel, D. L. Rossi, D. J. Wallace, and C. H. Chang, "Trogocytosis of multiple B-cell surface markers by CD22 targeting with epratuzumab," (in eng), *Blood*, vol. 122, no. 17, pp. 3020-9, Oct 24 2013, doi: 10.1182/blood-2012-12-473744.
- [290] P. Boross, J. H. Jansen, A. Pastula, C. E. van der Poel, and J. H. Leusen, "Both activating and inhibitory Fc gamma receptors mediate rituximab-induced trogocytosis of CD20 in mice," (in eng), *Immunol Lett*, vol. 143, no. 1, pp. 44-52, Mar 30 2012, doi: 10.1016/j.imlet.2012.01.004.
- [291] T. Pham, P. Mero, and J. W. Booth, "Dynamics of macrophage trogocytosis of rituximab-coated B cells," (in eng), *PLoS One*, vol. 6, no. 1, p. e14498, Jan 17 2011, doi: 10.1371/journal.pone.0014498.
- [292] Y. Zhang *et al.*, "Daclizumab reduces CD25 levels on T cells through monocyte-mediated trogocytosis," (in eng), *Mult Scler*, vol. 20, no. 2, pp. 156-64, Feb 2014, doi: 10.1177/1352458513494488.
- [293] S. Masuda *et al.*, "Mechanism of Fcγ receptor-mediated trogocytosis-based false-positive results in flow cytometry," (in eng), *PLoS One*, vol. 7, no. 12, p. e52918, 2012, doi: 10.1371/journal.pone.0052918.
- [294] S. Iwasaki *et al.*, "Plasma-dependent, antibody- and Fcγ receptor-mediated translocation of CD8 molecules from T cells to monocytes," (in eng), *Cytometry A*, vol. 79, no. 1, pp. 46-56, Jan 2011, doi: 10.1002/cyto.a.20984.
- [295] S. Daubeuf, M. A. Lindorfer, R. P. Taylor, E. Joly, and D. Hudrisier, "The direction of plasma membrane exchange between lymphocytes and accessory cells by trogocytosis is influenced by the nature of the accessory cell," (in eng), *J Immunol*, vol. 184, no. 4, pp. 1897-908, Feb 15 2010, doi: 10.4049/jimmunol.0901570.
- [296] T. He *et al.*, "Bidirectional membrane molecule transfer between dendritic and T cells," (in eng), *Biochem Biophys Res Commun*, vol. 359, no. 2, pp. 202-8, Jul 27 2007, doi: 10.1016/j.bbrc.2007.05.099.
- [297] D. Hudrisier *et al.*, "Ligand binding but undetected functional response of FcR after their capture by T cells via trogocytosis," (in eng), *J Immunol*, vol. 183, no. 10, pp. 6102-13, Nov 15 2009, doi: 10.4049/jimmunol.0900821.
- [298] D. Hudrisier, A. Aucher, A. L. Puaux, C. Bordier, and E. Joly, "Capture of target cell membrane components via trogocytosis is triggered by a selected set of surface molecules on T or B cells," (in eng), *J Immunol*, vol. 178, no. 6, pp. 3637-47, Mar 15 2007, doi: 10.4049/jimmunol.178.6.3637.
- [299] H. L. Matlung *et al.*, "Neutrophils Kill Antibody-Opsonized Cancer Cells by Trogoptosis," (in eng), *Cell Rep*, vol. 23, no. 13, pp. 3946-3959.e6, Jun 26 2018, doi: 10.1016/j.celrep.2018.05.082.
- [300] R. Velmurugan, D. K. Challa, S. Ram, R. J. Ober, and E. S. Ward, "Macrophage-Mediated Trogocytosis Leads to Death of Antibody-Opsonized Tumor Cells," (in eng), *Mol Cancer Ther*, vol. 15, no. 8, pp. 1879-89, Aug 2016, doi: 10.1158/1535-7163.Mct-15-0335.

- [301] S. Masuda, S. Iwasaki, U. Tomaru, T. Baba, K. Katsumata, and A. Ishizu, "Possible implication of Fc  $\gamma$  receptor-mediated trogocytosis in susceptibility to systemic autoimmune disease," (in eng), *Clin Dev Immunol*, vol. 2013, p. 345745, 2013, doi: 10.1155/2013/345745.
- [302] W. H. Organization. "The Global Health Observatory-Themes-HIV." <https://www.who.int/data/gho/data/themes/hiv-aids> (accessed 09.03.2023, 2023).
- [303] B. Müller, M. Anders, and J. Reinstein, "In vitro analysis of human immunodeficiency virus particle dissociation: gag proteolytic processing influences dissociation kinetics," (in eng), *PLoS One*, vol. 9, no. 6, p. e99504, 2014, doi: 10.1371/journal.pone.0099504.
- [304] M. Albanese *et al.*, "Rapid, efficient and activation-neutral gene editing of polyclonal primary human resting CD4(+) T cells allows complex functional analyses," (in eng), *Nat Methods*, vol. 19, no. 1, pp. 81-89, Jan 2022, doi: 10.1038/s41592-021-01328-8.
- [305] S. M. Dillon *et al.*, "HIV-1 infection of human intestinal lamina propria CD4+ T cells in vitro is enhanced by exposure to commensal Escherichia coli," (in eng), *J Immunol*, vol. 189, no. 2, pp. 885-96, Jul 15 2012, doi: 10.4049/jimmunol.1200681.
- [306] A. K. Steele *et al.*, "Microbial exposure alters HIV-1-induced mucosal CD4+ T cell death pathways Ex vivo," (in eng), *Retrovirology*, vol. 11, p. 14, Feb 4 2014, doi: 10.1186/1742-4690-11-14.
- [307] M. Strazza, I. Azoulay-Alfaguter, A. Pedoeem, and A. Mor, "Static adhesion assay for the study of integrin activation in T lymphocytes," (in eng), *J Vis Exp*, no. 88, Jun 13 2014, doi: 10.3791/51646.
- [308] J. Vermeire *et al.*, "Quantification of reverse transcriptase activity by real-time PCR as a fast and accurate method for titration of HIV, lenti- and retroviral vectors," (in eng), *PLoS One*, vol. 7, no. 12, p. e50859, 2012, doi: 10.1371/journal.pone.0050859.
- [309] M. Cavrois, J. Neidleman, and W. C. Greene, "HIV-1 Fusion Assay," (in eng), *Bio Protoc*, vol. 4, no. 16, Aug 20 2014, doi: 10.21769/bioprotoc.1212.
- [310] J. A. Horwitz *et al.*, "Non-neutralizing Antibodies Alter the Course of HIV-1 Infection In Vivo," (in eng), *Cell*, vol. 170, no. 4, pp. 637-648.e10, Aug 10 2017, doi: 10.1016/j.cell.2017.06.048.
- [311] D. N. Levy, G. M. Aldrovandi, O. Kutsch, and G. M. Shaw, "Dynamics of HIV-1 recombination in its natural target cells," (in eng), *Proc Natl Acad Sci U S A*, vol. 101, no. 12, pp. 4204-9, Mar 23 2004, doi: 10.1073/pnas.0306764101.
- [312] S. I. Richardson, C. Crowther, N. N. Mkhize, and L. Morris, "Measuring the ability of HIV-specific antibodies to mediate trogocytosis," (in eng), *J Immunol Methods*, vol. 463, pp. 71-83, Dec 2018, doi: 10.1016/j.jim.2018.09.009.
- [313] J. P. Moore, Y. Cao, J. Leu, L. Qin, B. Korber, and D. D. Ho, "Inter- and intraclade neutralization of human immunodeficiency virus type 1: genetic clades do not correspond to neutralization serotypes but partially correspond to gp120 antigenic serotypes," (in eng), *J Virol*, vol. 70, no. 1, pp. 427-44, Jan 1996, doi: 10.1128/jvi.70.1.427-444.1996.
- [314] C. Moog, H. J. Fleury, I. Pellegrin, A. Kirn, and A. M. Aubertin, "Autologous and heterologous neutralizing antibody responses following initial seroconversion in human immunodeficiency virus type 1-infected individuals," (in eng), *J Virol*, vol. 71, no. 5, pp. 3734-41, May 1997, doi: 10.1128/jvi.71.5.3734-3741.1997.
- [315] E. S. Gray *et al.*, "Neutralizing antibody responses in acute human immunodeficiency virus type 1 subtype C infection," (in eng), *J Virol*, vol. 81, no. 12, pp. 6187-96, Jun 2007, doi: 10.1128/jvi.00239-07.
- [316] B. F. Haynes *et al.*, "Cardiolipin polyspecific autoreactivity in two broadly neutralizing HIV-1 antibodies," (in eng), *Science*, vol. 308, no. 5730, pp. 1906-8, Jun 24 2005, doi: 10.1126/science.1111781.
- [317] B. F. Haynes, M. A. Moody, L. Verkoczy, G. Kelsoe, and S. M. Alam, "Antibody polyspecificity and neutralization of HIV-1: a hypothesis," (in eng), *Hum Antibodies*, vol. 14, no. 3-4, pp. 59-67, 2005.

- [318] E. Falkowska *et al.*, "Broadly neutralizing HIV antibodies define a glycan-dependent epitope on the prefusion conformation of gp41 on cleaved envelope trimers," (in eng), *Immunity*, vol. 40, no. 5, pp. 657-68, May 15 2014, doi: 10.1016/j.immuni.2014.04.009.
- [319] J. M. Hayes *et al.*, "Fc gamma receptor glycosylation modulates the binding of IgG glycoforms: a requirement for stable antibody interactions," (in eng), *J Proteome Res*, vol. 13, no. 12, pp. 5471-85, Dec 5 2014, doi: 10.1021/pr500414q.
- [320] D. Metes, L. K. Ernst, W. H. Chambers, A. Sulica, R. B. Herberman, and P. A. Morel, "Expression of functional CD32 molecules on human NK cells is determined by an allelic polymorphism of the FcgammaRIIC gene," (in eng), *Blood*, vol. 91, no. 7, pp. 2369-80, Apr 1 1998.
- [321] D. J. Katzmann, M. Babst, and S. D. Emr, "Ubiquitin-dependent sorting into the multivesicular body pathway requires the function of a conserved endosomal protein sorting complex, ESCRT-I," (in eng), *Cell*, vol. 106, no. 2, pp. 145-55, Jul 27 2001, doi: 10.1016/s0092-8674(01)00434-2.
- [322] J. Schöneberg, I. H. Lee, J. H. Iwasa, and J. H. Hurley, "Reverse-topology membrane scission by the ESCRT proteins," (in eng), *Nat Rev Mol Cell Biol*, vol. 18, no. 1, pp. 5-17, Jan 2017, doi: 10.1038/nrm.2016.121.
- [323] J. McCullough, L. A. Colf, and W. I. Sundquist, "Membrane fission reactions of the mammalian ESCRT pathway," (in eng), *Annu Rev Biochem*, vol. 82, pp. 663-92, 2013, doi: 10.1146/annurev-biochem-072909-101058.
- [324] M. Radulovic and H. Stenmark, "ESCRTs in membrane sealing," (in eng), *Biochem Soc Trans*, vol. 46, no. 4, pp. 773-778, Aug 20 2018, doi: 10.1042/bst20170435.
- [325] M. Babst, T. K. Sato, L. M. Banta, and S. D. Emr, "Endosomal transport function in yeast requires a novel AAA-type ATPase, Vps4p," (in eng), *Embo j*, vol. 16, no. 8, pp. 1820-31, Apr 15 1997, doi: 10.1093/emboj/16.8.1820.
- [326] M. Babst, D. J. Katzmann, W. B. Snyder, B. Wendland, and S. D. Emr, "Endosome-associated complex, ESCRT-II, recruits transport machinery for protein sorting at the multivesicular body," (in eng), *Dev Cell*, vol. 3, no. 2, pp. 283-9, Aug 2002, doi: 10.1016/s1534-5807(02)00219-8.
- [327] J. G. Carlton and J. Martin-Serrano, "Parallels between cytokinesis and retroviral budding: a role for the ESCRT machinery," (in eng), *Science*, vol. 316, no. 5833, pp. 1908-12, Jun 29 2007, doi: 10.1126/science.1143422.
- [328] J. Votteler and W. I. Sundquist, "Virus budding and the ESCRT pathway," (in eng), *Cell Host Microbe*, vol. 14, no. 3, pp. 232-41, Sep 11 2013, doi: 10.1016/j.chom.2013.08.012.
- [329] L. Ginaldi *et al.*, "Levels of expression of CD52 in normal and leukemic B and T cells: correlation with in vivo therapeutic responses to Campath-1H," (in eng), *Leuk Res*, vol. 22, no. 2, pp. 185-91, Feb 1998, doi: 10.1016/s0145-2126(97)00158-6.
- [330] N. Osuji *et al.*, "CD52 expression in T-cell large granular lymphocyte leukemia--implications for treatment with alemtuzumab," (in eng), *Leuk Lymphoma*, vol. 46, no. 5, pp. 723-7, May 2005, doi: 10.1080/10428190500052156.
- [331] J. A. Cohen *et al.*, "Alemtuzumab versus interferon beta 1a as first-line treatment for patients with relapsing-remitting multiple sclerosis: a randomised controlled phase 3 trial," (in eng), *Lancet*, vol. 380, no. 9856, pp. 1819-28, Nov 24 2012, doi: 10.1016/s0140-6736(12)61769-3.
- [332] A. J. Coles *et al.*, "Alemtuzumab for patients with relapsing multiple sclerosis after disease-modifying therapy: a randomised controlled phase 3 trial," (in eng), *Lancet*, vol. 380, no. 9856, pp. 1829-39, Nov 24 2012, doi: 10.1016/s0140-6736(12)61768-1.
- [333] Y. Hu *et al.*, "Investigation of the mechanism of action of alemtuzumab in a human CD52 transgenic mouse model," (in eng), *Immunology*, vol. 128, no. 2, pp. 260-70, Oct 2009, doi: 10.1111/j.1365-2567.2009.03115.x.
- [334] C. T. Dalgiç, E. N. M. Gökmen, M. Özişik, M. A. Baklan, and N. Yüceyar, "Successful Rapid Drug Desensitization with A Modified Protocol To Alemtuzumab in A Multiple

- Sclerosis Patient with Severe Immediate-Type Hypersensitivity Reaction," (in eng), *Noro Psikiyatr Ars*, vol. 59, no. 3, pp. 237-241, 2022, doi: 10.29399/npa.27371.
- [335] A. Stojanovic, M. P. Correia, and A. Cerwenka, "The NKG2D/NKG2DL Axis in the Crosstalk Between Lymphoid and Myeloid Cells in Health and Disease," (in eng), *Front Immunol*, vol. 9, p. 827, 2018, doi: 10.3389/fimmu.2018.00827.
- [336] M. Cavrois, C. De Noronha, and W. C. Greene, "A sensitive and specific enzyme-based assay detecting HIV-1 virion fusion in primary T lymphocytes," (in eng), *Nat Biotechnol*, vol. 20, no. 11, pp. 1151-4, Nov 2002, doi: 10.1038/nbt745.
- [337] X. Pan, H. M. Baldauf, O. T. Keppler, and O. T. Fackler, "Restrictions to HIV-1 replication in resting CD4+ T lymphocytes," (in eng), *Cell Res*, vol. 23, no. 7, pp. 876-85, Jul 2013, doi: 10.1038/cr.2013.74.
- [338] Z. Zhang *et al.*, "Sexual transmission and propagation of SIV and HIV in resting and activated CD4+ T cells," (in eng), *Science*, vol. 286, no. 5443, pp. 1353-7, Nov 12 1999, doi: 10.1126/science.286.5443.1353.
- [339] T. van Montfort, A. A. Nabatov, T. B. Geijtenbeek, G. Pollakis, and W. A. Paxton, "Efficient capture of antibody neutralized HIV-1 by cells expressing DC-SIGN and transfer to CD4+ T lymphocytes," (in eng), *J Immunol*, vol. 178, no. 5, pp. 3177-85, Mar 1 2007, doi: 10.4049/jimmunol.178.5.3177.
- [340] H. Bouhlal *et al.*, "Opsonization of HIV with complement enhances infection of dendritic cells and viral transfer to CD4 T cells in a CR3 and DC-SIGN-dependent manner," (in eng), *J Immunol*, vol. 178, no. 2, pp. 1086-95, Jan 15 2007, doi: 10.4049/jimmunol.178.2.1086.
- [341] B. Lee *et al.*, "cis Expression of DC-SIGN allows for more efficient entry of human and simian immunodeficiency viruses via CD4 and a coreceptor," (in eng), *J Virol*, vol. 75, no. 24, pp. 12028-38, Dec 2001, doi: 10.1128/jvi.75.24.12028-12038.2001.
- [342] J. T. Monteiro and B. Lepenies, "Myeloid C-Type Lectin Receptors in Viral Recognition and Antiviral Immunity," (in eng), *Viruses*, vol. 9, no. 3, Mar 22 2017, doi: 10.3390/v9030059.
- [343] S. Sarrazin, W. C. Lamanna, and J. D. Esko, "Heparan sulfate proteoglycans," (in eng), *Cold Spring Harb Perspect Biol*, vol. 3, no. 7, Jul 1 2011, doi: 10.1101/cshperspect.a004952.
- [344] R. Germi *et al.*, "Cellular glycosaminoglycans and low density lipoprotein receptor are involved in hepatitis C virus adsorption," (in eng), *J Med Virol*, vol. 68, no. 2, pp. 206-15, Oct 2002, doi: 10.1002/jmv.10196.
- [345] O. Lamas Longarela *et al.*, "Proteoglycans act as cellular hepatitis delta virus attachment receptors," (in eng), *PLoS One*, vol. 8, no. 3, p. e58340, 2013, doi: 10.1371/journal.pone.0058340.
- [346] C. Sureau and J. Salisse, "A conformational heparan sulfate binding site essential to infectivity overlaps with the conserved hepatitis B virus a-determinant," (in eng), *Hepatology*, vol. 57, no. 3, pp. 985-94, Mar 2013, doi: 10.1002/hep.26125.
- [347] L. Cruz and C. Meyers, "Differential dependence on host cell glycosaminoglycans for infection of epithelial cells by high-risk HPV types," (in eng), *PLoS One*, vol. 8, no. 7, p. e68379, 2013, doi: 10.1371/journal.pone.0068379.
- [348] D. Shukla *et al.*, "A novel role for 3-O-sulfated heparan sulfate in herpes simplex virus 1 entry," (in eng), *Cell*, vol. 99, no. 1, pp. 13-22, Oct 1 1999, doi: 10.1016/s0092-8674(00)80058-6.
- [349] S. A. Connolly, J. O. Jackson, T. S. Jardetzky, and R. Longnecker, "Fusing structure and function: a structural view of the herpesvirus entry machinery," (in eng), *Nat Rev Microbiol*, vol. 9, no. 5, pp. 369-81, May 2011, doi: 10.1038/nrmicro2548.
- [350] M. Patel *et al.*, "Cell-surface heparan sulfate proteoglycan mediates HIV-1 infection of T-cell lines," (in eng), *AIDS Res Hum Retroviruses*, vol. 9, no. 2, pp. 167-74, Feb 1993, doi: 10.1089/aid.1993.9.167.

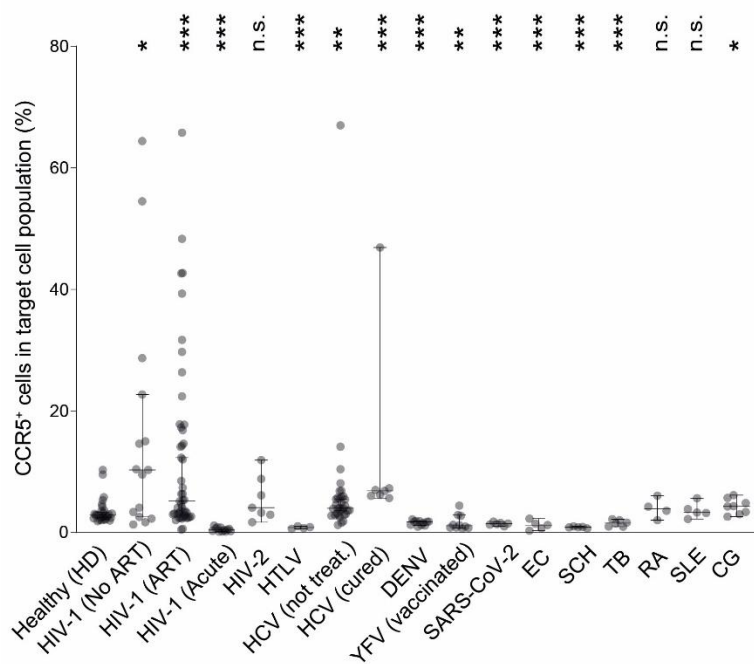
- [351] A. Ceballos *et al.*, "Spermatozoa capture HIV-1 through heparan sulfate and efficiently transmit the virus to dendritic cells," (in eng), *J Exp Med*, vol. 206, no. 12, pp. 2717-33, Nov 23 2009, doi: 10.1084/jem.20091579.
- [352] G. Roderiquez, T. Oravec, M. Yanagishita, D. C. Bou-Habib, H. Mostowski, and M. A. Norcross, "Mediation of human immunodeficiency virus type 1 binding by interaction of cell surface heparan sulfate proteoglycans with the V3 region of envelope gp120-gp41," (in eng), *J Virol*, vol. 69, no. 4, pp. 2233-9, Apr 1995, doi: 10.1128/jvi.69.4.2233-2239.1995.
- [353] A. C. Saphire, M. D. Bobardt, Z. Zhang, G. David, and P. A. Gallay, "Syndecans serve as attachment receptors for human immunodeficiency virus type 1 on macrophages," (in eng), *J Virol*, vol. 75, no. 19, pp. 9187-200, Oct 2001, doi: 10.1128/jvi.75.19.9187-9200.2001.
- [354] R. G. Parton and A. A. Richards, "Lipid rafts and caveolae as portals for endocytosis: new insights and common mechanisms," (in eng), *Traffic*, vol. 4, no. 11, pp. 724-38, Nov 2003, doi: 10.1034/j.1600-0854.2003.00128.x.
- [355] K. Simons and E. Ikonen, "Functional rafts in cell membranes," (in eng), *Nature*, vol. 387, no. 6633, pp. 569-72, Jun 5 1997, doi: 10.1038/42408.
- [356] M. M. Moreno-Altamirano, I. Aguilar-Carmona, and F. J. Sánchez-García, "Expression of GM1, a marker of lipid rafts, defines two subsets of human monocytes with differential endocytic capacity and lipopolysaccharide responsiveness," (in eng), *Immunology*, vol. 120, no. 4, pp. 536-43, Apr 2007, doi: 10.1111/j.1365-2567.2006.02531.x.
- [357] B. Ardman, K. Mayer, J. Bristol, M. Ryan, M. Settles, and E. Levy, "Surface immunoglobulin-positive T lymphocytes in HIV-1 infection: relationship to CD4+ lymphocyte depletion," (in eng), *Clin Immunol Immunopathol*, vol. 56, no. 2, pp. 249-58, Aug 1990, doi: 10.1016/0090-1229(90)90146-h.
- [358] C. Müller, S. Kukel, and R. Bauer, "Relationship of antibodies against CD4+ T cells in HIV-infected patients to markers of activation and progression: autoantibodies are closely associated with CD4 cell depletion," (in eng), *Immunology*, vol. 79, no. 2, pp. 248-54, Jun 1993.
- [359] A. Macela and K. Kubelkova, "Why Does SARS-CoV-2 Infection Induce Autoantibody Production?," (in eng), *Pathogens*, vol. 10, no. 3, Mar 22 2021, doi: 10.3390/pathogens10030380.
- [360] Y. C. Chuang, H. Y. Lei, Y. S. Lin, H. S. Liu, H. L. Wu, and T. M. Yeh, "Dengue virus-induced autoantibodies bind to plasminogen and enhance its activation," (in eng), *J Immunol*, vol. 187, no. 12, pp. 6483-90, Dec 15 2011, doi: 10.4049/jimmunol.1102218.
- [361] J. A. Quaresma, G. T. Yoshikawa, R. V. Koyama, G. A. Dias, S. Fujihara, and H. T. Fuzii, "HTLV-1, Immune Response and Autoimmunity," (in eng), *Viruses*, vol. 8, no. 1, Dec 24 2015, doi: 10.3390/v8010005.
- [362] D. Vergani and G. Mieli-Vergani, "Autoimmune manifestations in viral hepatitis," (in eng), *Semin Immunopathol*, vol. 35, no. 1, pp. 73-85, Jan 2013, doi: 10.1007/s00281-012-0328-6.
- [363] B. Dema and N. Charles, "Autoantibodies in SLE: Specificities, Isotypes and Receptors," (in eng), *Antibodies (Basel)*, vol. 5, no. 1, Jan 4 2016, doi: 10.3390/antib5010002.
- [364] M. A. M. van Delft and T. W. J. Huizinga, "An overview of autoantibodies in rheumatoid arthritis," (in eng), *J Autoimmun*, vol. 110, p. 102392, Jun 2020, doi: 10.1016/j.jaut.2019.102392.
- [365] Z. Luo *et al.*, "Pathological Role of Anti-CD4 Antibodies in HIV-Infected Immunologic Nonresponders Receiving Virus-Suppressive Antiretroviral Therapy," (in eng), *J Infect Dis*, vol. 216, no. 1, pp. 82-91, Jul 1 2017, doi: 10.1093/infdis/jix223.
- [366] K. Elkon and P. Casali, "Nature and functions of autoantibodies," (in eng), *Nat Clin Pract Rheumatol*, vol. 4, no. 9, pp. 491-8, Sep 2008, doi: 10.1038/ncprheum0895.
- [367] S. Nyamweya, A. Hegedus, A. Jaye, S. Rowland-Jones, K. L. Flanagan, and D. C. Macallan, "Comparing HIV-1 and HIV-2 infection: Lessons for viral

- immunopathogenesis," (in eng), *Rev Med Virol*, vol. 23, no. 4, pp. 221-40, Jul 2013, doi: 10.1002/rmv.1739.
- [368] F. Cambay *et al.*, "Glycosylation of Fcγ receptors influences their interaction with various IgG1 glycoforms," (in eng), *Mol Immunol*, vol. 121, pp. 144-158, May 2020, doi: 10.1016/j.molimm.2020.03.010.
- [369] A. L. Puaux *et al.*, "A very rapid and simple assay based on trogocytosis to detect and measure specific T and B cell reactivity by flow cytometry," (in eng), *Eur J Immunol*, vol. 36, no. 3, pp. 779-88, Mar 2006, doi: 10.1002/eji.200535407.
- [370] B. Vanherberghen *et al.*, "Human and murine inhibitory natural killer cell receptors transfer from natural killer cells to target cells," (in eng), *Proc Natl Acad Sci U S A*, vol. 101, no. 48, pp. 16873-8, Nov 30 2004, doi: 10.1073/pnas.0406240101.
- [371] B. D. Wines, M. S. Powell, P. W. Parren, N. Barnes, and P. M. Hogarth, "The IgG Fc contains distinct Fc receptor (FcR) binding sites: the leukocyte receptors Fc gamma RI and Fc gamma RIIa bind to a region in the Fc distinct from that recognized by neonatal FcR and protein A," (in eng), *J Immunol*, vol. 164, no. 10, pp. 5313-8, May 15 2000, doi: 10.4049/jimmunol.164.10.5313.
- [372] M. Sachse, G. J. Strous, and J. Klumperman, "ATPase-deficient hVPS4 impairs formation of internal endosomal vesicles and stabilizes bilayered clathrin coats on endosomal vacuoles," (in eng), *J Cell Sci*, vol. 117, no. Pt 9, pp. 1699-708, Apr 1 2004, doi: 10.1242/jcs.00998.
- [373] H. Fujita *et al.*, "A dominant negative form of the AAA ATPase SKD1/VPS4 impairs membrane trafficking out of endosomal/lysosomal compartments: class E vps phenotype in mammalian cells," (in eng), *J Cell Sci*, vol. 116, no. Pt 2, pp. 401-14, Jan 15 2003, doi: 10.1242/jcs.00213.
- [374] A. Aucher, E. Magdeleine, E. Joly, and D. Hudrisier, "Capture of plasma membrane fragments from target cells by trogocytosis requires signaling in T cells but not in B cells," (in eng), *Blood*, vol. 111, no. 12, pp. 5621-8, Jun 15 2008, doi: 10.1182/blood-2008-01-134155.
- [375] S. Daubeuf *et al.*, "Preferential transfer of certain plasma membrane proteins onto T and B cells by trogocytosis," (in eng), *PLoS One*, vol. 5, no. 1, p. e8716, Jan 14 2010, doi: 10.1371/journal.pone.0008716.
- [376] S. S. Somanchi, A. Somanchi, L. J. Cooper, and D. A. Lee, "Engineering lymph node homing of ex vivo-expanded human natural killer cells via trogocytosis of the chemokine receptor CCR7," (in eng), *Blood*, vol. 119, no. 22, pp. 5164-72, May 31 2012, doi: 10.1182/blood-2011-11-389924.
- [377] G. Chaudhri *et al.*, "T cell receptor sharing by cytotoxic T lymphocytes facilitates efficient virus control," (in eng), *Proc Natl Acad Sci U S A*, vol. 106, no. 35, pp. 14984-9, Sep 1 2009, doi: 10.1073/pnas.0906554106.
- [378] A. Noto *et al.*, "CD32(+) and PD-1(+) Lymph Node CD4 T Cells Support Persistent HIV-1 Transcription in Treated Aviremic Individuals," (in eng), *J Virol*, vol. 92, no. 20, Oct 15 2018, doi: 10.1128/jvi.00901-18.
- [379] J. Tabiasco, A. Vercellone, F. Meggetto, D. Hudrisier, P. Brousset, and J. J. Fournié, "Acquisition of viral receptor by NK cells through immunological synapse," (in eng), *J Immunol*, vol. 170, no. 12, pp. 5993-8, Jun 15 2003, doi: 10.4049/jimmunol.170.12.5993.
- [380] K. J. Doores, "The HIV glycan shield as a target for broadly neutralizing antibodies," (in eng), *Febs j*, vol. 282, no. 24, pp. 4679-91, Dec 2015, doi: 10.1111/febs.13530.
- [381] D. Sancho and C. Reis e Sousa, "Signaling by myeloid C-type lectin receptors in immunity and homeostasis," (in eng), *Annu Rev Immunol*, vol. 30, pp. 491-529, 2012, doi: 10.1146/annurev-immunol-031210-101352.
- [382] T. B. Geijtenbeek and Y. van Kooyk, "DC-SIGN: a novel HIV receptor on DCs that mediates HIV-1 transmission," (in eng), *Curr Top Microbiol Immunol*, vol. 276, pp. 31-54, 2003, doi: 10.1007/978-3-662-06508-2\_2.

- [383] Z. J. Xu *et al.*, "The M2 macrophage marker CD206: a novel prognostic indicator for acute myeloid leukemia," (in eng), *Oncoimmunology*, vol. 9, no. 1, p. 1683347, 2020, doi: 10.1080/2162402x.2019.1683347.
- [384] A. Domínguez-Soto *et al.*, "Dendritic cell-specific ICAM-3-grabbing nonintegrin expression on M2-polarized and tumor-associated macrophages is macrophage-CSF dependent and enhanced by tumor-derived IL-6 and IL-10," (in eng), *J Immunol*, vol. 186, no. 4, pp. 2192-200, Feb 15 2011, doi: 10.4049/jimmunol.1000475.
- [385] Z. Wu, Z. Chen, and D. M. Phillips, "Human genital epithelial cells capture cell-free human immunodeficiency virus type 1 and transmit the virus to CD4+ Cells: implications for mechanisms of sexual transmission," (in eng), *J Infect Dis*, vol. 188, no. 10, pp. 1473-82, Nov 15 2003, doi: 10.1086/379248.
- [386] M. D. Bobardt *et al.*, "Syndecan captures, protects, and transmits HIV to T lymphocytes," (in eng), *Immunity*, vol. 18, no. 1, pp. 27-39, Jan 2003, doi: 10.1016/s1074-7613(02)00504-6.
- [387] B. Fadnes *et al.*, "The proteoglycan repertoire of lymphoid cells," (in eng), *Glycoconj J*, vol. 29, no. 7, pp. 513-23, Oct 2012, doi: 10.1007/s10719-012-9427-9.
- [388] H. I. Henderson and T. J. Hope, "The temperature arrested intermediate of virus-cell fusion is a functional step in HIV infection," (in eng), *Virology*, vol. 3, p. 36, May 25 2006, doi: 10.1186/1743-422x-3-36.
- [389] S. A. Gallo, G. M. Clore, J. M. Louis, C. A. Bewley, and R. Blumenthal, "Temperature-dependent intermediates in HIV-1 envelope glycoprotein-mediated fusion revealed by inhibitors that target N- and C-terminal helical regions of HIV-1 gp41," (in eng), *Biochemistry*, vol. 43, no. 25, pp. 8230-3, Jun 29 2004, doi: 10.1021/bi049957v.
- [390] B. Helling *et al.*, "A specific CD4 epitope bound by tregalizumab mediates activation of regulatory T cells by a unique signaling pathway," (in eng), *Immunol Cell Biol*, vol. 93, no. 4, pp. 396-405, Apr 2015, doi: 10.1038/icb.2014.102.
- [391] D. Sharma *et al.*, "Protein minimization of the gp120 binding region of human CD4," (in eng), *Biochemistry*, vol. 44, no. 49, pp. 16192-202, Dec 13 2005, doi: 10.1021/bi051120s.
- [392] N. Cerutti *et al.*, "Stabilization of HIV-1 gp120-CD4 receptor complex through targeted interchain disulfide exchange," (in eng), *J Biol Chem*, vol. 285, no. 33, pp. 25743-52, Aug 13 2010, doi: 10.1074/jbc.M110.144121.
- [393] J. Shao, G. Liu, and G. Lv, "Mutation in the D1 domain of CD4 receptor modulates the binding affinity to HIV-1 gp120," (in eng), *RSC Adv*, vol. 13, no. 3, pp. 2070-2080, Jan 6 2023, doi: 10.1039/d2ra06628a.
- [394] A. Aucher, I. Puigdomènech, E. Joly, B. Clotet, D. Hudrisier, and J. Blanco, "Could CD4 capture by CD8+ T cells play a role in HIV spreading?," (in eng), *J Biomed Biotechnol*, vol. 2010, p. 907371, 2010, doi: 10.1155/2010/907371.
- [395] K. H. Roh, B. F. Lillemeier, F. Wang, and M. M. Davis, "The coreceptor CD4 is expressed in distinct nanoclusters and does not colocalize with T-cell receptor and active protein tyrosine kinase p56lck," (in eng), *Proc Natl Acad Sci U S A*, vol. 112, no. 13, pp. E1604-13, Mar 31 2015, doi: 10.1073/pnas.1503532112.
- [396] I. Parolini *et al.*, "Phorbol ester-induced disruption of the CD4-Lck complex occurs within a detergent-resistant microdomain of the plasma membrane. Involvement of the translocation of activated protein kinase C isoforms," (in eng), *J Biol Chem*, vol. 274, no. 20, pp. 14176-87, May 14 1999, doi: 10.1074/jbc.274.20.14176.
- [397] Singer, II *et al.*, "CCR5, CXCR4, and CD4 are clustered and closely apposed on microvilli of human macrophages and T cells," (in eng), *J Virol*, vol. 75, no. 8, pp. 3779-90, Apr 2001, doi: 10.1128/jvi.75.8.3779-3790.2001.
- [398] S. Bournazos, S. P. Hart, L. H. Chamberlain, M. J. Glennie, and I. Dransfield, "Association of FcγRIIIa (CD32a) with lipid rafts regulates ligand binding activity," (in eng), *J Immunol*, vol. 182, no. 12, pp. 8026-36, Jun 15 2009, doi: 10.4049/jimmunol.0900107.

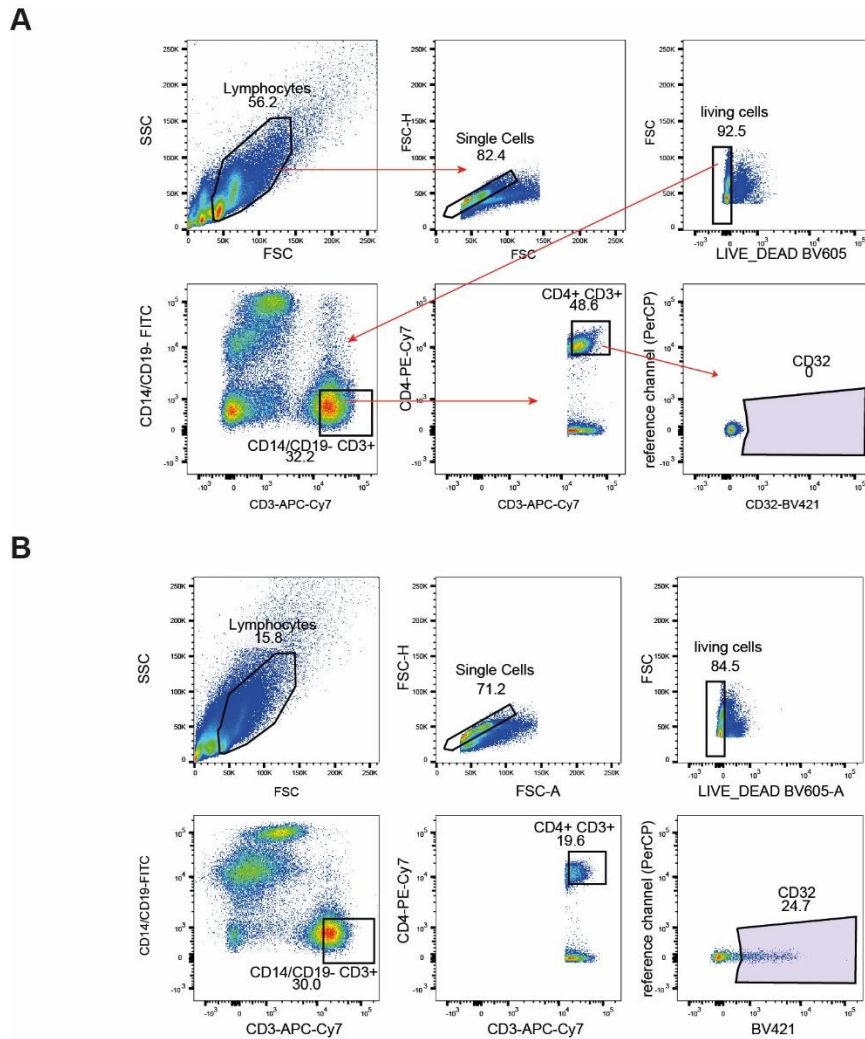
- [399] J. A. Vieth, M. K. Kim, D. Glaser, K. Stiles, A. D. Schreiber, and R. G. Worth, "FcγRIIa requires lipid rafts, but not co-localization into rafts, for effector function," (in eng), *Inflamm Res*, vol. 62, no. 1, pp. 37-43, Jan 2013, doi: 10.1007/s00011-012-0548-1.
- [400] J. A. Vieth, M. K. Kim, X. Q. Pan, A. D. Schreiber, and R. G. Worth, "Differential requirement of lipid rafts for FcγRIIA mediated effector activities," (in eng), *Cell Immunol*, vol. 265, no. 2, pp. 111-9, 2010, doi: 10.1016/j.cellimm.2010.07.011.
- [401] W. Popik, T. M. Alce, and W. C. Au, "Human immunodeficiency virus type 1 uses lipid raft-colocalized CD4 and chemokine receptors for productive entry into CD4(+) T cells," (in eng), *J Virol*, vol. 76, no. 10, pp. 4709-22, May 2002, doi: 10.1128/jvi.76.10.4709-4722.2002.
- [402] J. G. Burel *et al.*, "Circulating T cell-monocyte complexes are markers of immune perturbations," (in eng), *Elife*, vol. 8, Jun 25 2019, doi: 10.7554/eLife.46045.
- [403] D. Turner, M. Hoffman, I. Yust, M. Fried, M. Bleiberg, and B. Tartakovsky, "Overexpression of a novel lymphocyte population, positive for an intracellular CD14-like antigen, in patients positive for human immunodeficiency virus type 1," (in eng), *Clin Diagn Lab Immunol*, vol. 11, no. 6, pp. 1040-4, Nov 2004, doi: 10.1128/cdli.11.6.1040-1044.2004.
- [404] C. Ortolani, E. Forti, E. Radin, R. Cibir, and A. Cossarizza, "Cytofluorimetric identification of two populations of double positive (CD4+,CD8+) T lymphocytes in human peripheral blood," (in eng), *Biochem Biophys Res Commun*, vol. 191, no. 2, pp. 601-9, Mar 15 1993, doi: 10.1006/bbrc.1993.1260.
- [405] A. K. Viridi *et al.*, "CD32 is enriched on CD4dimCD8bright T cells," (in eng), *PLoS One*, vol. 15, no. 9, p. e0239157, 2020, doi: 10.1371/journal.pone.0239157.
- [406] T. Takahashi, S. Dejbakhsh-Jones, and S. Strober, "Expression of CD161 (NKR-P1A) defines subsets of human CD4 and CD8 T cells with different functional activities," (in eng), *J Immunol*, vol. 176, no. 1, pp. 211-6, Jan 1 2006, doi: 10.4049/jimmunol.176.1.211.

## 6. Supplemental data



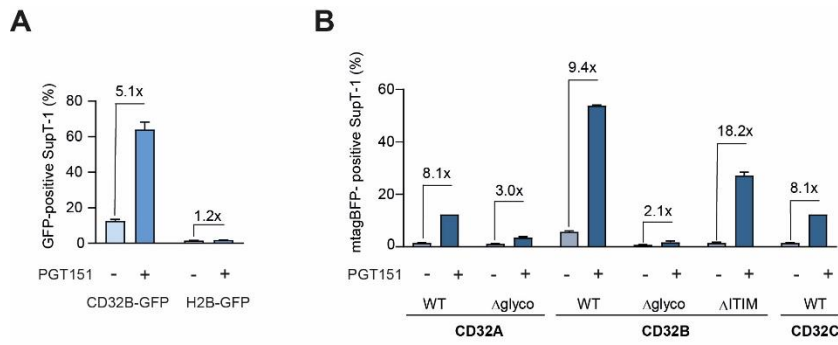
**Supplemental figure 1 | CCR5 transfer is enhanced by T-cell-autoreactive antibodies frequently seen in chronic infected HIV-1 patients.**

Levels of CCR5 transfer from the experiment described in the legend of Figure 11 p.57. Median with 95% CI are shown. Asterisks indicate statistical significance by Mann-Whitney test. \* $P \leq 0.05$ ; \*\* $P \leq 0.01$ ; \*\*\* $P \leq 0.001$ . n.s.: not significant.



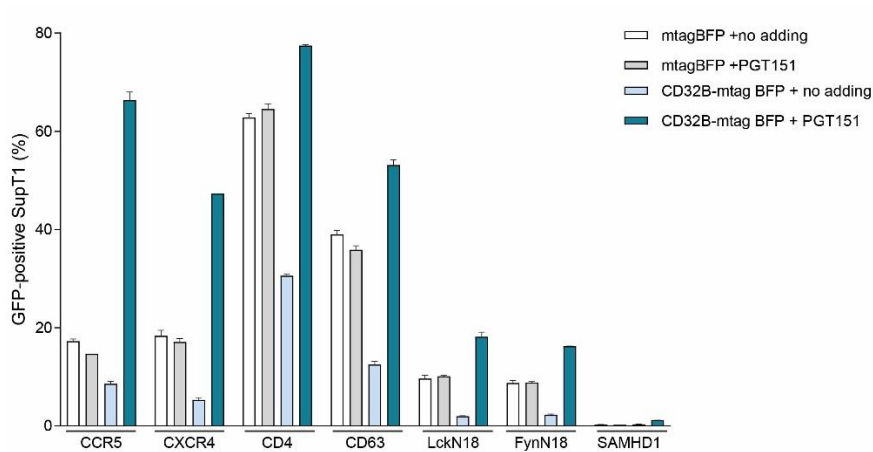
**Supplemental figure 2 | Gating strategy for identification of CD32+ CD4 T cells in PBMCs.**

Lymphocytes were gated using the forward and side scatter area (FSC-A versus SSC-A); doublets were removed by FSC-A to FSC-height (FSC-H). To exclude monocytes and B cells, the CD14<sup>-</sup> CD19<sup>-</sup> CD3<sup>+</sup> population was gated, followed by gating for CD4<sup>+</sup> CD3<sup>+</sup> cells. To quantify the fraction of CD32<sup>+</sup> CD4 T cells, a Fluorescence Minus One (FMO) control was used to set the gate. Representative examples of flow cytometry dot plots of one HD (A) and one HIV-1 patient (CHI) (B). Experiment described in legend Figure 11C p.46.



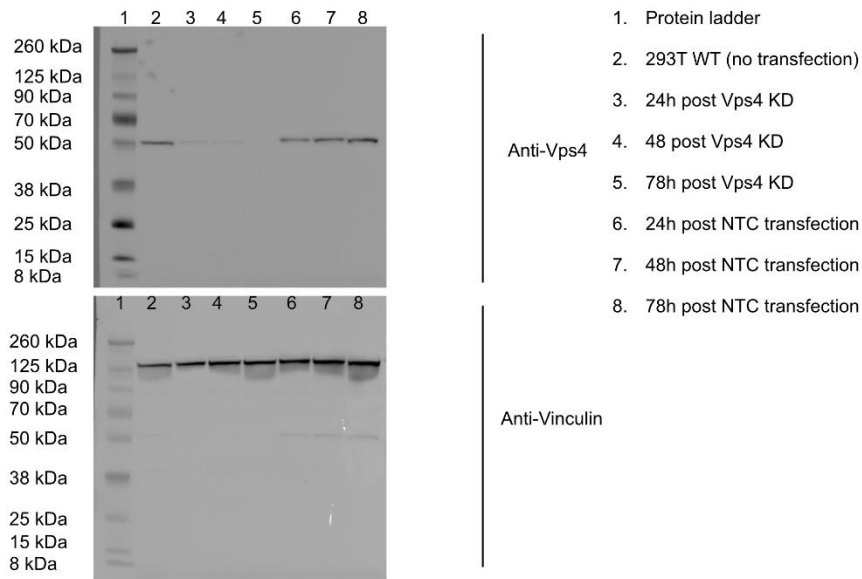
### Supplemental figure 3 | Transfer of CD32 isoforms and mutants promoted by bNAb PGT151

**A**, transfer of CD32B-GFP or H2B-GFP in experiment described in legend of Figure 12, p.59. **B**, transfer of CD32A, B and C and corresponding mutants of CD32A and B in experiment described in legend of Figure 12, p.59. Means of technical replicates  $\pm$  SD. are shown.



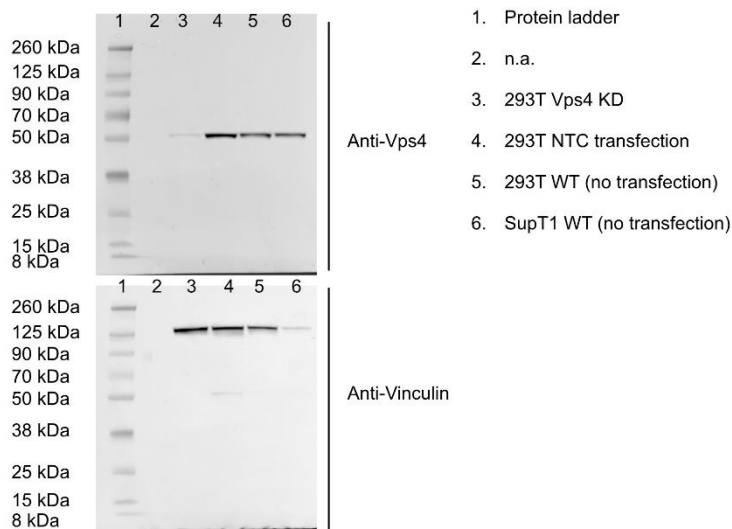
### Supplemental figure 4 | CD32 mediates transfer of plasma membrane-associated receptors.

Positive SupT-1 (%) after co-culture in experiment described in Figure 13, p.49. Transfer of indicated surface receptors (CCR5, CXCR4, CD4 or CD63), the first 18 amino acid of the N-terminal part of the intracellular membrane proteins of the Src kinase receptors Lck or Fyn or the intracellular protein SAMHD1 mediated by CD32B or mtagBFP (control) +/- presence of PGT151. Means of technical replicates  $\pm$  SD. are shown.



### Supplemental figure 5 | Knockdown of Vps4 in 293T monitored overtime.

Stably CD32B-T2A-mtagBFP expressing 293T cells were transfected with siRNA specific for human Vps4 or a non-targeting control siRNA (NTC). Vps4 (upper immunoblot) or Vinculin (control, lower immunoblot) expression in the 293T KD, NTC and wild type (WT) was analyzed 24 h, 48 h and 78 h post transfection.



### Supplemental figure 6 | Knockdown of Vps4 in donor cells does not impact CD32B transfer to recipient cell (full immunoblot).

Full image of immunoblots of experiment described in legend of Figure 15, p. 62.

**Supplemental table 1 | Surface receptor screening on M2 macrophages and autologous CD4 T cells, either co-cultured with M2 cells or kept alone for 48 h (antibodies screening panel of the BD Lyoplate™).**

Experiment described in legend of Figure 17, p.64

Receptor	MFI not co-cultured T cells	MFI co-cultured T cells	Ratio MFI not co-cultured T cells to co-cultured T cells	MFI not co-cultured M2 macrophages	Expression level on M2 cells
CD1a	24	25,1	1,0	2689	Medium
CD1b	46	40	0,9	5273	Medium
CD1d	37,6	39,3	1,0	1726	Low
CD2	18782	16908	0,9	1241	Low
CD3	26190	25481	1,0	1280	Low
CD4	25881	16658	0,6	5388	Medium
CD4v4	19623	18425	0,9	7761	High
CD5	25745	24964	1,0	1370	Low
CD6	22772	18704	0,8	1113	Low
CD7	9204	11631	1,3	808	Low
CD8a	32,9	61,6	1,9	757	Low
CD8b	63,8	57,9	0,9	1512	Low
CD9	4215	4048	1,0	13118	High
CD10	978	877	0,9	2003	Low
CD11a	22103	21353	1,0	5477	Medium
CD11b	47,2	40,5	0,9	21254	High
CD11c	448	520	1,2	35914	High
CD13	57,1	169	3,0	41284	High
CD14	1648	1380	0,8	28974	High
CD15	1020	733	0,7	830	Low
CD15s	587	187	0,3	1233	Low
CD16	27,8	29,7	1,1	4151	Medium
CD18	11540	12747	1,1	46932	High
CD19	85,3	86,2	1,0	1289	Low
CD20	113	107	0,9	3482	Medium
CD21	122	91,7	0,8	1745	Low
CD22	110	106	1,0	1492	Low
CD23	40,2	31,2	0,8	2482	Medium
CD24	45,2	48,6	1,1	2019	Low
CD25	704	894	1,3	2380	Medium
CD26	5558	7775	1,4	1537	Low
CD27	11874	11347	1,0	1620	Low
CD28	9503	7785	0,8	1870	Low
CD29	267	387	1,4	3897	Medium
CD30	580	530	0,9	1244	Low
CD31	2443	3651	1,5	9264	High
CD32	51,8	123	2,4	32166	High
CD33	42,1	43,6	1,0	7098	High
CD34	49,6	58	1,2	2026	Low
CD35	341	210	0,6	2059	Low
CD36	217	71,6	0,3	11130	High
CD37	1115	865	0,8	2558	Medium
CD38	3782	4095	1,1	2569	Medium
CD39	409	462	1,1	17381	High
CD40	70,7	124	1,8	17988	High
CD41a	37,7	38,4	1,0	1646	Low
CD41b	35,2	21,6	0,6	692	Low

\*table starts at page 127

Receptor	MFI not co-cultured T cells	MFI co-cultured T cells	Ratio MFI not co-cultured T cells to co-cultured T cells	MFI not co-cultured M2 macrophages	Expression level on M2 cells
CD42a	148	144	1,0	1058	Low
CD42b	23,2	24,3	1,0	1342	Low
CD43	25078	4830	0,2	26404	High
CD44	26348	11073	0,4	159220	High
CD45	26373	22806	0,9	32079	High
CD45RA	8871	6588	0,7	3880	Medium
CD45RB	24185	14674	0,6	16514	High
CD45RO	11306	7224	0,6	52751	High
CD46	18585	18643	1,0	15483	High
CD47	25980	18817	0,7	17206	High
CD48	8793	8666	1,0	4546	Medium
CD49a	84,4	62,8	0,7	1225	Low
CD49b	68,9	61,1	0,9	1127	Low
CD49c	768	627	0,8	2581	Medium
CD49d	5847	4643	0,8	7668	High
CD49e	2307	1971	0,9	14384	High
CD50	26306	23233	0,9	11610	High
CD51/CD61	37,9	23,5	0,6	1908	Low
CD53	18233	12557	0,7	13943	High
CD54	1163	2823	2,4	62996	High
CD55	12250	8377	0,7	5585	Medium
CD56	39,8	32,6	0,8	1683	Low
CD57	437	264	0,6	811	Low
CD58	3416	3580	1,0	43019	High
CD59	10460	7756	0,7	43263	High
CD61	101	88,3	0,9	2324	Medium
CD62E	37,8	32,9	0,9	1291	Low
CD62L	21878	18287	0,8	1059	Low
CD62P	68,9	59,4	0,9	980	Low
CD63	79,5	272	3,4	14543	High
CD64	27,3	33,7	1,2	2124	Low
CD66 (a,b,c,d,e)	217	651	3,0	2190	Low
CD66b	235	78	0,3	828	Low
CD66f	32,8	23,9	0,7	1403	Low
CD69	43,2	813	18,8	1233	Low
CD70	49,5	41	0,8	767	Low
CD71	132	240	1,8	11450	High
CD72	92,4	72,6	0,8	1836	Low
CD73	279	169	0,6	1393	Low
CD74	102	256	2,5	10321	High
CD75	299	134	0,4	952	Low
CD77	187	49,2	0,3	690	Low
CD79b	35,8	16,4	0,5	1167	Low
CD80	1012	749	0,7	6965	High
CD81	22788	19700	0,9	28221	High
CD83	175	158	0,9	1605	Low
CD84	872	1611	1,8	14546	High

\*table starts at page 127

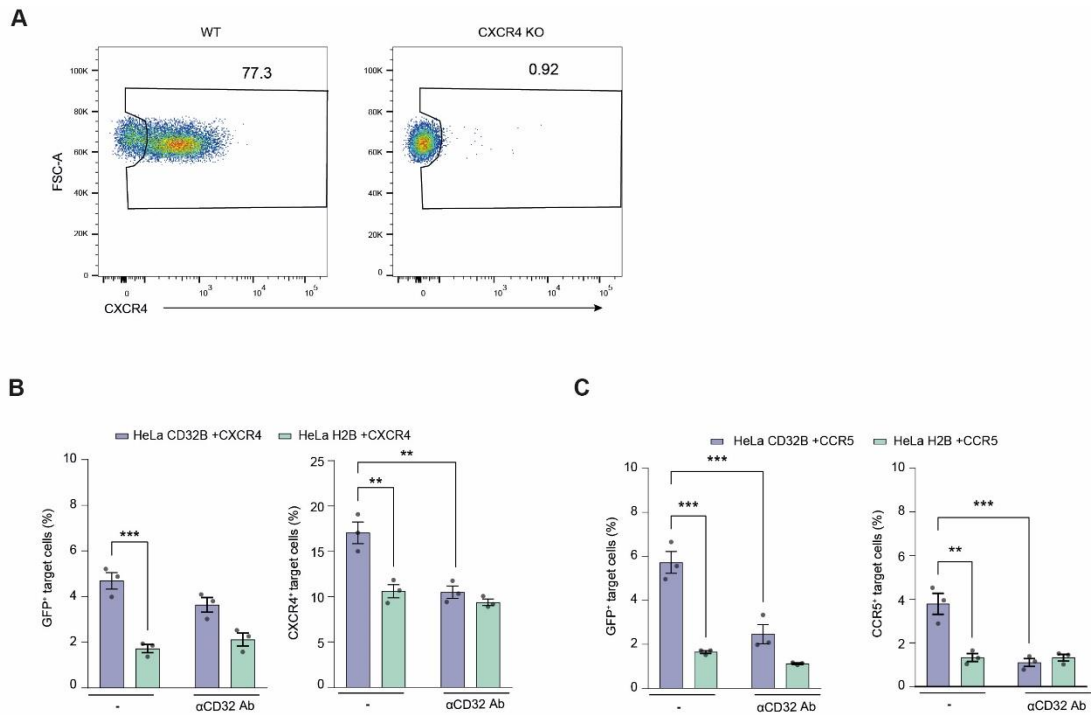
Receptor	MFI not co-cultured T cells	MFI co-cultured T cells	Ratio MFI not co-cultured T cells to co-cultured T cells	MFI not co-cultured M2 macrophages	Expression level on M2 cells
CD85	27,6	91,2	3,3	33286	High
buffer	28	19,5	0,7	425	Low
CD86	34,1	74	2,2	8633	High
CD87	32,9	42,6	1,3	966	Low
CD88	72,7	110	1,5	2312	Low
CD89	24,7	38,2	1,5	3765	Medium
CD90	64,5	73,6	1,1	700	Low
CD91	33,7	43,2	1,3	2442	Medium
CDw93	32,2	29,9	0,9	2280	Low
CD94	37,6	24,7	0,7	840	Low
CD95	2501	3830	1,5	3566	Medium
CD97	509	1779	3,5	9996	High
CD98	2493	3774	1,5	22768	High
CD99	12392	12279	1,0	23500	High
CD99R	804	572	0,7	1532	Low
CD100	3604	4609	1,3	1624	Low
CD102	13303	12481	0,9	3730	Medium
CD103	80,5	72,6	0,9	1385	Low
CD105	50,4	62,7	1,2	8600	High
CD106	28,8	45,5	1,6	1310	Low
CD107a	122	263	2,2	3534	Medium
CD107b	46,3	64,9	1,4	2532	Medium
CD108	38	38,8	1,0	2218	Low
CD109	43,3	42,8	1,0	2276	Low
CD112	38,9	27,3	0,7	4545	Medium
CD114	29,5	27,1	0,9	1282	Low
CD116	126	44,8	0,4	947	Low
CD117	61,6	36,4	0,6	2303	Low
CD118	38,1	28,1	0,7	1085	Low
CD119	222	300	1,4	6082	High
CD120a	82,6	111	1,3	3865	Medium
CD121a	27	20,3	0,7	1954	Low
CD121b	43	44,1	1,0	2245	Low
CD122	184	91,6	0,5	1368	Low
CD123	25,3	43,4	1,7	3524	Medium
CD124	207	70	0,3	2056	Low
CD126	696	254	0,4	1226	Low
CD127	2209	1132	0,5	1124	Low
CD128b	221	42,5	0,2	1262	low
CD130	420	347	0,8	2776	Medium
CD134	84,1	219	2,6	2603	Medium
CD135	39,5	38,2	1,0	1751	Low
CD137	34,4	57,4	1,7	2171	Low
CD137 Ligand	25,2	31,5	1,2	3277	Medium
CD138	40,1	31,1	0,8	1370	Low
CD140a	51,6	47,6	0,9	2154	Low
CD140b	34,4	27,8	0,8	2774	Medium

\*table starts at page 127

Receptor	MFI not co-cultured T cells	MFI co-cultured T cells	Ratio MFI not co-cultured T cells to co-cultured T cells	MFI not co-cultured M2 macrophages	Expression level on M2 cells
CD141	38,5	59	1,5	15464	High
CD142	34,3	34,7	1,0	2943	Medium
CD144	28,5	33,9	1,2	1152	Low
CD146	101	108	1,1	1255	Low
CD147	3374	5613	1,7	32916	High
CD150	264	309	1,2	2274	Low
CD151	3201	5135	1,6	10530	High
CD152	55,6	61	1,1	4470	Medium
CD153	43,8	42,3	1,0	3038	Medium
CD154	156	80,3	0,5	2153	Low
CD158a	211	48,8	0,2	693	Low
CD158b	46,5	47	1,0	2946	Medium
CD161	354	391	1,1	1153	Low
CD162	13440	10646	0,8	1759	Low
CD163	46,2	47,4	1,0	14048	High
CD164	558	1019	1,8	4015	Medium
CD165	192	316	1,6	2224	Low
CD166	123	128	1,0	8168	High
CD171	46	62,1	1,4	2533	Medium
CD172b	28,1	21,9	0,8	2458	Medium
CD177	65,1	53	0,8	1458	Low
CD178	31,7	29,5	0,9	1131	Low
CD180	67,4	72,2	1,1	5118	Medium
CD181	44,4	59,7	1,3	3200	Medium
CD183	1365	677	0,5	1298	Low
CD184	7397	14153	1,9	3161	Medium
CD193	57,3	75,2	1,3	1370	Low
CD195	125	395	3,2	7018	High
CD196	433	1175	2,7	1375	Low
CD197	687	590	0,9	730	Low
CD200	420	511	1,2	1464	Low
CD205	2987	4731	1,6	4903	Medium
CD206	29,8	50,1	1,7	11254	High
CD209	31,5	195	6,2	66385	High
CD220	36,5	49,5	1,4	1654	Low
CD221	190	220	1,2	1083	Low
CD226	1834	5380	2,9	2712	Medium
CD227	74	165	2,2	2773	Medium
CD229	1971	1169	0,6	1404	Low
CD231	32,9	46,4	1,4	832	Low
CD235a	58,2	46,8	0,8	1925	Low
CD243	93,1	62,2	0,7	2004	Low
CD244	40,4	60,3	1,5	1618	Low
CD255	35,2	35,3	1,0	618	Low
CD268	268	149	0,6	1412	Low
CD271	43,2	30,5	0,7	1639	Low
CD273	59,8	121	2,0	4610	Medium

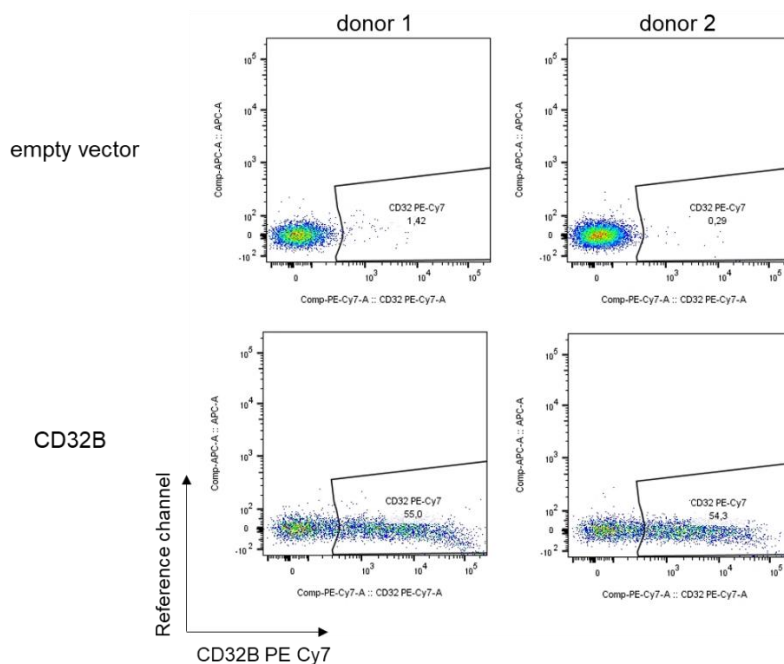
\*table starts at page 127

Receptor	MFI not co-cultured T cells	MFI co-cultured T cells	Ratio MFI not co-cultured T cells to co-cultured T cells	MFI not co-cultured M2 macrophages	Expression level on M2 cells
CD274	179	312	1,7	10053	High
CD275	56,1	42,6	0,8	8584	High
CD278	86,9	108	1,2	729	Low
buffer	26,2	23,3	0,9	498	Low
CD279	140	232	1,7	1444	Low
CD282	28,9	28,8	1,0	4486	Medium
CD305	1233	1452	1,2	12943	High
CD309	25	32,6	1,3	1201	Low
CD314	36,6	41,2	1,1	952	Low
CD321	2645	3283	1,2	9056	High
CDw327	29,4	59,3	2,0	791	Low
CDw328	24,3	35,7	1,5	5453	Medium
CD329	45,1	41	0,9	5762	Medium
CD335	34,3	35,1	1,0	864	Low
CD336	20,6	28	1,4	639	Low
CD337	41,7	35,6	0,9	1043	Low
CD338	31,4	48	1,5	2835	Medium
CD304	33,4	22,7	0,7	1623	Low
$\alpha\beta$ TCR	5301	6417	1,2	1583	Low
$\beta$ 2-microglobulin	18034	22553	1,3	23551	High
BLLTR-1	44	35,8	0,8	2343	Medium
CLIP	39,5	79,2	2,0	2939	Medium
CMRF-44	170	37	0,2	835	Low
CMRF-56	34,5	34,3	1,0	2336	Medium
EGF Receptor	39,1	32,9	0,8	2623	Medium
fMLP receptor	28,3	37,5	1,3	1687	Low
$\gamma\delta$ TCR	26,8	17,9	0,7	1253	Low
HPC	246	143	0,6	6559	High
HLA-A,B,C	26309	26357	1,0	38238	High
HLA-A2	22881	25760	1,1	45494	High
HLA-DQ	39,9	94,7	2,4	8021	High
HLA-DR	140	817	5,8	67940	High
HLA-DR, DP, DQ	306	1072	3,5	60783	High
Invariant NKT	46,3	35,1	0,8	1320	Low
Dsialoganglioside GD2	29,7	39,5	1,3	2647	Medium
MIC A/B	50,9	55	1,1	2312	Low
NKB1	31,8	35	1,1	1268	Low
SSEA-1	223	56,6	0,3	676	Low
SSEA-4	263	201	0,8	2015	Low
TRA-1-60	138	32,2	0,2	716	Low
TRA-1-81	148	75,6	0,5	883	Low
V $\beta$ 23	89,8	115	1,3	1768	Low
V $\beta$ 8	1347	1263	0,9	3081	Medium
CD326	41,5	23,4	0,6	1512	Low



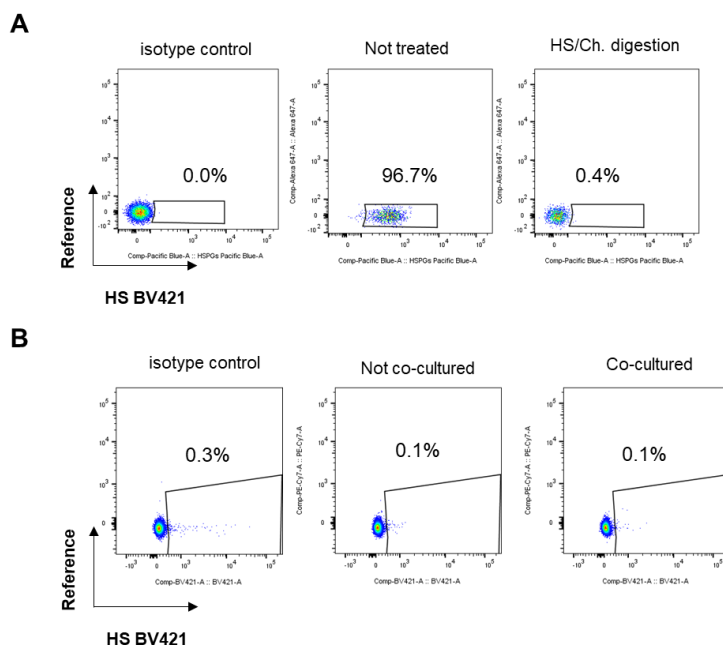
**Supplemental figure 7 | Knockout confirmation of CXCR4 in CD4 T cells and transfer of CXCR4 and CCR5 to CD4 T cells.**

**A**, KO confirmation: CXCR4 levels on WT (left panel) and CXCR4 KO (right panel) CD4 T cells were quantified with flow cytometry 7 days after RNP nucleofection. One out of three donors shown. Cells used in experiment described in legend of Figure 18A, p.65. **B**, **C**, transfer levels of CXCR4 (**B**) to CD4 T cells (described in **A**) or transfer levels of CCR5 (**B**) to primary CD4 T cells in experiment described in legend Figure 18A, p.54. Mean  $\pm$  s.e.m. is shown ( $n = 3$ ). Asterisks indicate statistical significance by two-way ANOVA. P values were corrected for multiple comparison (Tukey). \*\* $P \leq 0.01$ ; \*\*\* $P \leq 0.001$ .



**Supplemental figure 8 | Expression levels of CD32 on CD4 T cells 24 h post nucleofection with expression vector.**

CD32B levels were analyzed 24 h post nucleofection with empty vector or CD32B expression vector. Two representative donors shown, cells used in experiment described in legend of Figure 21C, p.68.



**Supplemental figure 9 | Flow cytometric staining for heparan sulfate on HeLa cells and CD4 T cells.**

**A**, HeLa cells were digested with Heparinase I/II/III (HS) and chondroitinase ABC (Ch) as in experiment described in legend of Figure 28 or left untreated. Subsequently the cells were stained for heparan sulfate and analyzed by flow cytometry, gating according to the staining with isotype control. **B**, CD4 T cells were co-cultured with M2 macrophages as described in Figure 16 and subsequently stained for heparan sulfate as described in (A). One representative donor shown.

## Acknowledgement

This thesis was carried out at the Max von Pettenkofer Institute Munich in the research group of Prof. Dr. Oliver T. Keppler. I would like to express my deepest gratitude to him. I was able to learn a lot under his supervision and I am thankful for all the inspiring meetings, discussions and his encouragement to develop myself further.

I am also very grateful to PD Dr. Barbara Adler and Prof. Dr. Ruth Brack-Werner for their time and supervision during my thesis advisory committee meetings, as well as my defense committee members for their time and evaluation.

I would also like to sincerely thank my two colleagues whom I shared this project with: Dr. Manuel Albanese and Dr. Hong-Ru Chen. All the experiments and insights we gained were achieved in a great team effort. I was able to learn so much from both of them and they were always willing to share their knowledge with me in a patient and supportive way.

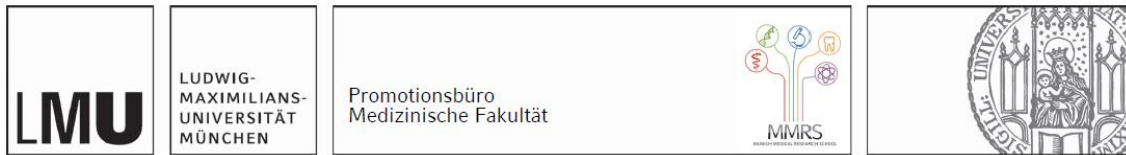
I would like to express my deepest appreciation to my colleague Stephanie Schneider. We walked the path to a PhD at the same time and shared all the good and the hard moments together. Having such a close colleague by my side, whom I can now call a dear close friend, is a priceless gift.

Many thanks to the “good fairies” Linda, Laura, Kathi and Thimo. Their help carried me through challenging times and I was so thankful to have them by my side. I am also thankful to all my colleagues, Marcel, Adrian, Robin, Ramya, Rebecca, Lin, Qianhao, Ernesto, Max, Gaia, Marie, Michele, Joao, Ina, Jasminka, and everyone else from the Virology department, for the great work environment. We organized many joyful social events together and had a lot of fun working in the lab. It was always a supportive atmosphere.

I would like to express my deepest gratitude to my parents, Sheila and Werner. They provided me with unfailing support and continuous encouragement throughout my years of study and during the process of researching and writing this thesis. They always inspired and supported me to follow my dreams. I am also grateful to my brother, Alexander, and sisters, Anneliese and Katharina, as well as the rest of my family, for always being by my side and cheering me on.

Last but not least, I would like to express a special thanks to my husband, Julian. You have always been by my side, from going to BTA school to starting and writing my PhD thesis. I could always count on you. Thank you for all the late night pick-ups from the lab with a cheese burger. You always cheered me up and encouraged me to continue my path. Thank you for being by my side!

## Affidavit



### Affidavit

#### Gapp, Madeleine Christine

I hereby declare, that the submitted thesis entitled:

*Mechanistic insight into the CD32-driven enhancement of HIV-1 susceptibility of resting CD4 T cells*

is my own work. I have only used the sources indicated and have not made unauthorised use of services of a third party. Where the work of others has been quoted or reproduced, the source is always given.

I further declare that the dissertation presented here has not been submitted in the same or similar form to any other institution for the purpose of obtaining an academic degree.

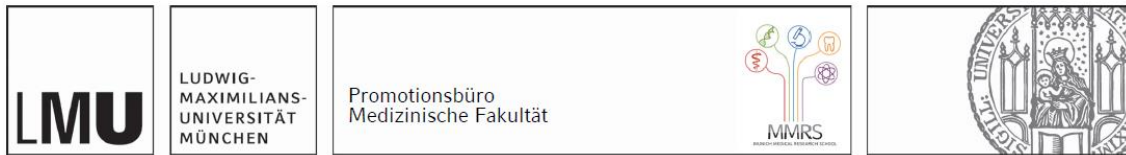
Munich, 10.05.2024

Madeleine Gapp

\_\_\_\_\_  
place, date

\_\_\_\_\_  
Signature doctoral candidate

## Confirmation of congruency



**Confirmation of congruency between printed and electronic version of  
the doctoral thesis**

**Gapp, Madeleine Christine**

I hereby declare, that the submitted thesis entitled:

*Mechanistic insight into the CD32-driven enhancement of HIV-1 susceptibility of resting CD4 T cells*

is congruent with the printed version both in content and format.

Munich, 10.05.2024

\_\_\_\_\_  
place, date

Madeleine Gapp

\_\_\_\_\_  
Signature doctoral candidate

## List of publications

### Publications related to this thesis:

Albanese M, Chen HR, **Gapp M**, Muenchhoff M, Yang HH, Peterhoff D, Hoffmann K, Xiao Q, Ruhle A, Ambiel I, Schneider S, Mejías-Pérez E, Stern M, Wratil PR, Hofmann K, Amann L, Jocham L, Fuchs T, Ulivi AF, Besson-Girard S, Weidlich S, Schneider J, Spinner CD, Sutter K, Dittmer U, Humpe A, Baumeister P, Wieser A, Rothenfusser S, Bogner J, Roeder J, Knolle P, Hengel H, Wagner R, Laketa V, Fackler OT, Keppler OT. *Receptor transfer between immune cells by autoantibody-enhanced, CD32-driven trogocytosis is hijacked by HIV-1 to infect resting CD4<sup>+</sup> T cells*. Cell Rep Med. 2024 Mar 28;101483. doi: 10.1016/j.xcrm.2024.101483. Epub ahead of print. PMID: 38579727.

Albanese M, Ruhle A, Mittermaier J, Mejías-Pérez E, **Gapp M**, Linder A, Schmacke NA, Hofmann K, Hennrich AA, Levy DN, Humpe A, Conzelmann KK, Hornung V, Fackler OT, Keppler OT. *Rapid, efficient and activation-neutral gene editing of polyclonal primary human resting CD4<sup>+</sup> T cells allows complex functional analyses*. Nat Methods. 2022 Jan;19(1):81-89. doi: 10.1038/s41592-021-01328-8. Epub 2021 Dec 23. PMID: 34949807; PMCID: PMC8748193.

Morath K, Sadhu L, Dyckhoff G, **Gapp M**, Keppler OT, Fackler OT. *Activation-neutral gene editing of tonsillar CD4<sup>+</sup> T cells for functional studies in human ex vivo tonsil cultures*. Cell Rep Methods. 2024 Jan 22;4(1):100685. doi: 10.1016/j.crmeth.2023.100685. Epub 2024 Jan 10. PMID: 38211593; PMCID: PMC10831948.

### Others:

Wratil PR, Schmacke NA, Karakoc B, Dulovic A, Junker D, Becker M, Rothbauer U, Osterman A, Spaeth PM, Ruhle A, **Gapp M**, Schneider S, Muenchhoff M, Hellmuth JC, Scherer C, Mayerle J, Reincke M, Behr J, Kääh S, Zwissler B, von Bergwelt-Baildon M, Eberle J, Kaderali L, Schneiderhan-Marra N, Hornung V, Keppler OT. *Evidence for increased SARS-CoV-2 susceptibility and COVID-19 severity related to pre-existing immunity to seasonal coronaviruses*. Cell Rep. 2021 Dec 28;37(13):110169. doi: 10.1016/j.celrep.2021.110169. Epub 2021 Dec 7. PMID: 34932974; PMCID: PMC8648802.

Faass L, Stein SC, Hauke M, **Gapp M**, Albanese M, Josenhans C. *Contribution of Heptose Metabolites and the cag Pathogenicity Island to the Activation of Monocytes/Macrophages by Helicobacter pylori*. Front Immunol. 2021 May 19;12:632154. doi: 10.3389/fimmu.2021.632154. PMID: 34093525; PMCID: PMC8174060.

Mumm JN, Ledderose S, Ostermann A, Rudelius M, Hellmuth JC, Münchhoff M, Munker D, Scherer C, Volz Y, Ebner B, Giessen-Jung C, Lampert C, Vilsmaier T, Schneider S, **Gapp M**, Milger-Kneidinger K, Behr J, von Bergwelt-Baildon M, Keppler OT, Stief C, Magistro G, Staehler M, Rodler S. *Dynamics of urinary and respiratory shedding of Severe acute respiratory syndrome virus 2 (SARS-CoV-2) RNA excludes urine as a relevant source of viral transmission*. Infection. 2022 Jun;50(3):635-642. doi: 10.1007/s15010-021-01724-4. Epub 2021 Oct 30. PMID: 34716901; PMCID: PMC8556791.

Muenchhoff M, Graf A, Krebs S, Quartucci C, Hasmann S, Hellmuth JC, Scherer C, Osterman A, Boehm S, Mandel C, Becker-Pennrich AS, Zoller M, Stubbe HC, Munker S, Munker D, Milger K, **Gapp M**, Schneider S, Ruhle A, Jocham L, Nicolai L, Pekayvaz K, Weinberger T, Mairhofer H, Khatamzas E, Hofmann K, Spaeth PM, Bender S, Kääh S, Zwissler B, Mayerle J, Behr J, von Bergwelt-Baildon M, Reincke M, Grabein B, Hinske CL, Blum H, Keppler OT. *Genomic epidemiology reveals multiple introductions of SARS-CoV-2 followed by community and nosocomial spread, Germany, February to May 2020*. Euro Surveill. 2021 Oct;26(43):2002066. doi: 10.2807/1560-7917.ES.2021.26.43.2002066. Erratum in: Euro Surveill. 2021 Nov;26(47): PMID: 34713795; PMCID: PMC8555370.

## Scientific presentations

### Presentation at science conference:

- 32nd Annual Meeting of the Society for Virology (2023)

### Poster presentation at science conference:

- 31nd Annual Meeting of the Society for Virology (2022)
- Cold Spring Harbor Laboratory – Retroviruses (2022)